FRIF retreat meeting 2014
VVF-Belambra of Dourdan, January 23-24, 2014

Holographic models for QCD

Elias Kiritsis

APC

CERN

UoC

Introduction

- My topic concerns the holographic correspondence between gauge theories and string theory.

- It has several ramifications and applications.

- There are many researchers in the Paris area and FRIF that are doing related research.

- I will not be able to cover all possible aspects.

- I will focus on potential applications to the physics of QCD.

- I will be mostly descriptive (no technical details) and will cut many corners (for simplicity and clarity)

- I will be happy to answer detailed questions, (if not urgent preferably at the end).

QCD

- Despite decades of progress, QCD remains a challenging theory for physicists, due to the strong coupling problem in the IR.

- Asymptotic freedom, combined with non-perturbative equilibrium approaches (numerical lattice gauge theory), a lot of phenomenological models and 4+ decades of experiments have convinced us today that QCD describes the strong interactions.

- But when we ask for the rate of a complex process in a collider at higher energies, we can still be easily off by 30%.

- We do think that we have good qualitative understanding of the many non-perturbative phenomena that appear in QCD (probably with the exception of finite density physics).

- We would like to eventually be able to precisely also calculate non-perturbative processes. This is, among other things, crucial for searching for new physics as the LHC has recently made the point.

• The only first principles approach we have so far, (numerical lattice gauge theory), has gone a long way since Wilson's foundational paper in 1974, but has two important limitations:

a) Finite computational resources

b) In principle limitations in computing dynamical processes at finite temperature and density.

• In 1974 't Hooft suggested that the large-N_c expansion in gauge theories may provide an alternative and controllable approximation to handle the strong coupling region and effects, (suggesting also a relationship to a string theory).

• For 20+ years the nature of this string theory remained elusive, despite a lot of theoretical effort in that direction.

• In 1997 Maldacena conjectured a precise correspondence for a more symmetric cousin of Yang-Mills (YM) theory.

• This conjecture (known today as the AdS/CFT correspondence) provides a duality between two very different looking theories:

(a) a 4d highly supersymmetric gauge theory (N=4 super YM theory= the 4d QFT with maximal supersymmetry)

and

(b) a ten-dimensional string theory in a background spacetime metric $AdS_5 \times S^5$ (with a single boundary that is $M_4 \times S^5$)

There were many surprises in this duality and new intuition that developed.

♠ There is the presence of extra dimensions. One of them (the holographic direction, transverse to the boundary) we understand today as the RG scale of the QFT.

♠ We also more-or-less understand why the metric $g_{\mu\nu}$ and other string theory fields, that are non-dynamical sources in the QFT, become dynamical fields in the string theory

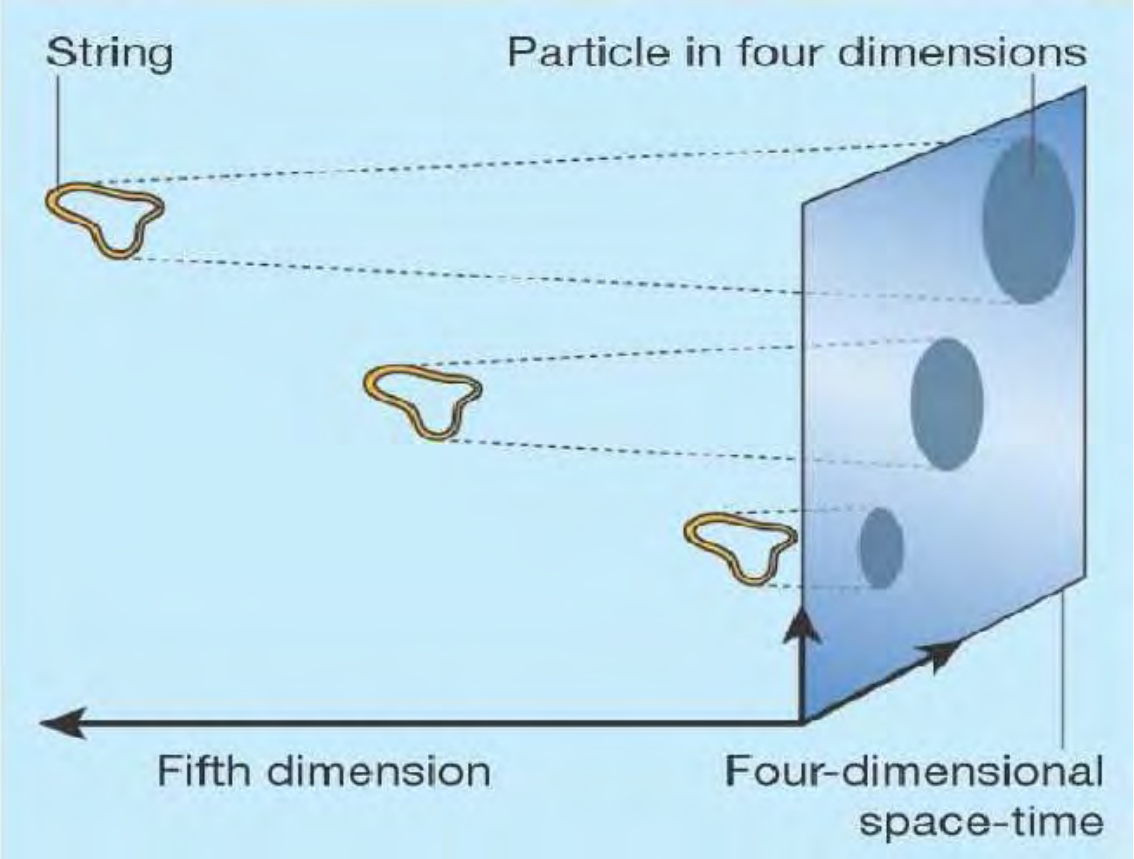

• There is one-to-one correspondence between on-shell string states $\Phi(r, x^\mu)$ and gauge-invariant (single-trace) operators $O(x^\mu)$ in the sYM theory

♠ The S^5 directions in the N=4 sYM dual are generated by the eigenvalue distributions of the extra SU(N_c)) matrix fields in the large N_c limit.

♠ For QFTs with less adjoint fields like standard QCD, they are not expected to appear in the dual string theory.

• The conjecture was tested in many controllable contexts but still remains a conjecture. Few doubt it validity.

• The duality was extended further to more QFTs but asymptotically-free theories remain out of controllable reach so far.

• We can use the duality to solve N=4 sYM at $N \to \infty$ and $\lambda \to \infty$ (supergravity approximation), but we have not solved yet the theory at $N_c \to \infty$ and arbitrary λ.

• However, the string-theory formulation gave rise to a system that is integrable, and a lot of progress has been made towards an exact solution (ex: the interquark potential has been calculated exactly as a function of λ, at $N_c \to \infty$).

• In the coming decade we will probably witness the first time a non-trivial 4d QFT will be solved exactly (albeit at $N_c \to \infty$)

• There are already ideas that suggest that even the finite-N_c N=4 sYM will be integrable.

• This is a big surprise because we were brought up to believe that $\lambda\phi^4$ and QED are the simplest QFTs in 4d, much simpler that non-abelian gauge theories.

• What we learn today is that N=4 sYM is in many respects the simplest 4d QFT.

• Interestingly, an analogous large N_c theory in 3 dimensions (N=8 ABJM theory=the CFT with maximal supersymmetry in 3d), seems much harder to tackle than $N = 4$ sYM in four dimensions.

• We have even for the first time strong evidence and a string theory formulation of a family of non-trivial Conformal Field Theories (CFTs) in 6 dimensions. Such theories were not suspected to exist because in 6d, all free field theories have only irrelevant operators.

• All of the above progress is realized by novel unexpected symmetries and unforseen relations between gluon amplitudes, Wilson loop expectation values, and supergravity scattering amplitudes.

Holography for pure YM theory

♠ Although the future looks rosy for N=4 sYM theory, however .....

• the theory we are directly interested in is SU(3) pure Yang-Mills theory coupled to Quarks.

• This is a theory with running coupling constants, weakly coupled in the UV, but strongly coupled in the IR.

• Several dualities between gauge theories and string theory helped understand the new ingredients that appear in YM, in particular the appearance of confinement and mass gap.

• The simplest such QFT is N=4 sYM theory in 5d.

• Its string theory dual is relative simple and known.

• Although this QFT is non-renormalizable, the associated string theory has a UV completion in terms of the 6d non-trivial CFT (this suggest a (highly innovative) UV completion by including monopole operators).

• This theory is compactified on a circle of radius R with antiperiodic boundary conditions for the fermions (breaking all of the supersymmetry).

• All fermions are massive in 4d, and all scalars acquire masses from quantum (loop) effects.

• At energies well-below these masses, the theory is identical to pure 4d YM theory. At very high energy the theory is 5d N=4 SYM.

• We therefore expect a discrete and gapped spectrum of glueballs, as well as extra massive states associated to the extra degrees of freedom at high energy.

• Indeed this is what is found by a classical calculation in the dual string theory.

• The Wilson loop can be also calculated to yield a nontrivial string tension for the YM theory.

• When however parameters are changed so as to separate the "UV junk" from the IR YM physics, the supergravity description becomes unreliable and the full string theory solutions are needed.

• This full string theory (so far) cannot be solved.

♠ Several more complicated and non-trivial QFTs with IR YM physics have been identified and their string theory duals found.

♠ When one tries to decouple the IR YM physics, they all have similar problems: one needs the full string theory solution.

♠ In all of the above, confinement related quantities (string tension, glueball masses, finite temperature effects etc) can be calculated controllably and analytically.

♠ But they cannot so far be used to provide precision calculations of non-perturbative YM observables.

♠ The progress with solving the string theory in AdS (dual to N=4 sYM) makes us hope that one day these string theories will be solved too.

"Holographic Phenomenology"

♠ A phenomenological approach has been tried in order to describe 4d YM physics using holography.

♠ The idea is to use all basic principles of holography, and some phenomenological input in order to construct a gravity dual for YM.

♠ There are good reasons to believe that well-chosen gravity duals will describe very well the IR Physics of QCD (if one uses appropriate UV boundary conditions).

♠ There are many such models on the market, from simple to sophisticated. I will describe here the state of the art.

A gravity dual for YM:(Very) basic expectations

• Pure SU(N_c) d=4 YM at large N_c is expected to be dual to a string theory in 5 dimensions only. Essentially a single adjoint field $\rightarrow$ a single extra dimension.

♠ In the UV, the theory becomes asymptotically free and conformal. We should expect a stringy-size AdS.

♠ In holographic CFTs only the metric $g_{\mu\nu}$ (dual to the stress tensor $T_{\mu\nu}$ of the CFT) is needed to describe the vacuum solution (large-N_c saddle point).

$$S_{gravity} = M^3 \int d^5x \, \sqrt{g} \left[R + \frac{d(d-1)}{\ell^2} \right] \quad , \quad (M\ell)^3 \sim N_c^2$$

The maximally symmetric solution is the AdS_5 metric

$$ds^2 = \frac{\ell^2}{r^2} \left(dr^2 + dx_\mu dx^\mu \right)$$

with O(4,1) symmetry (the conformal symmetry of a CFT in 4d).

• The radial direction r can be interpreted as a RG scale in the dual CFT $\rightarrow \mu = \frac{1}{r}$. Near the boundary of AdS (r=0) we are in the UV of the dual CFT.

• In YM however there is another important operator for the vacuum structure: the YM Lagrangian density, $Tr[F^2]$ dual to scalar field ϕ (known as the dilaton).

• It must have a non-trivial profile in the vacuum solution.

• The reason is that it corresponds to the YM coupling , and the variation in the radial direction should correspond to the running of the YM coupling.

• In YM (unlike a CFT) there is an ∞ number of operators that have non-trivial vevs in the vacuum. This means that we must include them in the gravity Lagrangian and also find their profiles.

• Simplification: we will ignore them. This is an non-controllable approximation. The justification is as usual complicated to explain.

• One can start adding them one by one back to improve the approximation. In other string theory contexts, this is known as "level truncation" and seems to give a convergent expansion.

Holographic YM: a model

• We should therefore write down the most general two-derivative gravitational action in 5d that contains the metric $g_{\mu\nu}$ and a single scalar ϕ.

• After redefinitions it can be written as

$$S = M^3 N_c^2 \int d^5x\sqrt{g}\left[R - \frac{4}{3}(\partial\phi)^2 + V(\phi)\right] \sim \int d^5x\sqrt{g}\left[R - \frac{4}{3}\frac{(\partial\lambda)^2}{\lambda^2} + V(\lambda)\right]$$

with the YM t' Hooft coupling identified as

$$\lambda = N_c\ e^{\phi}$$

• The dilaton potential is responsible for the running of the YM coupling and must be determined.

• To look for a vacuum solution we must write the (Lorentz invariant) metric and scalar as

$$ds^2 = e^{2A(r)}(dr^2 + dx_\mu dx^\mu) \quad , \quad \phi \to \phi(r)$$

• Roughly, e^A is the RG scale and e^ϕ the YM coupling.

The holographic RG flow

The Einstein equations for the functions $A(r)$ and $\phi(r)$ are

$$12\dot{A}^2 = \frac{1}{2}\dot{\phi}^2 + V(\phi) \quad , \quad 6\ddot{A} + 12\dot{A}^2 = -\frac{1}{2}\dot{\phi}^2 + V(\phi)$$

The Klein-Gordon equation is redundant

$$\ddot{\phi} + 4\dot{A}\dot{\phi} + V'(\phi) = 0,$$

• We can introduce a function of the scalar $W(\phi)$ (known as the superpotential) so that we can always write the equations as

$$\dot{A} = -\frac{W(\phi)}{6} \quad , \quad \dot{\phi} = W'(\phi) \quad \text{provided} \quad \frac{1}{3}W^2 - \frac{1}{2}W'^2 = V(\phi),$$

• The integration constants (3), include Λ_{QCD}, a gauge artifact, and one that is fixed by regularity (in W).

• We may now define the holographic β-function as in QFT

$$\frac{d\phi}{dA} \equiv \beta(\phi) = -6\frac{W'(\phi)}{W(\phi)}$$

• There is therefore a 1-1 correspondence between $V(\phi)$ and $\beta(\phi)$.

The UV regime

• In the UV regime, where $\lambda \to 0$, we can use the perturbative YM β-function to fix the $\lambda \to 0$ asymptotics of the potential.

• We obtain an expansion for the potential as

$$\lim_{\lambda \to 0} V(\lambda) = \frac{12}{\ell^2}\left(1 + \sum_{n=1}^{\infty} c_n \lambda^n\right)$$

• The coefficients c_n are determined uniquely, by the coefficients of the YM β-function.

The IR regime

• In the IR, $\lambda \to \infty$ and the only guidance we have is the existence of a mass gap and discrete spectrum for the glueballs.

• Remarkably, the requirement of a mass gap, discrete spectrum and linear asymptotic trajectories for the glueballs (ie. $m_n^2 \sim n$ for large n) fix uniquely the leading behavior of $V(\lambda)$ at large λ.

$$V(\lambda) \sim \lambda^{\frac{4}{3}} \sqrt{\log(\lambda)} \sim e^{\frac{4}{3}\phi} \sqrt{\phi}$$

• The rest of $V(\phi)$ is taken to be a smooth interpolation between the IR and UV asymptotics.

• This is where the phenomenological parameters are hidden.

• We will ultimately use two phenomenological parameters to tune this holographic model.

• It will describe well both zero-temperature glueball spectra as well as finite temperature thermodynamics. Both can be (favourably) compared to numerical lattice calculations.

Finite temperature

The theory at finite temperature can be described by:
(1) The "thermal vacuum solution". This is the zero-temperature solution we described so far with time periodically identified with period β.

(2) "black-hole" solutions

$$ds^2 = b(r)^2 \left[\frac{dr^2}{f(r)} - f(r) dt^2 + dx^i dx^i \right], \qquad \lambda = \lambda(r)$$

• By comparing their free energies we can determine which is dominating at a given temperature T.

• There is a minimal temperature T_{min} for the existence of Black-hole solutions

• When $T < T_{\text{min}}$ only the "thermal vacuum solution" exists: it describes the confined phase at small temperatures.

• For $T > T_{\text{min}}$ there are two black-hole solutions with the same temperature but different horizon positions. One is a "large" BH the other is "small".

• When $T > T_{\text{min}}$ three competing solutions exist. The large BH has the lowest free energy for $T > T_c > T_{min}$. It describes the deconfined "Gluon-plasma" phase.

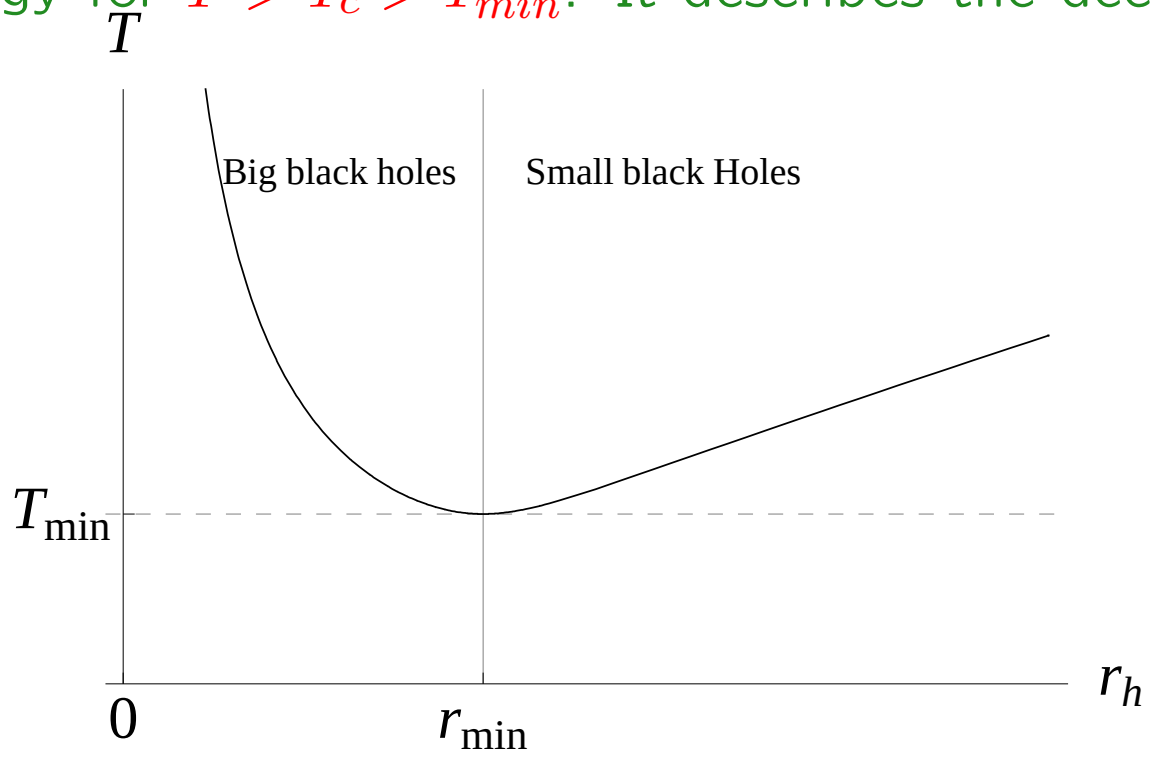

The pressure from the lattice at different N

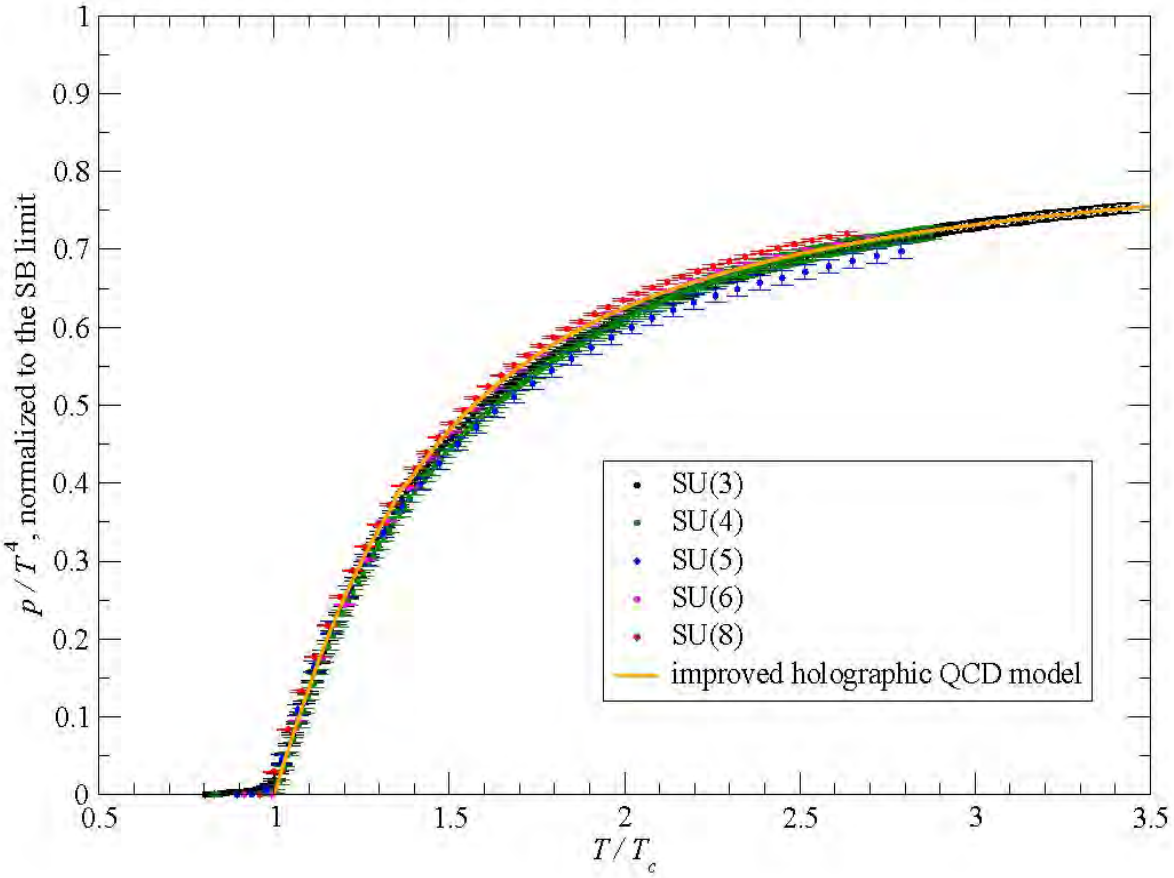

Figure 1: (Color online) The dimensionless ratio p/T^4, normalized to the lattice SB limit $\pi^2(N^2-1)R_I(N_t)/45$, *versus* T/T_c, as obtained from simulations of SU(N) lattice gauge theories on $N_t = 5$ lattices. Errorbars denote statistical uncertainties only. The results corresponding to different gauge groups are denoted by different colors, according to the legend. The yellow solid line denotes the prediction from the improved holographic QCD model from ref. [75] (with a trivial, parameter-free rescaling to our normalization).

Marco Panero arXiv: 0907.3719

The entropy from the lattice at different N

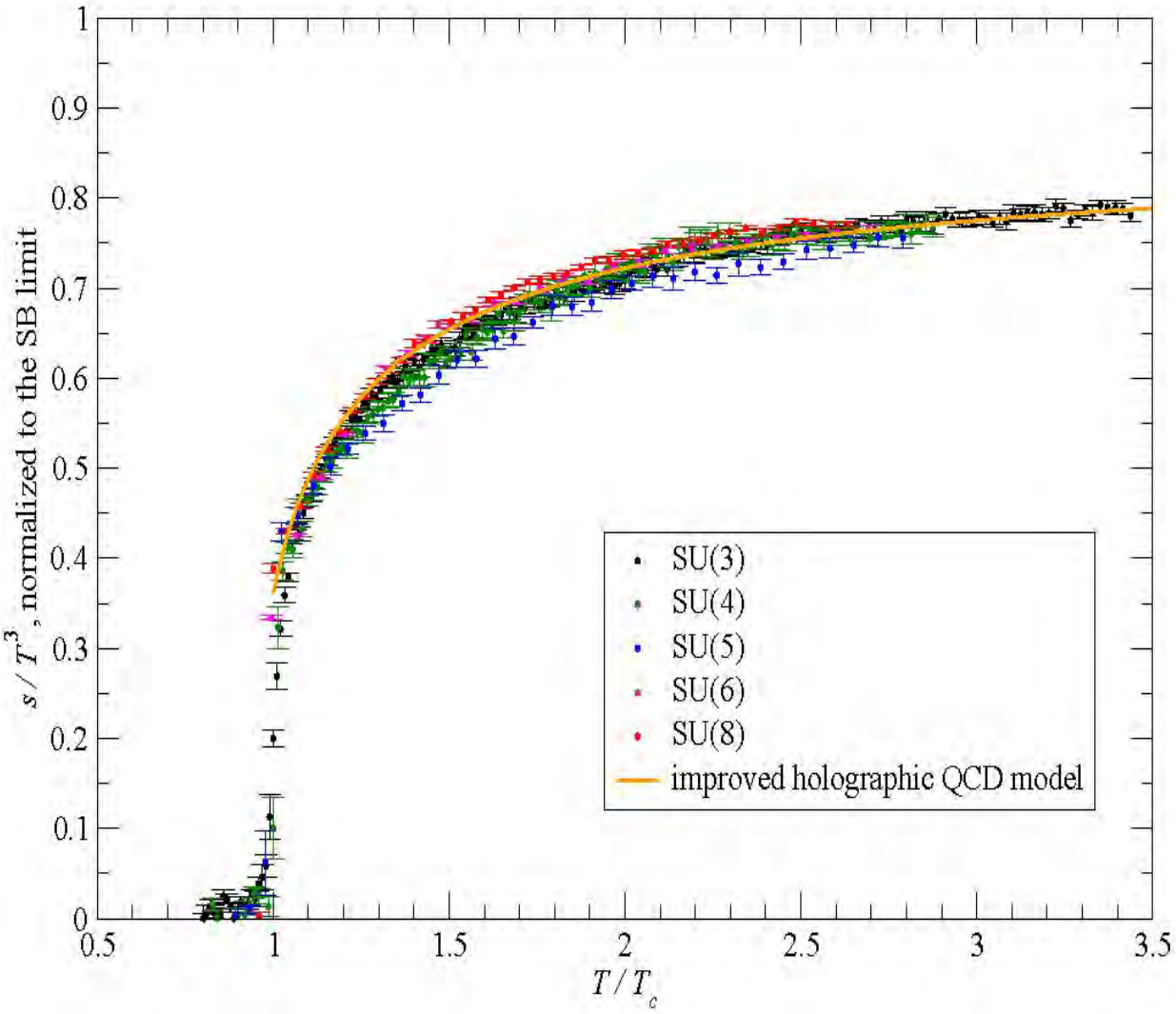

Figure 4: (Color online) Same as in fig. 1, but for the s/T^3 ratio, normalized to the SB limit.

Marco Panero arXiv: 0907.3719

The trace from the lattice at different N

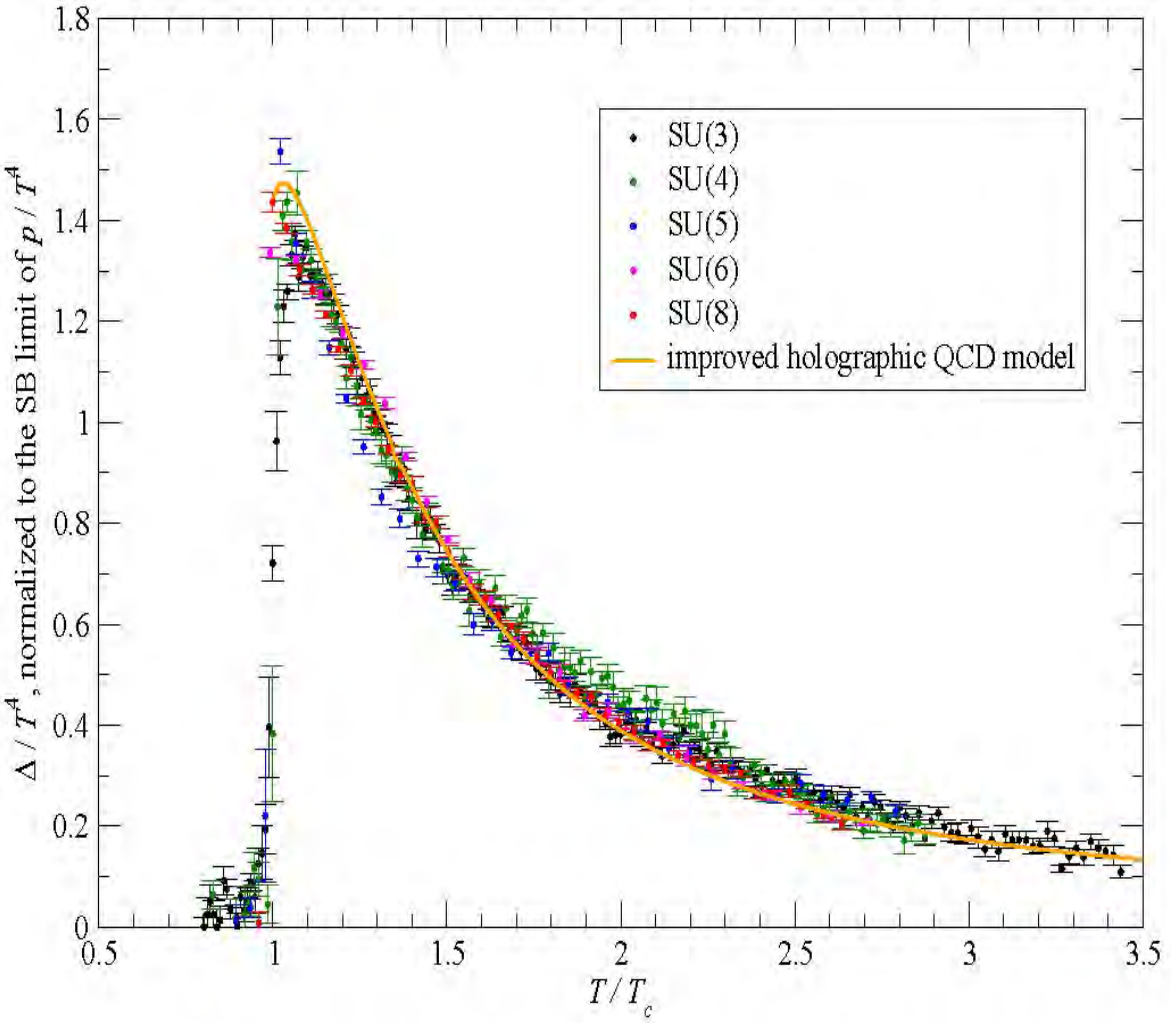

Figure 2: (Color online) Same as in fig. 1, but for the Δ/T^4 ratio, normalized to the SB limit of p/T^4.

Marco Panero arXiv: 0907.3719

The bulk $\frac{\zeta}{s}$ viscosity in IHQCD

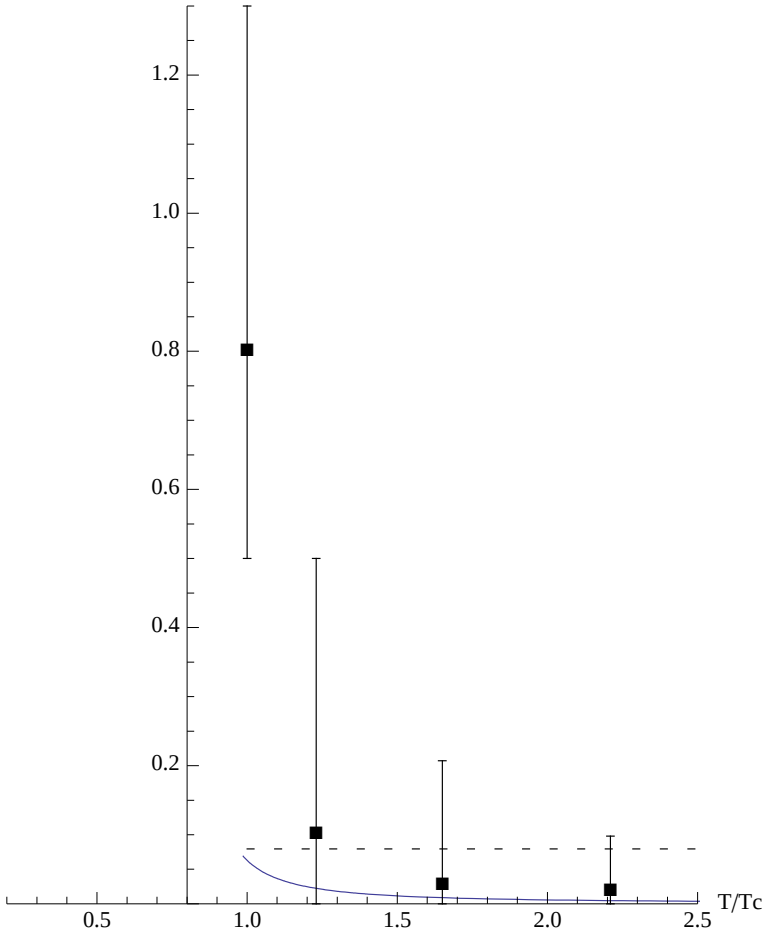

- Pure glue only.
- Calculations with other potentials show robustness.
- A good case of synergy between lattice gauge theory and holography.

Adding the quarks

- We would like to add N_f quarks q_L^I and antiquarks $q_R^{\bar{I}}$.

- We must add in the string theory (in 5d) space-filling N_f D_4 and N_f $\bar{D}_4$ branes.

- In the same spirit of keeping the most important (=relevant) operators, we will keep:

(a) The left and right-handed currents of the $\mathrm{U}(N_f)_L \times U(N_f)_R$ chiral symmetry. They are dual to $\mathrm{U}(N_f)_L \times U(N_f)_R$ gauge fields A_μ^L, A_μ^R.

(b) The quark mass operator $\bar{q}_L^i q_R^j$ dual to a complex $N_f \times N_f$ (bifundametal) complex scalar, T^{ij}, that in string theory is known as the open string tachyon.

- T^{ij} is the order parameter for the breaking of chiral symmetry.

The Veneziano limit

- The 't Hooft limit

$$N_c \to \infty, \qquad \lambda = g^2_{\rm YM} N_c \to \text{fixed}$$

always samples the quenched approximation as N_f is kept fixed as $N_c \to \infty$.

- To study phenomena in the large N_c approximation, where the quarks play an important role, we must take the limit introduced by Veneziano in (1976)

$$N_c \to \infty \quad , \quad N_f \to \infty \quad , \quad \frac{N_f}{N_c} = x_f \to \text{fixed} \quad , \quad \lambda = g^2_{\rm YM} N_c \to \text{fixed}$$

The Phase diagram

- From very general arguments we expect the following phase diagram

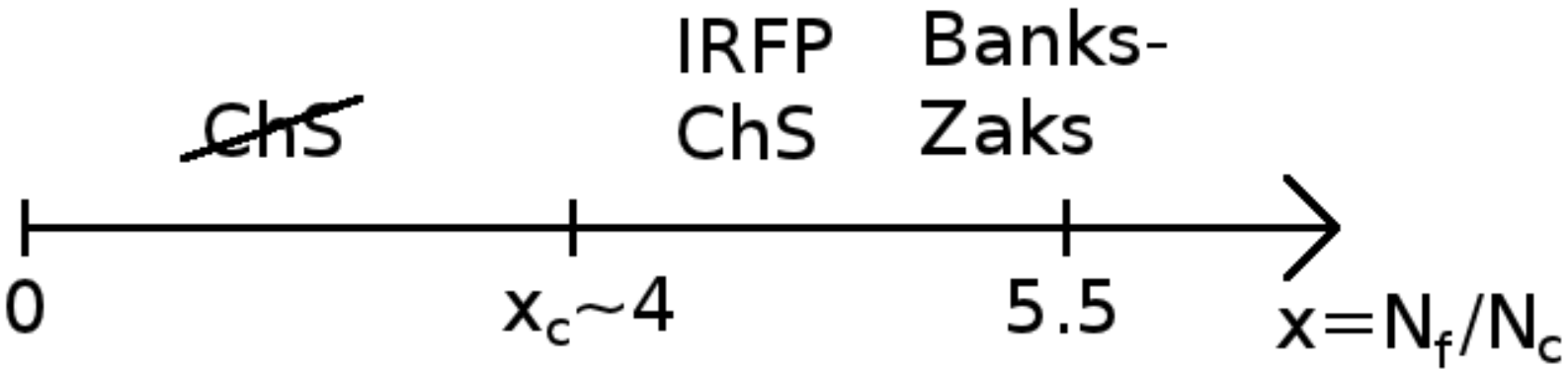

- The two end-points are $x = 0$ (pure YM) and $x = \frac{11}{2}$ (Banks-Zaks boundary)

- The big unknown is the phase transition (known as the conformal phase transition) where IR conformality is lost.

Results

• The position of the conformal transition x_c is determined by the violation of the BF bound in the holographic theory.

• It is in the Berezinsky-Kostelitz-Thouless class.

• Just below the transition, chiral symmetry is broken, but the chiral condensate is exponentially suppressed (Miransky scaling).

$$\sigma \sim \Lambda_{UV}^3 \ \exp\left(-\frac{2\hat{K}}{\sqrt{x_c - x}}\right) \ .$$

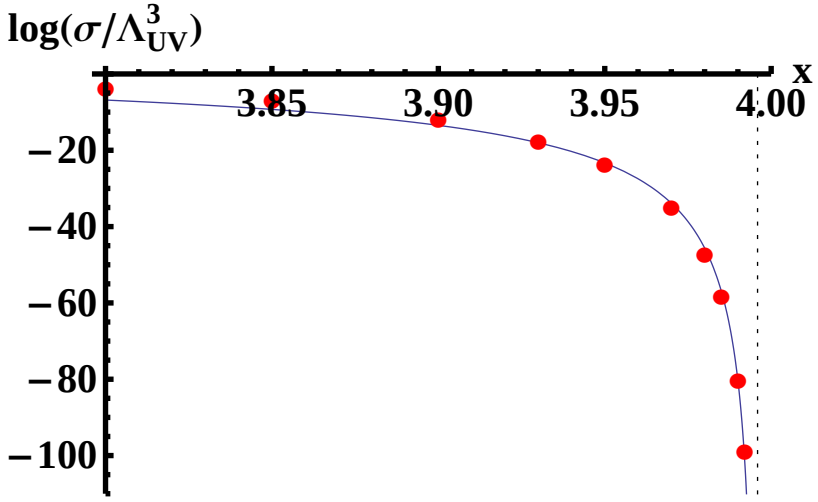

Efimov spiral

Ongoing work: $\sigma(m)$ dependence

- For $x < x_c$ spiral structure

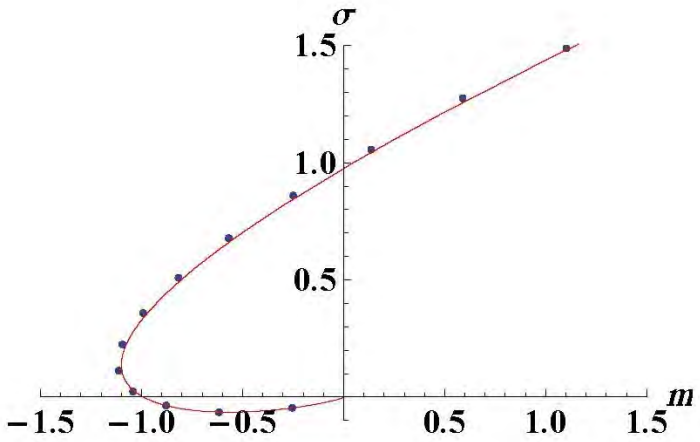

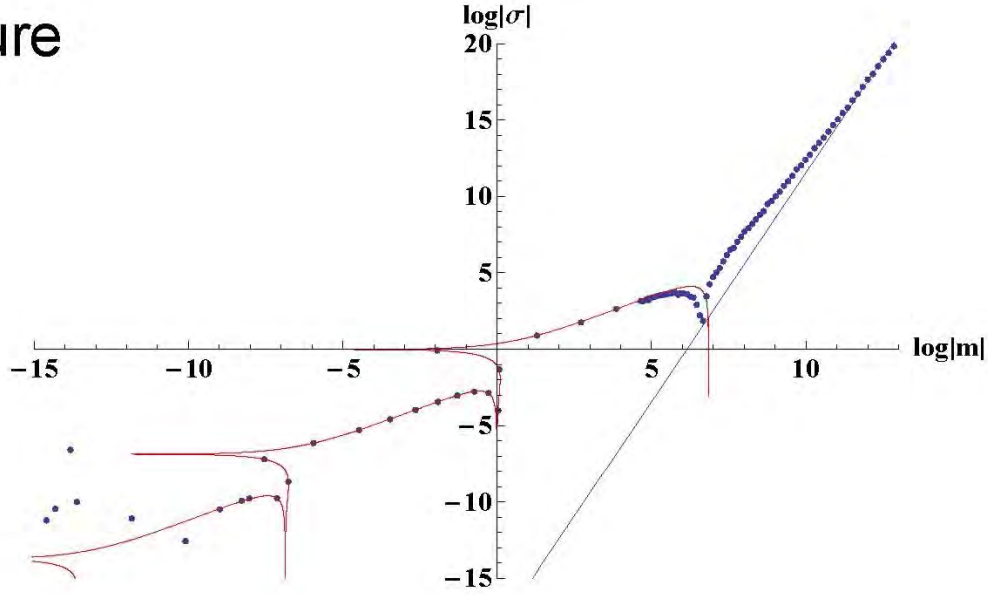

The phase structure at finite density

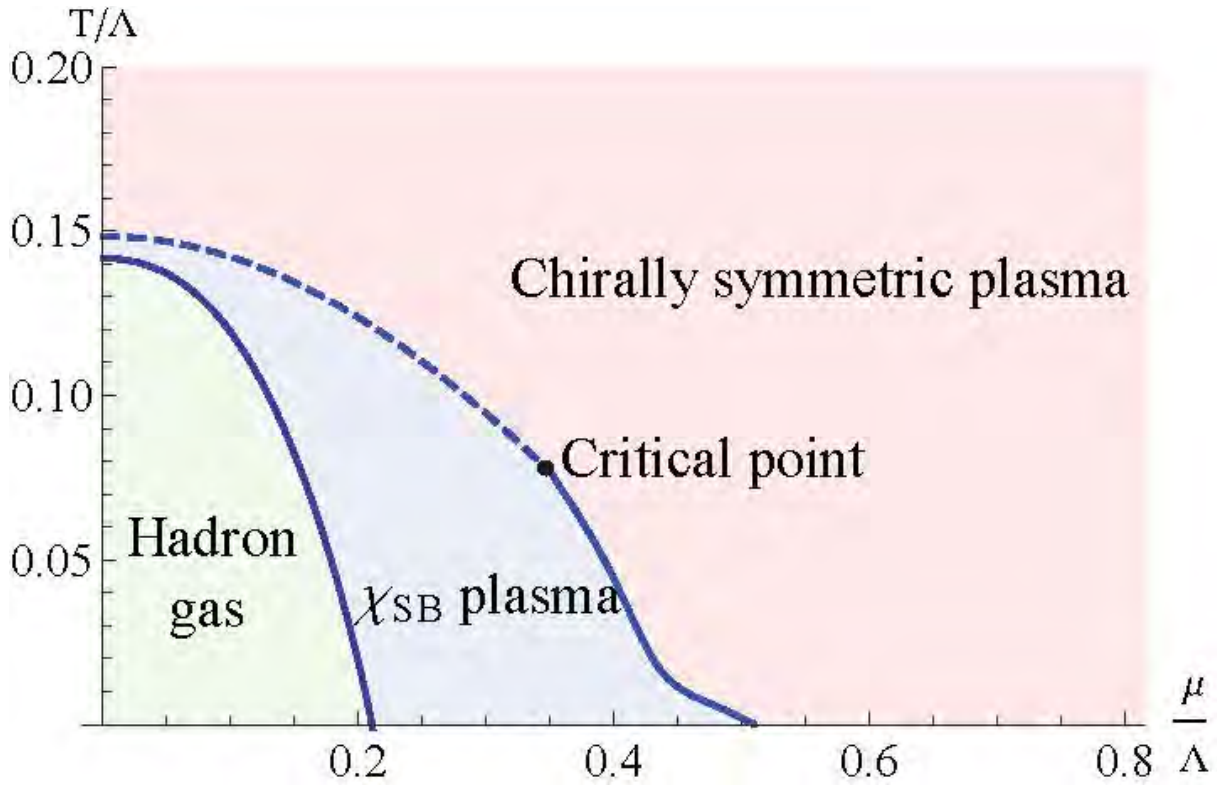

- The most remarkable new feature is a new quantum critical regime at $T = 0$ and finite μ.
- This is a phase with a $AdS_2 \times R^3$ geometry as in the RN black hole. Spacial points cannot communicate, it is like the speed of light is equal to 0.
- Such critical points are highly unstable, and are expected to give rise to superconducting states.

Outlook and open problems

- Many open ends remain and the essential problems need further attention

- There are many new conceptual issues to be addressed

- Several possible applications to QCD and systems at finite density (condensed matter)

- We have only scratched the tip of the iceberg.

THANK YOU!

Collaborators

- Timo Alho (Jyvaskyla University)
- Daniel Arean (SISSA)
- Umut Gursoy (Utrecht)
- Ioannis Iatrakis (StonyBrook)
- Matti Jarvinen (U. of Crete)
- Keijo Kajantie (University of Helsinki)
- Wen-Liang Li (APC, Paris)
- Liuba Mazzanti (Utrecht)
- George Michalogiorgakis (Duke)
- Fransesco Nitti (APC, Paris)
- Andy O'Bannon (Oxford)
- Angel Paredes (U. of Vigo)
- Anastasios Taliotis (VU Brussels)
- Kimo Tuominen (Jyvaskyla University)

Bibliography

- U. Gursoy, I. Iatrakis, E. Kiritsis, F. Nitti, A. O'Bannon.
The Chern-Simons Diffusion Rate in Improved Holographic QCD.
JHEP 1302 (2013) 119 e-Print: arXiv:1212.3894 [hep-th];

- D. Arean, I. Iatrakis, M. Jarvinen, E. Kiritsis.
V-QCD: Spectra, the dilaton and the S-parameter.
Phys. Lett. B720 (2013) 219-223e-Print: arXiv:1211.6125 [hep-ph]

- T. Alho, M. Jarvinen, K. Kajantie, E. Kiritsis and K. Tuominen
On finite-temperature holographic QCD in the Veneziano limit.
JHEP 1301 (2013) 093 arXiv:1210.4516 [hep-ph].

- Matti Jarvinen, Elias Kiritsis,
Holographic Models for QCD in the Veneziano Limit.
JHEP 1203 (2012) 002.arXiv:1112.1261 [hep-ph];

- Elias Kiritsis and Anastasios Taliotis,
Multiplicities from black-hole formation in heavy-ion collisions.
JHEP 1204 (2012) 065.arXiv:1111.1931 [hep-ph];

- Elias Kiritsis, Liuba Mazzanti and Francesco Nitti
Dressed spectral densities for heavy quark diffusion in holographic plasmas.
J.Phys.G G39 (2012) 054003arXiv:1111.1008 [hep-th];

- Ioannis Iatrakis and Elias Kiritsis,
Vector-axial vector correlators in weak electric field and the holographic dynamics of the chiral condensate.
JHEP 1202 (2012) 064.arXiv:1109.1282 [hep-ph]

- I. Iatrakis, E. Kiritsis and A. Paredes,
"An AdS/QCD model from tachyon condensation, II"
JHEP 1011 (2010) 123.. arXiv:1010.1364 [hep-ph]

- U. Gursoy, E. Kiritsis, L. Mazzanti and F. Nitti,
"Langevin diffusion of heavy quarks in non-conformal holographic backgrounds".
JHEP 1012 (2010) 088 . arXiv:1006.3261 [hep-th]

- I. Iatrakis, E. Kiritsis, A. Paredes.
An AdS/QCD model from Sen's tachyon action.
Phys.Rev.D81:115004,2010.[ArXiv:1003.2377][hep-ph

- REVIEW: U. Gursoy, E. Kiritsis, L. Mazzanti, G. Michalogiorgakis and F. Nitti,
"Improved Holographic QCD".
JHEP 0912:056,2009.;[ArXiv:1006.5461][hep-th],

- U. Gursoy, E. Kiritsis, G. Michalogiorgakis and F. Nitti,
" Thermal Transport and Drag Force in Improved Holographic QCD"
JHEP 0912:056,2009, [ArXiv:0906.1890][hep-ph],.

- U. Gursoy, E. Kiritsis, L. Mazzanti and F. Nitti,
"Improved Holographic Yang-Mills at Finite Temperature: Comparison with Data."
Nucl.Phys.B820:148-177,2009. [ArXiv:0903.2859][hep-th],.

- E. Kiritsis,
" Dissecting the string theory dual of QCD.,"
Fortsch.Phys.57:396-417,2009, [ArXiv:0901.1772][hep-th],.

• U. Gursoy, E. Kiritsis, L. Mazzanti and F. Nitti,
"Deconfinement and Gluon-Plasma Dynamics in Improved Holographic Holography and Thermodynamics of 5D Dilaton-gravity.,"
JHEP 0905:033,2009. [ArXiv:0812.0792][hep-th],.

• U. Gursoy, E. Kiritsis, L. Mazzanti and F. Nitti,
"Deconfinement and Gluon-Plasma Dynamics in Improved Holographic QCD,"
Phys. Rev. Lett. 101, 181601 (2008) [ArXiv:0804.0899][hep-th],.

• U. Gursoy and E. Kiritsis,
"Exploring improved holographic theories for QCD: Part I,"
JHEP **0802** (2008) 032[ArXiv:0707.1324][hep-th].

• U. Gursoy, E. Kiritsis and F. Nitti,
"Exploring improved holographic theories for QCD: Part II,"
JHEP **0802** (2008) 019[ArXiv:0707.1349][hep-th].

• Elias Kiritsis and F. Nitti
On massless 4D gravitons from asymptotically AdS(5) space-times.
Nucl.Phys.B772:67-102,2007;[arXiv:hep-th/0611344]

• R. Casero, E. Kiritsis and A. Paredes,
"Chiral symmetry breaking as open string tachyon condensation,"
Nucl. Phys. B **787** (2007) 98;[arXiv:hep-th/0702155].

.

Thank you for your Patience

This research has been co-financed by the European Union (European Social Fund, ESF) and Greek national funds through the Operational Program "Education and Lifelong Learning" of the National Strategic Reference Framework (NSRF), under the grants schemes "Funding of proposals that have received a positive evaluation in the 3rd and 4th Call of ERC Grant Schemes" and the program "Thales"

Additional (support) slides

"AdS/QCD"

♠ A basic phenomenological approach: use a slice of AdS_5, with a UV cutoff, and an IR cutoff.

Polchinski+Strassler

♠ It successfully exhibits confinement (trivially via IR cutoff), and power-like behavior in hard scattering amplitudes

♠ It may be equipped with a bifundamental scalar, T, and $U(N_f)_L \times U(N_f)_R$, gauge fields to describe mesons.

Erlich+Katz+Son+Stepanov, DaRold+Pomarol

Chiral symmetry is broken by hand, via IR boundary conditions. The low-lying meson spectrum looks "reasonable".

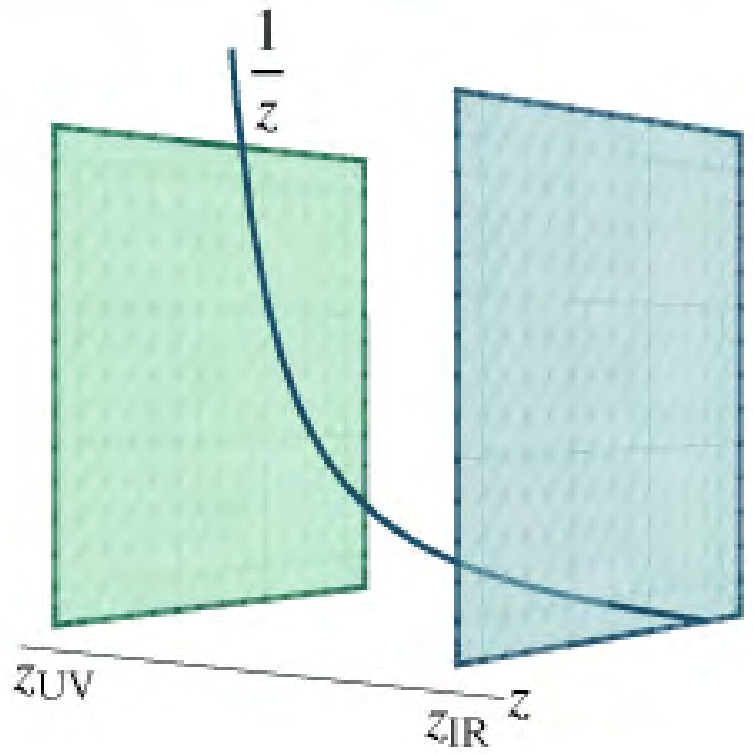

♠ Shortcomings:

- The glueball spectrum does not fit very well the lattice calculations. It has the wrong asymptotic behavior $m_n^2 \sim n^2$ at large n.

- Magnetic quarks are confined instead of screened.

- Chiral symmetry breaking is input by hand.

- The meson spectrum has also the wrong UV asymptotics $m_n^2 \sim n^2$.

- At finite temperature there is a deconfining transition but the equation of state is trivial (conformal) $(e - 3p = 0)$ and the speed of sound is $c_s^2 = \frac{1}{3}$.

The "soft wall"

♠ The asymptotic spectrum can be fixed by introducing a non-dynamical dilaton profile $\Phi \sim r^2$ (soft wall)

Karch+Katz+Son+Stephanov

• It is not a solution of equations of motion: the metric is still AdS: Neither $g_{\mu\nu}$ nor Φ solves the eq

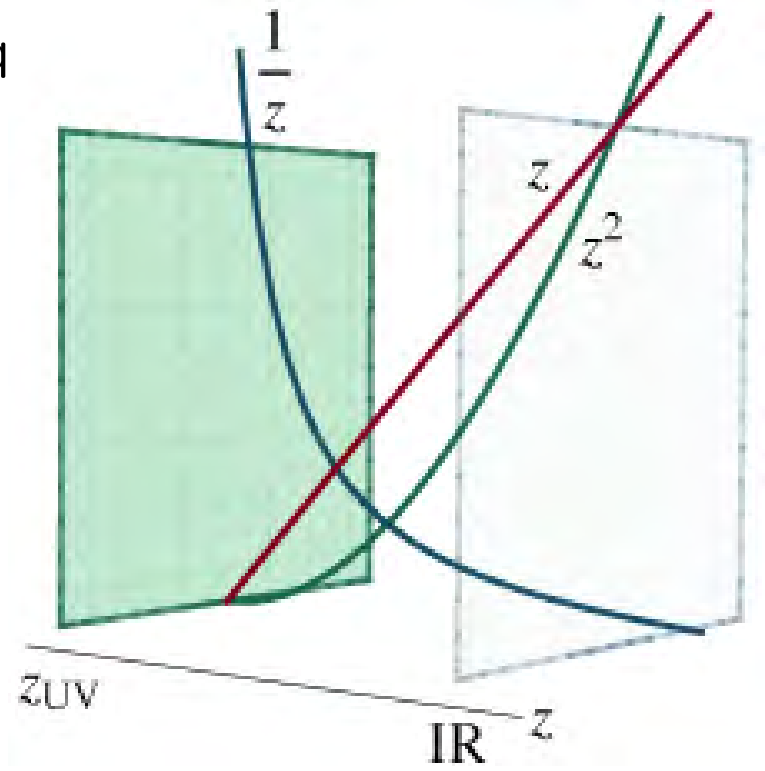

• This is really an "inconsistent" phenomenological model (except at the meson sector, in the probe limit).

The gauge-theory/gravity duality

• The gauge-theory/gravity duality is a duality that relates a string theory with a gauge theory.

• The prime example is the AdS/CFT correspondence

Maldacena 1997

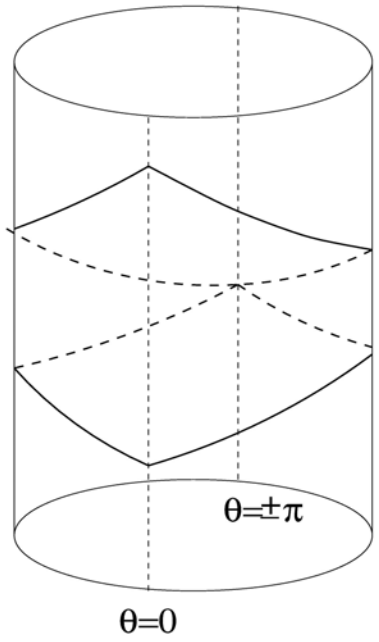

• It states that N=4 four-dimensional SU(N) gauge theory (gauge fields, 4 fermions, 6 scalars) is equivalent to ten-dimensional IIB string theory on $AdS_5 \times S^5$

$$ds^2 = \frac{\ell_{AdS}^2}{r^2}\left[dr^2 + dx^\mu dx_\mu\right] + \ell_{AdS}^2\ (d\Omega_5)^2$$

This space (AdS_5) has a single boundary, at $r = 0$.

• The string theory has as parameters, g_{string}, ℓ_{string}, ℓ_{AdS}. They are related to the gauge theory parameters as

$$g_{YM}^2 = 4\pi\ g_{\text{string}} \quad , \quad \lambda = g_{YM}^2\ N = \frac{\ell_{AdS}^4}{\ell_{\text{string}}^4}$$

• As $N \to \infty$, $g_{\text{string}} \sim \frac{\lambda}{N} \to 0$.

• As $N \to \infty$, $\lambda \gg 1$ implies that $\ell_{\text{string}} \ll \ell_{AdS}$ and the geometry is very weakly curved. String theory can be approximated by gravity in that regime and is weakly coupled.

• As $N \to \infty$, $\lambda \ll 1$ the gauge theory is weakly coupled, but the string theory is strongly curved.

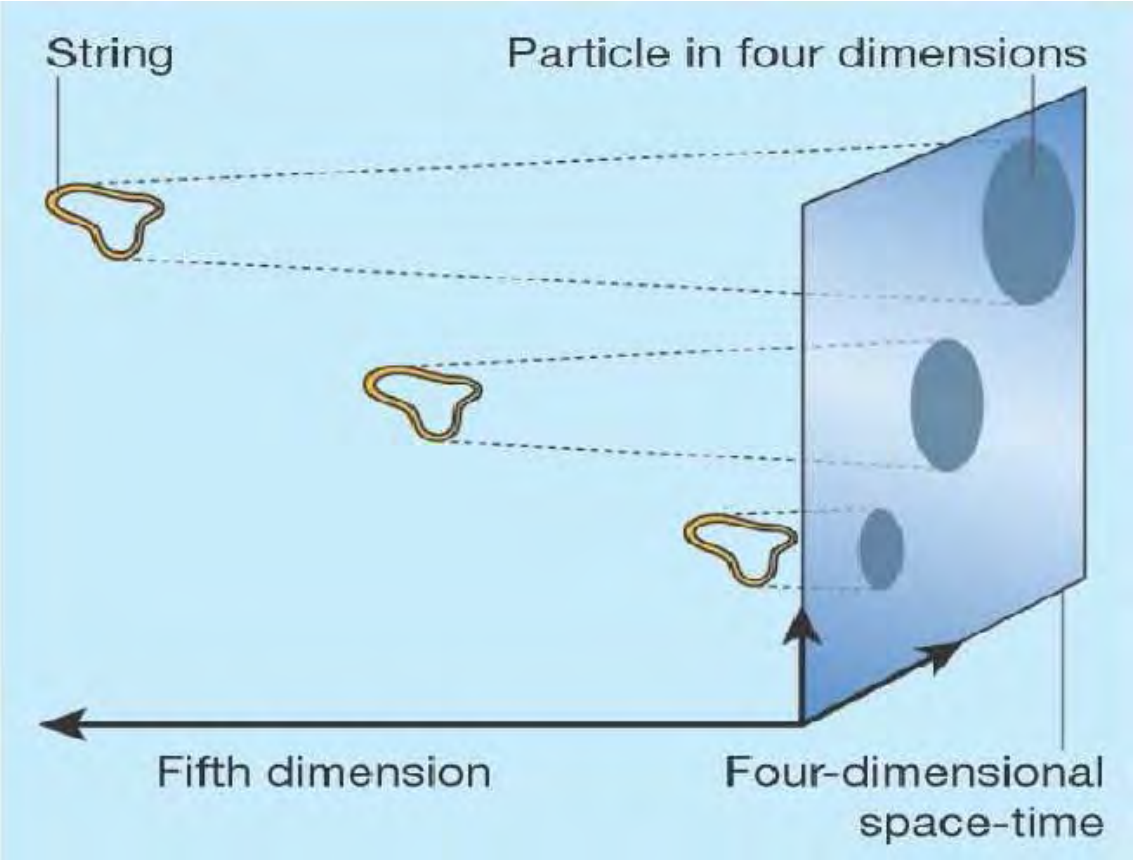

• There is one-to-one correspondence between on-shell string states $\Phi(r, x^\mu)$ and gauge-invariant (single-trace) operators $O(x^\mu)$ in the sYM theory

• In the string theory we can compute the "S-matrix" , $S(\phi(x^\mu))$ by studying the response of the system to boundary conditions $\Phi(r = 0, x^\mu) = \phi(x^\mu)$

• This is done by doing the string path integral with sources at the boundary

$$e^{-\widehat{S}(\phi(x))} = \int_{\Phi(r=0,x^\mu)=\phi(x^\mu)} D\Phi(r,x)\ e^{-S_{\text{string}}(\Phi)}$$

• At string tree level (large N), it is enough to solve the string equations of motion with the appropriate boundary conditions.

$$\frac{\delta S}{\delta \Phi} = 0 \quad , \quad \Phi(r=0,x^\mu) = \phi(x^\mu)$$

• Substituting the solution into the string action we obtain the "S"-matrix (a functional of the sources $\phi(x)$.

• The correspondence states that this is equivalent to the generating function of c-correlators of O

$$\langle e^{\int d^4x\ \phi(x)\ O(x)} \rangle \ = \ e^{-\widehat{S}(\phi(x))}$$

Therefore the source corresponds to the "coupling constant" for the operator

$$\Phi(r,x) = \phi(x) r^{4-\Delta} + \cdots + \widehat{\phi}(x) r^{\Delta} + \cdots \quad , \quad r \to 0$$

$\widehat{\phi} \simeq \langle \phi(x) \rangle$. ϕ and $\langle \phi(x) \rangle$ ARE NOT independent: regularity of the solution determines $\langle \phi(x) \rangle$ as a function of $\phi(x)$.

$B_2 - C_2$ mixing

- B_2 and C_2 are typically massless.
- In the presence of C_4 flux, this is not the case:

$$S = -M^3 \int d^5x\sqrt{g}\left[\frac{e^{-2\phi}}{2\cdot 3!}H_3^2 + \frac{1}{2\cdot 3!}F_3^2 + \frac{1}{2\cdot 5!}F_5^2\right] \ , \ F_3 = dC_2 \ , \ H_3 = dB_2 \ , \ F_5 = dC_4 - C_2 \wedge H_3$$

The equations of motion that stem from this action are*

$$\nabla^\mu(e^{-2\phi}H_{3,\mu\nu\rho}) + \frac{1}{4}F_{5,\nu\rho\alpha\beta\gamma}F_3{}^{\alpha\beta\gamma} = 0 \quad , \quad \nabla^\mu F_{3,\mu\nu\rho} + \frac{1}{4}F_{5,\nu\rho\alpha\beta\gamma}H_3{}^{\alpha\beta\gamma} = 0$$

$$\nabla^\mu F_{5,\mu\nu\rho\sigma\tau} = 0 \quad \rightarrow \quad F_{5,\mu\nu\rho\sigma\tau} = \frac{\epsilon_{\mu\nu\rho\sigma\tau}}{\sqrt{g}}\frac{2N_c}{3\ell_s}$$

Substituting

$$\nabla^\mu(e^{-2\phi}H_{3,\mu\nu\rho}) + \frac{N_c}{6\ell_s}\frac{\epsilon_{\nu\rho\alpha\beta\gamma}}{\sqrt{g}}F_3{}^{\alpha\beta\gamma} = 0 \quad , \quad \nabla^\mu F_{3,\mu\nu\rho} + \frac{N_c}{6\ell_s}\frac{\epsilon_{\nu\rho\alpha\beta\gamma}}{\sqrt{g}}H_3{}^{\alpha\beta\gamma} = 0$$

We finally decouple the equations:

$$\nabla^\mu\left[\nabla^\nu(e^{-2\phi}H_{3,\mu\rho\sigma} + \text{cyclic}\right] + \frac{N_c^2}{12\cdot 5!\ell_s^2}H_{3,\nu\rho\sigma} = 0$$

and a similar one for F_3. This equation has uniform N_c scaling for $e^\phi \sim \frac{\lambda}{N_c}$

- Both B_2 and C_2 combine to a massive two-tensor, that is dual to the $C-odd$ non-conserved operator $Tr[F_{[\mu a}F^{ab}F_{b\nu]} + \frac{1}{4}F_{ab}F^{ab}F_{\mu\nu}]$ with UV dimension 6.

RETURN

$D_0 - F_1$ charges

We may dualize $C_2 \to C_1$

$$(F_3)_{\mu\nu\rho} = \frac{\epsilon_{\mu\nu\rho\sigma\tau}}{2\sqrt{g}} \left(F^{\sigma\tau} + \frac{N_c}{\ell_s} B^{\sigma\tau} \right) \quad , \quad F = dC_1$$

The equations become

$$\nabla^\mu \left(e^{-2\phi} H_{\mu\nu\rho} \right) + \left(\frac{N_c}{2\ell_s} \right)^2 B_{\nu\rho} + \frac{N_c}{4\ell_s} F_{\nu\rho} = 0 \quad , \quad \nabla^\sigma \left(F_{\sigma\tau} + \frac{N_c}{\ell_s} B_{\sigma\tau} \right) = 0$$

and stem from a Stuckelberg-type action

$$S = -M^3 \int d^5x \sqrt{g} \left[\frac{e^{-2\phi}}{2 \cdot 3!} H_3^2 + \frac{1}{4} \left(F_{\mu\nu} + \frac{N_c}{\ell_s} B_{\mu\nu} \right)^2 + \frac{2N_c^2}{9\ell_s^2} \right]$$

Under B_2 gauge transformations C_1 transforms

$$\delta B_2 = d\Lambda_1 \quad , \quad \delta C_1 = -\frac{N_c}{\ell_s} \Lambda_1$$

- This implies that N_c units of fundamental string charge can cancel one unit of C_1 charge.

RETURN

$D_1 - NS_0$ charges

We now dualize $B_2 \to \tilde{B}_1$

$$e^{-2\phi}(H_3)_{\mu\nu\rho} = \frac{\epsilon_{\mu\nu\rho\sigma\tau}}{2\sqrt{g}}\left(\tilde{F}^{\sigma\tau} + \frac{N_c}{\ell_s}C^{\sigma\tau}\right) \quad , \quad \tilde{F} = d\tilde{B}_1$$

The equations become

$$\nabla^\mu\left((F_3)_{\mu\nu\rho}\right) + e^{2\phi}\left(\frac{N_c}{2\ell_s}\right)^2 C_{\nu\rho} + e^{2\phi}\frac{N_c}{4\ell_s}\tilde{F}_{\nu\rho} = 0 \quad , \quad \nabla^\sigma\left[e^{2\phi}\left(F_{\sigma\tau} + \frac{N_c}{\ell_s}B_{\sigma\tau}\right)\right] = 0$$

and stem from a Stuckelberg-type action

$$S = -M^3\int d^5x\sqrt{g}\left[\frac{1}{2\cdot 3!}F_3^2 + \frac{e^{2\phi}}{4}\left(\tilde{F}_{\mu\nu} + \frac{N_c}{\ell_s}C_{\mu\nu}\right)^2 + \frac{2N_c^2}{9\ell_s^2}\right]$$

Under C_2 gauge transformations C_1 transforms

$$\delta C_2 = d\Lambda_1 \quad , \quad \delta\tilde{B}_1 = -\frac{N_c}{\ell_s}\Lambda_1$$

- This implies that N_c units of fundamental D-string charge can cancel one unit of $\tilde{B}_1$ charge.

RETURN

bosonic string or superstring?

• The string theory must have no on-shell fermionic states at all because there are no gauge invariant fermionic operators in pure YM. (even in the presence of quarks and modulo baryons that are expected to be solitonic).

♠ We do expect a superstring however since there should be RR fields.

♠ A RR field we expect to have is the RR 4-form, as it is necessary to "seed" the D_3 branes responsible for the gauge group.

• It is non-propagating in 5D

• We will see later however that it is responsible for the non-trivial IR structure of the gauge theory vacuum.

• The most solid indication: There is a direct argument that the axion, dual to the instanton density $F \wedge F$ must be a RR field (as in $\mathcal{N} = 4$).

• Therefore the string theory must be a 5d-superstring theory resembling the II-0 class.

Bosonic string or superstring? II

- Consider the axion a dual to $Tr[F \wedge F]$. We can show that it must come from a RR sector.

In large-N$_c$ YM, the proper scaling of couplings is obtained from

$$\mathcal{L}_{YM} = N_c \; Tr\left[\frac{1}{\lambda} F^2 + \frac{\theta}{N_c} F \wedge F\right] \quad , \quad \zeta \equiv \frac{\theta}{N_c} \sim \mathcal{O}(1)$$

It can be shown

$$E_{YM}(\theta) = N_c^2 \; E_{YM}(\zeta) = N_c^2 \; E_{YM}(-\zeta) \simeq C_0 \; N_c^2 + C_1 \theta^2 + C_2 \frac{\theta^4}{N_c^2} + \cdots$$ *Witten*

In the string theory action

$$S \sim \int e^{-2\phi} \left[R + \cdots\right] + (\partial a)^2 + e^{2\phi} (\partial a)^4 + \cdots \quad , \quad e^{\phi} \sim g_{YM}^2 \quad , \quad \lambda \sim N_c e^{\phi}$$

$$\sim \int \frac{N_c^2}{\lambda^2} \left[R + \cdots\right] + (\partial a)^2 + \frac{\lambda^2}{N_c^2} (\partial a)^4 + \cdots \quad , \quad a = \theta[1 + \cdots]$$

RETURN

The minimal effective string theory spectrum

- NS-NS $\rightarrow$ $g_{\mu\nu} \leftrightarrow T_{\mu\nu}$, $B_{\mu\nu} \leftrightarrow Tr[F]^3$, $\phi \leftrightarrow Tr[F^2]$

- RR $\rightarrow$ $\text{Spinor}_5 \times \text{Spinor}_5 = F_0 + F_1 + F_2 + (F_3 + F_4 + F_5)$

♠ $F_0 \leftrightarrow F_5 \rightarrow$ C_4, background flux $\rightarrow$ no propagating degrees of freedom.

♠ $F_1 \leftrightarrow F_4 \rightarrow$ $C_3 \leftrightarrow C_0$: C_0 is the axion, C_3 its 5d dual that couples to domain walls separating oblique confinement vacua.

♠ $F_2 \leftrightarrow F_3 \rightarrow$ $C_1 \leftrightarrow C_2$: C_2 mixes with B_2 because of the C_4 flux, and is massive. C_1 is associated with baryon number (as we will also see later when we add flavor).

- In an ISO(3,1) invariant vacuum solution, only $g_{\mu\nu}, \phi, C_0 = a$ can be non-trivial.

$$ds^2 = e^{2A(r)}(dr^2 + dx_4^2) \quad , \quad a(r), \phi(r)$$

The relevant "defects"

• $B_{\mu\nu} \to$ Fundamental string (F_1). This is the YM (glue) string: fundamental tension $\ell_s^2 \sim \mathcal{O}(1)$

• Its dual $\tilde{B}_\mu \to NS_0$: Tension is $\mathcal{O}(N_c^2)$. It is an effective magnetic baryon vertex binding N_c magnetic quarks.

• $C_5 \to D_4$: Space filling flavor branes. They must be introduced in pairs: $D_4 + \bar{D}_4$ for charge neutrality/tadpole cancelation $\to$ gauge anomaly cancelation in QCD.

• $C_4 \to D_3$ branes generating the gauge symmetry.

.

• $C_3 \to D_2$ branes : domain walls separating different oblique confinement vacua (where $\theta_{k+1} = \theta_k + 2\pi$). Its tension is $\mathcal{O}(N_c)$

• $C_2 \to D_1$ branes: These are the magnetic strings:
(strings attached to magnetic quarks) with tension $\mathcal{O}(N_c)$

• $C_1 \to D_0$ branes. These are the baryon vertices: they bind N_c quarks, and their tension is $\mathcal{O}(N_c)$.
Its instantonic source when we add flavor is the (solitonic) baryon in the string theory.

• $C_0 \to D_{-1}$ branes: These are the Yang-Mills instantons.

The string effective action

- as $N_c \to \infty$, only string tree-level is dominant.

- Relevant field for the vacuum solution: $g_{\mu\nu}, a, \phi, F_5$.

- The vev of $F_5 \sim N_c\ \epsilon_5$. It appears always in the combination $e^{2\phi}F_5^2 \sim \lambda^2$, with $\lambda \sim N_c\ e^{\phi}$ All higher derivative corrections $(e^{2\phi}F_5^2)^n$ are $\mathcal{O}(1)$.
A non-trivial potential for the dilaton will be generated already at string tree-level.

- This is not the case for all other RR fields: in particular for the axion as $a \sim \mathcal{O}(1)$

$$(\partial a)^2 \sim \mathcal{O}(1) \quad , \quad e^{2\phi}(\partial a)^4 = \frac{\lambda^2}{N_c^2}(\partial a)^4 \sim \mathcal{O}\left(N_c^{-2}\right)$$

Therefore to leading order $\mathcal{O}(N_c^2)$ we can neglect the axion.

The UV regime

- In the far UV, the space should asymptote to AdS_5.

- The 't Hooft coupling should behave as $(r \to 0)$

$$\lambda \sim \frac{1}{\log(r\Lambda)} + \cdots \quad \to \quad 0 \quad , \quad r \sim \frac{1}{E}$$

- The effective action to leading order in N_c is

$$S_{eff} \sim \int d^5x\sqrt{g}\; e^{-2\phi}\; \Big(F(R\;,\;\xi\;) + \; 4(\partial\phi)^2 \Big) \quad , \quad \xi \equiv -e^{2\phi}\frac{F_5^2}{5!}$$

- For weak background fields

$$F = \frac{2}{3}\frac{\delta c}{\ell_s^2} + R + \frac{1}{2}\xi + \mathcal{O}(R^2, R\xi, \xi^2) \quad , \quad \delta c = 10 - 5 = 5$$

The equation for the four form is

$$\nabla^\mu \Big(F_\xi \; F_{\mu\nu\rho\sigma\tau} \Big) = 0 \quad , \quad F_\xi \; F_{\mu\nu\rho\sigma\tau} = \frac{N_c}{\lambda}\frac{\epsilon_{\mu\nu\rho\sigma\tau}}{\sqrt{g}} \to \xi \; F_\xi(\xi, R)^2 = \frac{\lambda^2}{\lambda^2}$$

We may use the alternative action where the 4-form is "integrated-out"

$$S_{\text{tree}} = M^3 N_c^2 \int d^5x\sqrt{g}\ \frac{1}{\lambda^2}\left[4\frac{\partial\lambda^2}{\lambda^2} + F(R,\xi) - 2\xi F_\xi(R,\xi)\right] \quad , \quad \xi\ F_\xi^2 = \frac{\lambda^2}{\lambda^2}$$

To continue further we must solve $\xi\ F_\xi^2 = \frac{\lambda^2}{\lambda^2}$. There are several possibilities:

(a) $\xi \to 0$ as $\lambda \to 0$ (turns out to be inconsistent with equations of motion).

(b) $\xi \to \xi_*(R)$ as $\lambda \to 0$.

$$F \simeq c_0(R) + \frac{c_1(R)}{2}(\xi - \xi_*(R))^2 + \mathcal{O}\left[(\xi - \xi_*(R))^3\right]$$

$$\xi \equiv \xi_*(R) + \delta\xi \simeq \xi_*(R) - \frac{\lambda}{c_1(R)\ \lambda\ \sqrt{\xi_*(R)}} + \mathcal{O}(\lambda^2)$$

The gravitational equation implies that for AdS to be the leading solution (at $\lambda = 0$) we must have

$$c_0(R_*) = 0 \quad , \quad \left.\frac{\partial c_0(R)}{\partial R}\right|_{R=R_*} = 0$$

F is therefore zero to next order and the first non-trivial contribution is at quadratic order

$$F(R,\xi) = \frac{\lambda^2}{2c_1(R_*)\ \lambda^2\ \xi_*(R_*)} + \frac{1}{2}\frac{\partial^2 c_0(R)}{\partial R^2}\Big|_{R=R_*}(R-R_*)^2 + \cdots$$

Solving the equations we find the one-loop β-function coefficients as

$$b_0 = \frac{\lambda\sqrt{\xi_*(R_*)}}{16}$$

and the correction subleading correction to the AdS_5 metric

$$e^A = \frac{\ell}{r}\left[1 + \frac{w}{\log(\Lambda r)} + \cdots\right] \quad , \quad \delta R = \frac{40w}{\ell^2\log(\Lambda r)} + \cdots$$

$$w = \frac{-5 + \frac{\frac{\delta\xi_*}{\delta R}(R*)}{\xi_*(R_*)}R_*}{c_0''(R_*)}\ \frac{\xi_*(R_*)}{80R_*}$$

- This turns out to be a regular expansion of the solution in powers of

$$\frac{P_n(\log\log(r\Lambda))}{(log(r\Lambda))^n}$$

• Effectively this can be rearranged as a "perturbative" expansion in $\lambda(r)$.

In the case of running coupling, the radial coordinate can be substituted by $\lambda(r)$.

• Using λ as a radial coordinate the solution for the metric can be written

$$E \equiv e^A = \frac{\ell}{r(\lambda)}\left[1 + c_1\lambda + c_2\lambda^2 + \cdots\right] = \ell\,(e^{-\frac{b_0}{\lambda}})\left[1 + c_1'\lambda + c_2'\lambda^2 + \cdots\right] \quad , \quad \lambda -$$

The UV geometry

- The theory becomes asymptotically free and conformal at high energy
- Following on N=4 intuition we might expect that $\ell_{AdS} \to 0 \quad \to \quad$ singularity.
- There are several possibilities for such singularities:

(a) They are "mirage": the geometry stabilizes at $\ell \sim \ell_s$. (different examples from WZW models and DBI actions).

(b) The singularity is resolved by the stringy or higher dimensional physics. The true string metric is regular (some examples from higher dimensional resolutions)

(c) The singularity remains (not our case we think)

- The N=4 relation $\ell^4 \sim \lambda \sim \frac{1}{\log r}$. seems to indicate a naked singularity.

- Another possibility is that the classical saddle point solution should asymptote to a regular but stringy ($\ell = \ell_s$) AdS_5. This option has several advantages and provides a lot of mileage:

♠ It allows in principle the machinery of holography to be applied

♠ It realizes the geometrical implementation of the asymptotic conformal symmetry of YM theory in the UV.

The low energy spectrum:details

♠ In YM only $Tr[FF]$ and maybe $Tr[F \wedge F]$ have a source. However many operators can have a vev. We expect $\langle O_\Delta \rangle \sim (\Lambda_{QCD})^\Delta$.

♠ If that is the case, this implies that many stringy states will have non-trivial profiles in the vacuum solution.

♠ Operators of higher dimension are not important in the UV (that's why we can truncate the RG flow). In the bulk, they have positive m^2, that suppresses their solutions.

These are scalar YM operators with $\Delta_{UV} > 4 \rightarrow m^2 > 0$ or higher spin fields.

- But higher dimension operators may become important in the IR.

♠ (Many) Indications from SVZ sum rules plus data suggest that the coefficients of higher dimension operators are "unnaturally" small.

• It seems a reasonable assumption to neglect all $\Delta > 4$ fields when looking for the vacuum solution.

• What are all gauge invariant YM operators of dimension 4 or less?

• They are given by $Tr[F_{\mu\nu}F_{\rho\sigma}]$.
Decomposing the lowest ones (in spin) are, the stress tensor, the scalar and the pseudoscalar

♠ Therefore we will consider

$$T_{\mu\nu} \leftrightarrow g_{\mu\nu},\ tr[F^2] \leftrightarrow \phi,\ tr[F \wedge F] \leftrightarrow a$$

• The "axion" action will be suppressed by $1/N_c^2$ since the axion is a RR field.

• It will not be discussed in these lectures but we will make up at the workshop talk :-)

general expectations

• In the UV (near the boundary) the coupling is small and stringy behavior is important. We expect an AdS space to emerge from the asymptotic conformal invariance and it will be of stringy size.

• The rest of the asymptotics are perturbative around the AdS space, and we obtain an expansion in powers of $(1/\log r)^n$.

• We do expect that $\lambda \to \infty$ (or becomes large) at the IR bottom.

• Intuition from N=4 and other 10d strongly coupled theories suggests that in this regime there should be an (approximate) two-derivative description of the physics.

• The simplest solution with this property is the linear dilaton solution with

$$\lambda \equiv e^{\phi} \sim e^{Qr} \quad , \quad V(\lambda) \sim \delta c = 10 - D \to \text{constant} \quad , \quad R = 0$$

• Self-consistency of this assumption implies that the string frame curvature should vanish in the IR.

• This property persists with potentials $V(\lambda) \sim (\log \lambda)^P$. Moreover all such cases have confinement, a mass gap and a discrete spectrum (except the P=0 case).

• At the IR bottom (in the string frame) the curvature vanishes and 5D space becomes (asymptotically) flat.

• Interestingly, these asymptotics $V(\lambda) \sim (\log \lambda)^P$ are the only ones that are not scaling in the IR.

On naked holographic singularities

- In this case all Poincaré invariant solutions end up in a naked IR singularity.

- In GR we abhor naked singularities.

- In holographic gravity some many be acceptable. The reason is that they do not always signal a breakdown of predictability. They could be resolved by stringy or KK physics and/or they could be shielded for finite energy configurations.

Something similar happens in the "Liouville wall" of 2d gravity: all finite energy physics is not affected by the $e^{\phi} \to \infty$ singularity.

- An important task in EHT is to therefore ascertain when such naked singularities are acceptable (alias "good")

♠ Gubser gave the first criterion for good singularities: They should be limits of solutions with a regular horizon. Such a singularity is expected to be resolvable.

Gubser

• The singularity is "repulsive" (like the Liouville wall). It has an overlap with the previous criterion. It involves the calculation of "Wilson loops"

Gursoy+E.K.+Nitti

• Another issue, when a singularity is "computable": is the low energy physics independent of the resolution?

• This criterion amounts to having a well-defined spectral problem for fluctuations around the solution: The second order equations describing all fluctuations are Sturm-Liouville problems (no extra boundary conditions needed at the singularity).

Gursoy+E.K.+Nitti

• It is not known whether the list is complete. The 1st and 2-3rd criteria are in general non-overlapping.

Organizing the vacuum solutions

- The β-function can be mapped uniquely to the dilaton potential $V(\lambda)$.
- We can introduce a (pseudo)superpotential

$$V(\lambda)=\left(\frac{4}{3}\right)^3\left[W^2-\left(\frac{3}{4}\right)^2\left(\frac{\partial W}{\partial\Phi}\right)^2\right]$$

and write the equations in a first order form:

$$A'=-\frac{4}{9}W \quad , \quad \Phi'=\frac{dW}{d\Phi}$$

$$\beta(\lambda)=-\frac{9}{4}\lambda\frac{d\log W}{d\log\lambda}$$

- $W(\phi)$ evaluated at the UV as a function of the boundary value of ϕ is the legendre transform of the (quantum) effective potential.

Kiritsis+Niarchos

An assessment of IR asymptotics

$$V(\lambda) \sim V_0 \lambda^{2Q} \quad , \quad \lambda \equiv e^{\phi} \to \infty$$

- The solutions can be parameterized in terms of a fake superpotential

$$V = \frac{64}{27} W^2 - \frac{4}{3} \lambda^2 \, W'^2 \quad , \quad W \geq \frac{3}{8} \sqrt{3V}$$

The crucial parameter resides in the solution to the diff. equation above. There are three types of solutions for $W(\lambda)$:

Gursoy+E.K.+Mazzanti+Nitti

1. Generic Solutions (bad IR singularity)

$$W(\lambda) \sim \lambda^{\frac{4}{3}} \quad , \quad \lambda \to \infty$$

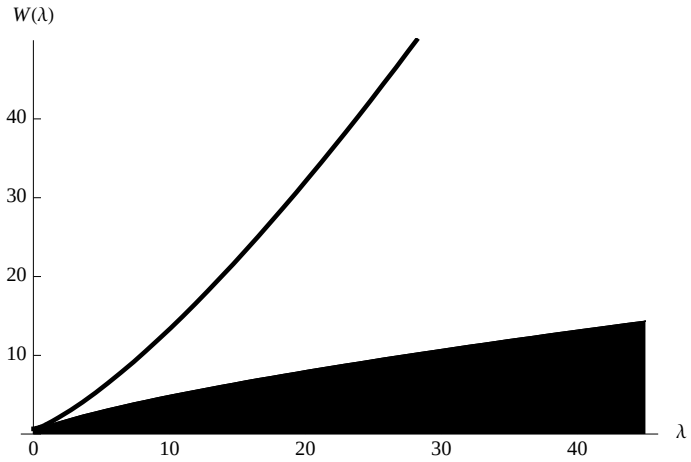

2. Bouncing Solutions (bad IR singularity)

$$W(\lambda) \sim \lambda^{-\frac{4}{3}} \quad , \quad \lambda \to \infty$$

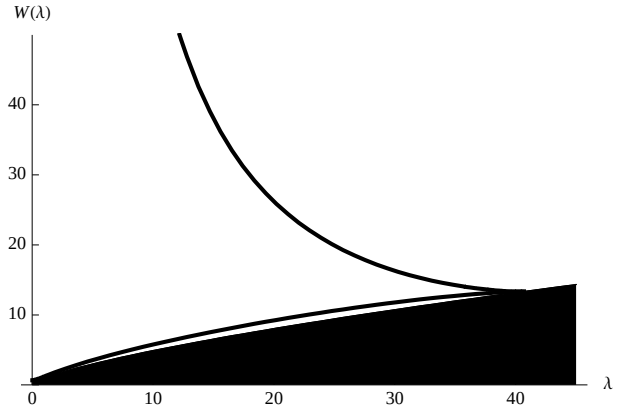

3. The "special" solution.

$$W(\lambda) \sim W_\infty \lambda^Q \quad , \quad \lambda \to \infty \quad , \quad W_\infty = \sqrt{\frac{27V_0}{4(4-9Q^2)}}$$

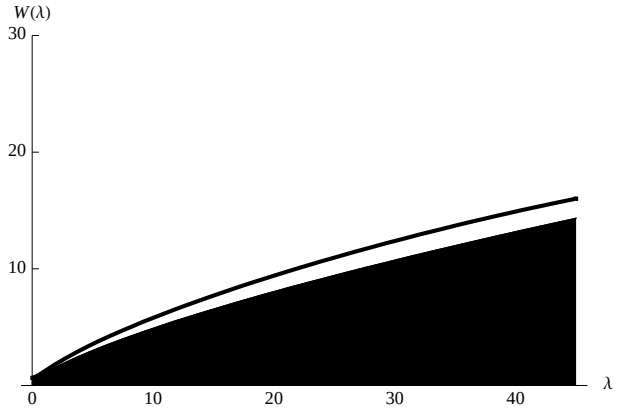

Good+computable IR singularity if $Q < \frac{4\sqrt{2}}{3}$

• For $Q > \frac{4}{3}$ all solutions are of the bouncing type (therefore bad).

• There is another special asymptotics in the potential namely $Q = \frac{2}{3}$. Below $Q = \frac{2}{3}$ the spectrum changes to continuous without mass gap.

In that region a finer parametrization of asymptotics is necessary

$$V(\lambda) \sim V_0 \ \lambda^{\frac{4}{3}} \ (\log \lambda)^P$$

• For $P > 0$ there is a mass gap, discrete spectrum and confinement of charges. There is also a first order deconfining phase transition at finite temperature.

• For $P < 0$, the spectrum is continuous, without mas gap, and there is a transition at T=0 (as in N=4 sYM).

• At $P = 0$ we have the linear dilaton vacuum. The theory has a mass gap but continuous spectrum. The order of the deconfining transition depends on the subleading terms of the potential and can be of any order larger than two.

Gursoy

Wilson-Loops and confinement

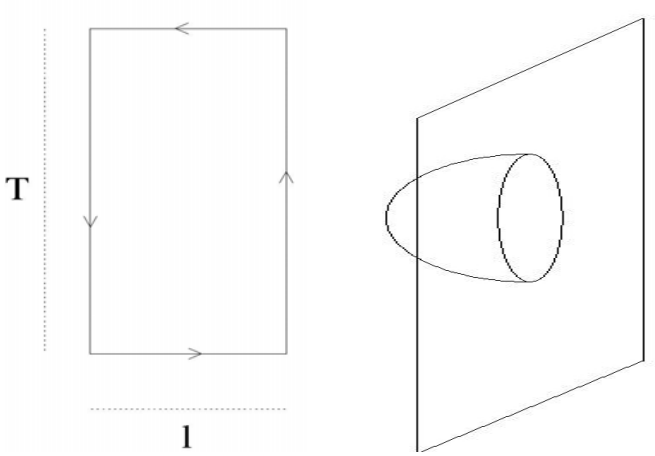

• Calculation of the static quark potential using the vev of the Wilson loop calculated via an F-string world-sheet.

Rey+Yee, Maldacena

$$T\ E(L) = S_{minimal}(X)$$

We calculate

$$L = 2\int_0^{r_0} dr \frac{1}{\sqrt{e^{4A_s(r)-4A_s(r_0)}-1}}.$$

It diverges when e^{A_s} has a minimum (at $r = r_*$). Then

$$E(L) \sim T_f\ e^{2A_S(r_*)}\ L$$

• Confinement $\rightarrow$ $A_s(r_*)$ is finite. This is a more general condition that considered before as A_s `is not monotonic in general`. $A_s = A_E + \frac{2}{3}\Phi$

• Effective string tension

$$T_{\text{string}} = T_f\ e^{2A_S(r_*)}$$

- In simple cases like AdS/QCD, Φ is constant, but r is bounded below.

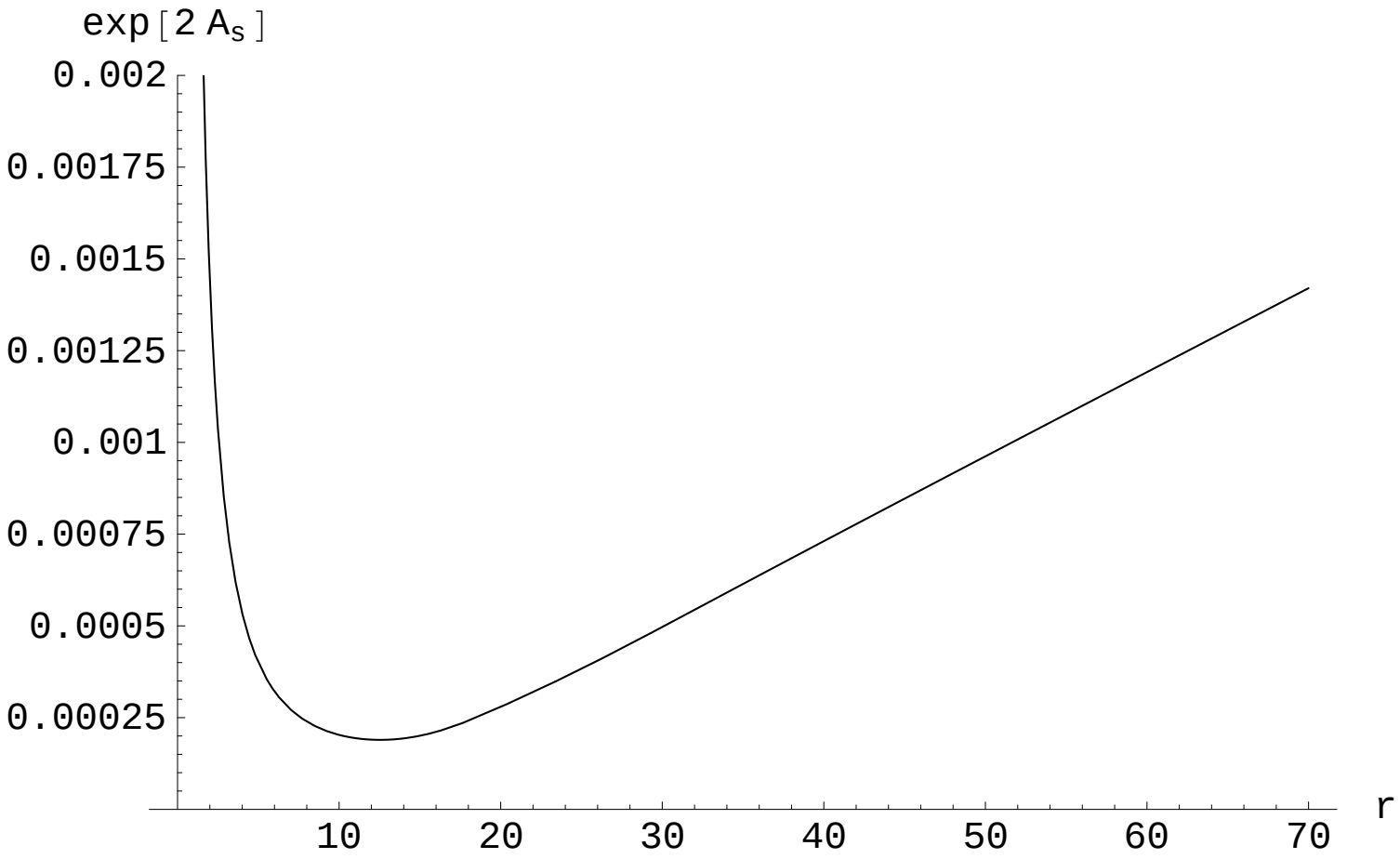

The string frame scale factor in a background that confines non-trivially.

Comments on confining backgrounds

• For all confining backgrounds with $r_0 = \infty$, although the space-time is singular in the Einstein frame, the string frame geometry is asymptotically flat for large r. Therefore only λ grows indefinitely.

• String world-sheets do not probe the strong coupling region, at least classically. The string stays away from the strong coupling region.

• Therefore: singular confining backgrounds have generically the property that the singularity is *repulsive*, i.e. only highly excited states can probe it. This will also be reflected in the analysis of the particle spectrum (to be presented later)

• The confining backgrounds must also screen magnetic color charges. This can be checked by calculating 't Hooft loops using D_1 probes:

♠ All confining backgrounds with $r_0 = \infty$ and most at finite r_0 screen properly

♠ On the other hand "hard-wall" AdS/QCD confines also the magnetic quarks.

General criterion for confinement

• `the geometric version`:
A geometry that shrinks to zero size in the IR is dual to a confining 4D theory if and only if the Einstein metric in conformal coordinates vanishes as (or faster than) e^{-Cr} as $r \to \infty$, for some $C > 0$.

• It is understood here that a metric vanishing at finite $r = r_0$ also satisfies the above condition.

♠ `the superpotential`
A 5D background is dual to a confining theory if the superpotential grows as (or faster than)

$$W \sim (\log \lambda)^{P/2} \lambda^{2/3} \quad \text{as} \quad \lambda \to \infty \quad , \quad P \geq 0$$

♠ `the` β`-function` A 5D background is dual to a confining theory if and only if

$$\lim_{\lambda \to \infty} \left(\frac{\beta(\lambda)}{3\lambda} + \frac{1}{2} \right) \log \lambda = K, \qquad -\infty \leq K \leq 0$$

(No explicit reference to any coordinate system) Linear trajectories correspond to $K = -\frac{3}{16}$

Classification of confining superpotentials

Classification of confining superpotentials $W(\lambda)$ as $\lambda \to \infty$ in IR:

$$W(\lambda) \sim (\log \lambda)^{\frac{P}{2}} \lambda^Q \quad , \quad \lambda \sim E^{-\frac{9}{4}Q} \left(\log \frac{1}{E}\right)^{\frac{P}{2Q}}, \qquad E \to 0.$$

- $Q > 2/3$ or $Q = 2/3$ and $P > 1$ leads to confinement and a singularity at finite $r = r_0$.

$$e^A(r) \sim \begin{cases} (r_0 - r)^{\frac{4}{9Q^2-4}} & Q > \frac{2}{3} \\ \exp\left[-\frac{C}{(r_0-r)^{1/(P-1)}}\right] & Q = \frac{2}{3} \end{cases}$$

- $Q = 2/3$, and $0 \leq P < 1$ leads to confinement and a singularity at $r = \infty$ The scale factor e^A vanishes there as

$$e^A(r) \sim \exp[-Cr^{1/(1-P)}].$$

- $Q = 2/3, P = 1$ leads to confinement but the singularity may be at a finite or infinite value of r depending on subleading asymptotics of the superpotential.

♠ If $Q < 2\sqrt{2}/3$, no *ad hoc* boundary conditions are needed to determine the glueball spectrum → One-to-one correspondence with the β-function This is unlike standard AdS/QCD and other approaches.

- when $Q > 2\sqrt{2}/3$, the spectrum is not well defined without extra boundary conditions in the IR because both solutions to the mass eigenvalue equation are IR normalizable.

Confining β-functions

A 5D background is dual to a confining theory if and only if

$$\lim_{\lambda\to\infty}\left(\frac{\beta(\lambda)}{3\lambda}+\frac{1}{2}\right)\log\lambda=K,\qquad -\infty\leq K\leq 0$$

(No explicit reference to any coordinate system). Linear trajectories correspond to $K=-\frac{3}{16}$

- We can determine the geometry if we specify K:
- $K=-\infty$: the scale factor goes to zero at some finite r_0, not faster than a power-law.
- $-\infty<K<-3/8$: the scale factor goes to zero at some finite r_0 faster than any power-law.
- $-3/8<K<0$: the scale factor goes to zero as $r\to\infty$ faster than $e^{-Cr^{1+\epsilon}}$ for some $\epsilon>0$.
- $K=0$: the scale factor goes to zero as $r\to\infty$ as e^{-Cr} (or faster), but slower than $e^{-Cr^{1+\epsilon}}$ for any $\epsilon>0$.

The borderline case, $K=-3/8$, is certainly confining (by continuity), but whether or not the singularity is at finite r depends on the subleading terms.

Selecting the IR asymptotics

The potentials with asymptotics $V \sim \lambda^{\frac{4}{3}}(\log\lambda)^{P})$ have a singularity at $r = \infty$. They are compatible with

- Confinement (it happens non-trivially: a minimum in the string frame scale factor)
- Mass gap+discrete spectrum (except P=0)
- "good+repulsive" singularity
- Curvature$\to$ 0 justifying the original assumption. More precisely: the string frame metric becomes flat at the IR .

♠ It is interesting that the lower endpoint: P=0 corresponds to linear dilaton and flat space (string frame). It is confining with a mass gap but continuous spectrum.

- For linear asymptotic trajectories for fluctuations (glueballs) we must choose $P = 1/2$

$$V(\lambda) =\sim \lambda^{\frac{4}{3}}\sqrt{\log\lambda} + \text{subleading} \qquad \text{as} \qquad \lambda \to \infty$$

- It is interesting above and near T_c, the YM Pressure behaves as

$$p \simeq a_0 T^4 + a_1 T^2$$

Pisarski

This T^2 is mysterious!

- Here, this power is correlated with P in $V(\lambda) \sim \lambda^{\frac{4}{3}} \, (\log \lambda)^P$

$$p \simeq a_0 T^4 + a_1 T^{\frac{1}{1-P}}$$

Gursoy

Particle Spectra: generalities

- Linearized equation:

$$\ddot{\xi} + 2\dot{B}\dot{\xi} + \Box_4 \xi = 0 \quad , \quad \xi(r,x) = \xi(r)\xi^{(4)}(x), \qquad \Box\xi^{(4)}(x) = m^2\xi^{(4)}(x)$$

- Can be mapped to Schrodinger problem

$$-\frac{d^2}{dr^2}\psi + V(r)\psi = m^2\psi \quad , \quad V(r) = \frac{d^2B}{dr^2} + \left(\frac{dB}{dr}\right)^2 \quad , \quad \xi(r) = e^{-B(r)}\psi(r)$$

- Mass gap and discrete spectrum visible from the asymptotics of the potential.

- Large n asymptotics of masses obtained from WKB

$$n\pi = \int_{r_1}^{r_2} \sqrt{m^2 - V(r)}\ dr$$

- Spectrum depends only on initial condition for λ ($\sim \Lambda_{QCD}$).

- scalar glueballs

$$B(r) = \frac{3}{2}A(r) + \frac{1}{2}\log\frac{\beta(\lambda)^2}{9\lambda^2}$$

- tensor glueballs

$$B(r) = \frac{3}{2}A(r)$$

- pseudo-scalar glueballs

$$B(r) = \frac{3}{2}A(r) + \frac{1}{2}\log Z(\lambda) \quad , \quad Z \sim \lambda^d$$

- Universality of asymptotics

$$\frac{m^2_{n\to\infty}(0^{++})}{m^2_{n\to\infty}(2^{++})} \to 1 \quad , \quad \frac{m^2_{n\to\infty}(0^{+-})}{m^2_{n\to\infty}(0^{++})} = \frac{1}{4}(d-2)^2$$

predicts $d = 4$ via

$$\frac{m^2}{2\pi\sigma_a} = 2n + J + c,$$

Summary

- We argued that an Einstein dilaton system with a potential can capture some important properties of YM: asymptotic freedom in the UV and confinement in the IR

$$S \sim \int \left[R - \frac{4}{3}(\partial\phi)^2 + V(\phi) \right]$$

- The potential is regular in the UV

$$V \to \frac{12}{\ell^2}\left[1 + c_1\lambda + c_2\lambda^2 + \cdots\right]$$

- In the IR it should behave as

$$V \sim \lambda^{\frac{4}{3}}(\log\lambda)^P$$

for linear trajectories $P = 1/2$.

- We can solve the equations of motion with $\lambda \to 0$ in the UV.
- The solutions have only one parameter: Λ_{QCD}
- The intermediate behavior of the potential is not fixed (phenomenological parameters).

Linearity of the glueball spectrum

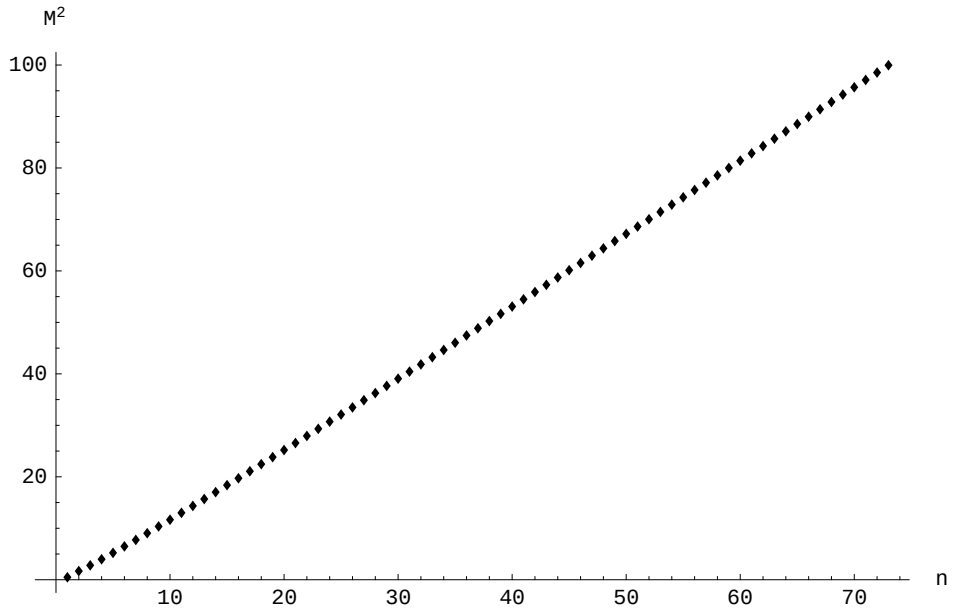

(a)

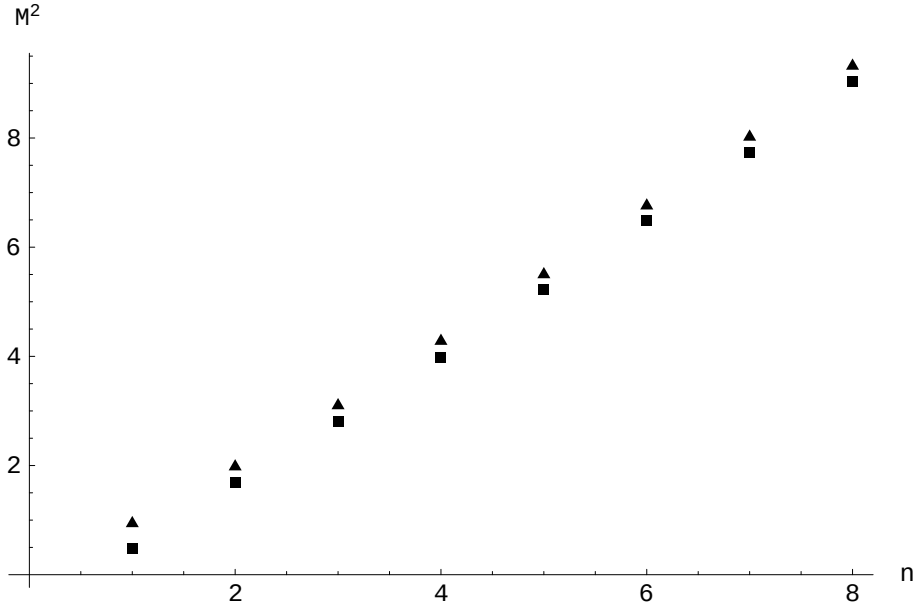

(b)

(a) Linear pattern in the spectrum for the first 70 0^{++} glueball states. M^2 is shown units of $0.015\ell^{-2}$.

(b) The first 8 0^{++} (squares) and the 2^{++} (triangles) glueballs. These spectra are obtained in the background I with $b_0 = 4.2, \lambda_0 = 0.05$.

Comparison with lattice data (Meyer)

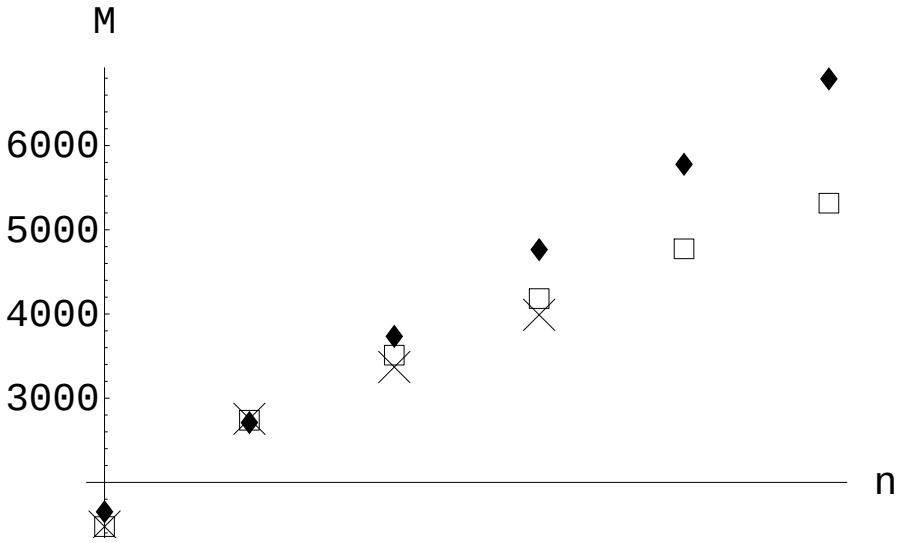

(a)

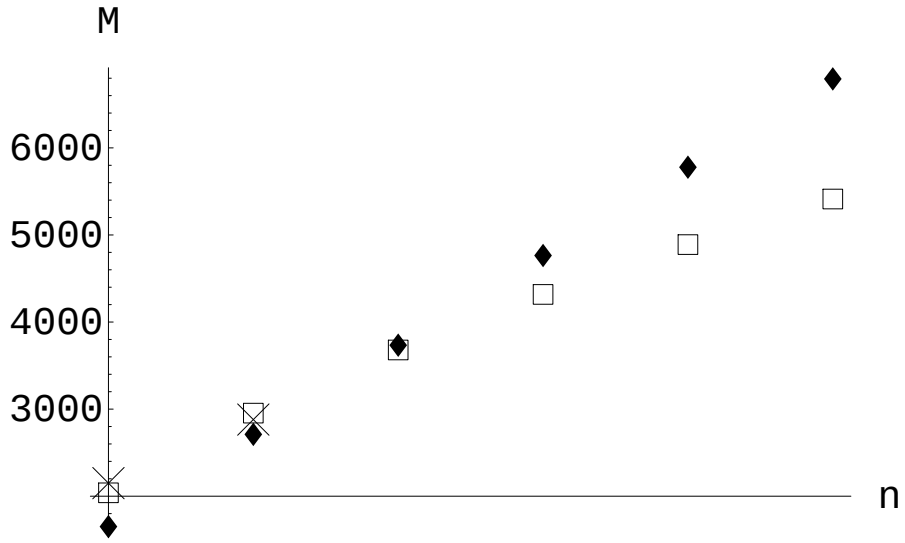

(b)

Comparison of glueball spectra from our model with $b_0 = 4.2, \lambda_0 = 0.05$ (boxes), with the lattice QCD data from Ref. I (crosses) and the AdS/QCD computation (diamonds), for (a) 0^{++} glueballs; (b) 2^{++} glueballs. The masses are in MeV, and the scale is normalized to match the lowest 0^{++} state from Ref. I.

Shortcomings of the glue description

Not everything is perfect: There are some shortcomings localized at the UV

- The conformal anomaly (proportional to the curvature) is incorrect.

- Shear viscosity ratio is constant and equal to that of N=4 sYM.

(This is not expected to be a serious error in the experimentally interesting $T_c \leq T \leq 4T_c$ range.)

Both of the above need Riemann curvature corrections.

- Many other observables come out very well both at T=0 and finite T

The lattice glueball data

J^{++}	Ref. I $(m/\sqrt{\sigma})$	Ref. I (MeV)	Ref. II (mr_0)	Ref. II (MeV)	$N_c \to \infty (m/$
0	$3.347(68)$	$1475(30)(65)$	$4.16(11)(4)$	$1710(50)(80)$	$3.37(15)$
0^*	$6.26(16)$	$2755(70)(120)$	$6.50(44)(7)$	$2670(180)(130)$	$6.43(50)$
0^{**}	$7.65(23)$	$3370(100)(150)$	NA	NA	NA
0^{***}	$9.06(49)$	$3990(210)(180)$	NA	NA	NA
2	$4.916(91)$	$2150(30)(100)$	$5.83(5)(6)$	$2390(30)(120)$	$4.93(30)$
2^*	$6.48(22)$	$2880(100)(130)$	NA	NA	NA
R_{20}	$1.46(5)$	$1.46(5)$	$1.40(5)$	$1.40(5)$	$1.46(11)$
R_{00}	$1.87(8)$	$1.87(8)$	$1.56(15)$	$1.56(15)$	$1.90(17)$

Available lattice data for the scalar and the tensor glueballs. Ref. I =H. B. Meyer, [arXiv:hep-lat/0508002]. and Ref. II = C. J. Morningstar and M. J. Peardon, [arXiv:hep-lat/9901004] + Y. Chen *et al.*, [arXiv:hep-lat/0510074]. The first error corresponds to the statistical error from the the continuum extrapolation. The second error in Ref.I is due to the uncertainty in the string tension $\sqrt{\sigma}$. (Note that this does not affect the mass ratios). The second error in the Ref. II is the estimated uncertainty from the anisotropy. In the last column we present the available large N_c estimates according to B. Lucini and M. Teper, [arXiv:hep-lat/0103027]. The parenthesis in this column shows the total possible error followed by the estimations in the same reference.

The glueball wavefunctions

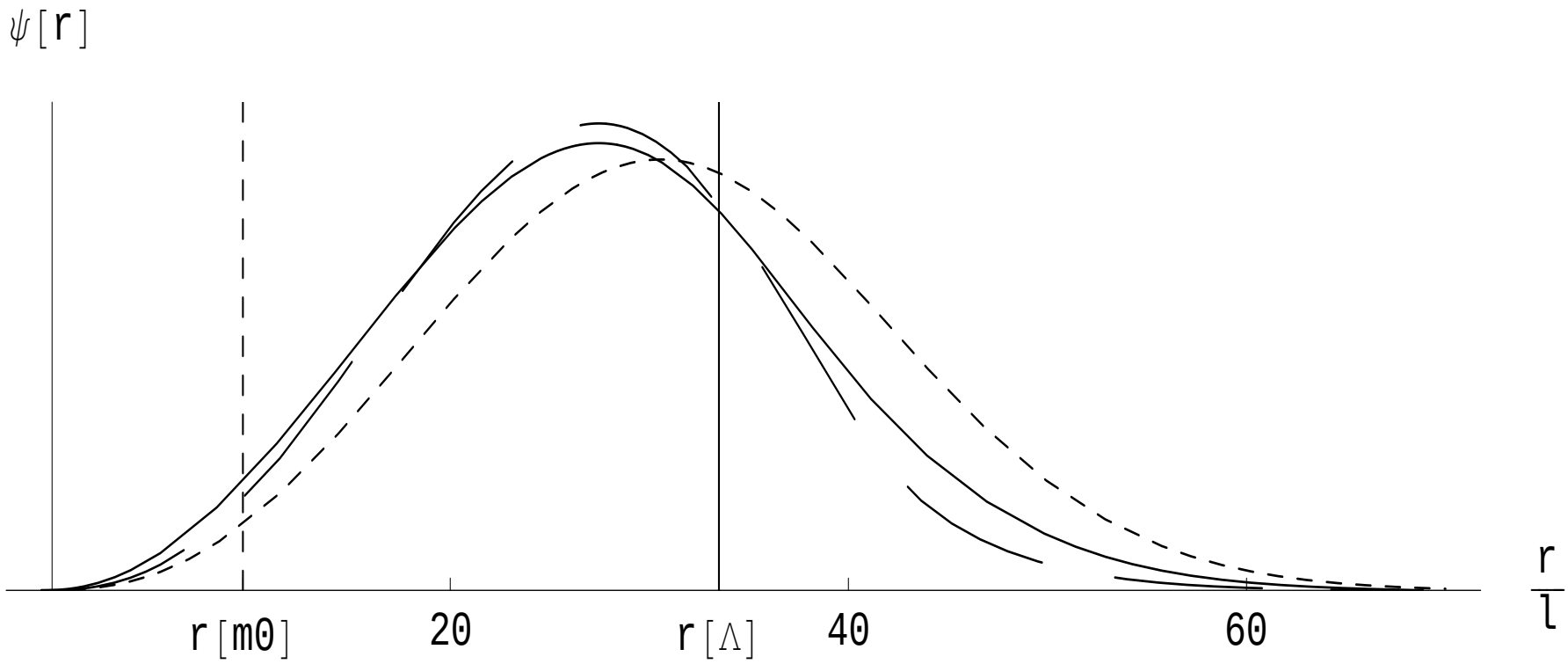

Normalized wave-function profiles for the ground states of the 0^{++} (solid line) ,0^{-+} (dashed line), and 2^{++} (dotted line) towers, as a function of the radial conformal coordinate. The vertical lines represent the position corresponding to $E = m_{0^{++}}$ and $E = \Lambda_p$.

Comparison of scalar and tensor potential

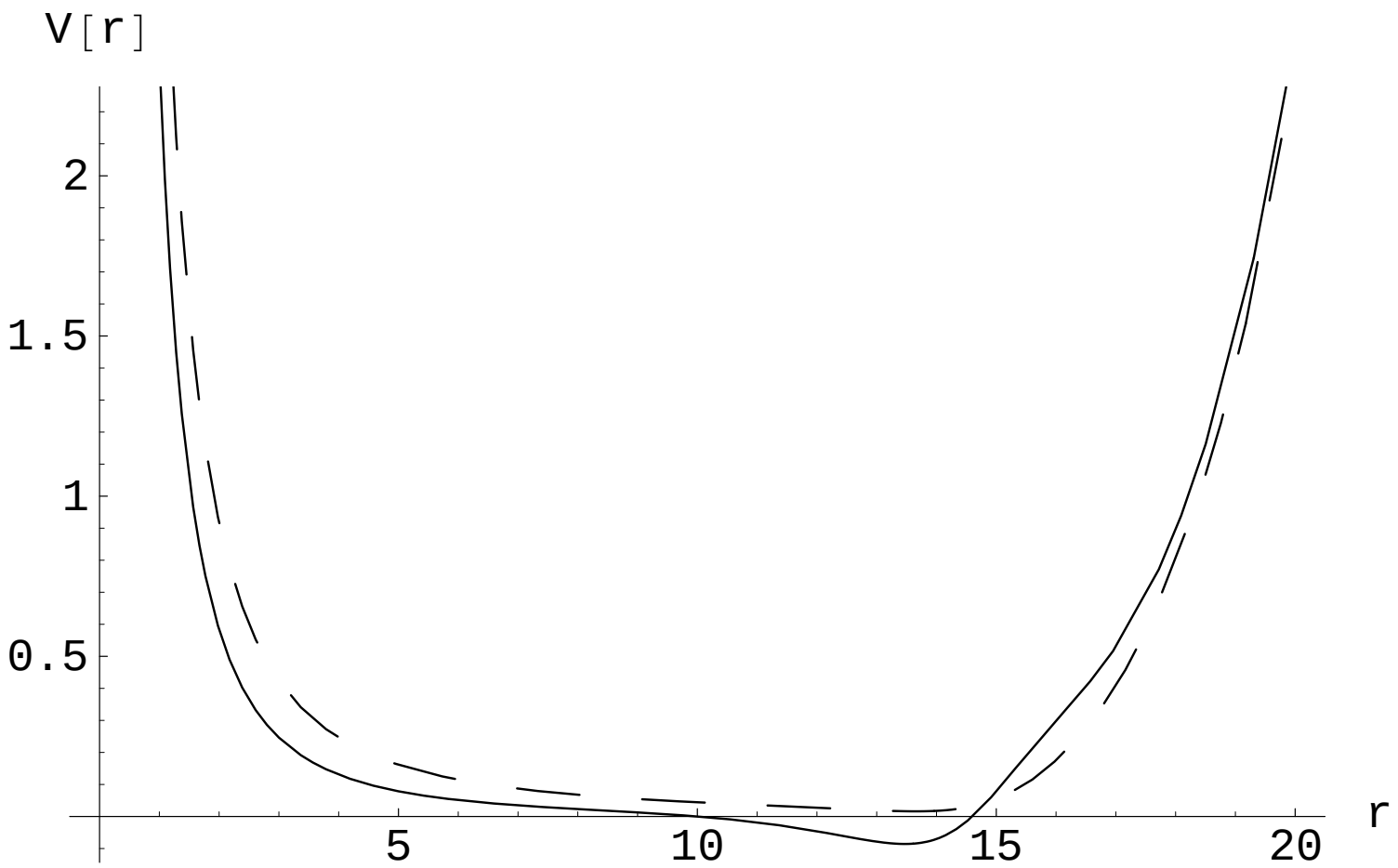

Effective Schrödinger potentials for scalar (solid line) and tensor (dashed line) glueballs. The units are chosen such that $\ell = 0.5$.

α-dependence of scalar spectrum

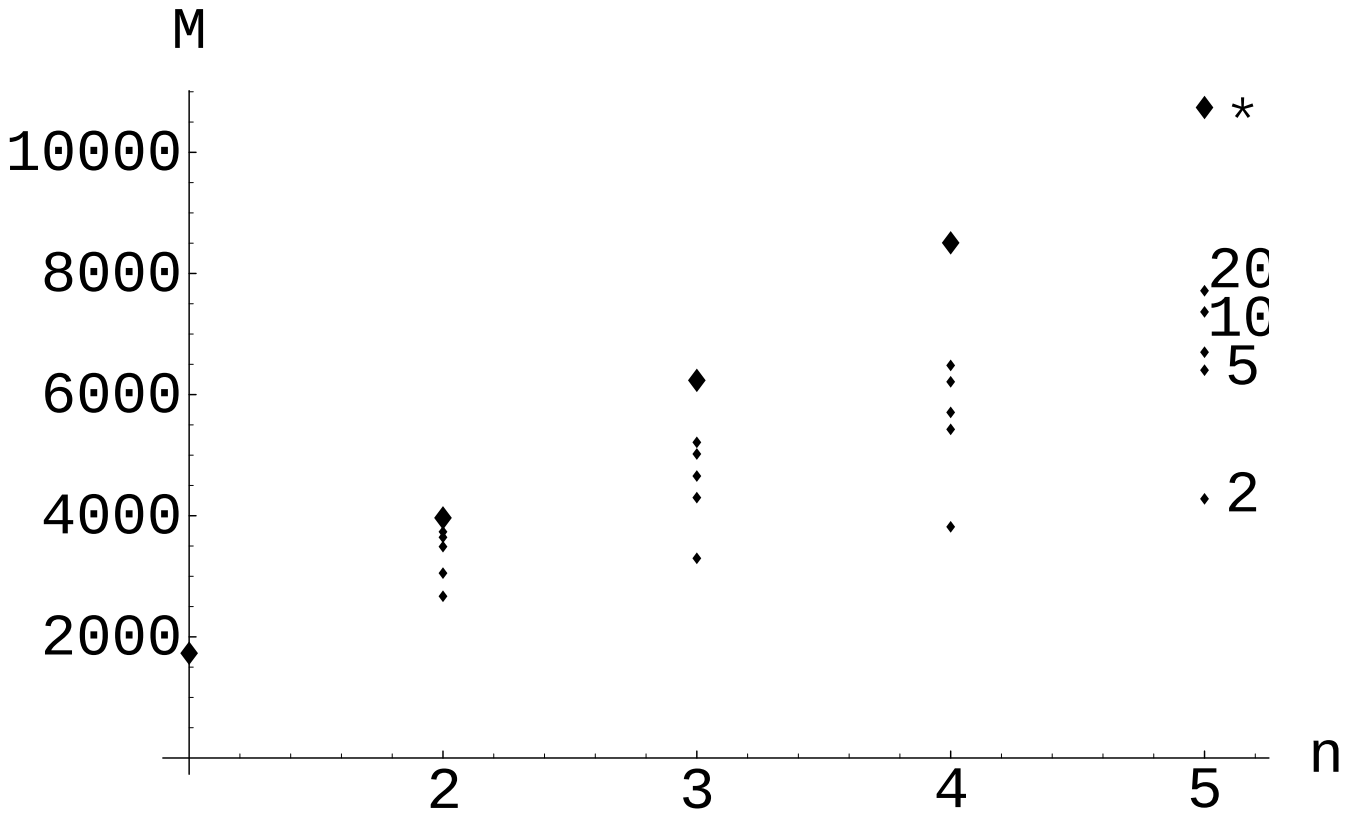

The 0^{++} spectra for varying values of α that are shown at the right end of the plot. The symbol * denotes the AdS/QCD result.

The fit to glueball lattice data

J^{PC}	Ref I (MeV)	Our model (MeV)	Mismatch	$N_c \to \infty$	Mismat
0^{++}	**1475 (4%)**	**1475**	0	**1475**	0
2^{++}	2150 (5%)	2055	4%	2153 (10%)	5%
0^{-+}	**2250 (4%)**	**2243**	0		
0^{++*}	**2755 (4%)**	**2753**	0	2814 (12%)	2%
2^{++*}	2880 (5%)	2991	4%		
0^{-+*}	3370 (4%)	3288	2%		
0^{++**}	3370 (4%)	3561	5%		
0^{++***}	3990 (5%)	4253	6%		

Comparison between the glueball spectra in Ref. I and in our model. The states we use as input in our fit are marked in red. The parenthesis in the lattice data indicate the percent accuracy.

The gauge-theory at finite temperature

• The finite temperature ground state of the gauge theory corresponds to a different solution in the dual string theory: the AdS-Black-hole solution

E. Witten, 1998

$$ds^2 = \frac{\ell_{AdS}^2}{r^2}\left[\frac{dr^2}{f(r)} + f(r)dt^2 + dx^i dx_i\right] + \ell_{AdS}^2\ (d\Omega_5)^2 \quad , \quad f(r) = 1 - (\pi T)^4 r^4$$

• The horizon is at $r = \frac{1}{\pi T}$

• The dynamics of low-energy gravitational fluctuations is governed by the relativistic Navier-Stokes equation.

Temperature versus horizon position

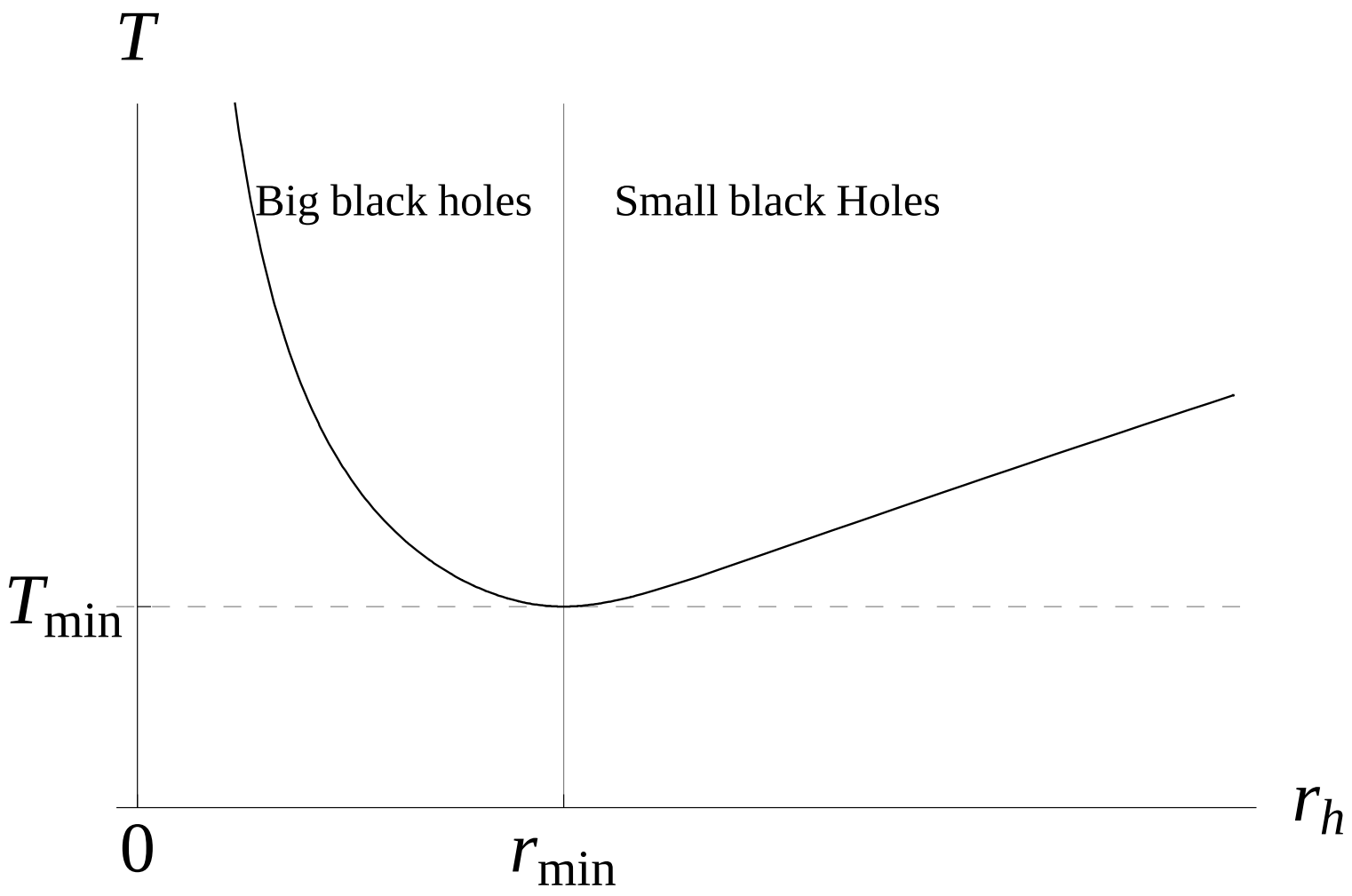

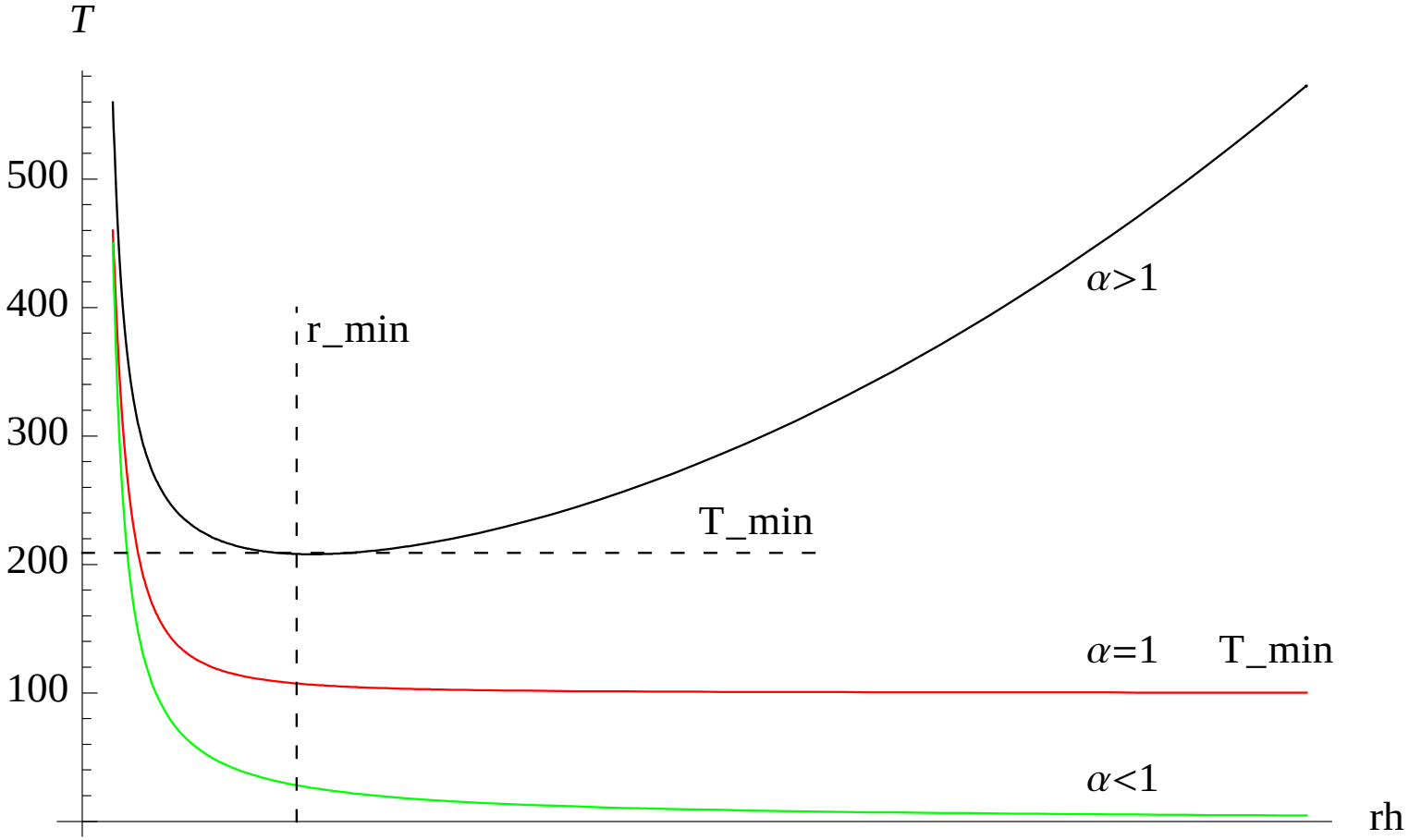

We plot the relation $T(r_h)$ for various potentials parameterized by a. $a = 1$ is the critical value below which there is only one branch of black-hole solutions.

The free energy

• The free energy is calculated from the action as a boundary term for both the black-holes and the thermal vacuum solution. They are all UV divergent but their differences are finite.

$$\frac{\mathcal{F}}{M_p^3 V_3} = 12\mathcal{G}(T) - T\ S(T)$$

• $\mathcal{G}$ is the temperature-depended gluon condensate $\langle Tr[F^2]\rangle_T - \langle Tr[F^2]\rangle_{T=0}$ defined as

$$\lim_{r\to 0} \quad \lambda_T(r) - \lambda_{T=0}(r) = \mathcal{G}(T)\ r^4 + \cdots$$

• It is $\mathcal{G}$ the breaks conformal invariance essentially and leads to a non-trivial deconfining transition (as $S > 0$ always)

• The axion solution must be constant above the phase transition (black-hole). This is the only regular solution. (the would be normalizable solution diverges at the BH horizon). Therefore $\langle F \wedge F\rangle$ vanishes in agreement with indications from lattice data.

Free energy versus horizon position

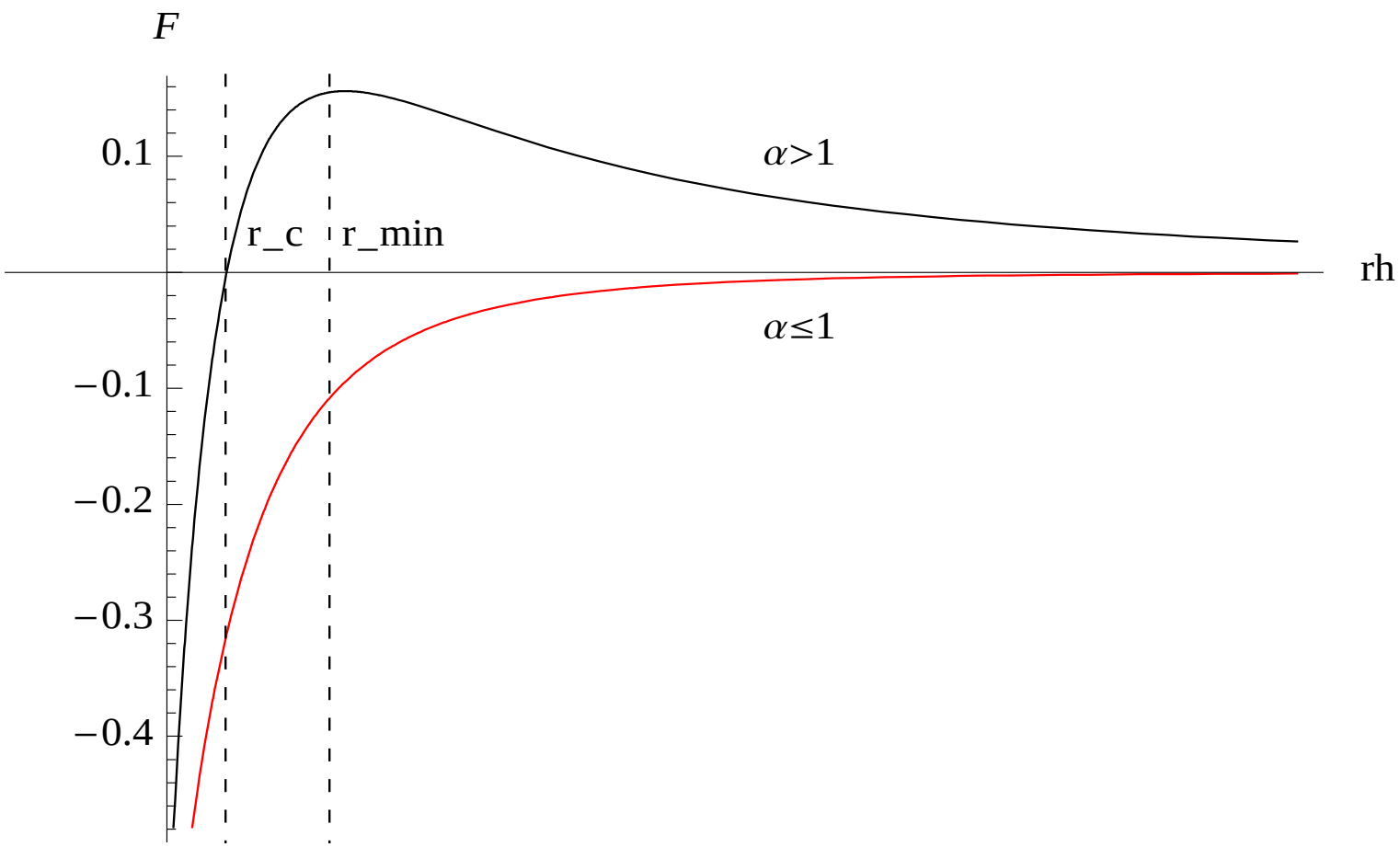

We plot the relation $\mathcal{F}(r_h)$ for various potentials parameterized by a. $a = 1$ is the critical value below which there is no first order phase transition .

The transition in the free energy

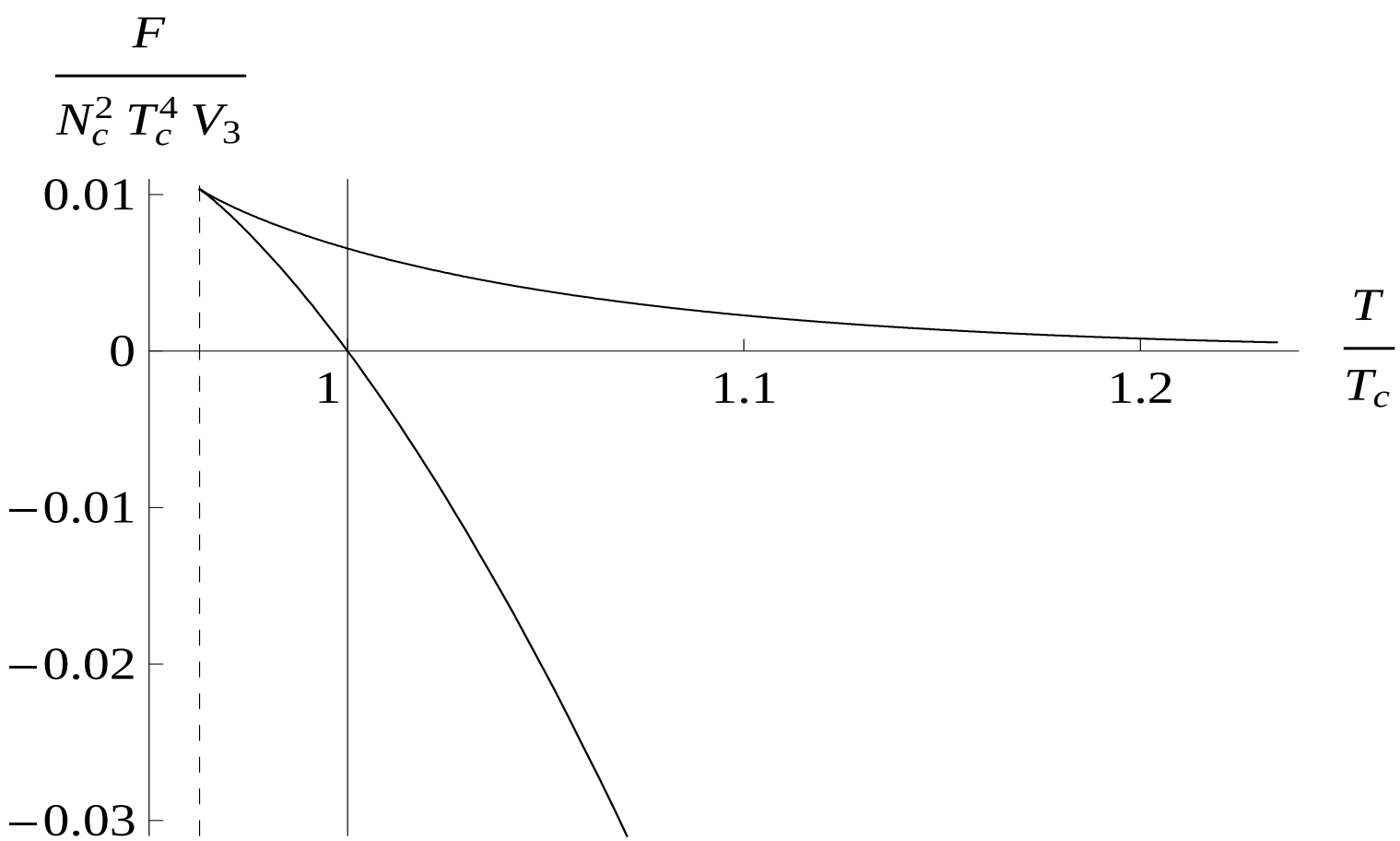

Parameters

- We have 3 initial conditions in the system of graviton-dilaton equations:

♠ One is fixed by picking the branch that corresponds asymptotically to $\lambda \sim \frac{1}{\log(r\Lambda)}$

♠ The other fixes $\Lambda \to \Lambda_{QCD}$.

♠ The third is a gauge artifact as it corresponds to a choice of the origin of the radial coordinate.

- We parameterize the potential as

$$V(\lambda) = \frac{12}{\ell^2}\left\{1 + V_0\lambda + V_1\lambda^{4/3}\left[\log\left(1 + V_2\lambda^{4/3} + V_3\lambda^2\right)\right]^{1/2}\right\},$$

- We fix the one and two loop β-function coefficients:

$$V_0 = \frac{8}{9}b_0 \quad , \quad V_2 = b_0^4\left(\frac{23 + 36b_1/b_0^2}{81V_1^2}\right)^2 , \quad \frac{b_1}{b_0^2} = \frac{51}{121}.$$

and remain with two leftover arbitrary (phenomenological) coefficients.

Fit and comparison

	HQCD	lattice $N_c = 3$	lattice $N_c \to \infty$	Parameter
$[p/(N_c^2T^4)]_{T=2T_c}$	**1.2**	**1.2**	-	$V1 = 14$
$L_h/(N_c^2T_c^4)$	**0.31**	0.28 (Karsch)	**0.31** (Teper+Lucini)	$V3 = 170$
$[p/(N_c^2T^4)]_{T\to+\infty}$	$\pi^2/45$	$\pi^2/45$	$\pi^2/45$	$M_p\ell = [45\pi^2]^{-1/3}$
$m_{0^{++}}/\sqrt{\sigma}$	**3.37**	3.56 (Chen)	**3.37** (Teper+Lucini)	$\ell_s/\ell = 0.15$
$m_{0^{-+}}/m_{0^{++}}$	**1.49**	**1.49** (Chen)	-	$c_a = 0.26$
χ	$(191MeV)^4$	$(191MeV)^4$ (DelDebbio)	-	$Z_0 = 133/4$
$T_c/m_{0^{++}}$	0.167	-	0.177(7)	
$m_{0^{*++}}/m_{0^{++}}$	1.61	1.56(11)	1.90(17)	
$m_{2^{++}}/m_{0^{++}}$	1.36	1.40(4)	1.46(11)	
$m_{0^{*-+}}/m_{0^{++}}$	2.10	2.12(10)	-	

- G. Boyd, J. Engels, F. Karsch, E. Laermann, C. Legeland, M. Lutgemeier and B. Petersson, *"Thermodynamics of SU(3) Lattice Gauge Theory,"* Nucl. Phys. B **469**, 419 (1996) [arXiv:hep-lat/9602007].

- B. Lucini, M. Teper and U. Wenger, *"Properties of the deconfining phase transition in SU(N) gauge theories,"* JHEP **0502**, 033 (2005) [arXiv:hep-lat/0502003];
"SU(N) gauge theories in four dimensions: Exploring the approach to $N = \infty$," JHEP **0106**, 050 (2001) [arXiv:hep-lat/0103027].

- Y. Chen *et al.*, *"Glueball spectrum and matrix elements on anisotropic lattices,"* Phys. Rev. D **73** (2006) 014516 [arXiv:hep-lat/0510074].

- L. Del Debbio, L. Giusti and C. Pica, *"Topological susceptibility in the SU(3) gauge theory,"* Phys. Rev. Lett. **94**, 032003 (2005) [arXiv:hep-th/0407052].

Thermodynamic variables

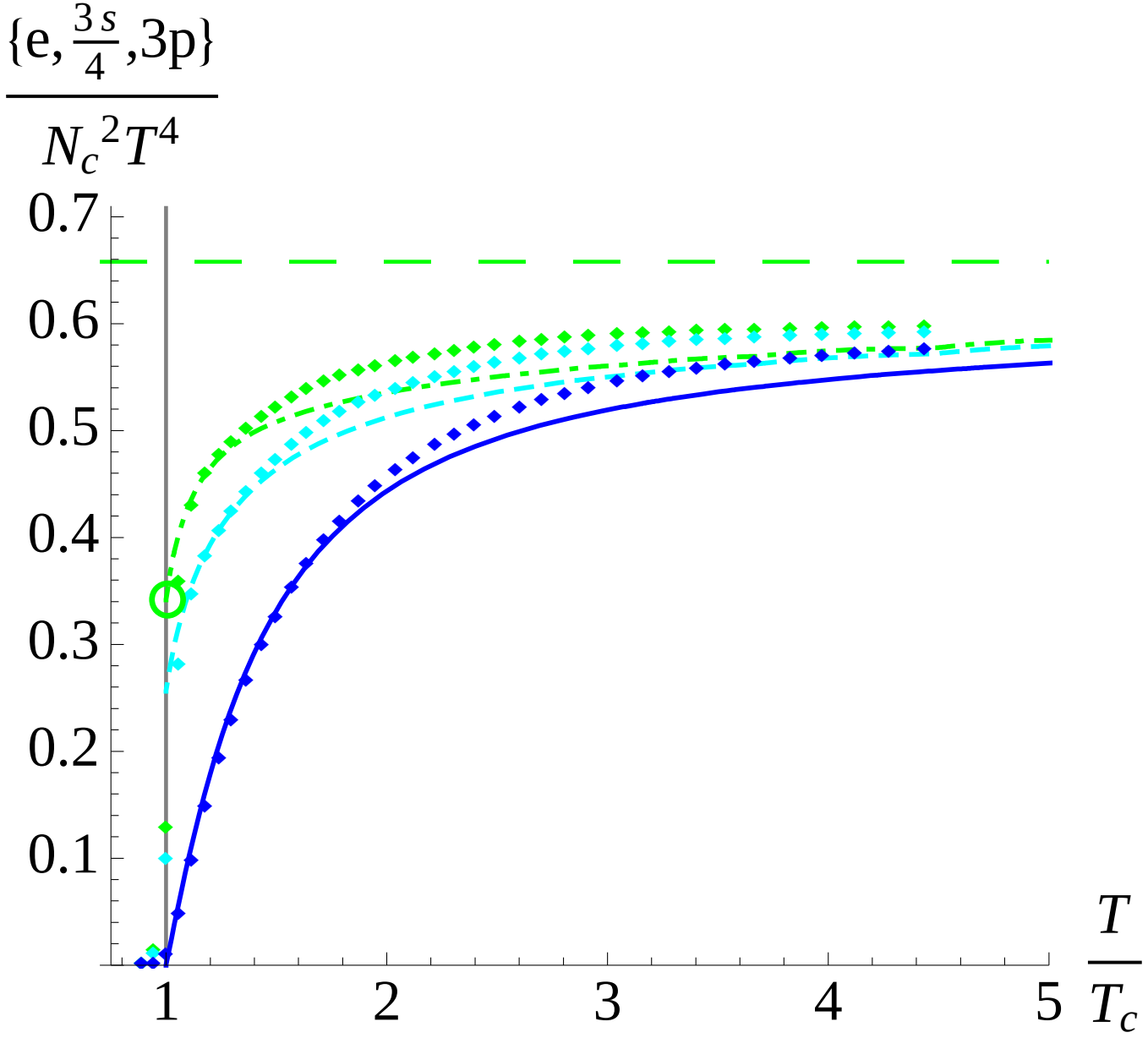

Equation of state

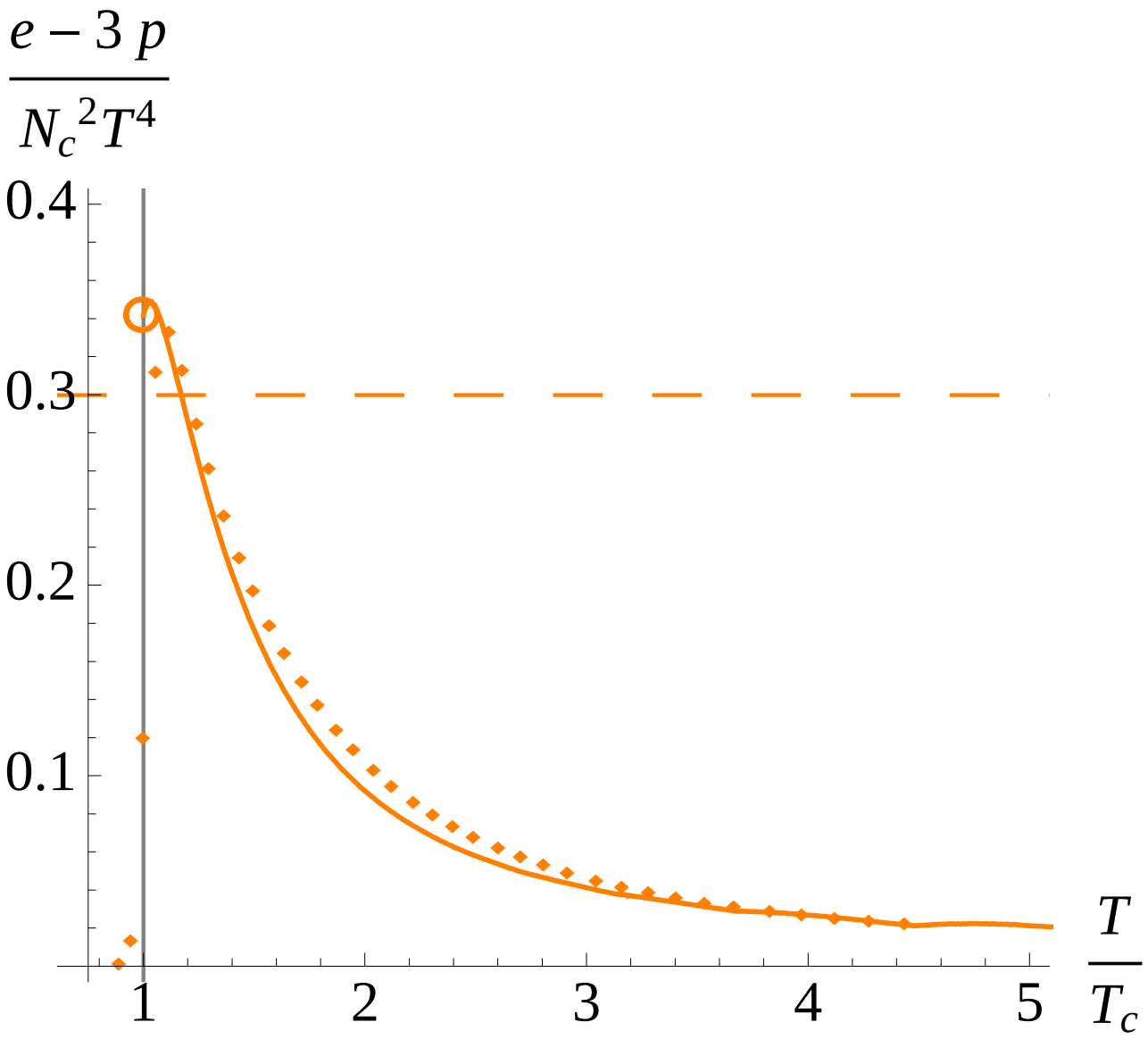

The conformal anomaly in flat space

- In YM we have the following anomaly equation in flat space:

$$T^{\mu}_{\mu} = \frac{\beta(\lambda_t)}{4\lambda_t^2} Tr[F^2],$$

- Defining the pressure p and energy density ρ,

$$p = -\frac{\mathcal{F}}{V_3}, \qquad \rho = \frac{\mathcal{F} + TS}{V_3},$$

the trace is

$$\langle T^{\mu}_{\mu} \rangle_R = \rho - 3p = 60 M_p^3 N_c^2 \mathcal{G}(T) = \frac{\beta(\lambda_t)}{4\lambda_t^2} (\langle Tr[F^2] \rangle_T - \langle Tr[F^2] \rangle_o),$$

- The left hand side is the trace of the renormalized thermal stress tensor, $\langle T^{\mu}_{\mu} \rangle_R = \langle T^{\mu}_{\mu} \rangle - \langle T^{\mu}_{\mu} \rangle_o$, and it is proportional to $\mathcal{G} \sim \langle Tr[F^2] \rangle$,

The specific heat

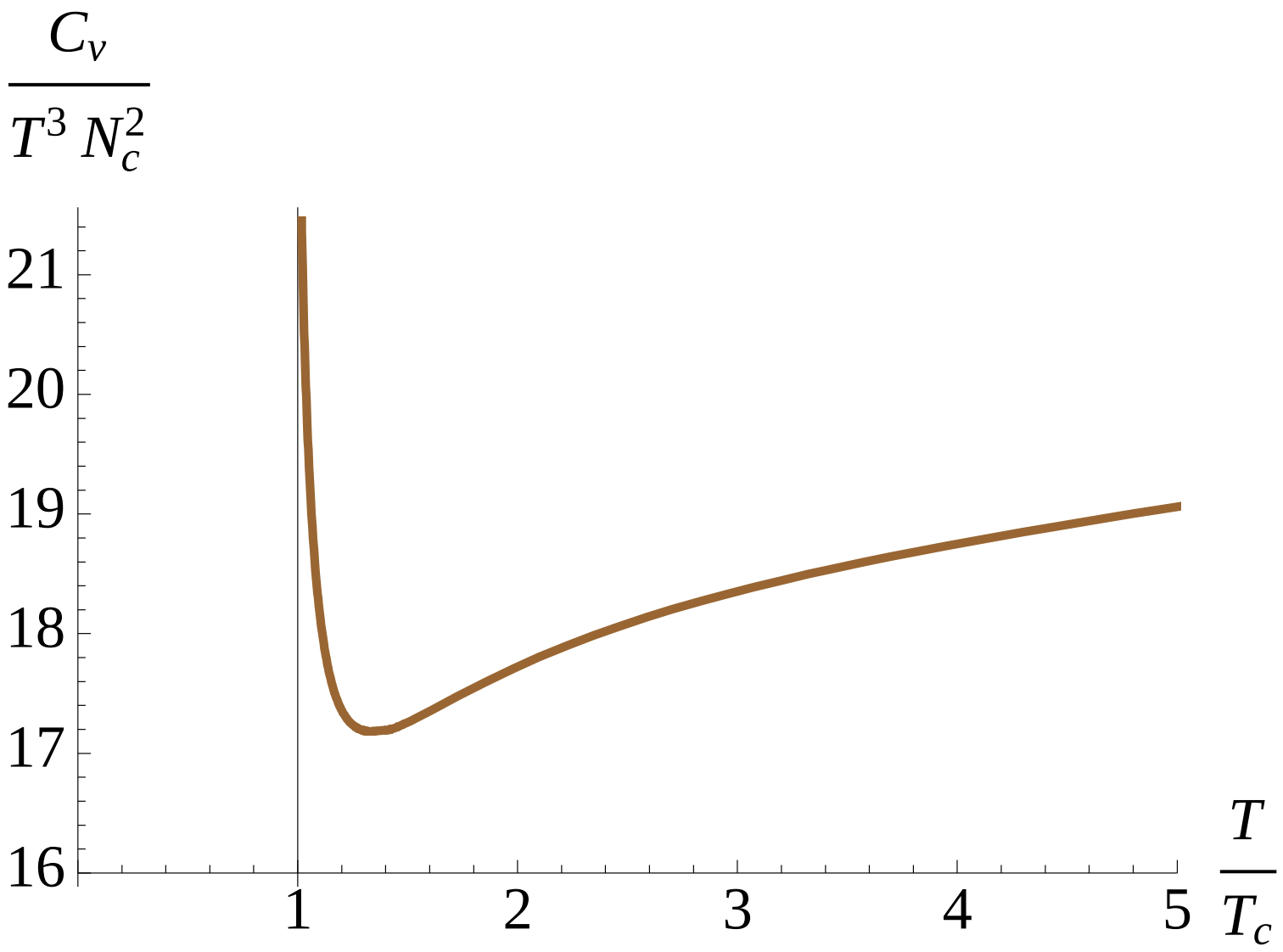

Parameters

- We have 3 initial conditions in the system of graviton-dilaton equations:

♠ One is fixed by picking the branch that corresponds asymptotically to $\lambda \sim \frac{1}{\log(r\Lambda)}$

♠ The other fixes $\Lambda \to \Lambda_{QCD}$.

♠ The third is a gauge artifact as it corresponds to a choice of the origin of the radial coordinate.

- We parameterize the potential as

$$V(\lambda) = \frac{12}{\ell^2}\left\{1 + V_0\lambda + V_1\lambda^{4/3}\left[\log\left(1 + V_2\lambda^{4/3} + V_3\lambda^2\right)\right]^{1/2}\right\},$$

- We fix the one and two loop β-function coefficients:

$$V_0 = \frac{8}{9}b_0 \quad , \quad V_2 = b_0^4\left(\frac{23 + 36b_1/b_0^2}{81V_1^2}\right)^2 , \quad \frac{b_1}{b_0^2} = \frac{51}{121}.$$

and remain with two leftover arbitrary (phenomenological) coefficients.

• We also have the Planck scale M_p

Asking for correct $T \to \infty$ thermodynamics (free gas) fixes

$$(M_p \ell)^3 = \frac{1}{45\pi^2} \quad , \quad M_{\text{physical}} = M_p N_c^{\frac{2}{3}} = \left(\frac{8}{45\pi^2 \ell^3}\right)^{\frac{1}{3}} \simeq 4.6 \text{ GeV}$$

• The fundamental string scale. It can be fixed by comparing with lattice string tension

$$\sigma = \frac{b^2(r_*)\lambda^{4/3}(r_*)}{2\pi \ell_s^2},$$

• ℓ is not a parameter for bulk calculations due to a special "scaling" pseudosymmetry in the Einstein frame:

$$e^{\phi} \to \kappa\ e^{\phi} \quad , \quad g_{\mu\nu} \to g_{\mu\nu} \quad , \quad \ell \to \ell \quad , \quad \ell_s \to \kappa^{\frac{2}{3}}\ \ell_s \quad , \quad V(e^{\phi}) \to V(\kappa\ e^{\phi})$$

• It is a parameter when using the Nambu-Goto action.

Comparing to Gubser+Nelore's formula

• Gubser+Nelore proposed the following approximate formula for the speed of sound

$$c_s^2 \simeq \frac{1}{3} - \frac{1}{2}\frac{V'^2}{V^2}\Big|_{\phi=\phi_h}$$

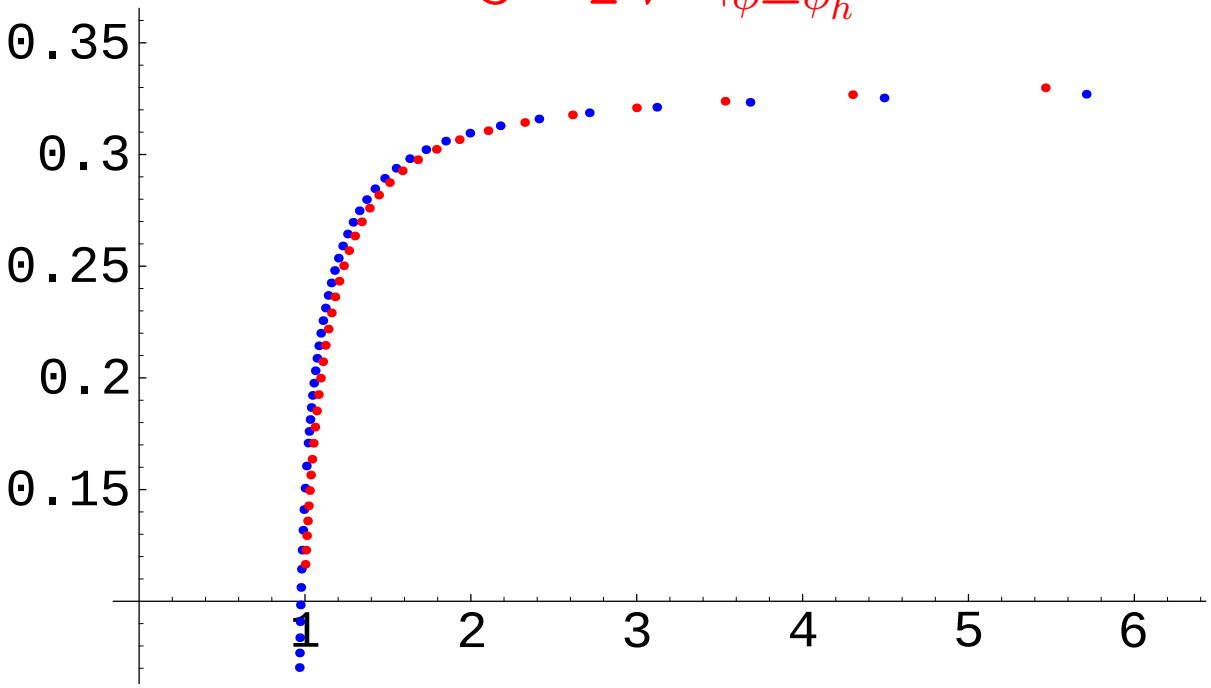

Gursoy (unpublished) 2009

• Red curve=numerical calculation, Blue curve=Gubser's adiabatic/approxima formula.

The axion

Similar arguments lead to an action of the form

$$S = N_c^2 \; S_{g,\phi} + S_{axion} + \cdots$$

$$S_{axion} \sim \int d^5x \sqrt{g} \; G(R,\lambda) \; (\partial a)^2$$

- Higher powers of $(\partial a)^2$ are subleading in N_c.

- We may therefore find the solution using the solution of the metric-dilaton system.

The axion background

- The axion solution can be interpreted as a "running" θ-angle

- This is in accordance with the absence of UV divergences (all correlators $\langle Tr[F \wedge F]^n \rangle$ are UV finite), and Seiberg-Witten type solutions.

- The axion action is down by $1/N_c^2$

$$S_{axion} = -\frac{M_p^3}{2} \int d^5x \sqrt{g}\ Z(\lambda)\ (\partial a)^2$$

$$\lim_{\lambda \to 0} Z(\lambda) = Z_0 \left[1 + c_1 \lambda + c_2 \lambda^2 + \cdots\right] \quad , \quad \lim_{\lambda \to \infty} Z(\lambda) = c_a \lambda^d + \cdots \quad , \quad d = 4$$

- The equation of motion is

$$\ddot{a} + \left(3\dot{A} + \frac{\dot{Z}(\lambda)}{Z(\lambda)}\right) \dot{a} = 0 \quad \rightarrow \quad \dot{a} = \frac{C\ e^{-3A}}{Z(\lambda)}$$

- The full solution is

$$a(r) = \theta_{UV} + 2\pi k + C \int_0^r dr \frac{e^{-3A}}{Z(\lambda)} \quad , \quad C = \langle Tr[F \wedge F] \rangle$$

- $a(r)$ is a running effective θ-angle. Its running is non-perturbative,

$$a(r) \sim r^4 \sim e^{-\frac{4}{b_0 \lambda}}$$

- The vacuum energy is

$$E(\theta_{UV}) = -\frac{M^3}{2} \int d^5x \sqrt{g}\ Z(\lambda)\ (\partial a)^2 = -\frac{M^3}{2} C a(r) \Big|_{r=0}^{r=r_0}$$

- Consistency requires to impose that $a(r_0) = 0$. This determines C and

$$E(\theta_{UV}) = \frac{M^3}{2} \text{Min}_k \frac{(\theta_{UV} + 2\pi k)^2}{\int_0^{r_0} \frac{dr}{e^{3A} Z(\lambda)}}$$

$$\frac{a(r)}{\theta_{UV} + 2\pi k} = \frac{\int_r^{r_0} \frac{dr}{e^{3A} Z(\lambda)}}{\int_0^{r_0} \frac{dr}{e^{3A} Z(\lambda)}}$$

- The topological susceptibility is given by

$$E(\theta) = \frac{1}{2} \chi\ \theta^2 + \mathcal{O}(\theta^4) \quad , \quad \chi = \frac{M^3}{\int_0^{r_0} \frac{dr}{e^{3A} Z(\lambda)}}$$

• The effective θ-angle "runs" also in the D4 model for QCD, and also vanishes in the IR

$$\theta(U) = \theta(1 - U_0^3/U^3)$$

• In Improved Holographic QCD:

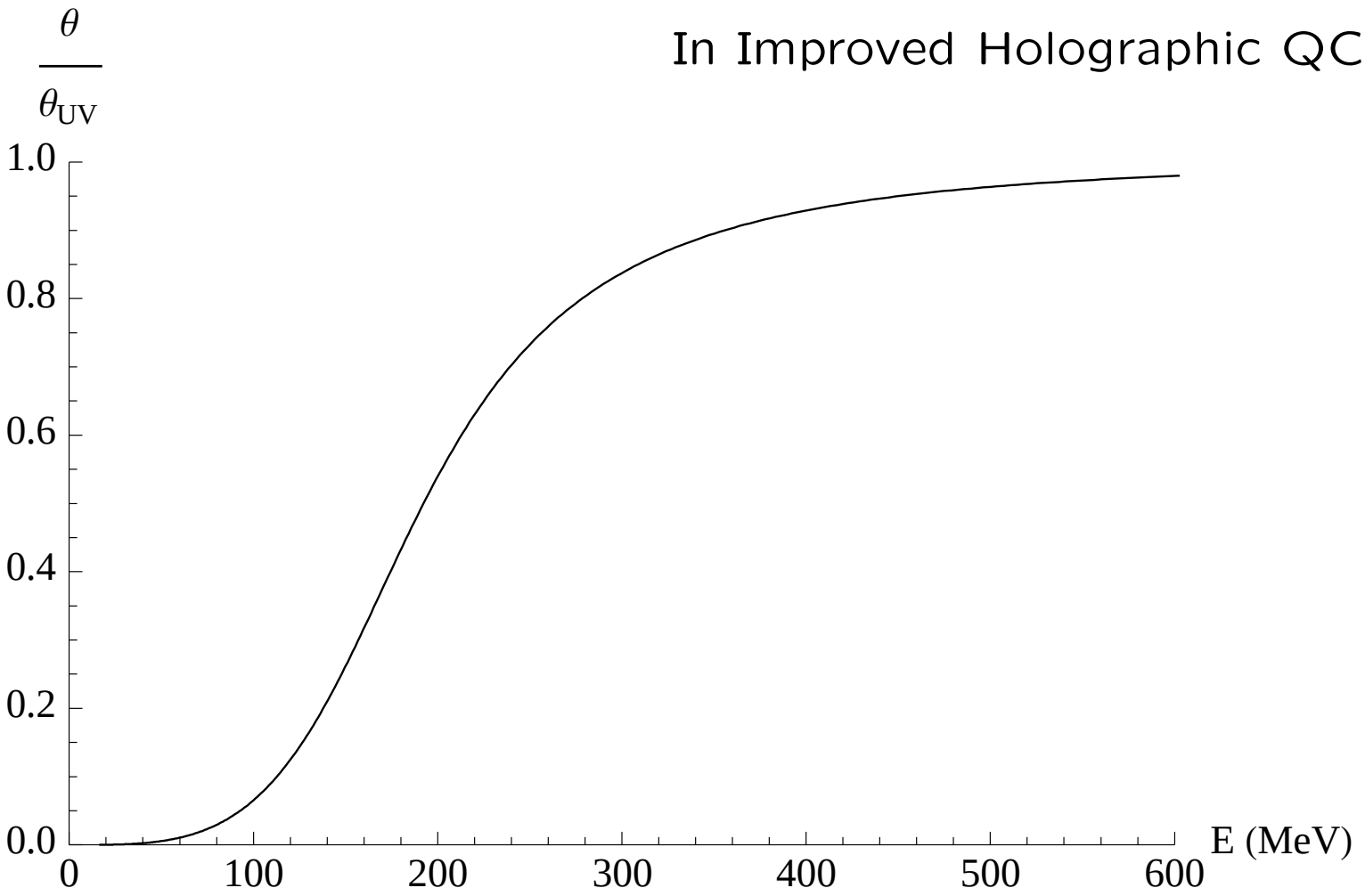

We have taken: $Z(\lambda) = Z_0(1 + c_a\lambda^4) \simeq 133(1 + 0.26\lambda^4)$

shear viscosity data

- V_2 is the elliptic flow coefficient

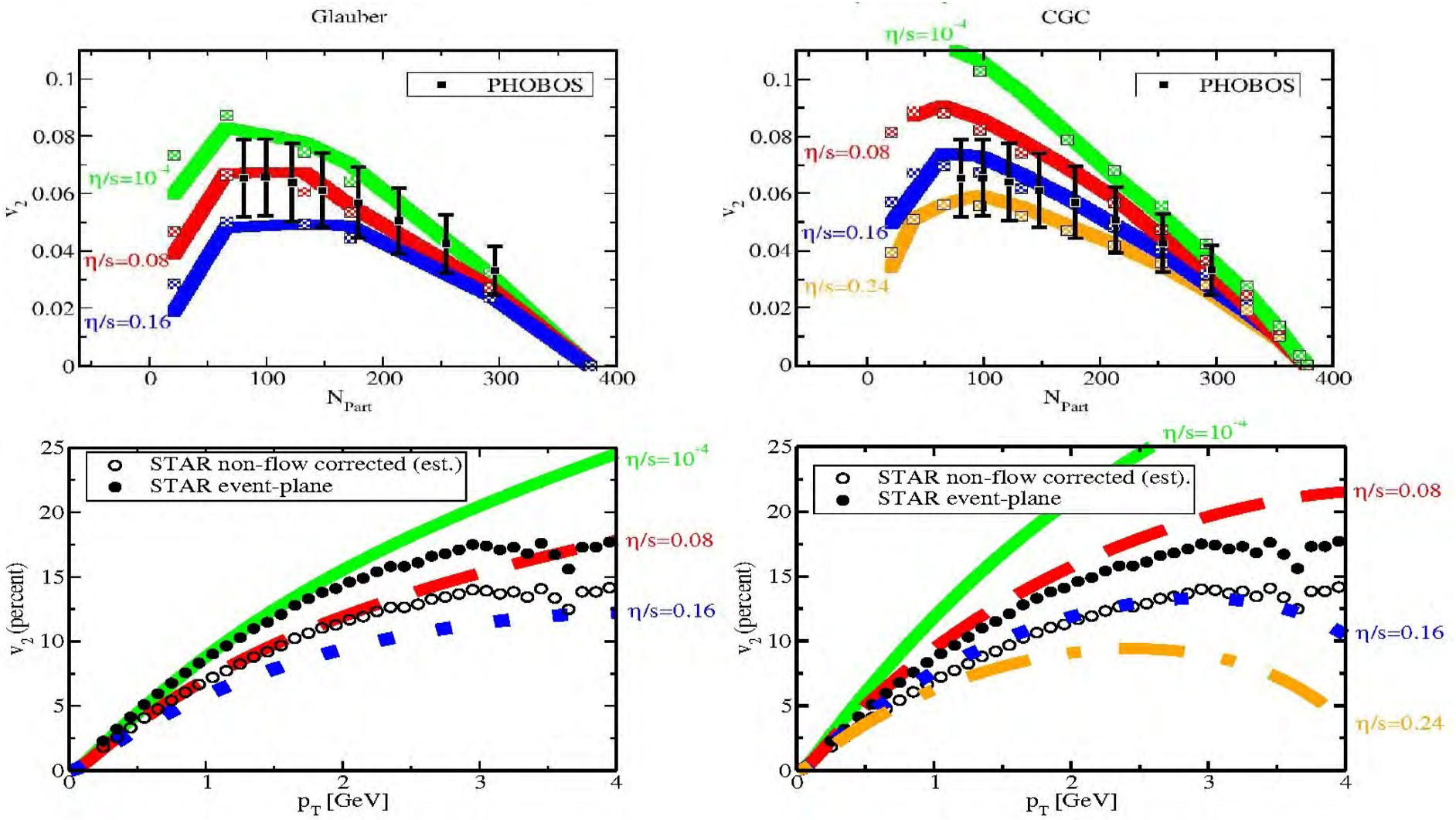

Luzum+Romatchke 2008

Viscosity

- Viscosity (shear and bulk) is related to dissipation and entropy production

$$\frac{\partial s}{\partial t}=\frac{\eta}{T}\left[\partial_i v_j+\partial_j v_i-\frac{2}{3}\delta_{ij}\partial\cdot v\right]^2+\frac{\zeta}{T}(\partial\cdot v)^2$$

- Hydrodynamics is valid as an effective description when relevant length scales $\gg$ mean-free-path:
- Conformal invariance imposes that $\zeta=0$.
- Viscosity can be calculated from a Kubo-like formula (fluctuation-dissipation)

$$\eta\left(\delta_{ik}\delta_{jl}+\delta_{il}\delta_{jk}-\frac{2}{3}\delta_{ij}\delta_{kl}\right)+\zeta\delta_{ij}\delta_{kl}=-\lim_{\omega\to 0}\frac{Im\ G^R_{ij;kl}(\omega)}{\omega}$$

$$G^R_{ij;kl}(\omega)=-i\int d^3x\int dt\ e^{i\omega t}\theta(t)\ \langle 0|[T_{ij}(\vec{x},t),T_{kl}(\vec{0},0)]|0\rangle$$

- In all theories with gravity duals ($\lambda\to\infty$) at two-derivative level

$$\frac{\eta}{s}=\frac{1}{4\pi}$$

Policastro+Starinets+Son 2001, Kovtun+Son+Starinets 2003, Buchel+Liu 2003

- In Einstein-dilaton gravity shear viscosity is equal to the universal value.

The bulk viscosity in lattice

H. Meyer 2007

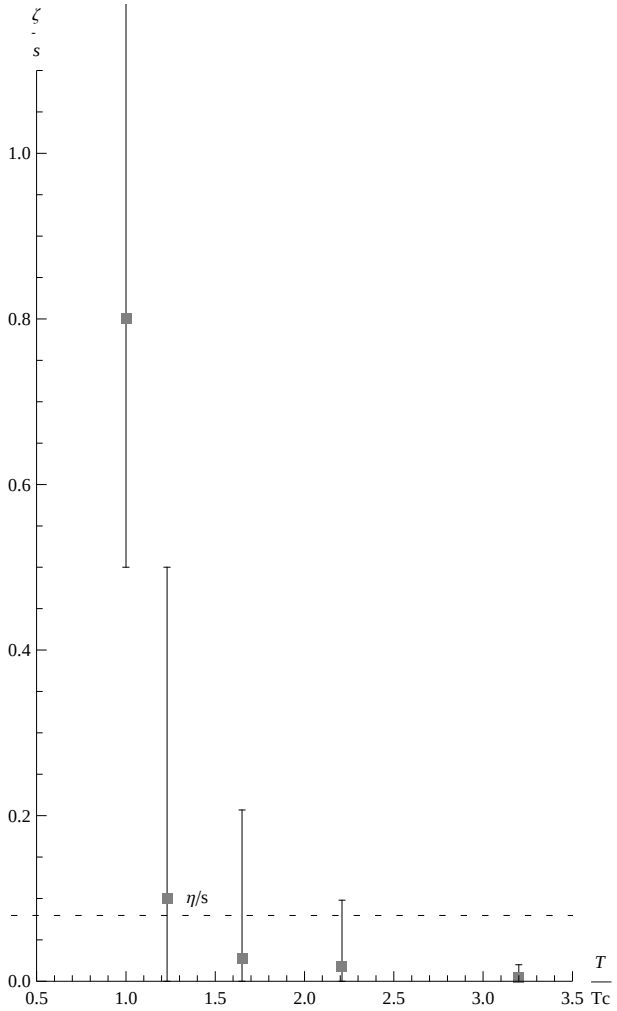

Pure YM only. Error bar are statistical only.

The Buchel parametrization (bound)

$$\frac{\zeta}{\eta} \geq 2\left(\frac{1}{3} - c_s^2\right)$$

Buchel 2007

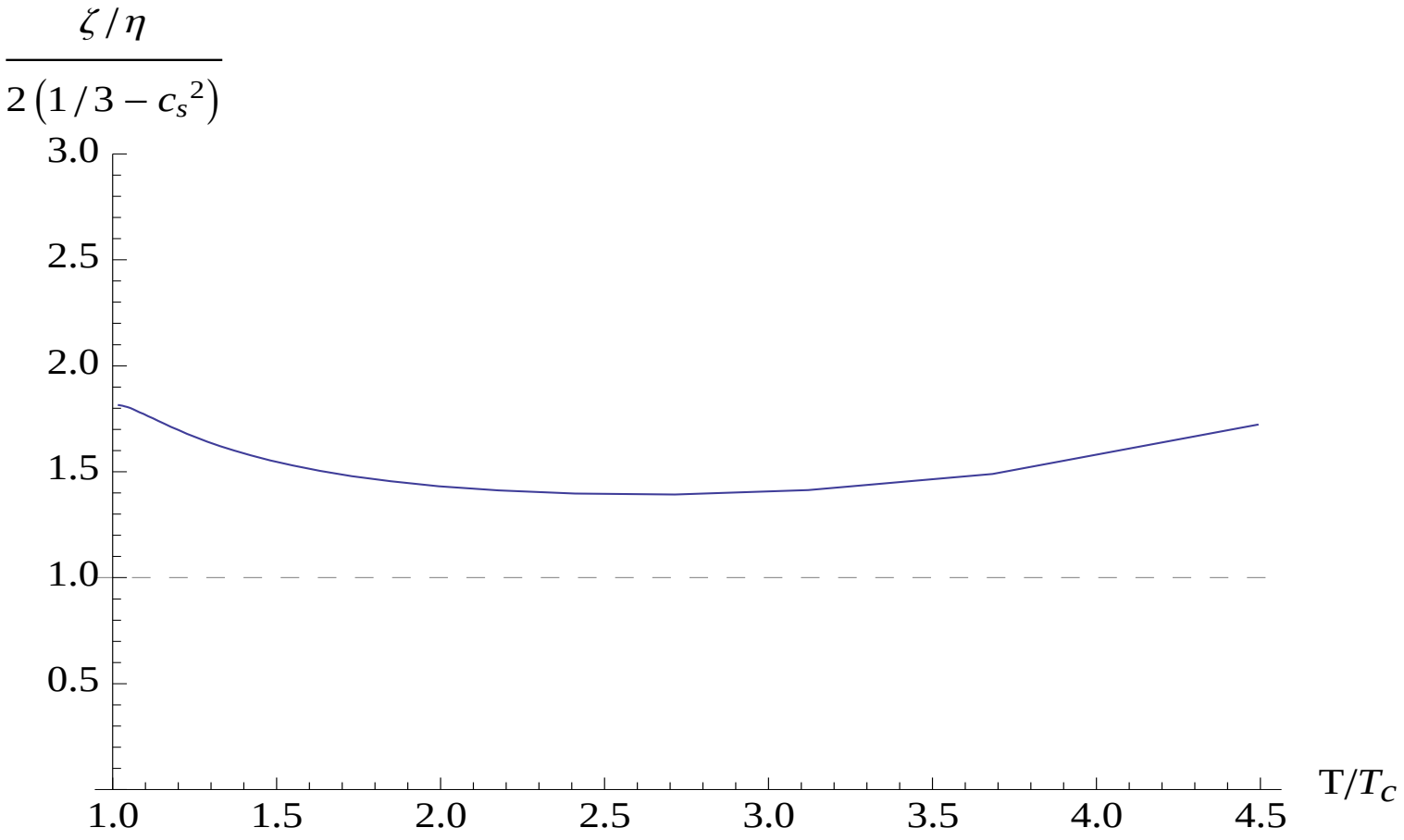

The sum rule method

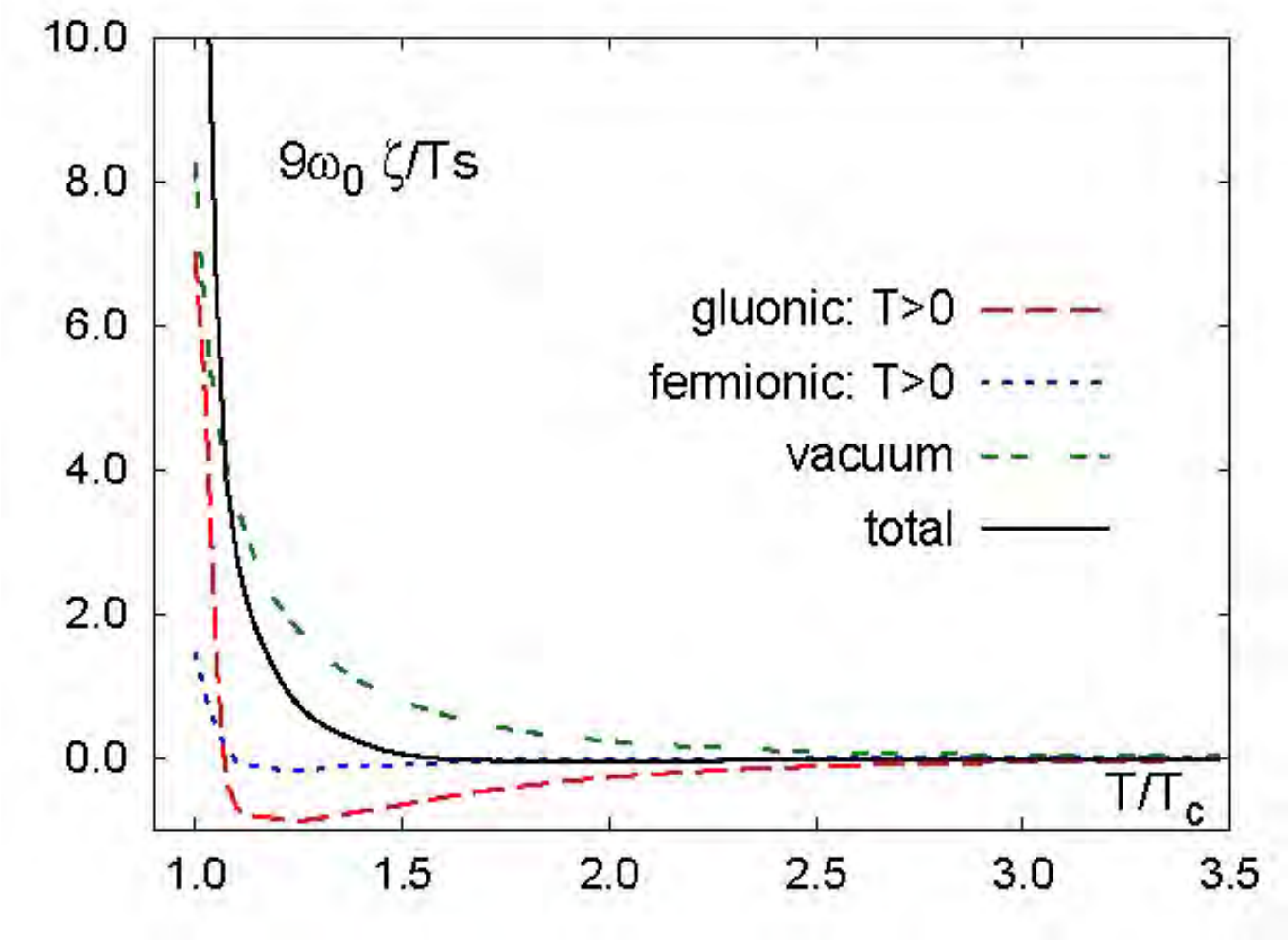

Karsch+Kharzeev+Tuchin, 2008

- A rise near the phase transition but the scale cannot be fixed.

Elliptic Flow vs bulk viscosity

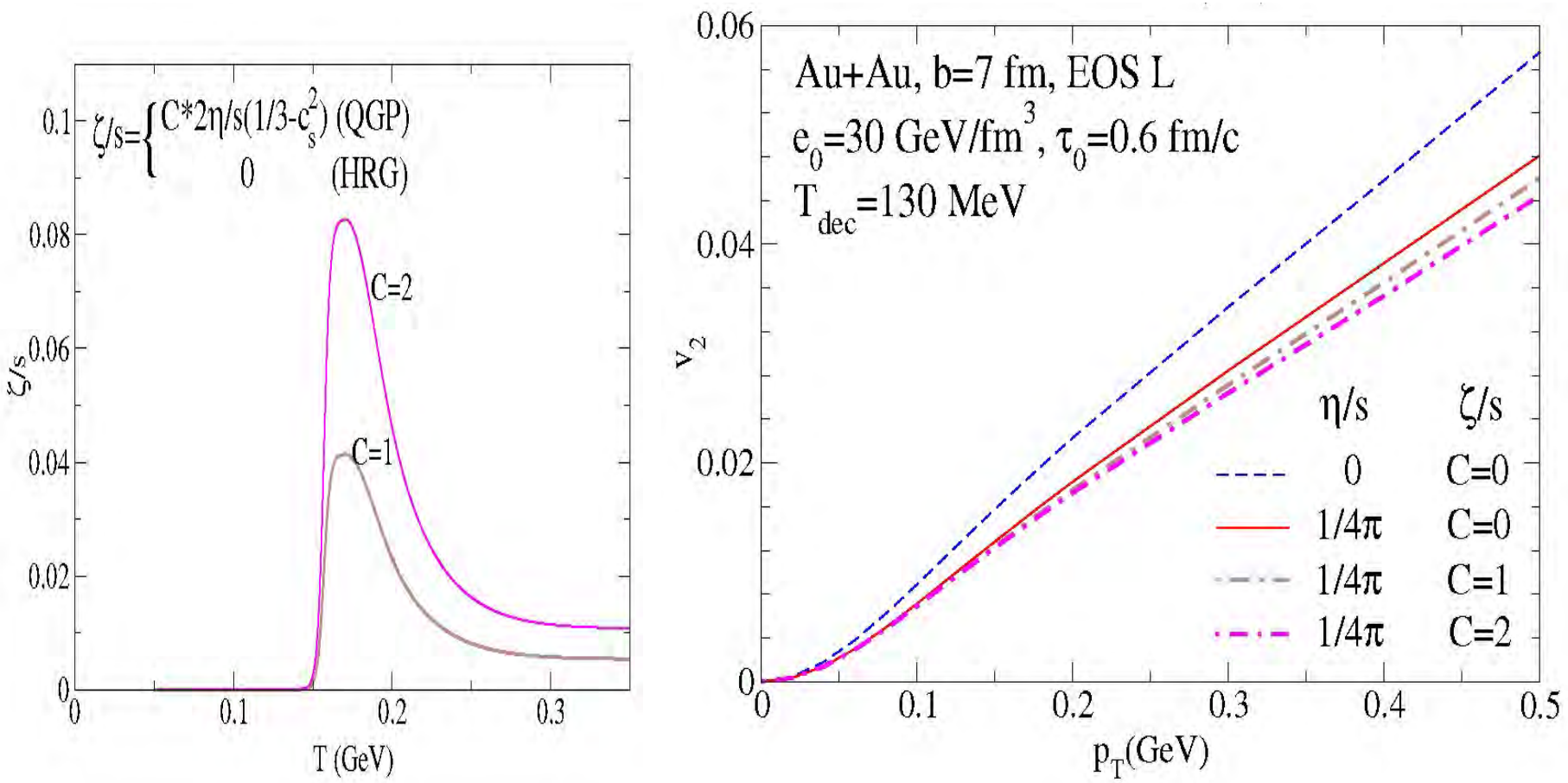

U Heinz+H.Song 2008

Spatial string tension

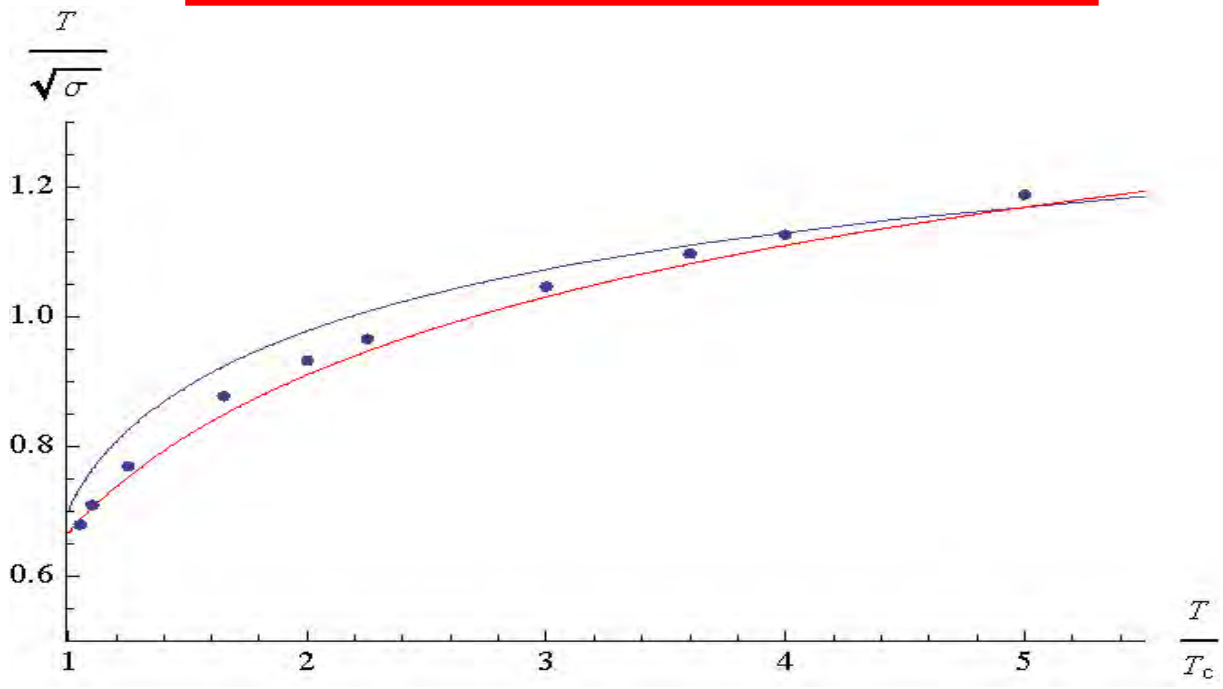

G. Boyd et al. 1996

- The blue line is the spatial string tension as calculated in Improved hQCD, with no additional fits.

Nitti (unpublished) 2009

- The red line is a semi-phenomenological fit using

$$\frac{T}{\sqrt{\sigma_s}} = 0.51 \left[\log\frac{\pi T}{T_c} + \frac{51}{121}\log\left(2\log\frac{\pi T}{T_c}\right)\right]^{\frac{2}{3}}$$

Alanen+Kajantie+Suur-Uski, 2009

Heavy quarks, energy loss and Langevin diffusion

- An important class of probes in Heavy ion collisions are heavy quarks.

- They are heavy and relatively easily identifiable from end products.

- They can provide useful "localized" information about the quark-gluon fireball in a heavy-ion collision.

- They have not been so prominent in the initial phases of RHIC due to energy availability.

- They are becoming more prominent recently and they play a leading role now both at RHIC and LHC, complementing the collective observables.

Brownian Motion and Langevin Dynamics

• Heavy particles moving inside a thermal bath undergo Brownian motion: once in a while they collide with fluid particles and suddenly change path.

• This phenomenon has an elegant description in terms of the (local) Langevin equation which in its simplest form is

$$\frac{dp^i(t)}{dt} = -\eta^{ij}\ p^j(t) + \xi^i(t) \quad , \quad \langle \xi^i(t) \rangle = 0 \quad , \quad \langle \xi^i(t)\xi^j(t') \rangle = 2\kappa^{ij}\ \delta(t-t')$$

η^{ij} is an average "viscous" (dissipative) force

κ^{ij} is the diffusions coefficients.

• Physically both of them have a common origin: the interactions of the heavy probe with the heat-bath.

• The first describes the averaged out (smooth) motion, while the second the (stochastic) fluctuations around the average motion.

• The Langevin equation is a stochastic equation and as such makes sense only in a (time) discretized form (Itô calculus).

The Kramers Equation

• The Brownian motion induced by the Langevin equation can be remodeled as an evolution in phase space

• Let $P(x^i, p^i, t)\ d^3x d^3p$ be the probability of an ensemble of probes. The Langevin evolution translates to

$$\left(\frac{\partial}{\partial t} + \frac{\vec{p}}{E}\cdot\frac{\partial}{\partial \vec{x}}\right) P = \frac{\partial}{\partial p^i}\left(\eta^{ij} p^j + \frac{1}{2}\frac{\partial}{\partial p^j}\kappa^{ij}\right) P$$

• The equilibrium distribution in a homogeneous ensemble is expected to satisfy,

$$\frac{\partial}{\partial p^i}\left(\eta^{ij} p^j + \frac{1}{2}\frac{\partial}{\partial p^j}\kappa^{ij}\right) P = 0$$

• It will be a (non-relativistic) Boltzmann distribution $P \sim e^{-\frac{E}{T}}$ if the Einstein relation holds

$$\kappa^{ij} = 2MT\ \eta^{ij} \quad , \quad E = \frac{\vec{p}^2}{2M}$$

where T is the bath temperature.

Solution of the Langevin Equation

$$\dot{p} = -\eta p + \xi \quad , \quad \langle \xi(t)\xi(t') \rangle = \kappa \delta(t - t')$$

with solution

$$p(t) = p(0)e^{-\eta t} + \int_0^t dt' e^{\eta(t'-t)} \xi(t')$$

$$\langle p(t) \rangle = p(0)e^{-\eta t}$$

$$\langle p(t)^2 \rangle - \langle p(t) \rangle^2 = \int_0^t dt' e^{\eta(t'-t)} \int_0^t dt'' e^{\eta(t''-t)} \langle \xi(t)\xi(t') \rangle = \frac{\kappa}{2\eta} \left(1 - e^{-2\eta t}\right)$$

- Long times: $t \gg \frac{1}{\eta}$: $\langle p \rangle \to 0$ and $\langle \Delta p^2 \rangle \to \frac{\kappa}{2\eta}$.
- Short times: $t \ll \frac{1}{\eta}$: $\langle p \rangle \simeq p(0)$ and $\langle \Delta p^2 \rangle \to \kappa\ t$.

- Consider a multidimensional motion and separate

$$\vec{p} = p^{||} + p^{\perp} \quad , \quad \vec{v} \cdot p^{\perp} = 0$$

- The transverse momentum obeys a Langevin process with (by definition) $\langle p^{\perp} \rangle = 0$ but with an increasing dispersion

$$\langle (\Delta p^{\perp})^2 \rangle \to 2\kappa^{\perp} \; t$$

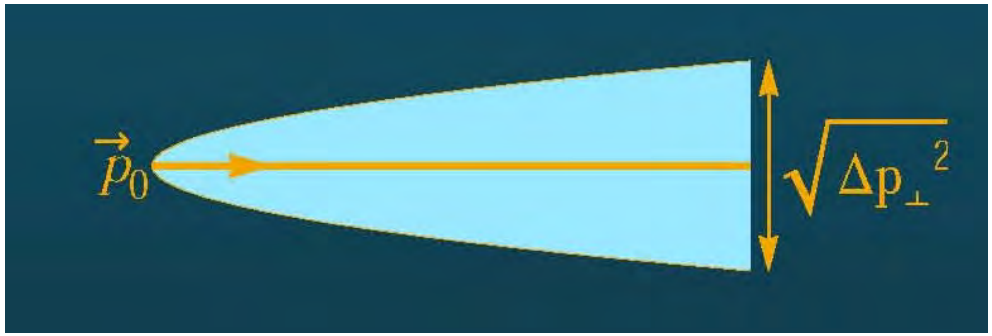

- This defines the "jet quenching parameter"

$$\widehat{q} = \frac{\langle (\Delta p^{\perp})^2 \rangle}{vt} = 2\frac{\kappa^{\perp}}{v}$$

- This is a "local" (in time) transport coefficient.

Jet quenching influence

• A non-zero value for the jet quenching parameter for light quarks is essential in explaining the RHIC data. Below we show the nuclear modification factor

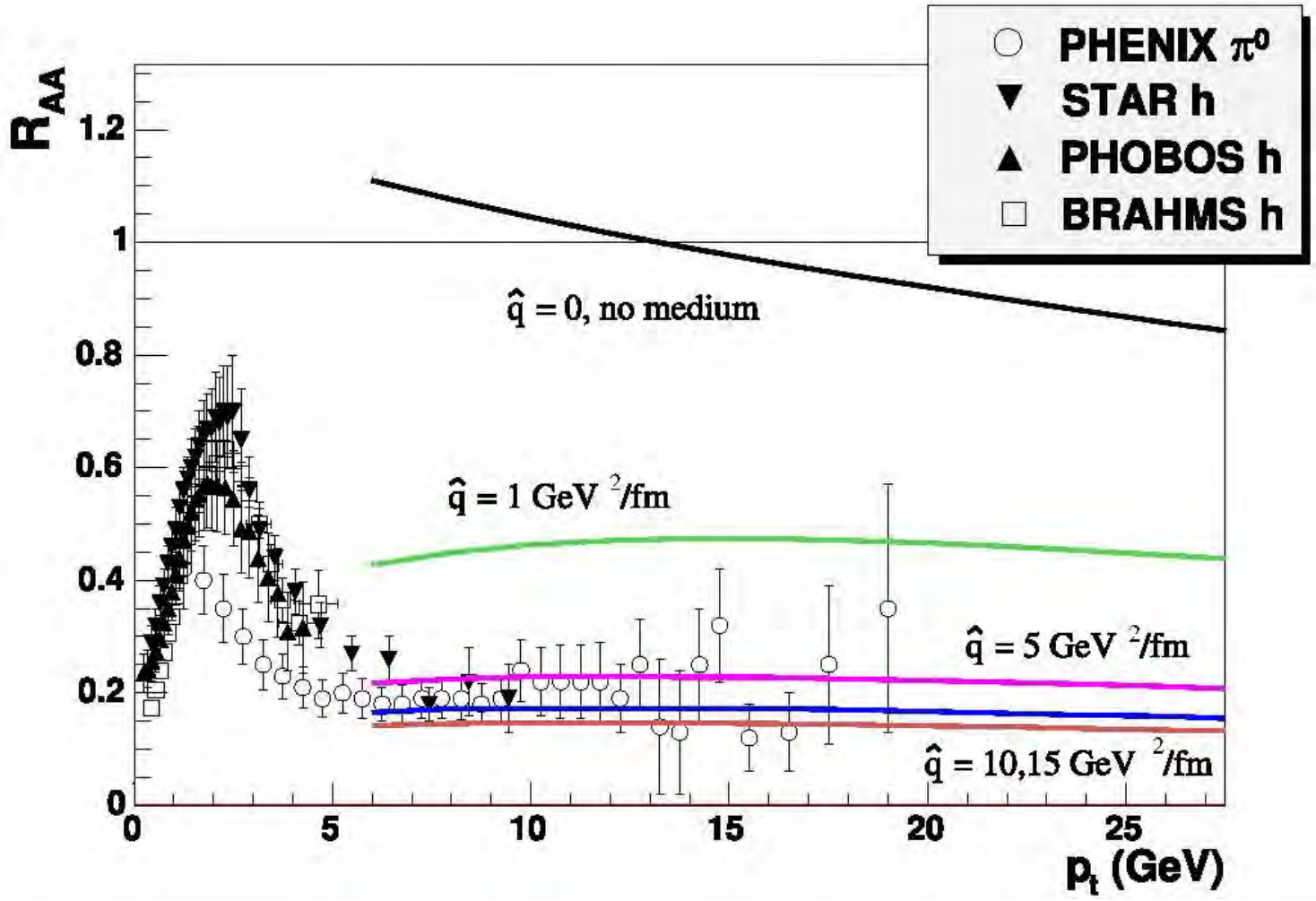

Eskola et al. 2005

The generalized Langevin equation

• For our purposes a more general analysis is necessary. We consider the coupling of the coordinates of the probe with the bath degrees of freedom

$$S_{int} = \int d\tau \vec{X}(\tau) \cdot \vec{\mathcal{F}}$$

where $\mathcal{F}^i$ is the force from the heat-bath.

• The generalized Langevin equation in general has memory and reads

$$\dot{P}^i + \int_0^\infty dt' \gamma^{ij}(t') \dot{X}^j(t-t') = \xi^i(t) \ , \ \dot{\gamma}^{ij}(t) = G_R^{ij}(t) \ , \ \langle \xi^i(t) \xi^j(0) \rangle = G_{sym}^{ij}(t)$$

where

$$G_R(t) = -i\theta(t) \langle [\mathcal{F}(t), \mathcal{F}(0)] \rangle \quad , \quad G_A(t) = i\theta(-t) \langle [\mathcal{F}(t), \mathcal{F}(0)] \rangle$$

$$G_{sym}(t) = -\frac{i}{2} \langle \{\mathcal{F}(t), \mathcal{F}(0)\} \rangle \quad , \quad G_{anti-sym}(t) = -\frac{i}{2} \langle [\mathcal{F}(t), \mathcal{F}(0)] \rangle$$

$$\langle T\mathcal{F}(t)\mathcal{F}(0) \rangle \equiv \theta(t) \langle \mathcal{F}(t)\mathcal{F}(0) \rangle + \theta(-t) \langle \mathcal{F}(0)\mathcal{F}(t) \rangle = G_{sym} + \frac{1}{2}(G_R + G_A)$$

• The main goal is to use holography in order to evaluate G_{sym} and G_R for the forces of interest in QGP

The local limit

- For $t \gg t_c$ the autocorrelation time of the force

$$\int_0^\infty dt' \gamma(t') \dot{X}(t-t') \to \eta \dot{X}(t) \quad , \quad \eta = \int_0^\infty dt' \gamma(t')$$

$$G_{sym}(t-t') \to \kappa \delta(t-t') \quad , \quad \kappa = \int_0^\infty dt \; G_{sym}(t)$$

$$\dot{P} + \eta \dot{X} = \xi \quad \to \quad \dot{P} + \eta_D P = \xi \quad , \quad \eta_D = \frac{\dot{X}}{P}\eta = \frac{\eta}{\gamma M}$$

- In Fourier space

$$\kappa = G_{sym}(\omega = 0) \quad , \quad \eta = -\lim_{\omega \to 0} \frac{Im \; G_R(\omega)}{\omega}$$

- The relation between G_R and G_R is ensemble-dependent. For a thermal ensemble

$$G_{sym}(\omega) = \coth\left(\frac{\omega}{2T}\right) Im \; G_R(\omega) \quad \Rightarrow \quad \kappa = 2T\eta = 2MT\eta_D$$

we recover the non-relativistic Einstein relation.

The holographic strategy

• To determine the stochastic motion of heavy quarks we must therefore calculate the force correlator in QCD as

$$e^{iS_{eff}} = \langle e^{i\int X\mathcal{F}} \rangle$$

• We will calculate them using a holographic dual.

1. We must identify the force operator $\mathcal{F}$.

2. We must solve the classical equations of motion

3. Calculate the correlators from the boundary on-shell action using the Son-Starinets prescription for the real-time correlators.

The holographic setup

• There is a 5D bulk described by a general 5D black hole with metric (in the string frame)

$$ds^2 = b^2(r)\left[\frac{dr^2}{f(r)} - f(r)dt^2 + d\vec{x}^2\right]$$

• The boundary is at

$$r \to 0 \quad , \quad f \to 1 \quad , \quad b \to \frac{\ell}{r} + \cdots$$

and at the BH horizon

$$r \to r_h \quad , \quad f(r_h) = 0 \quad , \quad 4\pi T = |\dot{f}(r_h)|$$

• This is the holographic description of a general strongly coupled plasma (deconfined phase) in a heat bath.

Classical Heavy quark motion

• A heavy quark is modeled by a string moving in the BH background with (constant) velocity $\vec{v}$.

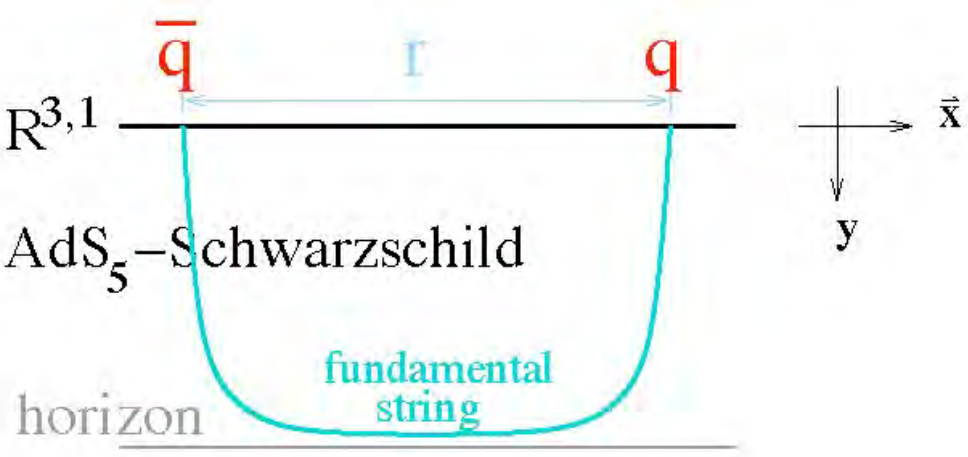

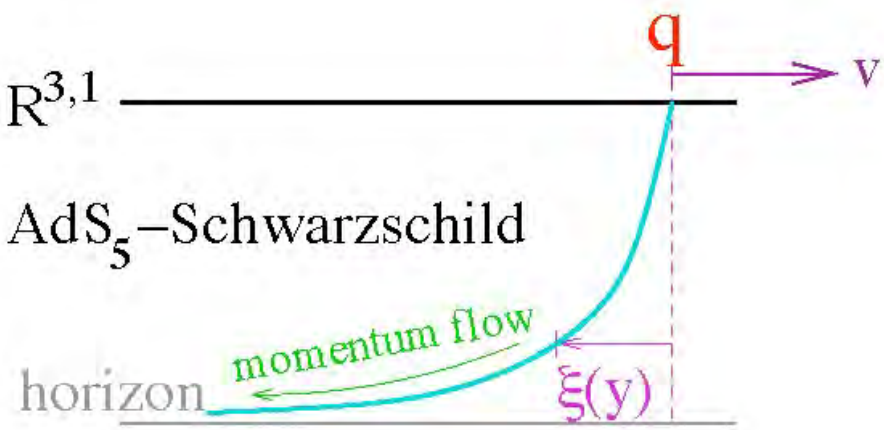

Herzog+Karch+kovtun+Kozcac+Yaffe, Gubser
CasalderreySolana+Teaney, Liu+Rajagopal+Wiedeman

• The dynamics of the string is given by the Nambu-Goto action

$$S_{NG} = -\frac{1}{2\pi\ell_s^2}\int d^2\xi\sqrt{\det\ \hat{g}} \quad , \quad \hat{g}_{\alpha\beta} = g_{\mu\nu}\ \partial_\alpha X^\mu \partial_\beta X^\nu$$

The drag force

- The classical dragging string solution is

$$X^{\perp}=0 \quad , \quad X^{||}=vt+\xi(r) \quad , \quad \xi(0)=0$$

$$\xi'(r)=\frac{C}{f(r)}\sqrt{\frac{f(r)-v^2}{b^4(r)f(r)-C^2}} \quad , \quad f(r_s)=v^2 \quad , \quad C=b^2(r_s)f(r_s)$$

- The "drag" force is in the longitudinal direction

$$\frac{dp^{||}}{dt}=-\frac{b^2(r_s)}{2\pi\ell_s^2}\,v=-\eta_D^{class}p^{||} \quad , \quad \eta_D^{class}=\frac{1}{M\gamma}\frac{b^2(r_s)}{2\pi\ell_s^2} \quad , \quad \gamma=\frac{1}{\sqrt{1-v^2}}$$

Gursoy+Kiritsis+Michalogiorgakis+Nitti,2009

The world-sheet black hole

- Change coordinates to

$$t = \tau + \zeta(r) \quad , \quad \zeta' = \frac{v\xi'}{f - v^2}$$

and write the induced world-sheet metric as

$$ds^2 = b^2(r)\left[-(f(r) - v^2)d\tau^2 + \frac{b^4(r)}{b^4(r)f(r) - C^2}dr^2\right] \quad ,$$

- This has a (world-sheet) horizon at $r = r_s$.

- It is an asymptotically AdS_2, two-dimensional black-hole.

- The Hawking temperature can be calculated to be

$$T_s = \frac{1}{4\pi}\sqrt{f(r_s)f'(r_s)\left[4\frac{b'(r_s)}{b(r_s)} + \frac{f'(r_s)}{f(r_s)}\right]}$$

- In general T_s depends on T, Λ, v. In the conformal case, $T_s = \frac{T}{\sqrt{\gamma}}$.

Giecold+Iancu+Mueller, 2009

$$T_s \to T \quad as \quad v \to 0 \quad , \quad T_s \to \frac{T}{\sqrt{\gamma}} \quad as \quad v \to 1$$

- In all examples we analyzed, $T_s \leq T$.

- We always have $0 \leq r_s \leq r_h$. $r_s = 0$ when $v = 1$ and $r_s = r_h$ when $v = 0$.

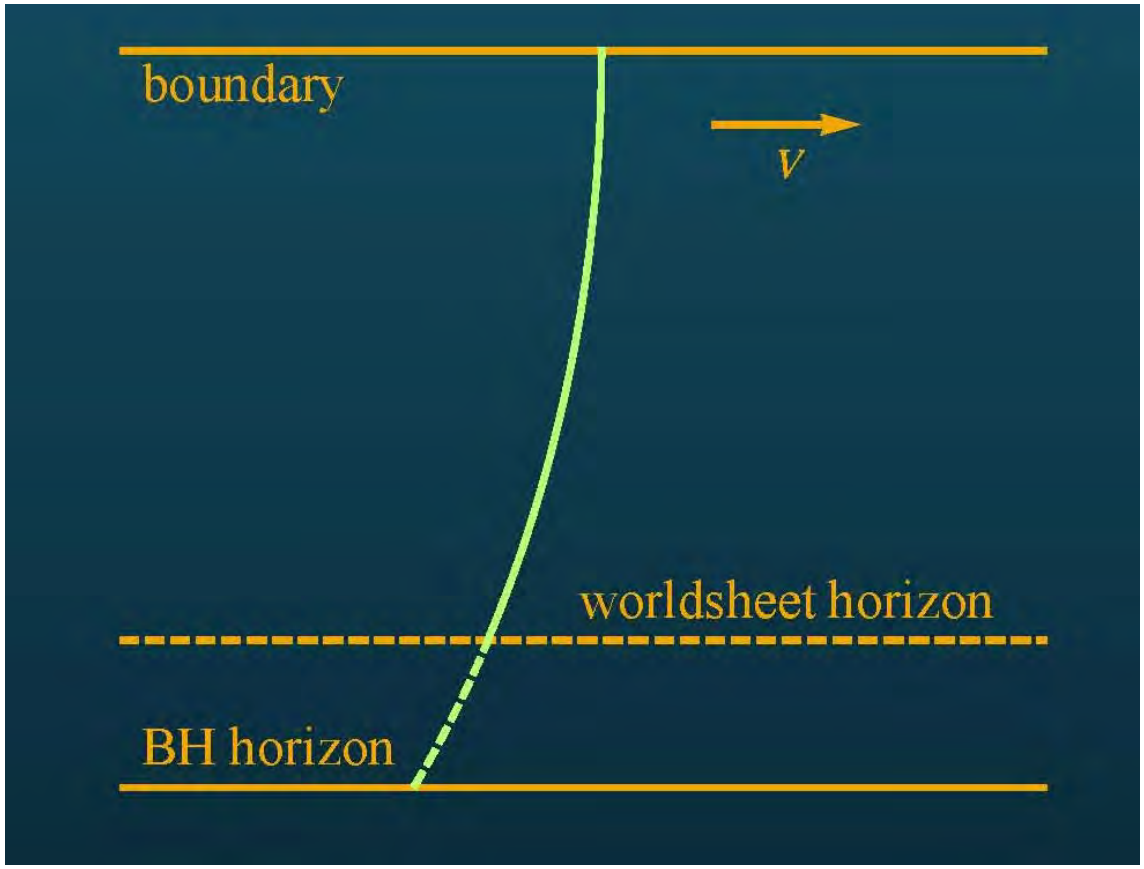

Fluctuations of the trailing string

• So far we have calculated the average $damped$ motion of the trailing string.

• To study the fluctuations we set

$$\vec{X}(r,t) = (vt + \xi(r))\frac{\vec{v}}{v} + \delta\vec{X}(r,t)$$

• From the boundary coupling

$$S_{bdr} = \int dt\ X_i(t)\ \mathcal{F}^i(t) \simeq S^0_{bdr} + \int dt\ \delta X_i(t)\ \mathcal{F}^i(t)$$

• Correlators of $\mathcal{F}$ in the dual QFT are given by holographic correlators of $\delta X_i(t)$ in the bulk string theory.

• They can be obtained according to the standard holographic prescriptions by solving the second order fluctuation equations for $\delta X_i(t)$.

• For the retarded correlator we must impose "incoming" boundary conditions at the world-sheet horizon and unit normalization at the boundary.

- Introducing the Fourier modes of fluctuations

$$\delta\vec{X}(r,t) = e^{i\omega\tau}\delta\vec{X}(r,\omega)$$

the second-order radial equations are of the form

$$\partial_r\left[\sqrt{(f-v^2)(b^4f-C^2)}\;\partial_r\left(\delta X^{\perp}\right)\right]+\frac{\omega^2b^4}{\sqrt{(f-v^2)(b^4f-C^2)}}\delta X^{\perp}=0$$

$$\partial_r\left[\frac{1}{Z^2}\sqrt{(f-v^2)(b^4f-C^2)}\;\partial_r\left(\delta X^{\parallel}\right)\right]+\frac{\omega^2b^4}{Z^2\sqrt{(f-v^2)(b^4f-C^2)}}\delta X^{\parallel}=0$$

$$Z(r)\equiv b(r)^2\sqrt{\frac{f(r)-v^2}{b(r)^4f(r)-C^2}}.$$

- They are different for longitudinal and transverse fluctuations.

World-Sheet Hawking temperature

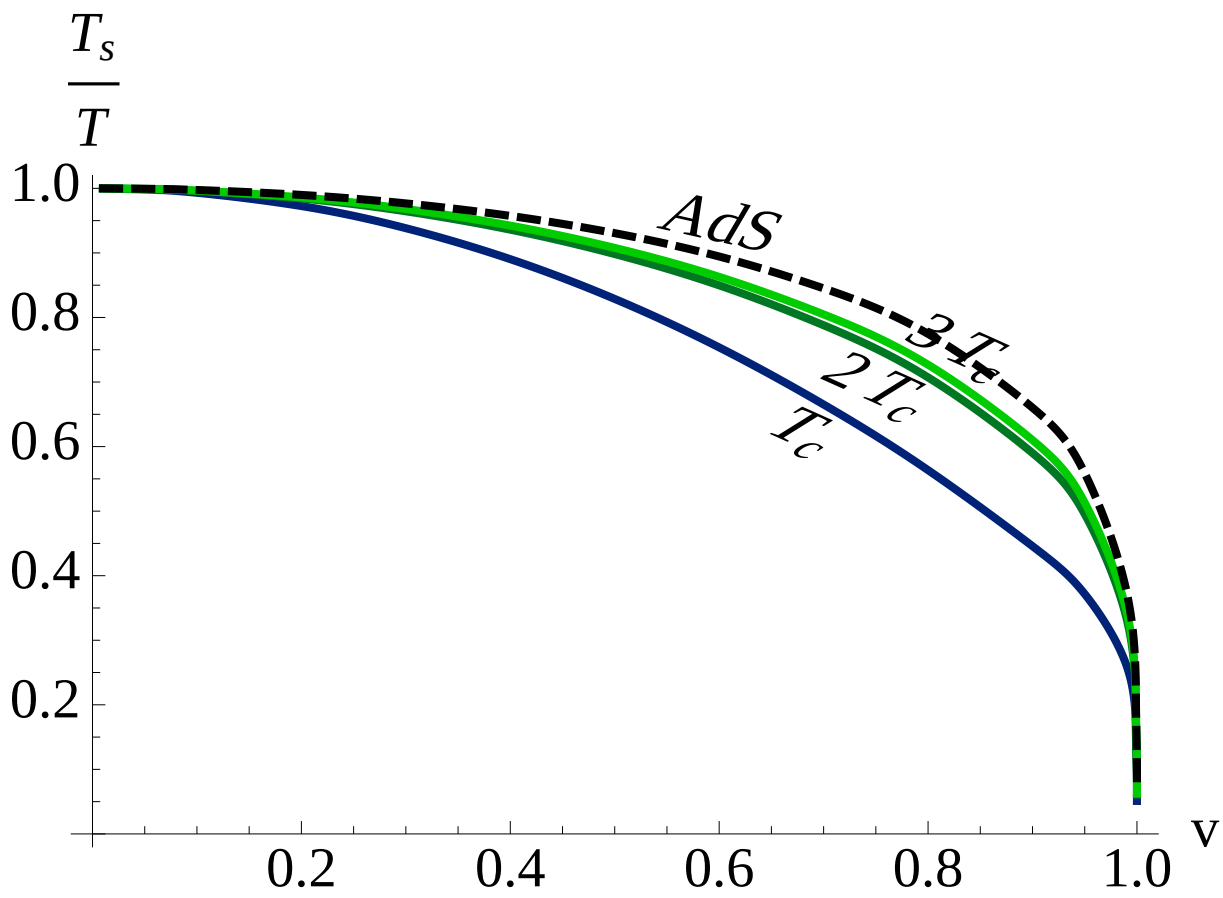

The ratio of the world-sheet temperature to the bulk black hole temperature, as a function of velocity, for different values of the bulk temperature. The dashed line indicates the AdS-Schwarzschild curve, $T_s = T/\sqrt{\gamma}$.

Asymmetry factor (Z)

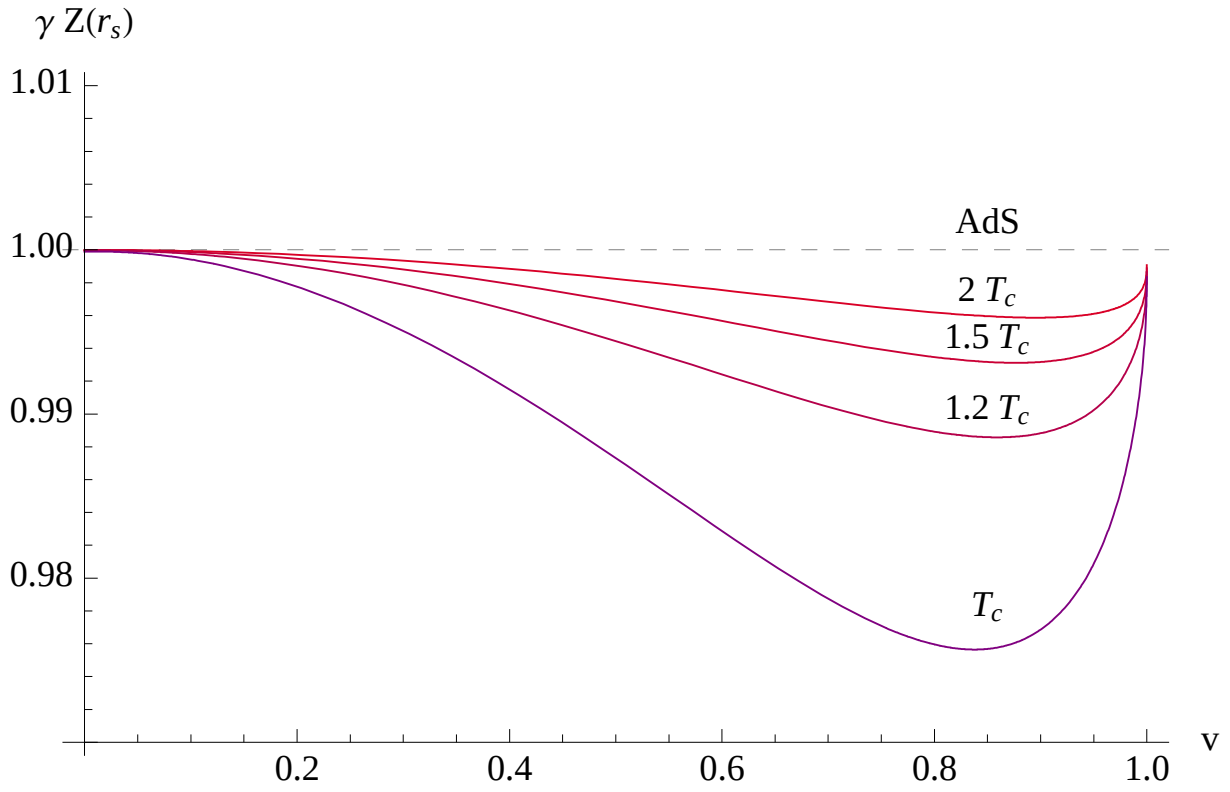

The function $\gamma Z(r_s)$ as a function of velocity, $(\gamma \equiv 1/\sqrt{1-v^2})$, computed numerically varying the velocity, at different temperatures. The dashed line represents the conformal limit, in which $\gamma Z = 1$ exactly.

Jet quenching parameters

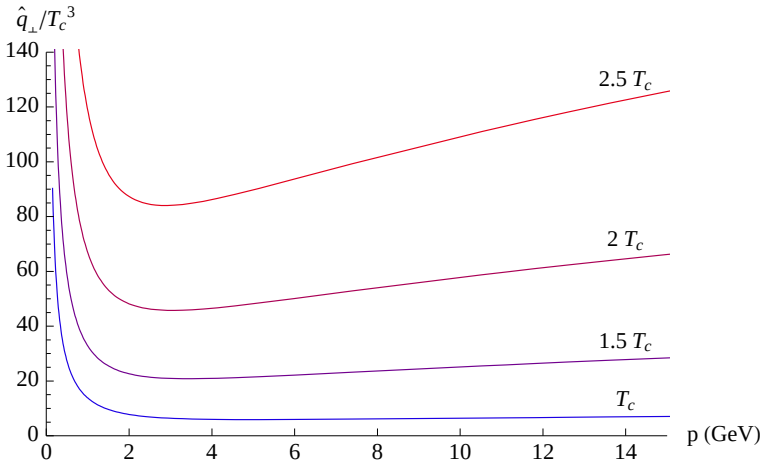

$\widehat{q}_\perp$ charm

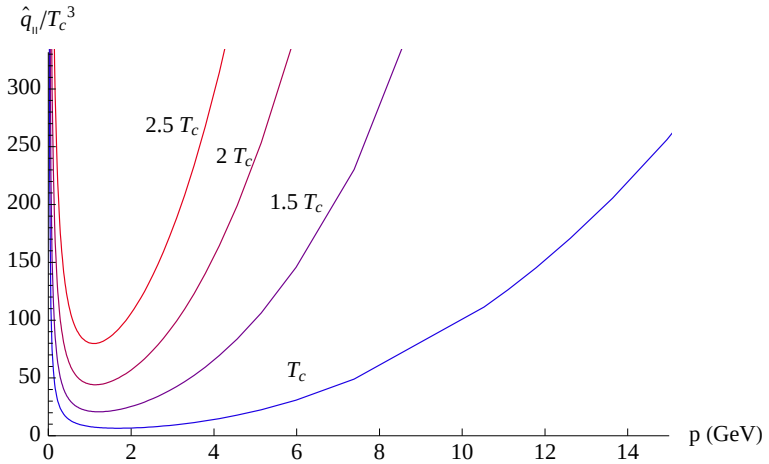

$\widehat{q}_{||}$ charm

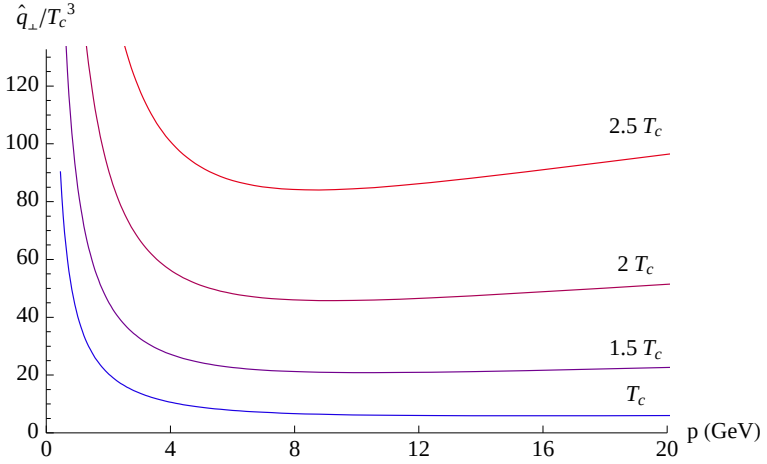

$\widehat{q}_\perp$ bottom

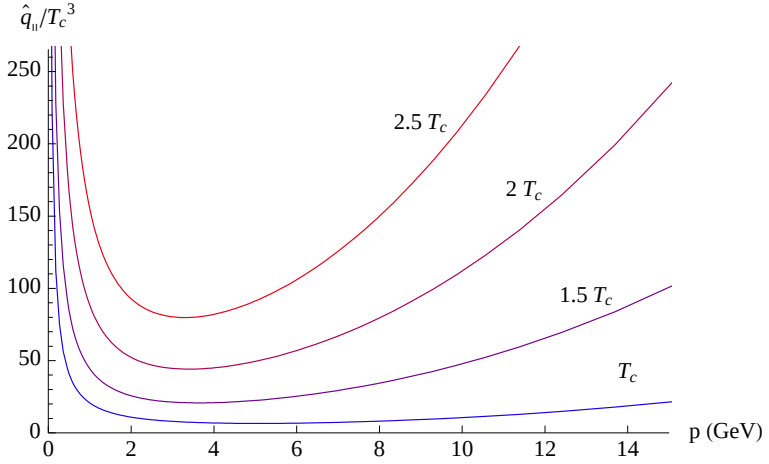

$\widehat{q}_{||}$ bottom

The quantities $\widehat{q}_\perp/T_c^3$ and $\widehat{q}_{||}/T_c^3$ plotted as a function of the quark momentum p. The plots for the charm and the bottom quark differ by a scaling of the horizontal direction.

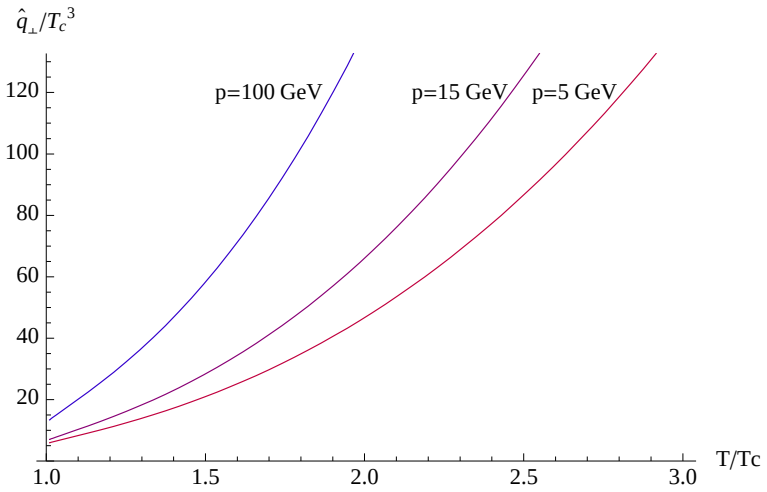

$\widehat{q}_\perp$ charm

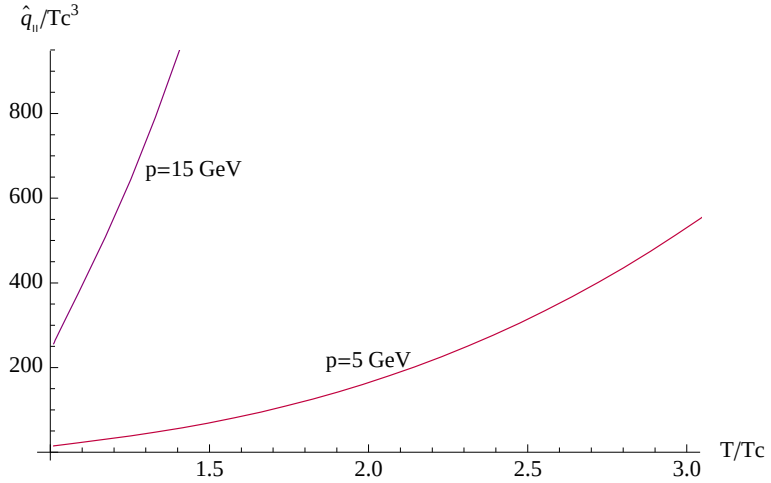

$\widehat{q}_{||}$ charm

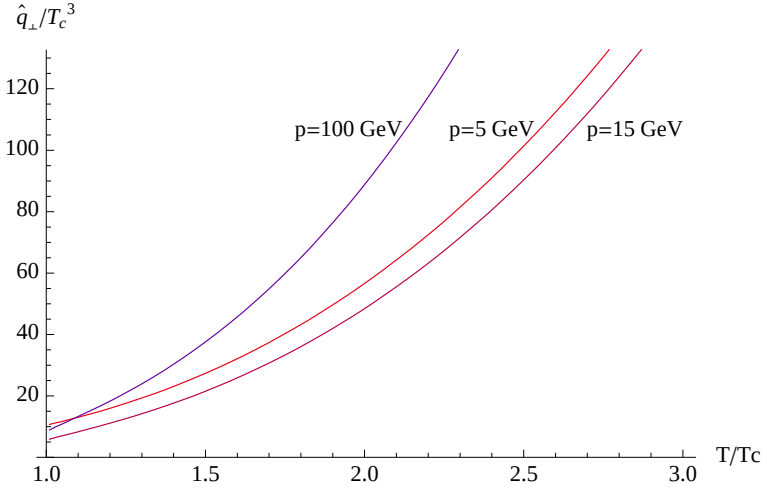

$\widehat{q}_\perp$ bottom

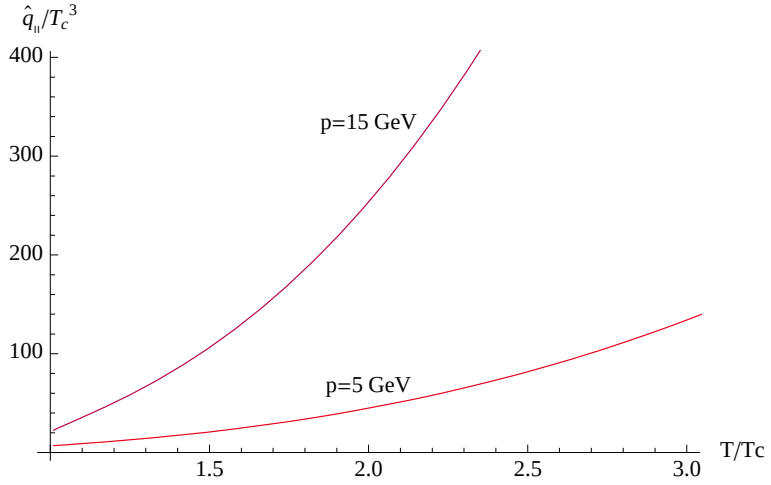

$\widehat{q}_{||}$ bottom

The jet-quenching parameters $\widehat{q}_\perp$ and $\widehat{q}_{||}$ plotted as a function of T/T_c, for different quark momenta.

Locality of Langevin evolution

- The validity of the local approximation demands that

$$t \gg t_{correlation} \sim \frac{1}{T_s}$$

- For $(\Delta p^{\perp})^2$ to be characterized by $\kappa^{\perp}$ we must have

$$t \ll t_{\text{relaxation}} \sim \frac{1}{\eta_D}$$

Therefore we need

$$\frac{1}{\eta_D} \gg \frac{1}{T_s}$$

If this fails we need the full non-local (in time) Langevin evolution.

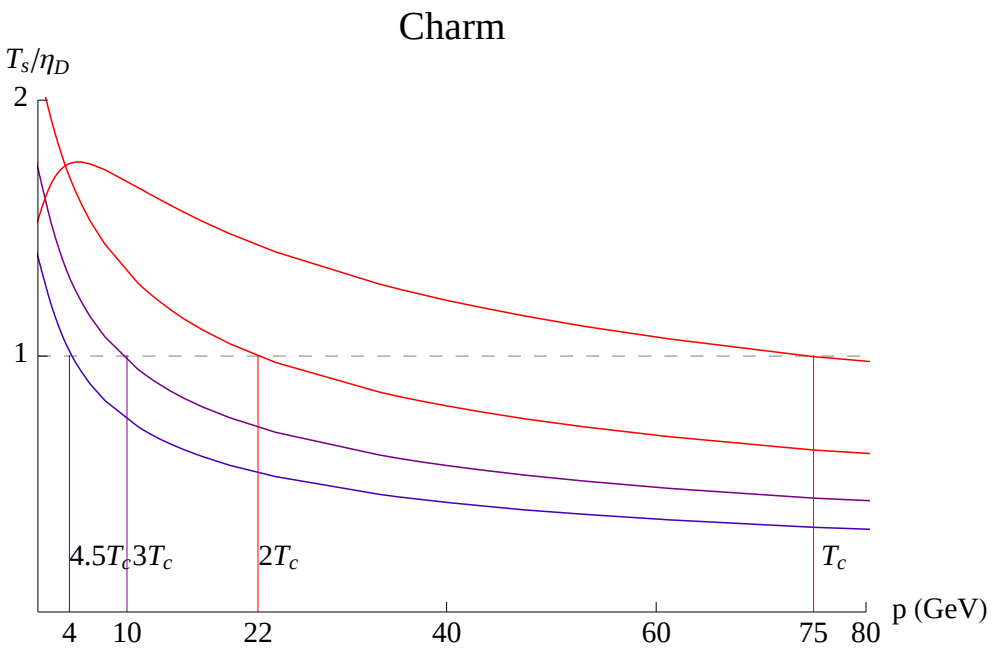

(a)

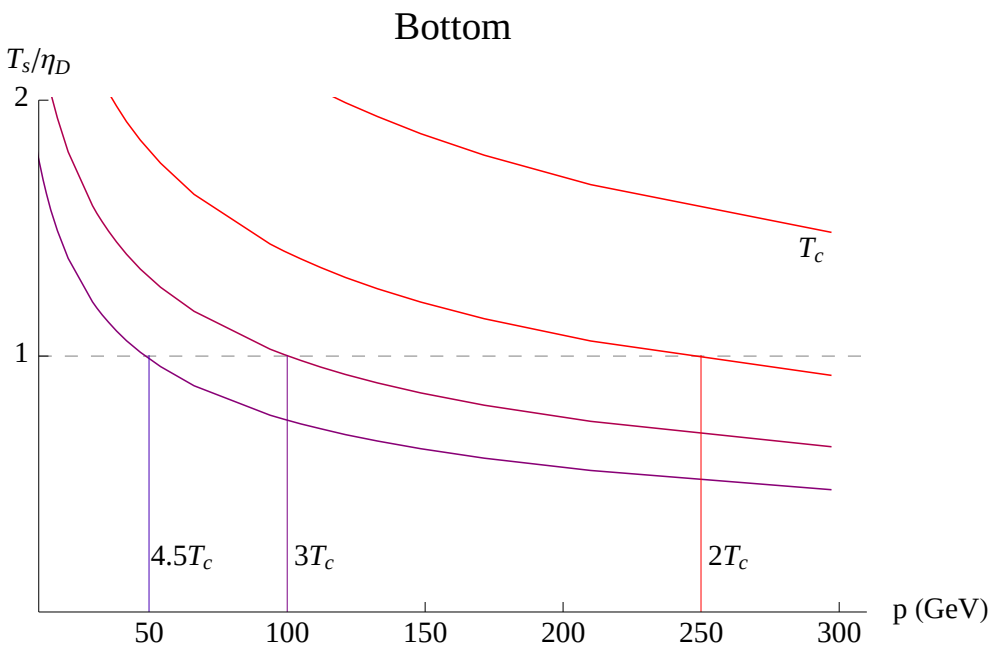

(b)

The quantity T_s/η_D is plotted against quark momentum, for different bulk temperatures. Figures refer to the charm and bottom quark, respectively. For each temperature, the validity of the local Langevin equation constrains p to the left of the corresponding vertical line, which marks the transition of T_s/η_D across unity.

Schwinger-Keldysh derivation

Consider a system with degrees of freedom $\{ Q \}$ and density matrix $\rho(Q, Q', t)$. that evolves as

$$\rho(Q_f, Q'_f, t) = U(Q_f, Q_0, t, t_0)\rho(Q_0, Q'_0, t_0)U^\dagger(Q'_f, Q'_0, t, t_0)$$

where the evolution operator is given by the path integral

$$U(Q_f, Q_0, t, t_0) = \int DQ\ e^{iS(Q)} = \int DQ\ e^{i\int_{t_0}^{t} L(Q,\dot{Q})} \quad , \quad Q(t_0) = Q_0 \quad , \quad Q(t) = Q_f$$

Therefore the density matrix is a double path integral

$$\rho(Q_f, Q'_f, t) = \int DQ \int DQ'\ e^{i(S(Q)-S(Q'))}\rho(Q_0, Q'_0, t_0)$$

It is natural to double the fields, call $Q = Q_+$, $Q' = Q_-$, and consider $Q_\pm$ the values of Q on the double (Keldysh) contour

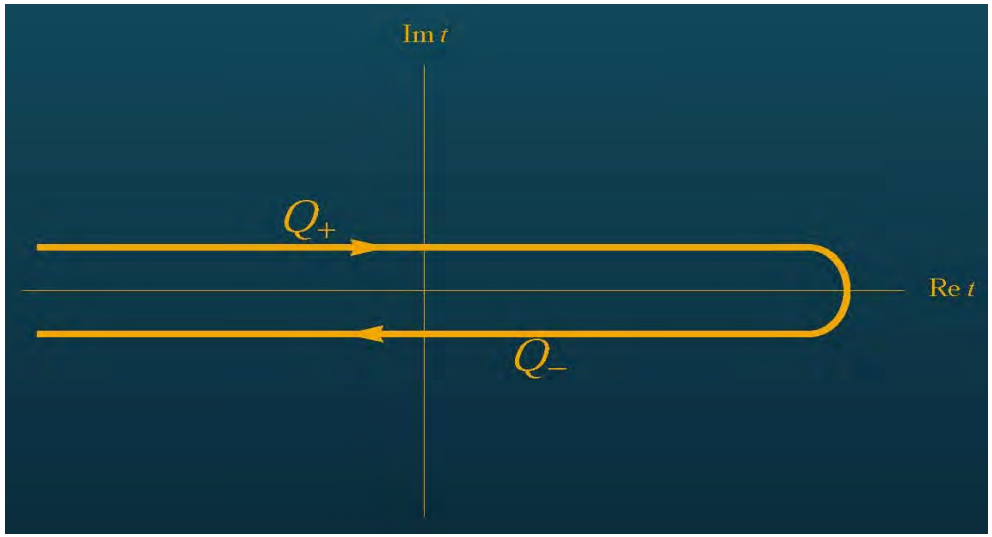

We now consider a single particle described by $X(t)$, and a statistical ensemble, described by a QFT with degrees of freedom $\Phi(x,t)$. We assume a linear interaction between X and some functional $\mathcal{F}(t)$ of the QFT fields Φ.

$$S = S_0(X) + S_{QFT}(\Phi) + S_{int}(X,\Phi) \quad , \quad S_{int}(X,\Phi) = \int dt\ X(t)\mathcal{F}(t)$$

We assume that the particle starts at $X = x_i$ at $t_i = -\infty$

$$\rho_i = \delta(X - x_i)\delta(X' - x_i)\rho_i(\Phi,\Phi')$$

We would like to compute the reduced density matrix at time t:

$$\rho(X,X',t) = Tr_\Phi \rho(X,X',\Phi,\Phi',t)$$

That we can now write as a path integral using a doubled set of fields

$$\rho(X,X',t) = \int DX_+ \int DX_-\ e^{iS_0(X_+)-iS_0(X_-)} \int D\Phi_+ D\Phi_-\ e^{iS_+(X_+,\Phi_+)-iS_-(X_-,\Phi_-)}\rho_i(\Phi_+,\Phi_-)$$

where the the trace in the QFT path integral is obtained by setting $(\Phi_+)_f = (\Phi_-)_f$ and

$$S_\pm = S_{QFT} + \int X\mathcal{F}$$

Therefore the effective density matrix evolves according to the effective action

$$S_{eff}(X_+,X_-) = S_0(X_+) - S_0(X_-) + S_{IF}(X_+,X_-)$$

$$e^{iS_{IF}} = \langle e^{i\int X_+\mathcal{F}_+ - i\int X_-\mathcal{F}_-}\rangle_{\text{QFT ensemble}}$$

Feynman+Vernon, 1963

We expand the exponential to quadratic order

$$\langle e^{i\int X_+\mathcal{F}_+ - i\int X_-\mathcal{F}_-}\rangle_{\text{QFT ensemble}} \simeq 1 + i\int dt\ \langle\mathcal{F}(t)\rangle(X_+ - X_-) -$$

$$-\frac{i}{2}\int dt\int dt'\left[-X_+(t)\ i\langle\mathcal{F}_+(t)\mathcal{F}_+(t')\rangle X_+(t') + X_-(t)\ i\langle\mathcal{F}_-(t)\mathcal{F}_+(t')\rangle X_+(t') + \right.$$

$$\left. + X_+(t)\ i\langle\mathcal{F}_+(t)\mathcal{F}_-(t')\rangle X_-(t') - X_-(t)\ i\langle\mathcal{F}_-(t)\mathcal{F}_-(t')\rangle X_-(t')\right]$$

$$\simeq \exp\left[i\int dt\ \langle\mathcal{F}(t)\rangle(X_+ - X_-) - \frac{i}{2}\int X_a(t)\ G_{ab}(t,t')X_b(t')\right]$$

with

$$G_{ab}(t,t') \equiv i\langle\mathcal{P}\mathcal{F}_a(t)\mathcal{F}_b(t')\rangle$$

with $\mathcal{P}$ being path ordering along the keldysh contour:

- $+$ operators are time-ordered, $-$ operators are anti-time-ordered
- $-$ operators are always in the future of $+$ operators.

$$G_{++}(t,t') = -i\left\langle T\,\mathcal{F}_+(t)\mathcal{F}_+(t')\right\rangle \qquad G_{-+}(t,t') = -i\left\langle \mathcal{F}_-(t)\mathcal{F}_+(t')\right\rangle$$

$$G_{+-}(t,t') = -i\left\langle \mathcal{F}_-(t')\mathcal{F}_+(t)\right\rangle \qquad G_{--}(t,t') = -i\left\langle \overline{T}\,\mathcal{F}_-(t)\mathcal{F}_-(t')\right\rangle$$

The Keldysh propagators can be written in terms of the standard ones:

$$G_R(t) = -i\theta(t)\langle[\mathcal{F}(t),\mathcal{F}(0)]\rangle \quad , \quad G_A(t) = i\theta(-t)\langle[\mathcal{F}(t),\mathcal{F}(0)]\rangle$$

$$G_{sym}(t) = -\frac{i}{2}\langle\{\mathcal{F}(t),\mathcal{F}(0)\}\rangle \quad , \quad G_{anti-sym}(t) = -\frac{i}{2}\langle[\mathcal{F}(t),\mathcal{F}(0)]\rangle$$

$$\langle T\mathcal{F}(t)\mathcal{F}(0)\rangle \equiv \theta(t)\langle\mathcal{F}(t)\mathcal{F}(0)\rangle + \theta(-t)\langle\mathcal{F}(0)\mathcal{F}(t)\rangle = G_{sym} + \frac{1}{2}(G_R + G_A)$$

$$G_{++} = G_{sym} + \frac{1}{2}(G_R + G_A) \quad , \quad G_{--} = G_{sym} - \frac{1}{2}(G_R + G_A)$$

$$G_{+-} = G_{sym} + \frac{1}{2}(-G_R + G_A) \quad , \quad G_{-+} = G_{sym} + \frac{1}{2}(G_R - G_A)$$

$$G_{++} + G_{--} - G_{+-} - G_{-+} = 0$$

Using this we can rewrite the effective action as

$$S_{eff} = S_0(X_+) - S_0(X_-) + \int (X_+ - X_-)G_R(X_+ + X_-) + \frac{1}{2}(X_+ - X_-)G_{\text{sym}}(X_+ - X_-)\int$$

We now define

$$X_{\text{class}} = \frac{1}{2}(X_+ + X_-) \quad , \quad y = X_+ - X_-$$

In the semiclassical limit $y \ll X_{\text{class}}$ and we can expand

$$S_0(X_+) - S_0(X_-) \simeq \int dt \ \frac{\delta S_0}{\delta X_{\text{class}}} \ y + \mathcal{O}(y^3)$$

to obtain

$$S_{eff} = \int dt \ y(t) \left[\frac{\delta S_0}{\delta X_{\text{class}}(t)} + \int dt' G_R(t,t') X_{\text{class}}(t') \right] + \frac{1}{2} \int dt \int dt' y(t) G_{\text{sym}}(t,t') y(t')$$

Therefore the X path integral becomes

$$Z = \int DX_{\text{classs}} \int Dy \ e^{i \int dt \ y(t) \left[\frac{\delta S_0}{\delta X_{\text{class}}(t)} + \int dt' G_R(t,t') X_{\text{class}}(t') \right] + \frac{1}{2} \int dt \int dt' y(t) G_{\text{sym}}(t,t') y(t')}$$

We integrate-in a gaussian variable $\xi(t)$ with variance G_{sym}. This will linearize the y integration

$$Z = \int D\xi \int DX_{\text{class}} \int Dy \exp \left[i \int dt \ y \left(\frac{\delta S_0}{\delta X_{\text{class}}} + G_R X_{\text{class}} - \xi \right) - \frac{1}{2} \xi G_{sym} \xi \right]$$

Integrating over y we obtain a δ functional,

$$Z = \int D\xi \int DX_{\text{class}} \ \delta \left(\frac{\delta S_0}{\delta X_{\text{class}}} + G_R X_{\text{class}} - \xi \right) \ e^{-\frac{1}{2} \xi G_{sym} \xi}$$

Therefore the path integral is localized in a solution of the generalized Langevin equation

$$\frac{\delta S_0}{\delta X_{\text{class}}(t)} + \int_{-\infty}^{t} dt' \ G_R(t,t') X_{\text{class}}(t') = \xi(t) \quad , \quad \langle \xi(t) \xi(t') \rangle = G_{\text{sym}}(t,t')$$

String fluctuations and force correlators

In the diagonal wold-sheet frame

$$S^{(2)}_{NG} = -\frac{1}{2\pi\ell_s^2}\int d\tau\ dr\ \frac{H^{\alpha\beta}}{2}\left[\frac{\partial_\alpha X^{||}\partial_\beta X^{||}}{Z^2} + \sum_{i=1}^{2}\partial_\alpha X_i^{\perp}\partial_\beta X_i^{\perp}\right]$$

and the fluctuation equations are

$$\partial_\alpha(H^{\alpha\beta}\partial_\beta)X^{\perp} = 0 \quad , \quad \partial_\alpha\left(\frac{H^{\alpha\beta}}{Z^2}\partial_\beta\right)X^{||} = 0$$

$$H^{\alpha\beta} = \begin{pmatrix} -\frac{b^4}{\sqrt{(f-v^2)(b^4f-C^2)}} & 0 \\ 0 & \sqrt{(f-v^2)(b^4f-C^2)} \end{pmatrix} \quad , \quad Z \equiv b^2\sqrt{\frac{f-v^2}{b^4f-C^2}}.$$

We look for harmonic solutions $\delta X(r,t) = e^{i\omega\tau}\ \delta X(r,\omega)$

$$\partial_r\left[\sqrt{(f-v^2)(b^4f-C^2)}\ \partial_r\left(\delta X^{\perp}\right)\right] + \frac{\omega^2 b^4}{\sqrt{(f-v^2)(b^4f-C^2)}}\delta X^{\perp} = 0$$

$$\partial_r\left[\frac{1}{Z^2}\sqrt{(f-v^2)(b^4f-C^2)}\ \partial_r\left(\delta X^{||}\right)\right] + \frac{\omega^2 b^4}{Z^2\sqrt{(f-v^2)(b^4f-C^2)}}\delta X^{||} = 0$$

- Near the boundary the equations is symmetric

$$\Psi'' - \frac{2}{r}\Psi' + \gamma^2\omega^2\Psi = 0 \quad , \quad \Psi(r,\omega) \sim C_s(\omega) + C_v(\omega)r^3 + \cdots$$

- Near the world-sheet horizon, $r \to r_s$

$$\Psi'' + \frac{1}{r_s - r}\Psi' + \left(\frac{\omega}{4\pi T_s (r_s - r)}\right)^2 \Psi = 0 \quad , \quad \Psi(r,\omega) \sim C_{out}(\omega)\,(r_s - r)^{\frac{i\omega}{4\pi T_s}} + C_{in}(\omega)\,(r_s - r)^{-\frac{i\omega}{4\pi T_s}}$$

- To calculate the retarded correlator we have

$$S = \int dr d\tau\ \mathcal{H}^{\alpha\beta}\ \partial_\alpha \Psi \partial_\beta \Psi \quad , \quad \mathcal{H}^{\alpha\beta} = \begin{cases} \dfrac{H^{\alpha\beta}}{2\pi \ell_s^2} & , \ \perp, \\ \dfrac{H^{\alpha\beta}}{2\pi \ell_s^2\ Z^2} & , \ \parallel, \end{cases}$$

- For the retarded correlator

$$G_R(\omega) = \mathcal{H}^{r\alpha}(r)\Psi^*(r,\omega)\partial_\alpha \Psi(r,\omega)\Big|_{\text{boundary}} \quad , \quad \Psi(0,\omega) = 1 \quad , \quad \Psi(r \to r_s,\omega) \sim (r_s - r)^{-\frac{i\omega}{4\pi T_s}}$$

- The metric entering the wave equations for fluctuations is 2d BH metric, with temperature T_s. Using the Schwinger-Keldysh formalism we can show that

$$G^i_{sym}(\omega) = \coth\left(\frac{\omega}{2T_s}\right) G^i_R(\omega)$$

and therefore the temperature entering the fluctuation-dissipation relations is T_s.

- This is NOT the thermal equilibrium relation of the plasma.

Langevin diffusion constants

$$\kappa = G_{sym}(\omega = 0) = -2T_s \frac{G_R(\omega)}{\omega}\Big|_{\omega=0}$$

$$ImG_r(r,t) = \frac{\mathcal{H}^{rr}}{2i}\Psi^* \overleftrightarrow{\partial} \Psi = J^r(r,t) \quad , \quad \partial_r J^r = 0$$

We can compute $ImG_R(\omega)$, anywhere, and the easiest is at the horizon, $r = r_s$:

$$\Psi = C_h\,(r_s - r)^{-\frac{i\omega}{4\pi T_s}} + \cdots \quad , \quad ImG_R = \frac{\mathcal{H}^{rr}}{4\pi T_s (r_s - r)}\Big|_{r_s} |C_h|^2 \omega$$

- Ψ can be computed exactly as $\omega \to 0$

$$\Psi \simeq 1 + \omega \int_0^r \mathcal{H}^{rr}(r')\, dr' \quad \Rightarrow \quad C_h = 1 \quad \Rightarrow \quad \kappa = \frac{\mathcal{H}^{rr}}{2\pi(r_s - r)}\Big|_{r_s} = \frac{1}{\pi \ell_s^2} \begin{cases} b^2(r_s) T_s & , \quad \perp, \\ (4\pi)^2 \dfrac{b^2(r_s)}{f'(r_s)^2} T_s^3 & , \quad \| , \end{cases}$$

Langevin friction terms

We have

$$\dot{\vec{p}} = -\eta_D^{||}\ p^{||}\ \hat{v} - \eta_D^{\perp}\ p^{\perp} + \vec{\xi}(t)$$

To connect to the holographic equations we must rewrite them as equations for δX

$$\dot{\vec{X}} = \vec{v} + \delta\dot{\vec{X}} \quad , \quad \vec{p} = \frac{M\dot{\vec{X}}}{\sqrt{1-\dot{\vec{X}}\cdot\dot{\vec{X}}}} = \gamma M\vec{v} + \delta\vec{p}$$

We expand to first order to obtain the equations for the position fluctuations

$$\gamma M\delta\ddot{X}^{\perp} = -\eta^{\perp}\delta\dot{X}^{\perp} + \xi^{\perp} \quad , \quad \gamma^3 M\delta\ddot{X}^{||} = -\eta^{||}\delta\dot{X}^{||} + \xi^{||}$$

$$\eta^{\perp} = \frac{1}{\gamma M}\eta_D^{\perp} \quad , \quad \eta^{||} = \frac{1}{\gamma^3 M}\left[\eta_D^{||} + \gamma M v\frac{\partial\eta_D^{||}}{\partial p}\right]$$

We have computed holographically

$$\eta^{||,\perp} = \frac{\kappa^{||,\perp}}{2T_s}$$

which lead to the modified Einstein relations

$$\kappa^{\perp} = 2\gamma M T_s \; \eta_D^{\perp} = 2E T_s \; \eta_D^{\perp} \quad , \quad \kappa^{||} = 2\gamma^3 M T_s \left[\eta_D^{||} + \gamma M v \frac{\partial \eta_D^{||}}{\partial p} \right]$$

to be compared with the standard one $\kappa = 2MT\eta_D$.

- Consistency check

$$\eta_D^{||} = \eta_D^{\perp} = \frac{b^2(r_s)}{M\gamma(2\pi\ell_s^2)}$$

satisfies both Einstein relations.

The diffusion constants

- From direct calculation we obtain

$$\kappa^{\perp} = \frac{b^2(r_s)}{\pi \ell_s^2} T_s \quad , \quad \kappa^{||} = \frac{b^2(r_s)}{\pi \ell_s^2} \frac{(4\pi)^2}{f'(r_s)^2} T_s^3$$

- We also obtain the relation

$$G^i_{sym}(\omega) = \coth\left(\frac{\omega}{2T_s}\right) G^i_R(\omega)$$

and therefore the temperature entering the fluctuation-dissipation relations is T_s.

- Because the diffusion and friction coefficients are generically momentum dependent there are non-trivial relations between Langevin equations for momenta and position fluctuations.

$$\dot{\vec{p}} = -\eta_D^{||}\ p^{||}\ \hat{v} - \eta_D^{\perp}\ p^{\perp} + \vec{\xi}(t)$$

In configuration space

$$\gamma M \delta\ddot{X}^{\perp} = -\eta^{\perp}\delta\dot{X}^{\perp} + \xi^{\perp} \quad , \quad \gamma^3 M \delta\ddot{X}^{||} = -\eta^{||}\delta\dot{X}^{||} + \xi^{||}$$

$$\eta^{\perp} = \frac{1}{\gamma M}\eta_D^{\perp} \quad , \quad \eta^{||} = \frac{1}{\gamma^3 M}\left[\eta_D^{||} + \gamma M v \frac{\partial \eta_D^{||}}{\partial p}\right]$$

- We have computed holographically

$$\eta^{||,\perp} = \frac{\kappa^{||,\perp}}{2T_s}$$

which lead to the modified Einstein relations

$$\kappa^{\perp} = 2\gamma M T_s\ \eta_D^{\perp} = 2ET_s\ \eta_D^{\perp} \quad , \quad \kappa^{||} = 2\gamma^3 M T_s \left[\eta_D^{||} + \gamma M v \frac{\partial \eta_D^{||}}{\partial p}\right]$$

to be compared with the standard one $\kappa = 2MT\eta_D$.

- Consistency check:

$$\eta_D^{||} = \eta_D^{\perp} = \frac{b^2(r_s)}{M\gamma(2\pi\ell_s^2)}$$

satisfies both Einstein relations.

- This type of relativistic Langevin evolution is different from what has been described so far in the mathematical physics literature.

Debasch+Mallick+Ribet, 1997

- The diffusion constants satisfy the general inequality (in the deconfined phase)

$$\frac{\kappa_{||}}{\kappa_{\perp}} = \left(\frac{4\pi T_s}{f'(r_s)}\right)^2 = 1 + 4v^2\ \frac{b'(r_s)}{f'(r_s)b(r_s)} \geq 1$$

equality is attained at $v = 0$.

- For systems similar to QCD, the WKB approximation valid for large ω seems to be valid down to very low frequencies, providing an analytical control over the Langevin correlators.

Adding the quarks

- We would like to add N_f quarks q_L^I and antiquarks $q_R^{\bar{I}}$.

- We must add in the string theory (in 5d) space-filling N_f D_4 and N_f $\bar{D}_4$ branes.

- In the same spirit of kicking the most important (=relevant) operators we will keep:

(a) The left and right-handed currents of the $\mathrm{U}(N_f)_L \times U(N_f)_R$ chiral symmetry. They are dual to $\mathrm{U}(N_f)_L \times U(N_f)_R$ gauge fields A_μ^L, A_μ^R.

(b) The quark mass operator $\bar{q}_L^i q_R^j$ dual to a complex $N_f \times N_f$ (bifundametal) complex scalar, T^{ij}, that in string theory is known as the open string tachyon.

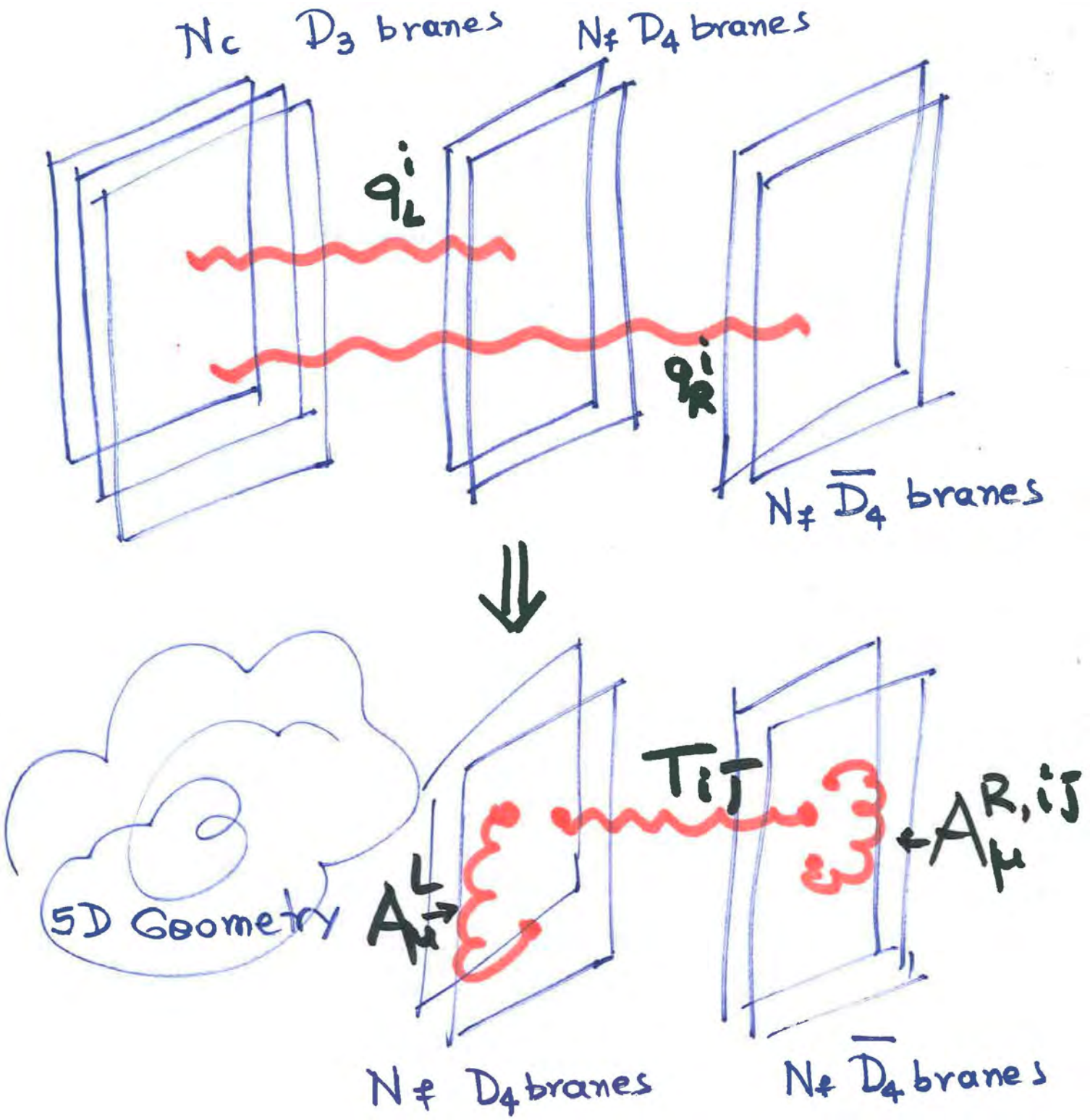
N_c D_3 branes
N_f D_4 branes
q_L^i
q_R^i
N_f $\overline{D}_4$ branes
5D Geometry
A_μ^L
T_{ij}
$A_\mu^{R,ij}$
N_f D_4 branes
N_f $\overline{D}_4$ branes

• The interactions on the flavor branes are weak, so that $A_\mu^{L,R}, T$ are as sources for the quarks.

• Integrating out the quarks, generates an effective action $S_{flavor}(A_\mu^{L,R}, T)$, so that $A_\mu^{L,R}, T$ can be thought as effective $q\bar{q}$ composites, that is : mesons

• On the string theory side: integrating out $D_3 - D_4$ and $D_3 - \bar{D}_4$ strings gives rise to the DBI action for the $D_4 - \bar{D}_4$ branes in the D_3 background:

$$S_{flavor}(A_\mu^{L,R}, T) \quad \longleftrightarrow \quad S_{DBI}(A_\mu^{L,R}, T) \quad \text{holographically}$$

• In the "vacuum" only T can have a non-trivial profile: $T^{I\bar{J}}(r)$. Near the AdS_5 boundary ($r \to 0$)

$$T^{I\bar{J}}(r) = M_{I\bar{J}}\, r + \cdots + \langle \bar{q}_L^I \; q_R^{\bar{J}} \rangle r^3 + \cdots$$

Casero+Kiritsis+Paredes

General properties

• A typical solution has (a) T vanishing in the UV and (b) $T \to \infty$ in the IR.

• At the point $r = r_*$ where $T = \infty$, the D_4 and $\bar{D}_4$ branes "fuse". The true vacuum is a brane that enters folds on itself and goes back to the boundary.

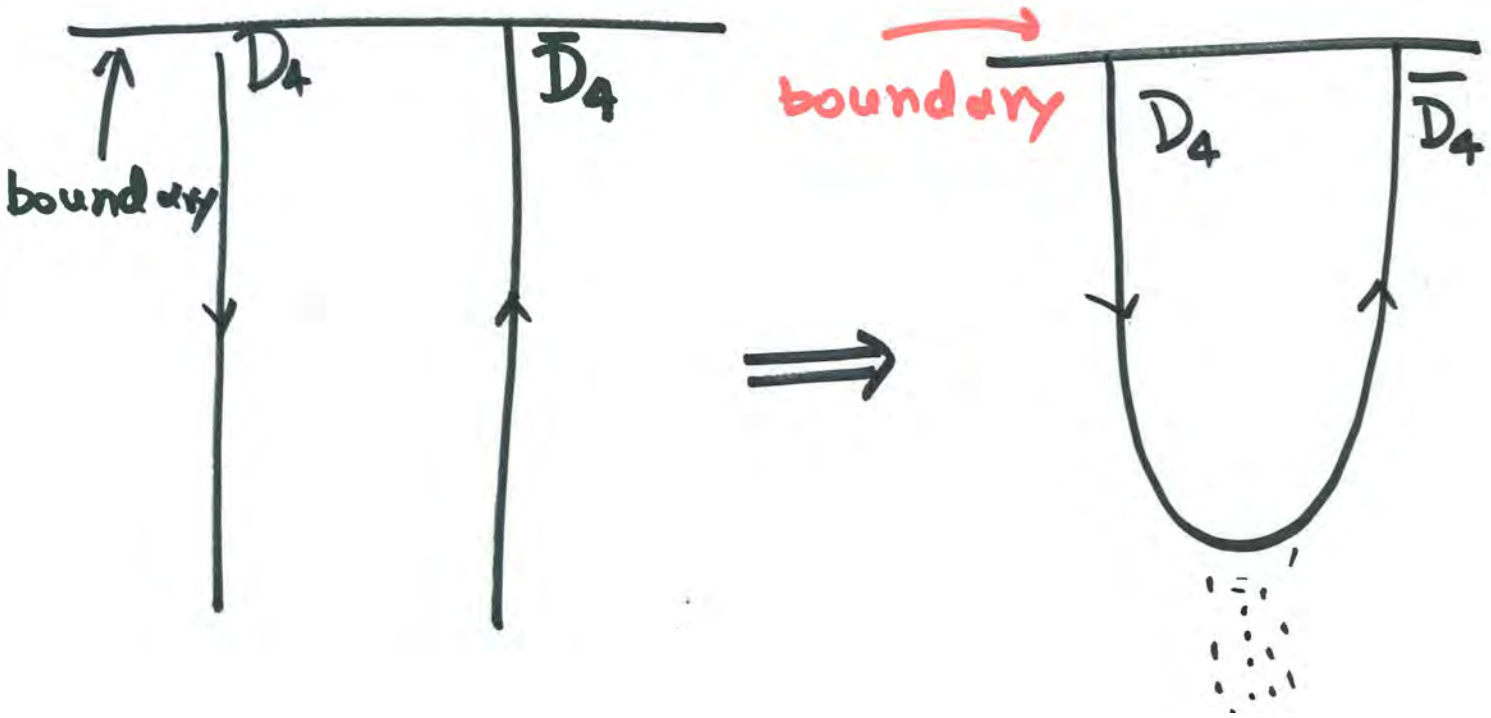

• A non-zero T breaks chiral symmetry.

• When $m_q = 0$, the meson spectrum contains N_f^2 massless pseudoscalars, the $U(N_f)_A$ Goldstone bosons.

• The WZ part of the flavor brane action gives the $U(1)_A$ axial anomaly and an associated Stuckelberg mechanism gives an $O\left(\frac{N_f}{N_c}\right)$ mass to the would-be Goldstone boson η', (agreeing with Veneziano-Witten).

• We can derive formulae for the anomalous divergences of flavor currents, when they are coupled to an external source.

• T=0 is a solution. In case of confinement, it is excluded from the absence of IR boundary for the branes: Holographic Coleman-Witten theorem.

• Fluctuations around the $T(r)$ solution for $T, A_\mu^{L,R}$ give the spectra (and interactions) of various meson trajectories.

• A GellMann-Oaks-Renner relation is always satisfied (for an asymptotic AdS_5 space)

$$m_\pi^2 = -2\frac{m_q}{f_\pi^2}\,\langle \bar{q}q\rangle \quad , \quad m_q \to 0$$

The tachyon DBI action

- The flavor action is the $D_4 - \bar{D}_4$ action: $S[T, A^L, A^R] = S_{DBI} + S_{WZ}$

$$S_{DBI} = \int dr d^4x \, \frac{N_c}{\lambda} \, \mathbf{Str} \left[V(T) \left(\sqrt{-\det\left(g_{\mu\nu} + D_{\{\mu} T^\dagger D_{\nu\}} T + F^L_{\mu\nu}\right)} + \right.\right.$$

$$\left.\left. + \sqrt{-\det\left(g_{\mu\nu} + D_{\{\mu} T^\dagger D_{\nu\}} T + F^R_{\mu\nu}\right)} \right) \right]$$

$$D_\mu T \equiv \partial_\mu T - i T A^L_\mu + i A^R_\mu T \quad , \quad D_\mu T^\dagger \equiv \partial_\mu T^\dagger - i A^L_\mu T^\dagger + i T^\dagger A^R_\mu$$

transforming covariantly under flavor gauge transformations

$$T \to V_R T V_L^\dagger \quad , \quad A^L \to V_L (A^L - i V_L^\dagger d V_L) V_L^\dagger \quad , \quad A^R \to V_R (A^R - i V_R^\dagger d V_R) V_R^\dagger$$

- For the vacuum structure and spectrum $Str = Tr$.

- The tachyon potential in flat space can be computed from boundary CFT.

Kutasov+Marino+Moore

$$V(T) = K_0 \, e^{-\mu^2 T T^\dagger}$$

- Two extrema: $T = 0$ (unbroken chiral symmetry) and $T = \infty$ (broken chiral symmetry).

The tachyon WZ action

- The WZ action is given by

Kennedy+Wilkins, Kraus+Larsen, Takayanagi+Terashima+Uesugi

$$S_{WZ} = T_4 \int_{M_5} C \wedge \mathrm{Str}\ \exp\left[i2\pi\alpha' \mathcal{F}\right]$$

- M_5 is the world-volume of the D4-$\overline{\text{D4}}$ branes that coincides with the full space-time.

- C is a formal sum of the RR potentials $C = \sum_n (-i)^{\frac{5-n}{2}} C_n$,

- $\mathcal{F}$ is the curvature of a superconnection $\mathcal{A}$:

$$i\mathcal{A} = \begin{pmatrix} iA_L & T^\dagger \\ T & iA_R \end{pmatrix}, \qquad i\mathcal{F} = \begin{pmatrix} iF_L - T^\dagger T & DT^\dagger \\ DT & iF_R - TT^\dagger \end{pmatrix}$$

$$\mathcal{F} = d\mathcal{A} - i\mathcal{A} \wedge \mathcal{A} \quad , \quad d\mathcal{F} - i\mathcal{A} \wedge \mathcal{F} + i\mathcal{F} \wedge \mathcal{A} = 0$$

- Under (flavor) gauge transformation it transforms homogeneously

$$\mathcal{F} \to \begin{pmatrix} V_L & 0 \\ 0 & V_R \end{pmatrix} \mathcal{F} \begin{pmatrix} V_L^\dagger & 0 \\ 0 & V_R^\dagger \end{pmatrix}$$

- Expanding:

$$S_{WZ} = T_4 \int C_5 \wedge Z_0 + C_3 \wedge Z_2 + C_1 \wedge Z_4 + C_{-1} \wedge Z_6$$

where Z_{2n} are appropriate forms coming from the expansion of the exponential of the superconnection.

- $Z_0 = 0$, signaling the global cancelation of 4-brane charge, which is equivalent to the cancelation of the gauge anomaly in QCD.

$$Z_2 = d\Omega_1 \quad , \quad \Omega_1 = iSTr(V(T^\dagger T))Tr(A_L - A_R) - \log\det(T) d(StrV(T^\dagger T))$$

Casero+Kiritsis+Paredes

- This term provides the Stuckelberg mixing between $Tr[A_\mu^L - A_\mu^R]$ and the QCD axion that is dual to C_3. Dualizing the full action we obtain

$$S_{CP-odd} = \frac{M^3}{2N_c^2} \int d^5x \sqrt{g} Z(\lambda) \left(\partial a + i\Omega_1\right)^2$$

$$= \frac{M^3}{2}\int d^5x\sqrt{g}Z(\lambda)\left(\partial_\mu a + \zeta\partial_\mu V(\tau) - \sqrt{\frac{N_f}{2}}V(\tau)A^A_\mu\right)^2$$

$$\zeta = \Im \log\det T \quad , \quad A_L - A_R \equiv \frac{1}{2N_f}A^A\mathbf{I} + (A^a_L - A^a_R)\lambda^a$$

• This term is invariant under the $U(1)_A$ transformations, reflecting the QCD $U(1)_A$ anomaly.

$$\zeta \to \zeta + \epsilon \quad , \quad A^A_\mu \to A^A_\mu - \sqrt{\frac{2}{N_f}}\partial_\mu\epsilon \quad , \quad a \to a - N_f\epsilon V(\tau)$$

• This is responsible for the mixing between the QCD axion and the η' $\to$ we have two scalars a, ζ and an (axial) vector, A^A_μ. Then an appropriate linear combination of the two scalars will become the 0^{-+} glueball field while the other will be the η'. The transverse (5d) vector will provide the tower of $U(1)_A$ vector mesons.

• The term $C_1 \times Z_4 \sim V\ C_1\left[F_L\wedge F_L + F_R\wedge F_R\right] + \cdots$ couples the flavor instanton density to the baryon vertex.

• Using $Z_6 = d\Omega_5$ we may rewrite the last term as

$$\int F_0\wedge\Omega_5 \quad , \quad F_0 = dC_{-1}$$

$F_0 \sim N_c$ is nothing else but the dual of the five-form field strength. This term then provides the correct Chern-Simons form that reproduces the flavor anomalies of QCD. It contains the tachyon non-trivially

Casero+Kiritsis+Paredes

• To proceed further and analyze the vacuum solution we set $T = \tau$ 1 and set the vectors to zero. Then the DBI action collapses to

$$S[\tau, A_M] = N_c N_f \int dr d^4x \; e^{-\Phi} V(\tau) \sqrt{-\det\left(g_{\mu\nu} + \partial_\mu \tau \partial_\nu \tau\right)}$$

We assume the following tachyon potential, motivated/calculated in studies of tachyon condensation:

$$V(\tau) = V_0 e^{-\frac{\mu^2}{2}\tau^2}$$

where μ has dimension of mass. It is fixed by the requirement that τ has the correct bulk mass to couple to the quark bilinear operator on the boundary.

Tachyon dynamics

- In the vacuum the gauge fields vanish and $T \sim 1$. Only DBI survives

$$S[\tau] = T_{D_4} \int dr d^4x \, \frac{e^{4A_s(r)}}{\lambda} \, V(\tau) \, \sqrt{e^{2A_s(r)} + \dot{\tau}(r)^2} \quad , \quad V(\tau) = e^{-\frac{\mu^2}{2}\tau^2}$$

- We obtain the nonlinear field equation:

$$\ddot{\tau} + \left(3\dot{A}_S - \frac{\dot{\lambda}}{\lambda}\right)\dot{\tau} + e^{2A_S}\mu^2\tau + e^{-2A_S}\left[4\dot{A}_S - \frac{\dot{\lambda}}{\lambda}\right]\dot{\tau}^3 + \mu^2\tau\,\dot{\tau}^2 = 0.$$

- In the UV we expect

$$\tau = m_q \, r + \sigma \, r^3 + \cdots \quad , \quad \mu^2\ell^2 = 3$$

- We expect that the tachyon must diverge before or at $r = r_0$. We find that indeed it does at the (dilaton) singularity. For the $r_0 = \infty$

backgrounds

$$\tau \sim \exp\left[\frac{2}{a}\,\frac{R}{\ell^2}\,r\right] \qquad \text{as} \qquad r \to \infty$$

• Generically the solutions have spurious singularities: $\tau(r_*)$ stays finite but its derivatives diverges because:

$$\tau \sim \tau_* + \gamma\sqrt{r_* - r}.$$

The condition that they are absent determines σ as a function of m_q.

• The easiest spectrum to analyze is that of vector mesons. We find ($r_0 = \infty$)

$$\Lambda_{glueballs} = \frac{1}{R}, \qquad \Lambda_{mesons} = \frac{3}{\ell}\left(\frac{\alpha\ell^2}{2R^2}\right)^{(\alpha-1)/2} \propto \frac{1}{R}\left(\frac{\ell}{R}\right)^{\alpha-2}.$$

This suggests that $\alpha = 2$ preferred also from the glue sector (linear trajectories).

A "warmup" model

Take a simple confining background: AdS_6 soliton, a solution of non-critical string theory (a 6d version of the black-D4 Witten model for glue)

$$ds_6^2 = \frac{R^2}{z^2}\left[dx_{1,3}^2 + f_\Lambda^{-1} dz^2 + f_\Lambda\, d\eta^2\right] \quad , \quad f_\Lambda = 1 - \frac{z^5}{z_\Lambda^5} \quad , \quad z \in [0, z_\Lambda]$$

with η periodic, $\Phi \to$ constant.

Kuperstein+Sonnenschein

• We consider N_f $D_4 + \bar{D}_4$ branes at a fixed η, and we will will neglect the coordinate of the branes transverse to the η circle.

$$S = -\int d^4x dz V(|T|)\left(\sqrt{-\det \mathbf{A}_L} + \sqrt{-\det \mathbf{A}_R}\right)$$

$$\mathbf{A}_{(i)MN} = g_{MN} + 2\pi\alpha' F^{(i)}_{MN} + \pi\alpha'\left((D_M T)^*(D_N T) + (D_N T)^*(D_M T)\right)$$

$$D_M T = (\partial_M + iA^L_M - iA^R_M)T.$$

• The active fields are two 5-d gauge fields and a complex scalar $T = \tau\, e^{i\theta}$, which are dual to the low-lying quark bilinear operators which correspond to states with $J^{PC} = 1^{--}, 1^{++}, 0^{-+}, 0^{++}$,

- We will take $T = \tau\ 1$

$$V = \mathcal{K}\, e^{-\frac{\pi}{2}\tau^2} \quad , \quad R^2 = 6\ell_s^2$$

so that $\Delta_T = 3$.

- Tachyon equation:

$$\tau'' - \frac{4\pi\, z\, f_\Lambda}{3}\tau'^3 + (-\frac{3}{z} + \frac{f_\Lambda'}{2f_\Lambda})\tau' + \left(\frac{3}{z^2 f_\Lambda} + \pi\,\tau'^2\right)\tau = 0$$

- Near the boundary $z = 0$, the solution can be expanded in terms of two integration constants as:

$$\tau = c_1 z + \frac{\pi}{6} c_1^3 z^3 \log z + c_3 z^3 + \mathcal{O}(z^5)$$

- c_1, c_3 are related to the quark mass and condensate

- There is a one-parameter family of diverging solutions in the IR:

$$\tau = \frac{C}{(z_\Lambda - z)^{\frac{3}{20}}} - \frac{13}{6\pi C}(z_\Lambda - z)^{\frac{3}{20}} + \dots$$

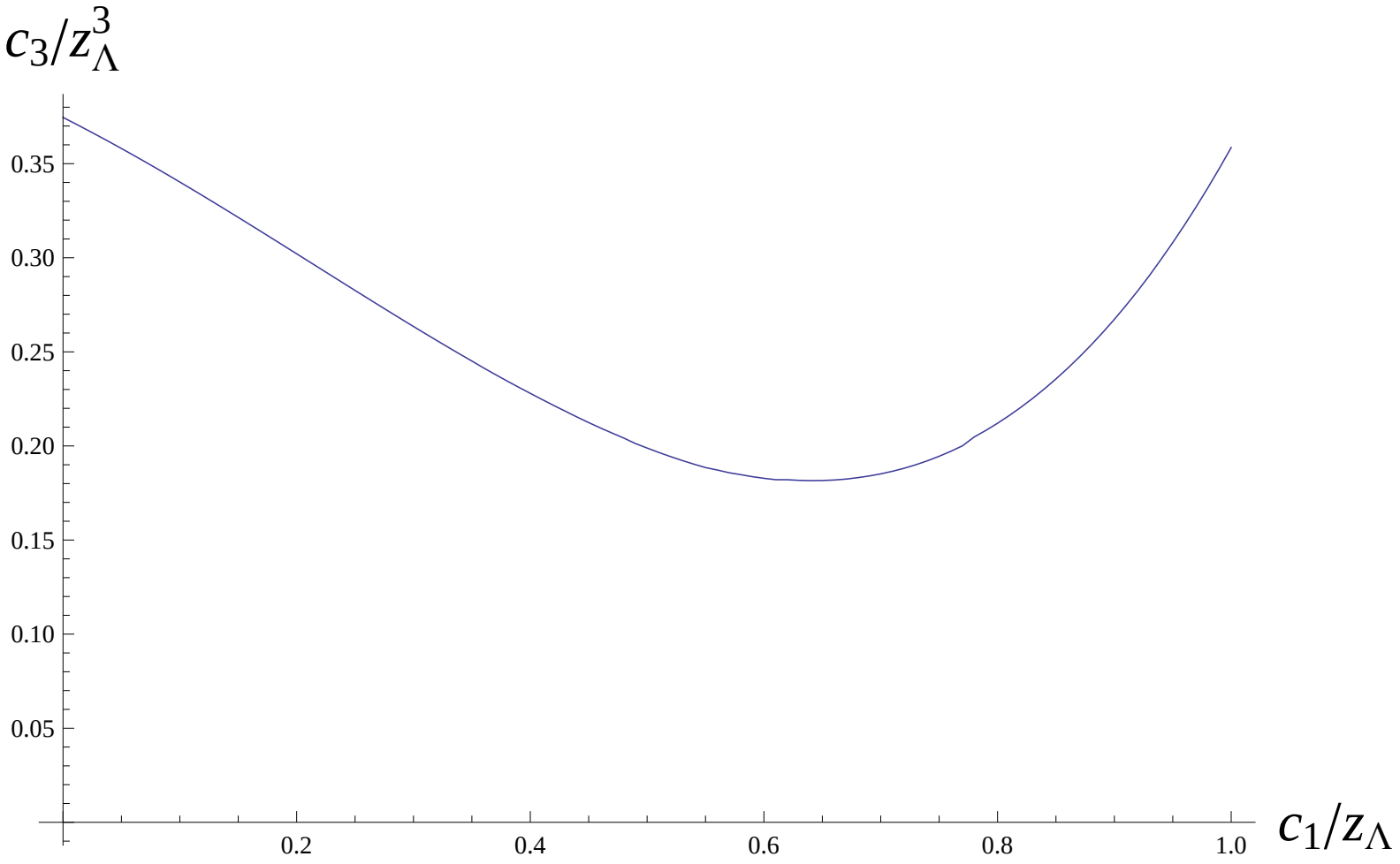

- Chiral symmetry breaking is manifest.

For the vectors

$$z_\Lambda\, m_V^{(1)} = 1.45 + 0.718 c_1\ , \qquad z_\Lambda\, m_V^{(2)} = 2.64 + 0.594 c_1\ , \qquad z_\Lambda\, m_V^{(3)} = 3.45 + 0.581 c_1\ ,$$
$$z_\Lambda\, m_V^{(4)} = 4.13 + 0.578 c_1\ , \qquad z_\Lambda\, m_V^{(5)} = 4.72 + 0.577 c_1\ , \qquad z_\Lambda\, m_V^{(6)} = 5.25 + 0.576 c_1\ .$$

For the axial vectors:

$$z_\Lambda\, m_A^{(1)} = 1.93 + 1.23 c_1\ , \quad z_\Lambda\, m_A^{(2)} = 3.28 + 1.04 c_1\ , \quad z_\Lambda m_A^{(3)} = 4.29 + 0.997 c_1$$
$$z_\Lambda m_A^{(4)} = 5.13 + 0.975 c_1\ , \quad z_\Lambda\, m_A^{(5)} = 5.88 + 0.962 c_1\ , \quad z_\Lambda\, m_A^{(6)} = 6.55 + 0.954 c_1$$

For the pseudoscalars:

$$z_\Lambda\, m_P^{(1)} = \sqrt{2.47 c_1^2 + 5.32 c_1}\ , \qquad z_\Lambda\, m_P^{(2)} = 2.79 + 1.16 c_1\ , \qquad z_\Lambda\, m_P^{(3)} = 3.87 + 1.08 c_1\ ,$$
$$z_\Lambda\, m_P^{(4)} = 4.77 + 1.04 c_1\ , \qquad z_\Lambda\, m_P^{(5)} = 5.54 + 1.01 c_1\ , \qquad z_\Lambda\, m_P^{(6)} = 6.24 + 0.997 c_1\ .$$

For the scalars:

$$z_\Lambda\, m_S^{(1)} = 2.47 + 0.683 c_1\ , \qquad z_\Lambda\, m_S^{(2)} = 3.73 + 0.488 c_1\ , \qquad z_\Lambda\, m_S^{(3)} = 4.41 + 0.507 c_1\ ,$$
$$z_\Lambda\, m_S^{(4)} = 4.99 + 0.519 c_1\ , \qquad z_\Lambda\, m_S^{(5)} = 5.50 + 0.536 c_1\ , \qquad z_\Lambda\, m_S^{(6)} = 5.98 + 0.543 c_1\ .$$

- Valid up to $c_1 = 1$
- In qualitative agreement with lattice results

Laerman+Schmidt., Del Debbio+Lucini+Patela+Pica, Bali+Bursa

We fit the two parameters to the "confirmed" isospin 1 mesons

$$\frac{1}{z_\Lambda} = 503 MeV \quad , \quad c_1^{\text{light}} = 0.0135$$

J^{PC}	Meson	Measured (MeV)	Model (MeV)
1^{--}	$\rho(770)$	775	735
	$\rho(1450)$	1465	1331
	$\rho(1700)$	1720	1742
	$\rho(1900)$	1900	2083
	$\rho(2150)$	2150	2380
1^{++}	$a_1(1260)$	1230	980
	$a_1(1640)$	1647	1661
0^{-+}	π_0	135.0	135.3
	$\pi(1300)$	1300	1411
	$\pi(1800)$	1816	1955
0^{++}	$a_0(1450)$	1474	1249

- The RMS error defined as $100 \times \frac{1}{\sqrt{n}} \sqrt{\sum_O \frac{\delta O^2}{O^2}}$ with n=11-2 is 11%

- "less confirmed mesons"

J^{PC}	Meson	Measured (MeV)	Model (MeV)
1^{--}	$\rho(2270)$	2270	2649
1^{++}	$a_1(1930)$	1930	2166
	$a_1(2096)$	2096	2591
	$a_1(2270)$	2270	2965
	$a_1(2340)$	2340	3303
0^{-+}	$\pi(2070)$	2070	2406
	$\pi(2360)$	2360	2798
0^{++}	$a_0(2020)$	2025	1883

- The RMS error here is 23%

- Axial vector mesons are consistently overestimated.

Advantages of this simple model

• Compared to the SS model it contains all trajectories corresponding to $1^{--}, 1^{++}, 0^{-+}, 0^{++}$ and can accommodate a mass of the quarks. The asymptotic masses of mesons are $m_n^2 \sim n$ are they should.

• Compared to the hard wall AdS/QCD model chiral symmetry breaking is dynamical and not input by hand. Asymptotic masses behave as $m_n^2 \sim n^2$.

• In the soft wall model, chiral symmetry breaking is not dynamical and different aspects of that model are inconsistent.

• It needs to be improved along the lines of the glue sector+add the non-abelian structure.

The chiral vacuum structure

- We take the potential to be the flat space one

$$V = V_0 \; e^{-T^2}$$

with a maximum at $T = 0$ and a minimum at $T = \infty$.

- Near the boundary $z = 0$, the solution can be expanded in terms of two integration constants as:

$$\tau = c_1 z + \frac{\pi}{6} c_1^3 z^3 \log z + c_3 z^3 + \mathcal{O}(z^5)$$

- c_1, c_3 are related to the quark mass and condensate.

- At the tip of the cigar, the generic behavior of solutions is

$$\tau \sim constant_1 + constant_2 \sqrt{z - z_\Lambda}$$

- With special tuned condition there is a one-parameter family of diverging solutions in the IR depending on a single parameter:

$$\tau = \frac{C}{(z_\Lambda - z)^{\frac{3}{20}}} - \frac{13}{6\pi C} (z_\Lambda - z)^{\frac{3}{20}} + \dots$$

• This is the correct "regularity condition" in the IR as τ is allowed to diverge only at the tip.

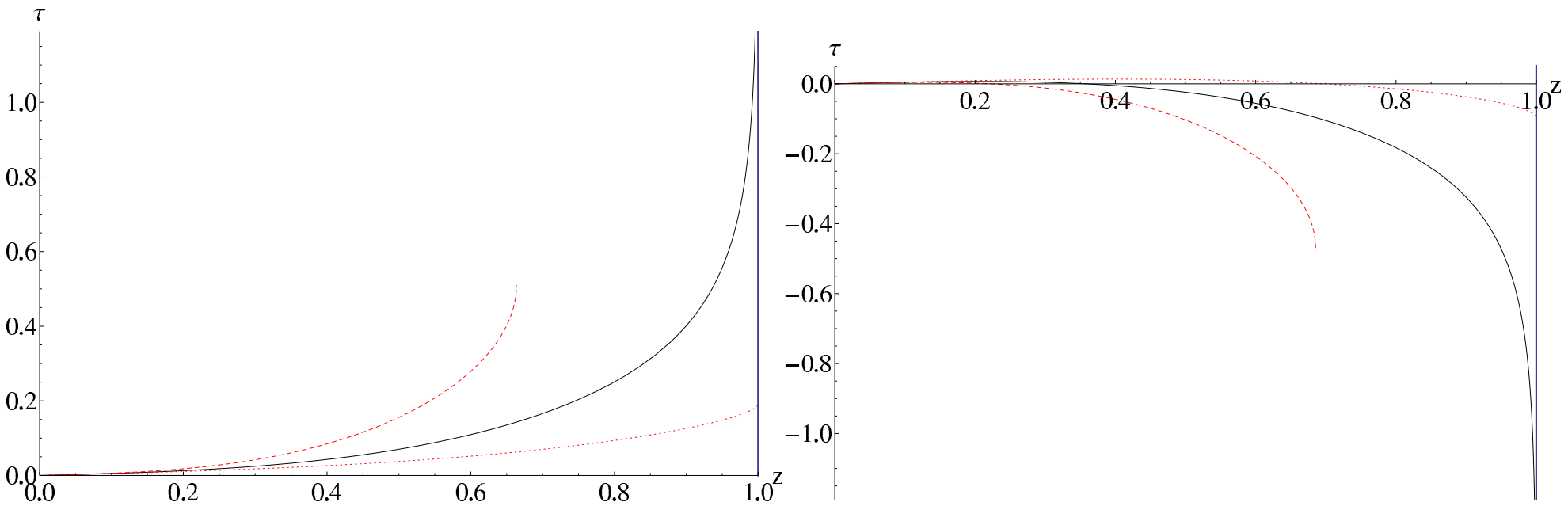

All the graphs are plotted using $z_\Lambda = 1$, $\mu^2 = \pi$ and $c_1 = 0.05$. The tip of the cigar is at $z = z_\Lambda = 1$. On the left, the solid black line represents a solution with $c_3 \approx 0.3579$ for which τ diverges at z_Λ. The red dashed line has a too large c_3 ($c_3 = 1$) - such that there is a singularity at $z = z_s$ where $\partial_z \tau$ diverges while τ stays finite. This is unacceptable since the solution stops at $z = z_s$ where the energy density of the flavor branes diverges. The red dotted line corresponds to $c_3 = 0.1$; this kind of solution is discarded because the tachyon stays finite everywhere. The plot in the right is done with the same conventions but with negative values of $c_3 = -0.1, -0.3893, -1$. For $c_3 \approx -0.3893$ there is a solution of the differential equation such that τ diverges to $-\infty$. This solution is unstable.

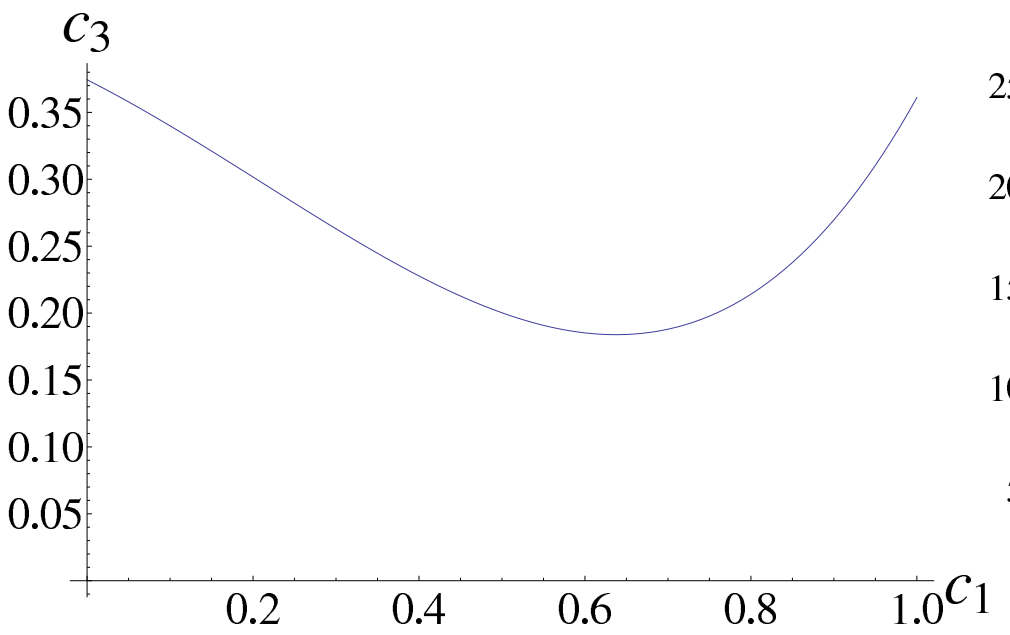

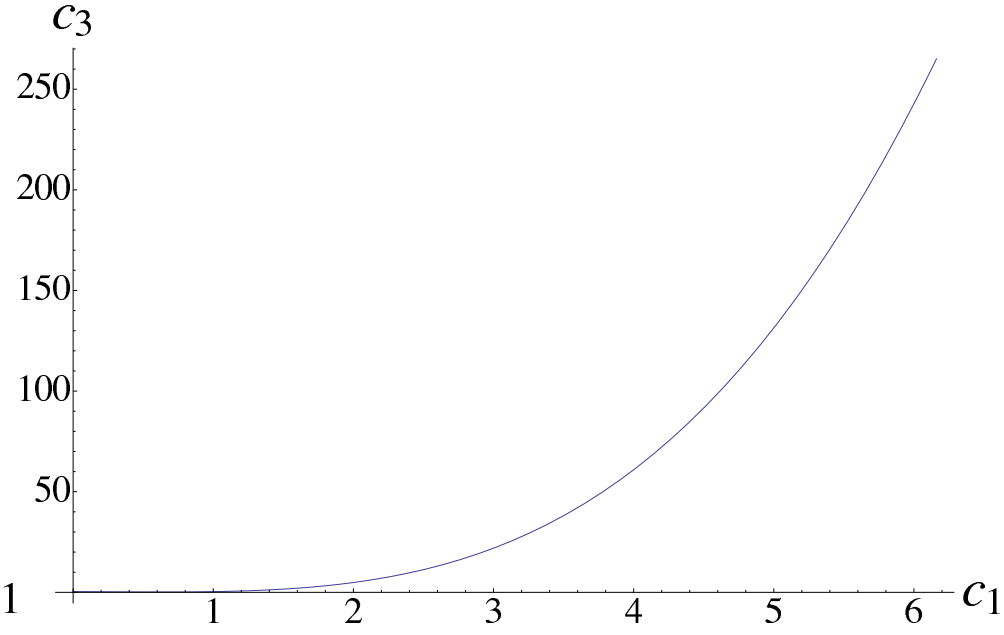

- Chiral symmetry breaking is manifest.

Chiral restauration at deconfinement

- In the deconfined phase, the bulk metric is that of a bh.

- The branes now are allowed to enter the horizon without recombining.

- To avoid intermediate singularities of the solution the boundary conditions must be tuned so that tachyon is finite at the horizon.

- Near the horizon the correct solution behaves as a one-parameter family

$$\tau = c_T - \frac{3c_T}{5z_T}(z_T - z) - \frac{9c_T}{200z_T}(8 + \mu^2 {c_T}^2)(z_T - z)^2 + \dots$$

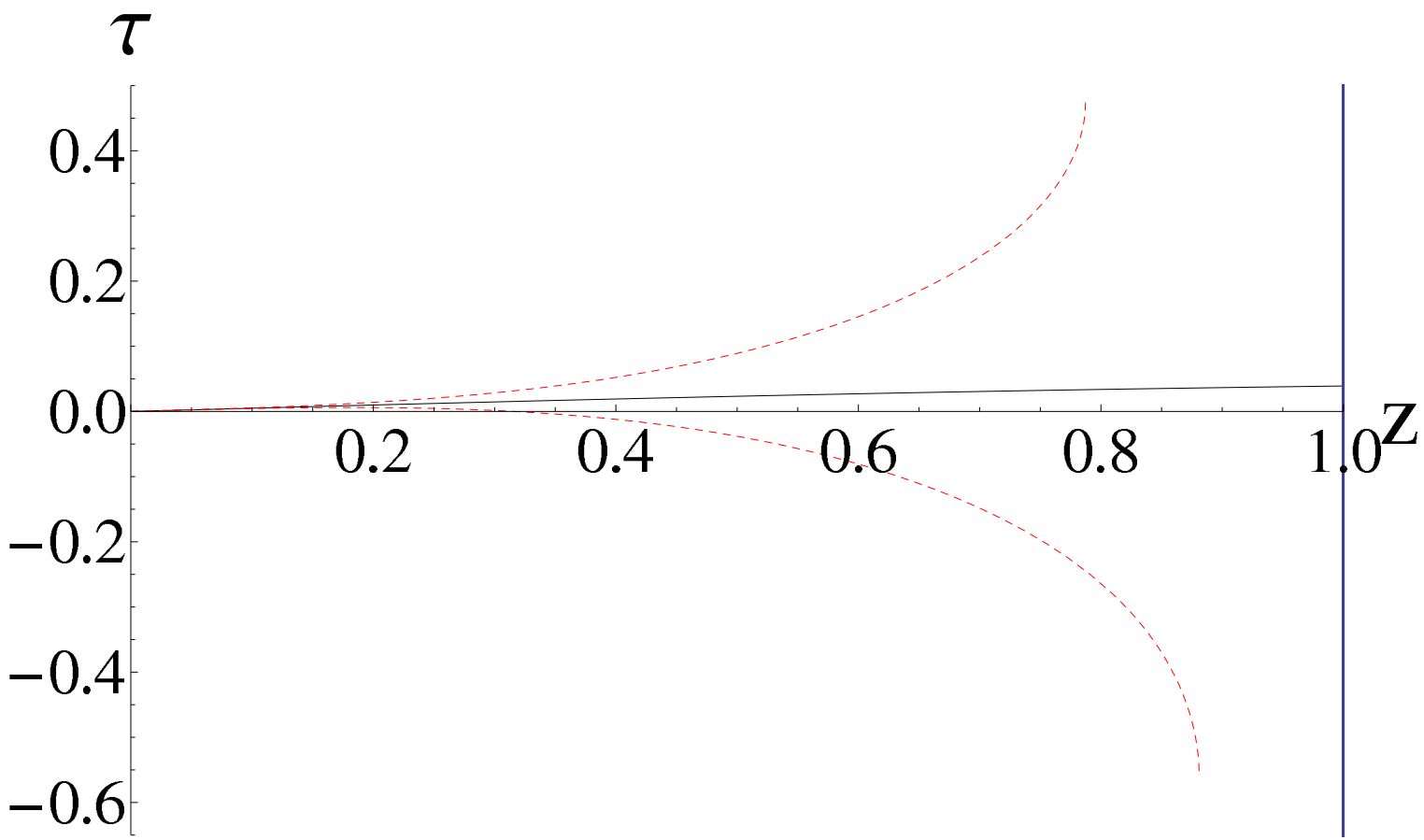

Plots corresponding to the deconfined phase. We have taken $c_1 = 0.05$. The solid line displays the physical solution $c_3 = -0.0143$ whereas the dashed lines ($c_3 = -0.5$ and $c_3 = 0.5$) are unphysical and end with a behavior of the type $\tau = k_1 - k_2\sqrt{z_s - z}$.

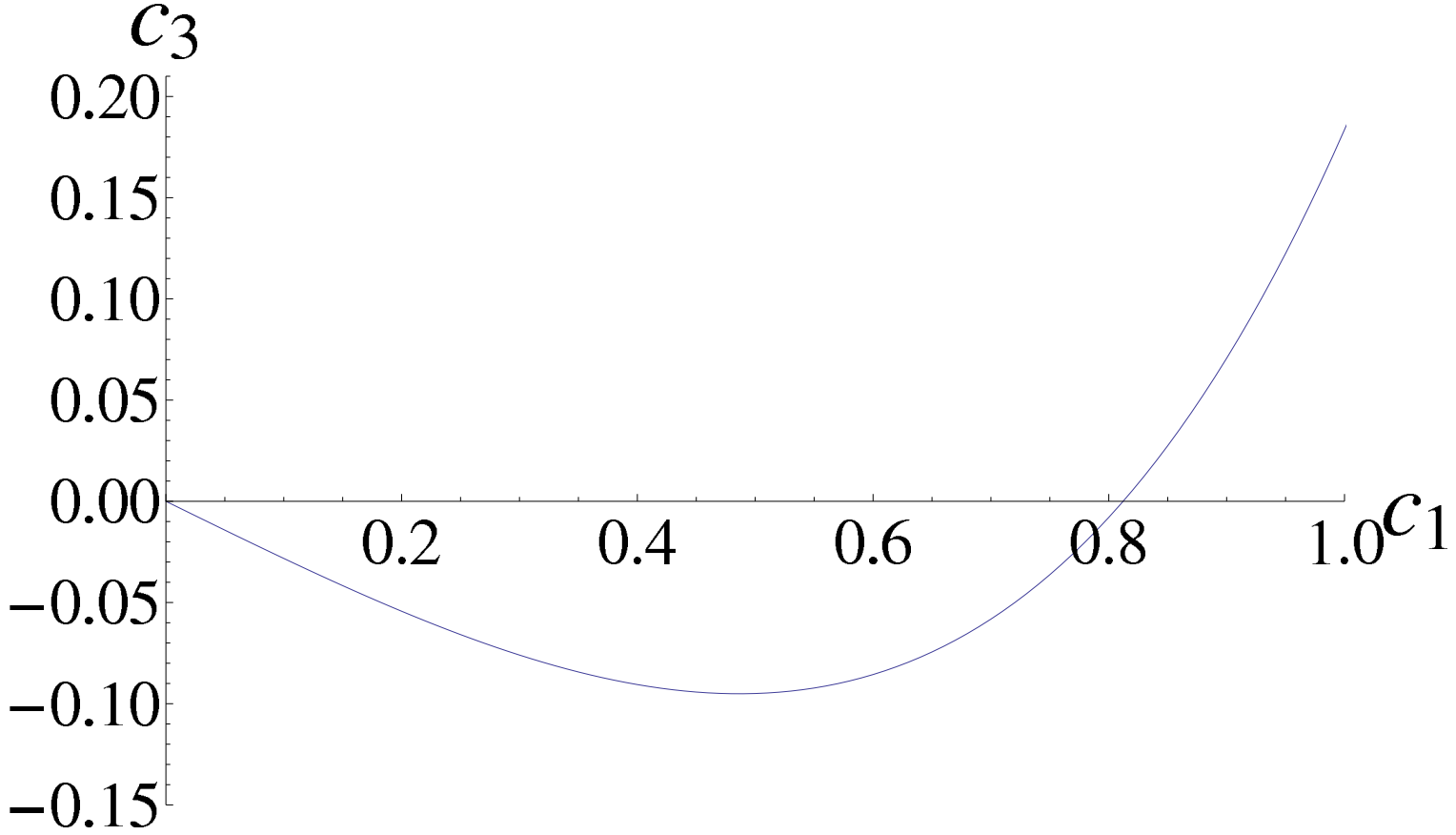

These plots give the values of c_3 determined numerically by demanding the correct IR behavior of the solution, as a function of c_1.

Jump of the condensate at the phase transition

- From holographic renormalization we obtain

$$\langle \bar{q}q \rangle = \frac{1}{\beta}(2\pi\alpha' \mathcal{K} R^3 \lambda) \left(-4c_3 + \left(\frac{m_q}{\beta}\right)^3 \mu^2 (1+\alpha) \right) \quad , \quad m_q = \beta \; c_1$$

- We calculate the jump at the phase transition that is scheme independent for a fixed quark mass.

$$\Delta\langle \bar{q}q \rangle \equiv \langle \bar{q}q \rangle_{conf} - \langle \bar{q}q \rangle_{deconf} = -4\frac{1}{\beta}(2\pi\alpha' \mathcal{K} R^3 \lambda)\Delta c_3$$

- This is equivalent to Δc_3

- We plot it as a function of the quark mass.

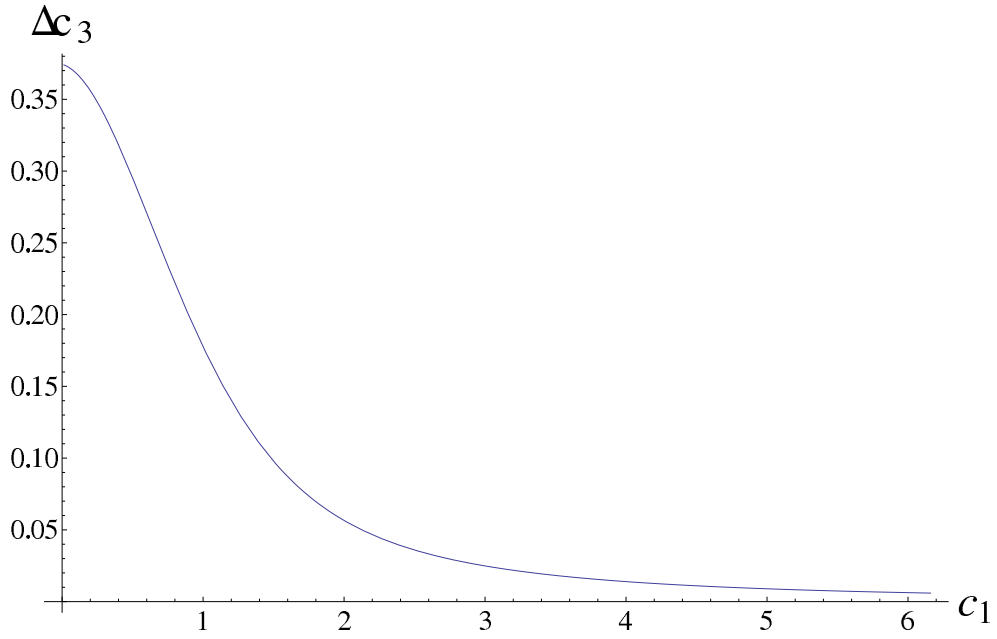

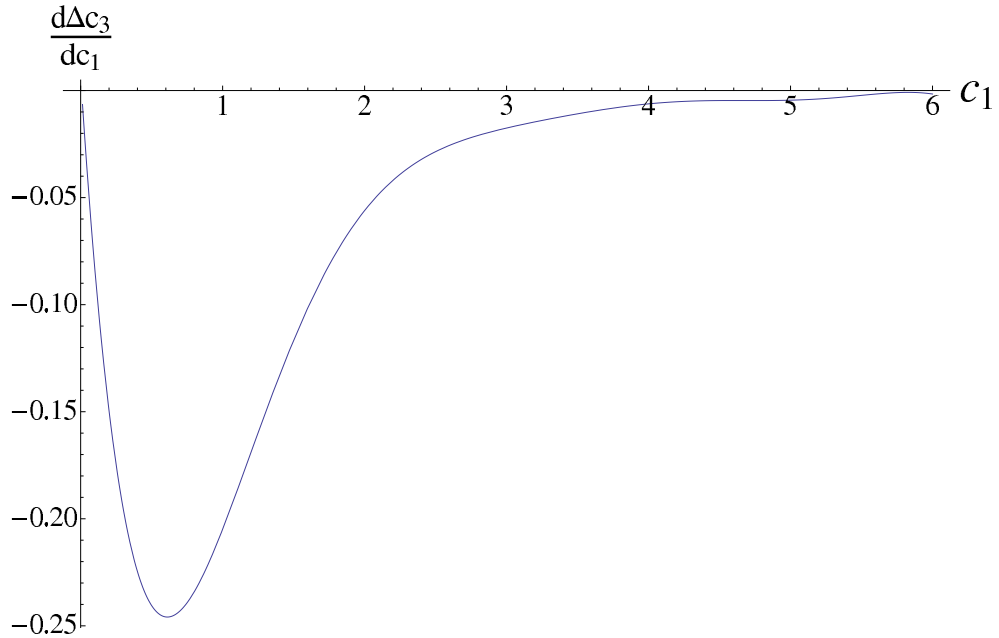

The finite jump of the quark condensate and its derivative with respect to c_1 when the confinement-deconfinement transition takes place. The important features appear when $m_q \sim \Lambda_{QCD}$

Meson spectra

For the vectors

$$z_\Lambda m_V^{(1)} = 1.45 + 0.718 c_1 \,, \quad z_\Lambda m_V^{(2)} = 2.64 + 0.594 c_1 \,, \quad z_\Lambda m_V^{(3)} = 3.45 + 0.581 c_1 \,,$$
$$z_\Lambda m_V^{(4)} = 4.13 + 0.578 c_1 \,, \quad z_\Lambda m_V^{(5)} = 4.72 + 0.577 c_1 \,, \quad z_\Lambda m_V^{(6)} = 5.25 + 0.576 c_1 \,.$$

For the axial vectors:

$$z_\Lambda m_A^{(1)} \approx 2.05 + 1.46 c_1 \,, \quad z_\Lambda m_A^{(2)} \approx 3.47 + 1.24 c_1 \,, \quad z_\Lambda m_A^{(3)} \approx 4.54 + 1.17 c_1 \,,$$
$$z_\Lambda m_A^{(4)} \approx 5.44 + 1.13 c_1 \,, \quad z_\Lambda m_A^{(5)} \approx 6.23 + 1.11 c_1 \,, \quad z_\Lambda m_A^{(6)} \approx 6.95 + 1.10 c_1 \,.$$

For the pseudoscalars:

$$z_\Lambda m_P^{(1)} \approx \sqrt{3.53 c_1^2 + 6.33 c_1} \,, \quad z_\Lambda m_P^{(2)} \approx 2.91 + 1.40 c_1 \,, \quad z_\Lambda m_P^{(3)} \approx 4.07 + 1.27 c_1 \,,$$
$$z_\Lambda m_P^{(4)} \approx 5.04 + 1.21 c_1 \,, \quad z_\Lambda m_P^{(5)} \approx 5.87 + 1.17 c_1 \,, \quad z_\Lambda m_P^{(6)} \approx 6.62 + 1.15 c_1 \,.$$

For the scalars:

$$z_\Lambda m_S^{(1)} = 2.47 + 0.683 c_1 \,, \quad z_\Lambda m_S^{(2)} = 3.73 + 0.488 c_1 \,, \quad z_\Lambda m_S^{(3)} = 4.41 + 0.507 c_1 \,,$$
$$z_\Lambda m_S^{(4)} = 4.99 + 0.519 c_1 \,, \quad z_\Lambda m_S^{(5)} = 5.50 + 0.536 c_1 \,, \quad z_\Lambda m_S^{(6)} = 5.98 + 0.543 c_1 \,.$$

- Valid up to $c_1 \sim 1$.
- In qualitative agreement with lattice results *Laerman+Schmidt., Del Debbio+Lucini+Patela+Pica, Bali+Bursa*

Mass dependence of f_π

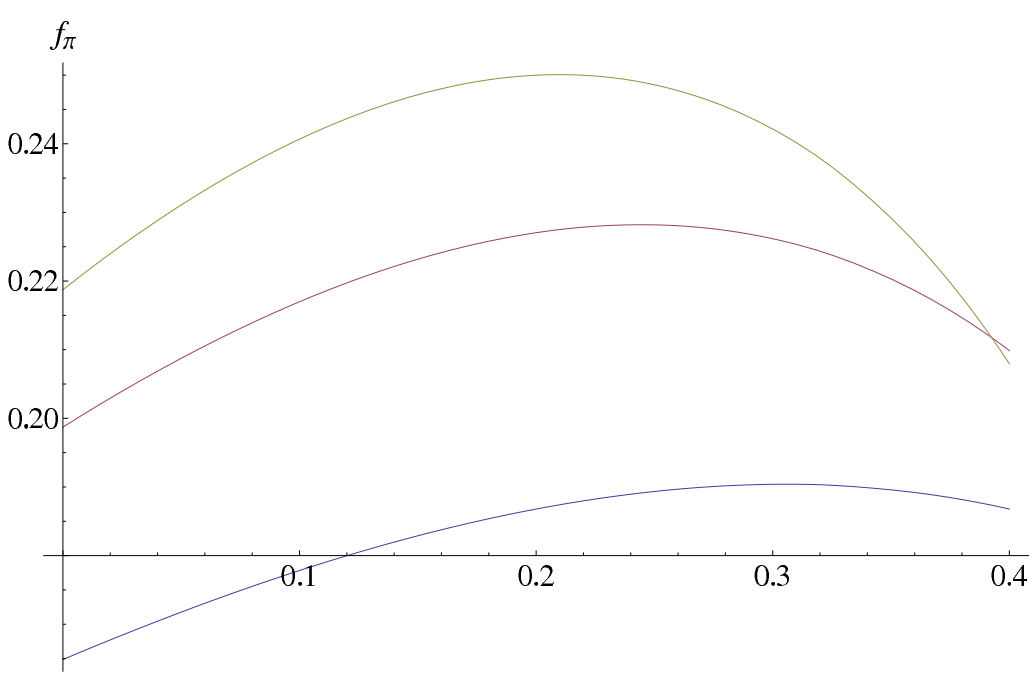

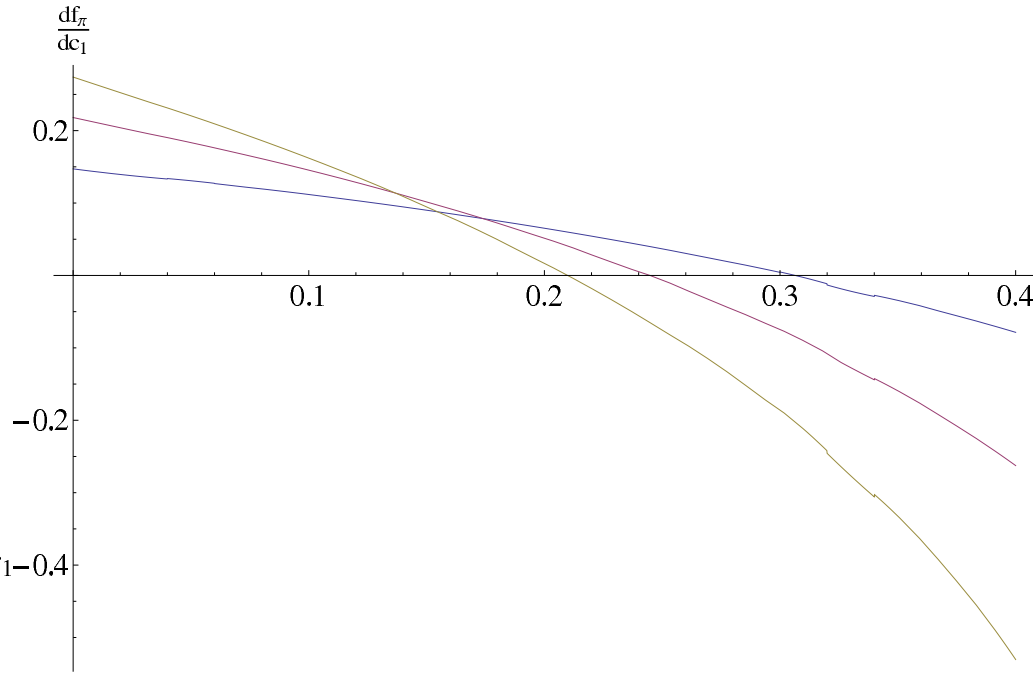

The pion decay constant and its derivative as a function of c_1 - the quark mass. The different lines correspond to different values of k. From bottom to top (on the right plot, from bottom to top in the vertical axis) $k = \frac{12}{\pi^2}, \frac{24}{\pi^2}, \frac{36}{\pi^2}$. The pion decay constant comes in units of z_Λ^{-1}.

Linear Regge Trajectories

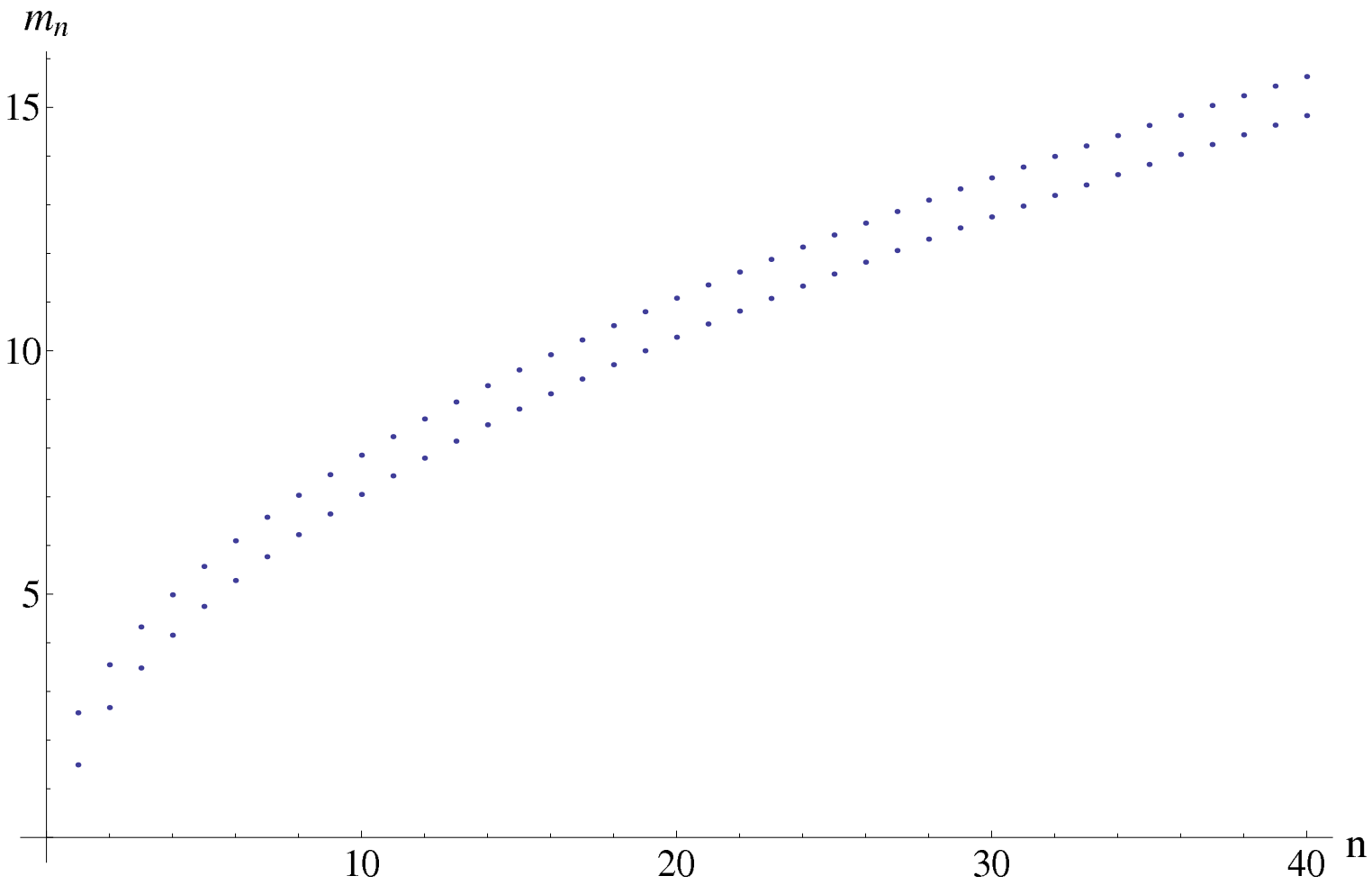

Results corresponding to the forty lightest vector states with $c_1 = 0.05$ and $c_1 = 1.5$.

Spectra of "$s\bar{s}$ states

They can be "estimated" using

$$m(\text{"}\eta\text{"}) = \sqrt{2m_K^2 - m_\pi^2} \quad , \quad m(\text{"}\phi(1020)\text{"}) = 2m(K^*(892)) - m(\rho(770)) \quad ,$$

Alton+Gimenez+Giusti+Rapuano

J^{PC}	Meson	Measured (MeV)	Model (MeV)
1^{--}	"$\phi(1020)$"	1009	857
	"$\phi(1680)$"	1363	1432
1^{++}	"$f_1(1420)$"	1440	1188
0^{-+}	"η"	691	740
	"$\eta(1475)$"	1620	1608
0^{++}	"$f_0(1710)$"	1386	1365

The "mass" of the s-quark is $c_{1,s} = 0.350$. The rms error for this set of observables ($n = 6 - 1$) is $\varepsilon_{rms} = 11\%$.

- $\frac{2m_s}{m_u + m_d} \simeq \frac{c_{1,s}}{c_{1,l}} \simeq 26$
- $T_{deconf} = \frac{5}{45\pi z_\Lambda} \simeq 200 MeV$.

The Veneziano limit: motivation

• For several phenomena in QCD (=$SU(N_c)$ theory with N_f quarks) the presence of quarks is important

• Sometimes the relevant physics can be studied in the "Quenched Approximation": quarks are probes in the glue dynamics. Several interesting phenomena have been studied in this context.

• For others however, one should include propagating quarks inducing quantum corrections in order to see them. In this second class we can mention:

♠ The conformal window: the theory flows to an IR CFT for $x_f \equiv \frac{N_f}{N_c} \geq x_c$ if quarks are massless. Chiral symmetry is expected to remain unbroken in this phase. The conformal window ends at the Banks-Zaks point, $x_f = \frac{11}{2}$.

♠ The phase transition at $x_f = x_c$ that is conjectured to be in the BKT class. This type of transition where for $x_f < x_c$ there is a condensate is known as a conformal transition.

Miransky, Kaplan+Stephanov+Son

♠ The region just below x_c where the theory is expected to exhibit walking behavior. This type of behavior has been advocated to be crucially useful for technicolor models.

♠ The QCD thermodynamics as a function of x_f.

♠ The phase diagram as a function of baryon density. Here we expect a color superconducting phase, as well as a color-flavor locking phase.

Alford+Rajagopal+Wilczek

• All of the phenomena above except the Banks-Zaks region are at strong coupling and therefore hard to analyze.

• Several (uncontrolable) techniques were applied so far for their study: Truncated Schwinger-Dyson equations, lattice calculations, guesswork on β functions, etc. It is with such techniques that some of the expectations above were found.

• The purpose of this effort is to explore the construction of holographic models that exhibit similar phenomena, so that: (a) Explore the landscape of possibilities (b) Construct realistic strong coupling models of QCD in the Veneziano Limit.

N=1 sQCD

The case of $\mathcal{N} = 1$ $SU(N_c)$ superQCD with N_f quark multiplets is known and provides an interesting (although much more complex) example for the non-supersymmetric case.

Seiberg

• $x = 0$ the theory has confinement, a mass gap and N_c distinct vacua associated with a spontaneous breaking of the leftover R symmetry Z_{N_c}.

• At $0 < x < 1$, the theory has a runaway ground state.

• At $x = 1$, the theory has a quantum moduli space with no singularity. This reflects confinement with χSB.

• At $x = 1 + \frac{1}{N_c}$, the moduli space is classical (and singular). The theory confines, but there is no χSB.

• At $1+\frac{2}{N_c} < x < \frac{3}{2}$ the theory is in the non-abelian magnetic IR-free phase, with the magnetic gauge group $SU(N_f - N_c)$ IR free.

• At $\frac{3}{2} < x < 3$, the theory flows to a CFT in the IR. (conformal window)

Near $x = 3$ this is the Banks-Zaks region where the original theory has an IR fixed point at weak coupling. Moving to lower values, the coupling of the IR $SU(N_c)$ gauge theory grows.

However near $x = \frac{3}{2}$ the dual magnetic $SU(N_f - N_c)$ is in its Banks-Zaks region, and provides a weakly coupled description of the IR fixed point theory.

• At $x > 3$, the theory is IR free.

Walking region+Technicolor

• Technicolor: EW symmetry breaking is due to a new strong gauge interaction with $\Lambda_{TC} \sim 1 TeV$.

• The EW Higgs is scalar TC meson and the vev is due to a condensate of TC fermions $\langle H \rangle \sim \langle \bar{\psi}_{TC} \psi_{TC} \rangle$ from TC chiral symmetry breaking.

• The Higgs vev is the TechniColor f_π and should be set to ~ 250 GeV.

• The composite Higgs couplings to the SM fermions χ are now four-fermi terms,

$$H \bar{\chi} \chi \sim \bar{\psi}_{TC} \psi_{TC} \ \bar{\chi} \chi$$

and should be generated by a new (ETC) interaction at a higher scale, Λ_{ETC}.

• There are some important problems with this idea:

♠ At the qualitative level: it relies on non-perturbative physics and therefore is not easily controlable/calculable.

♠ There can be important flavor changing processes (that are suppressed in the SM)

♠ To get the correct size for all masses, the dimension of operators $\psi_{TC}\psi_{TC}$ must be close to two (instead of 3 in perturbation theory).

♠ The dimensionless quantity

Peskin+Takeuchi

$$S = \frac{d}{dq^2}(\Pi_V(q^2) - \Pi_A(q^2))\Big|_{q^2=0} \quad , \quad \left(\delta_{\mu\nu} - \frac{q_\mu q_\nu}{q^2}\right)\Pi_i(q^2) \equiv \langle J^i_\mu(q) J^i_\nu(0)\rangle$$

controls the correction to the EW coupling constants and the EW gaueg boson propagators.

• It is $\mathcal{O}(1)$ in generic theories from the spectral decomposition+sum rules, but EW data imply that its should be $\mathcal{O}(10^{-2})$.

♠ It has been argued by many scientists that a way out of the above is a TC theory that is near conformal ("walking") in the TC regime,

Holdom, Appelquist+Karabali+Wijewardhana

♠ Because $S = 0$ in the conformal window it was argued by continuity that $S \to 0$ in the walking region.

Appelquist+Sannino

♠ Because of approximate scale invariance, the theory was expected to have a light scalar, "the dilaton", namely the singlet scalar meson (σ-meson).

Yamawaki+Bando+Matumoto

♠ Despite a lot of work in the last 15 years, whether such a theory exists, and whether it has the required properties has remained elusive till now, especially because lattice techniques are hard to apply to almost massless setups.

The Banks-Zaks region

- The QCD β function in the V-limit is

$$\dot{\lambda} = \beta(\lambda) = -b_0\lambda^2 + b_1\lambda^3 + \mathcal{O}(\lambda^4) \ , \ b_0 = \frac{2}{3}\frac{(11-2x_f)}{(4\pi)^2} \ , \ b_1 = -\frac{2}{3}\frac{(34-13x_f)}{(4\pi)^4}$$

- The Banks-Zaks region is

$$x_f = \frac{11}{2} - \epsilon \quad with \quad 0 < \epsilon \ll 1$$

We obtain a fixed point of the β-function at

$$\lambda_* \simeq \frac{(8\pi)^2}{75}\epsilon + \mathcal{O}(\epsilon^2)$$

which is trustable in perturbation theory, as λ_* can be made arbitrarily small.

• The mass operator, $\bar{\psi}_L \psi_R$ has now dimension smaller than three, from the perturbative anomalous dimension (in the V-limit)

$$-\frac{d\log m}{d\log \mu} \equiv \gamma = \frac{3}{(4\pi)^2}\lambda + \frac{(203-10x_f)}{12\,(4\pi)^4}\lambda^2 + \mathcal{O}(\lambda^3, N_c^{-2})$$

• Extrapolating to lower x we expect the phase diagram

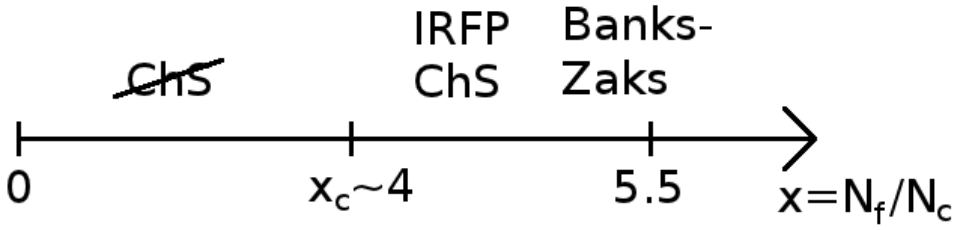

The strategy

- Construct (toy) holographic models resembling QCD in the Veneziano limit.

- Put together two ingredients: the holographic model for glue developed earlier: IHQCD

Gursoy+E.K+Nitti

- and the model for flavor based in Sen's tachyon action.

Casero+E.K.+Paredes, Iatrakis+E.K.+Paredes

Fusion

The idea is to put together the two ingredients in order to study the chiral dynamics and its backreaction to glue.

$$\mathcal{S} = N_c^2\ M^3 \int d^5x\sqrt{g}\left[R - \frac{4}{3}\frac{(\partial\lambda)^2}{\lambda^2} + V_g(\lambda)\right] -$$

$$-N_f N_c\ M^3 \int d^5x V_f(\lambda,T)\sqrt{-\det(g_{ab}+h(\lambda)\partial_a T\partial_b T)}$$

with

$$V_f(\lambda,T) = V_0(\lambda)\ \exp(-a(\lambda)T^2)$$

- We must choose $V_0(\lambda), a(\lambda), h(\lambda)$.

♠ The simplest and most reasonable choices, compatible with glue dynamics do the job! The phase structure at $T=0$ is robust against many different choices in the IR.

Parameters

• A theory with a single relevant (or marginally relevant) coupling like YM has no parameters.

• The same applies to QCD with massless quarks.

• QCD with all quarks having mass m has a single (dimensionless) parameter : $\frac{m}{\Lambda_{QCD}}$.

• After various rescalings this single parameter can be mapped to the parameter T_0 that controls the diverging tachyon in the IR.

• There is also x_f that has become continuous in the large N_c Veneziano limit.

The effective potential

For solutions $T = T_* = constant$ the relevant non-linear action simplifies

$$\mathcal{S} = M^3 N_c^2 \int d^5x \sqrt{g} \left[R - \frac{4}{3} \frac{(\partial\lambda)^2}{\lambda^2} + V_g(\lambda) - x_f V_f(\lambda, T) \right]$$

$$V_f(\lambda, T) = V_0(\lambda)\ e^{-a(\lambda) T_*^2}$$

• Minimizing for T_* we obtain $T_* = 0$ and $T_* = \infty$. The effective potential for λ is

♠ $T_* = 0$, $V_{eff} = V_g(\lambda) - x_f V_0(\lambda)$ with a IR fixed point at $\lambda = \lambda_*(x_f)$.

♠ $T_* = \infty$, $V_{eff} = V_g(\lambda)$ with no fixed points.

Condensate dimension at the IR fixed point

• By expanding the DBI action we obtain the IR tachyon mass at the IR fixed point $\lambda = \lambda_*$ which gives the chiral condensate dimension:

$$-m_{\rm IR}^2 \ell_{\rm IR}^2 = \Delta_{\rm IR}(4-\Delta_{\rm IR}) = \frac{24a(\lambda_*)}{h(\lambda_*)(V_g(\lambda_*) - x_f V_0(\lambda_*))}$$

• Must reach the Breitenlohner-Freedman (BF) bound (horizontal line) at some x_c.

• x_c marks the *conformal phase transition*

Kaplan+Lee+Son+Stephanov

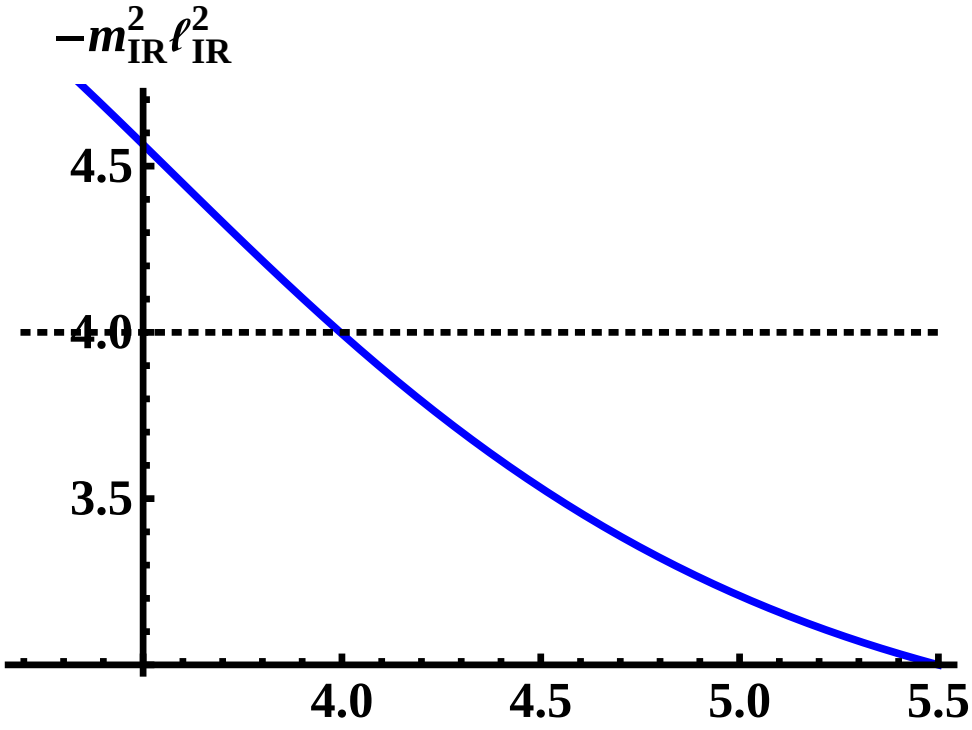

We obtain: $3.7 \lesssim x_c \lesssim 4.2$

UV mass vs IR parameter

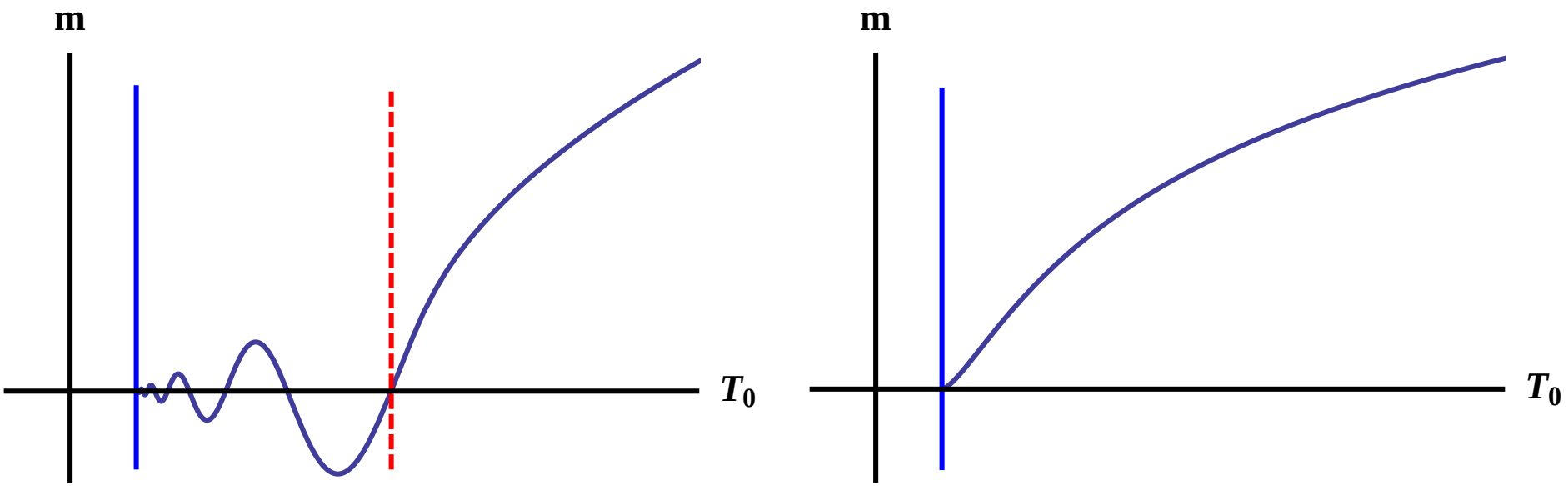

• Left figure: Plot of the UV Mass parameter m, as a function of the IR T_0 scale, for $x < x_c$.

• Right figure: Similar plot for $x \geq x_c$.

• Such plots are sketched from the numerics, analytical expansions and some guesses.

• The tachyon starts at the boundary, evolves into the sinusoidal form for a while, $T \sim r^2 \sin[k \log r + \phi]$, and then at the end diverges. Similar behavior seen at

Kutasov+Lin+Parnachev

• For the n-th solution, the tachyon changes sign n times before diverging in the IR.

• At $m = 0$ there is an ∞ number of saddle point solutions (Efimov-like minima)

• The Efimov minima have free energies ΔE_n with

$$\Delta E_0 > \Delta E_1 > \Delta E_2 > \cdots$$

Efimov spiral

Ongoing work: $\sigma(m)$ dependence

❑ For $x < x_c$ spiral structure

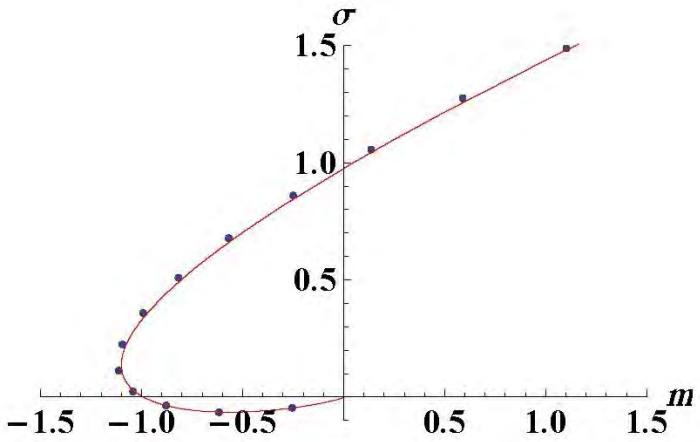

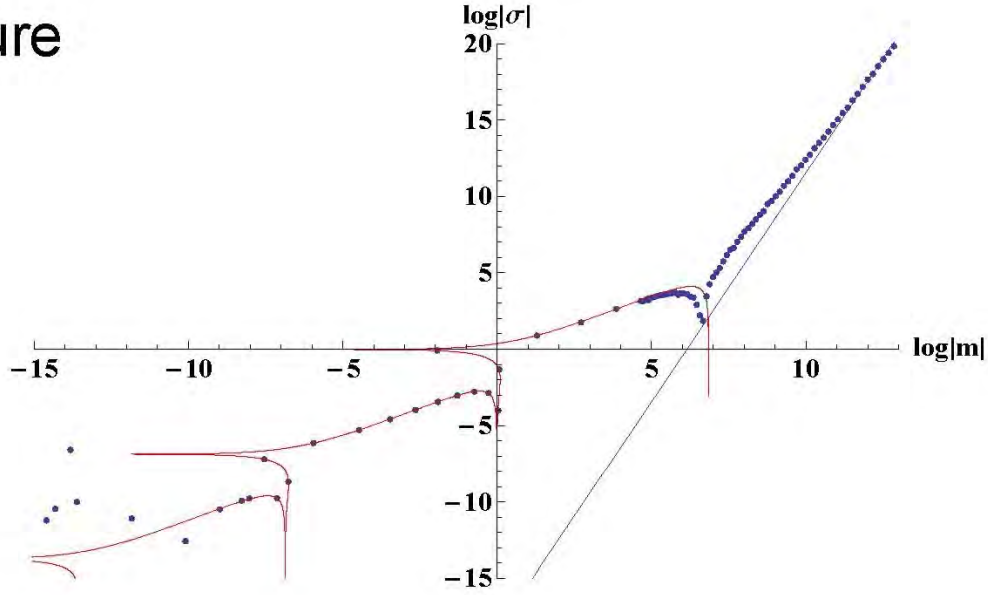

• This suggests that the presence of double trace deformations can alter the ground state of the system and make the second Effimov vacuum be the ground state.

Recap

- For $x = 0$, the theory has a mass gap, and confines.

- $0 < x < x_c \simeq 4$ the theory has chiral symmetry breaking, massless pions, and gapped spectrum otherwise.

- $x_c < x < \frac{11}{2}$ the theory is chirally symmetric, and flows to a non-trivial fixed point in the IR.

Below the BF bound

- Correlation of the violation of BF bound and the conformal phase transition

- For $\Delta_{\rm IR}(4-\Delta_{\rm IR})<4$

$$T(r)\sim m_q r^{4-\Delta_{\rm IR}}+\sigma r^{\Delta_{\rm IR}}$$

- For $\Delta_{\rm IR}(4-\Delta_{\rm IR})>4$

$$T(r)\sim Cr^2\sin\left[(\mathrm{Im}\Delta_{\rm IR})\log r+\phi\right]$$

Two possibilities:

- $x>x_c$: BF bound satisfied at the fixed point $\Rightarrow$ only trivial massless solution ($T\equiv 0$, ChS intact, fixed point hit)

- $x<x_c$: BF bound violated at the fixed point $\Rightarrow$ a nontrivial massless solution exists, which drives the system away from the fixed point.

Conclusion: *phase transition* at $x=x_c$

Matching to QCD: UV

- As $\lambda \to 0$ we can match:

♠ $V_g(\lambda)$ with (two-loop) Yang-Mills β-function.

♠ $V_g(\lambda) - xV_0(\lambda)$ with QCD β-function.

♠ $a(\lambda)/h(\lambda)$ with anomalous dimension of the quark mass/chiral condensate

- The matching allows to mark the BZ point, that we normalize at $x = \frac{11}{2}$.

- After the matching above we are left with a single undetermined parameter in the UV:

$$V_g \sim V_0 + \mathcal{O}(\lambda) \quad , \quad V_0 \sim W_0 + \mathcal{O}(\lambda)$$

$$V_0 - xW_0 = \frac{12}{\ell_{UV}^2}$$

Potential Choices

- Potentials I vs II

$$V_g = \frac{12}{\ell_0^2} + \mathcal{O}(\lambda) \quad , \quad V_f = -x_f \left(\frac{12}{\ell_f^2} + \mathcal{O}(\lambda) \right) \quad , \quad \frac{1}{\ell_{UV}^2} = \frac{1}{\ell_0^2} - \frac{x_f}{\ell_f^2}$$

- Value of $0 < W_0 < \frac{24}{11}$ with $x_f \ell_0^2 W_0 = 12 \left(1 - \frac{\ell_0^2}{\ell_{UV}^2} \right)$.

- Fixed point of $V_g(\lambda) - V_f(\lambda)$ exists for all x, or for $x_* < x < \frac{11}{2}$

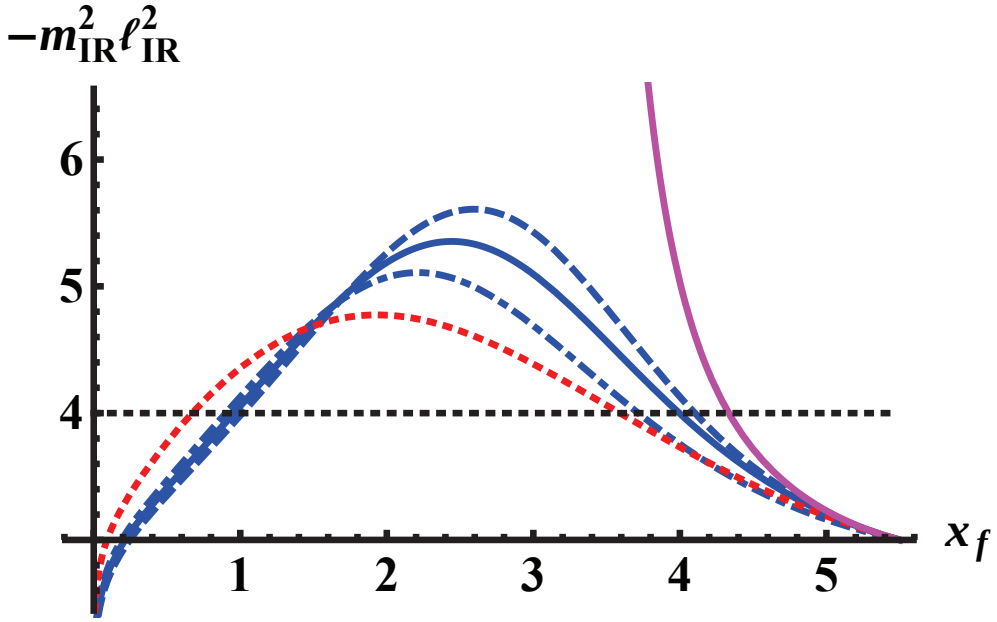

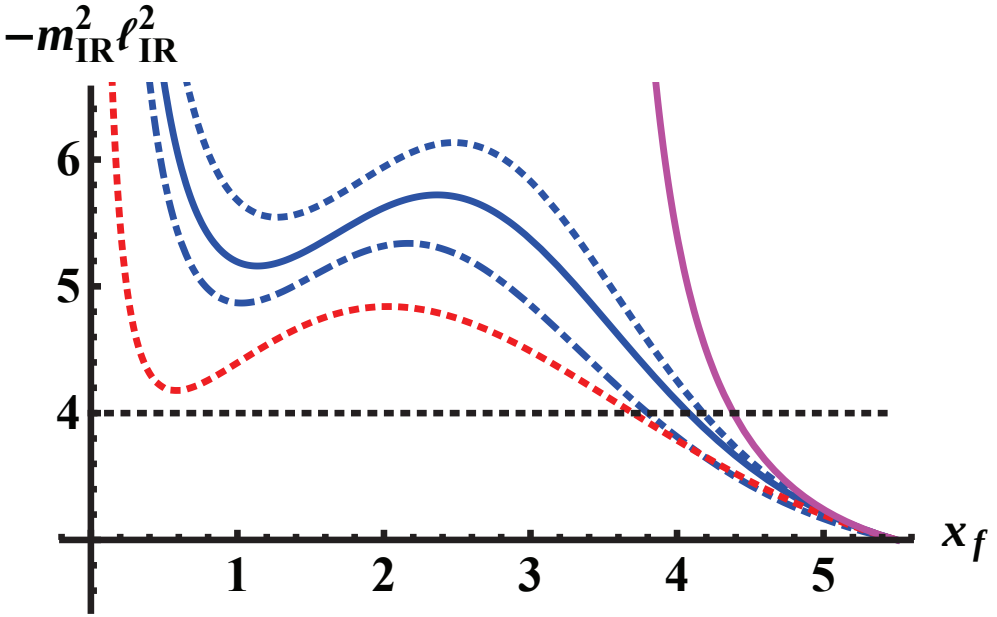

Varying the model

"prediction" for x_c

After fixing UV coefficients from QCD, there is still freedom in choosing the leading coefficient of V_0 at $\lambda \to 0$ and the IR asymptotics of the potentials

Thick blue $\to V_I$

Thin red $\to V_{II}$

Resulting variation of the edge of conformal window

$$3.7 \lesssim x_c \lesssim 4.2$$

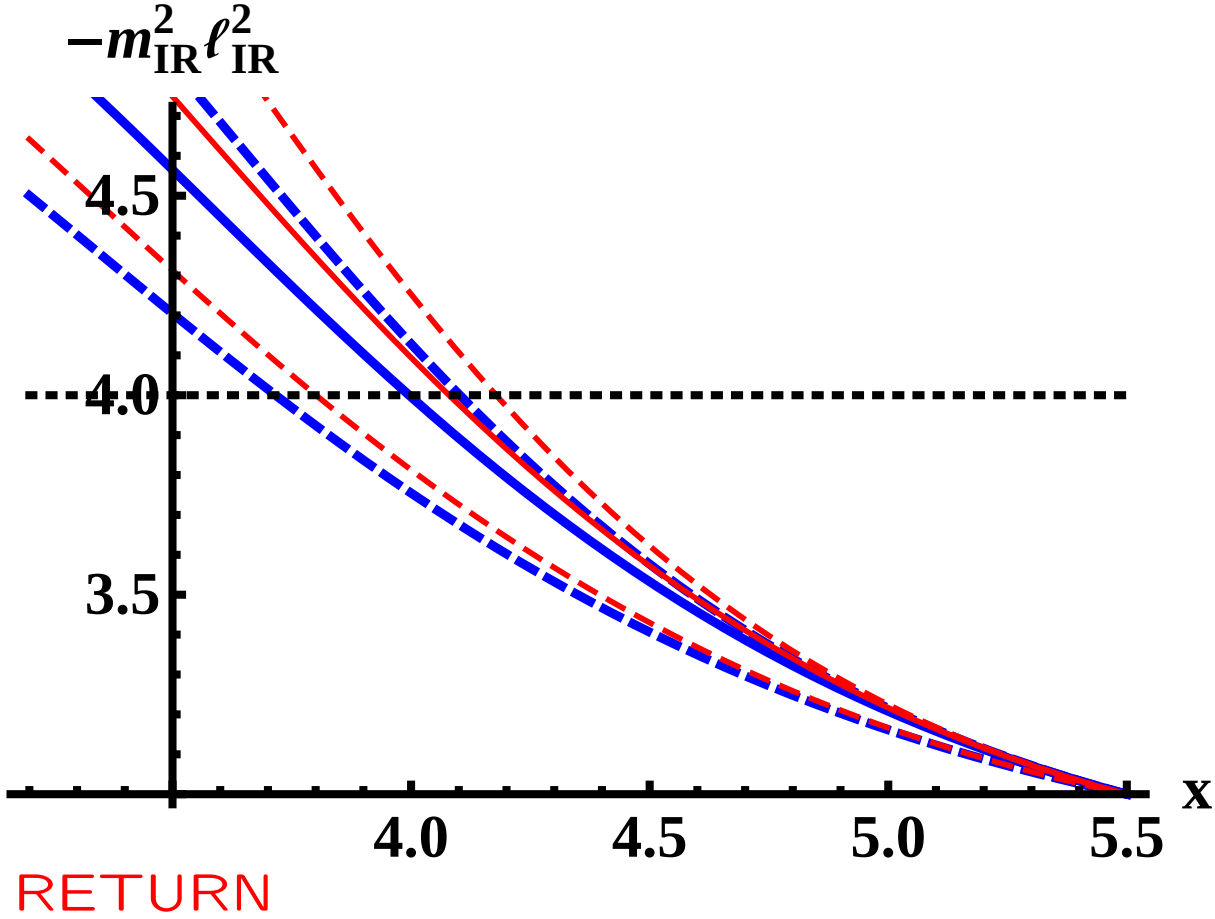

RETURN

The IR fixed point

$$V_{\text{eff}}(\lambda) = V_g(\lambda) - xV_0(\lambda)$$

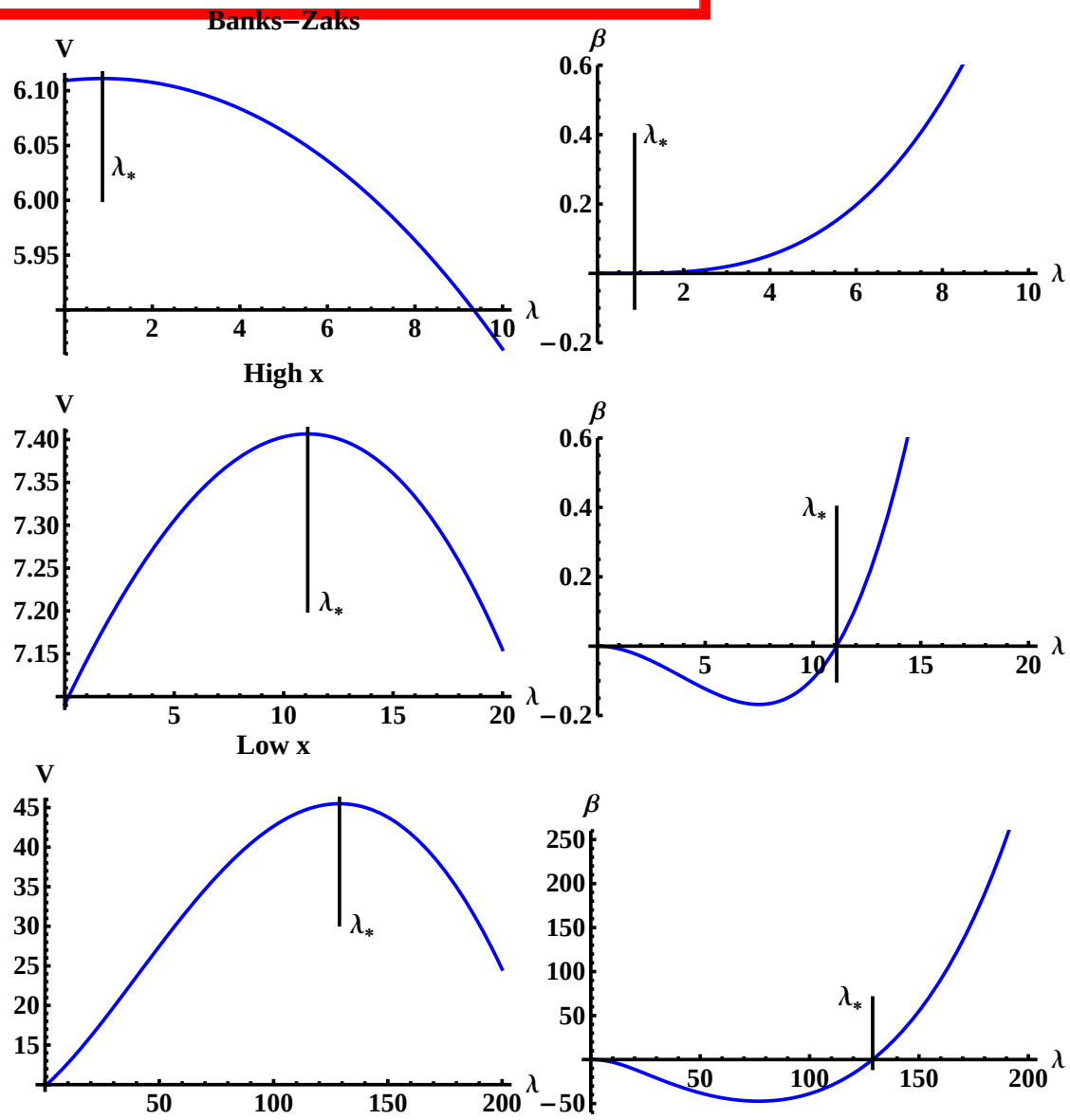

Two possibilities: (a) The maximum exists for all x. (b) The maximum exists for $x > x_*$.

Matching to QCD: IR

• In the IR, the tachyon has to diverge $\Rightarrow$ the tachyon action $\propto e^{-T^2}$ becomes small

♠ $V_g(\lambda) \simeq \lambda^{\frac{4}{3}}\sqrt{\lambda}$ chosen as for Yang-Mills, so that a "good" IR singularity exists etc.

♠ $V_0(\lambda)$, $a(\lambda)$, and $h(\lambda)$ chosen to produce tachyon divergence: there are several possibilities.

♠ The phase structure is essentially independent of IR choices.

Choice I, for which in the IR

$$T(r) \sim T_0 \exp\left[\frac{81\ 3^{5/6}(115-16x)^{4/3}(11-x)}{812944\ 2^{1/6}}\frac{r}{R}\right] \quad , \quad r \to \infty$$

R is the IR scale of the solution. T_0 is the control parameter of the UV mass.

Choice II: for which in the IR

$$T(r) \sim \frac{27\ 2^{3/4}3^{1/4}}{\sqrt{4619}}\sqrt{\frac{r-r_1}{R}} \quad , \quad r \to \infty$$

R is the IR scale of the solution. r_1 is the control parameter of the UV mass.

The free energy

The free energy difference between the ChS and ChSB $m_q = 0$ solutions

Chiral symmetry breaking solution favored whenever it exists ($x < x_c$)

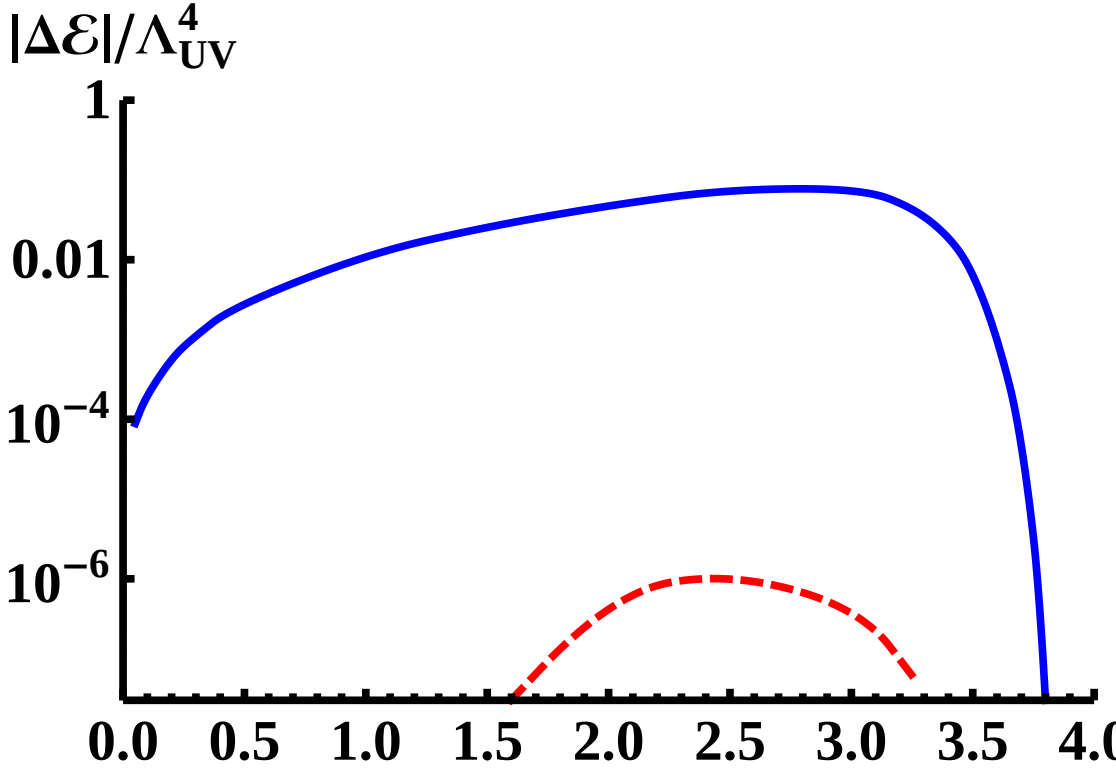

- The Efimov minima have free energies ΔE_n with

$$\Delta E_0 > \Delta E_1 > \Delta E_2 > \cdots$$

Walking

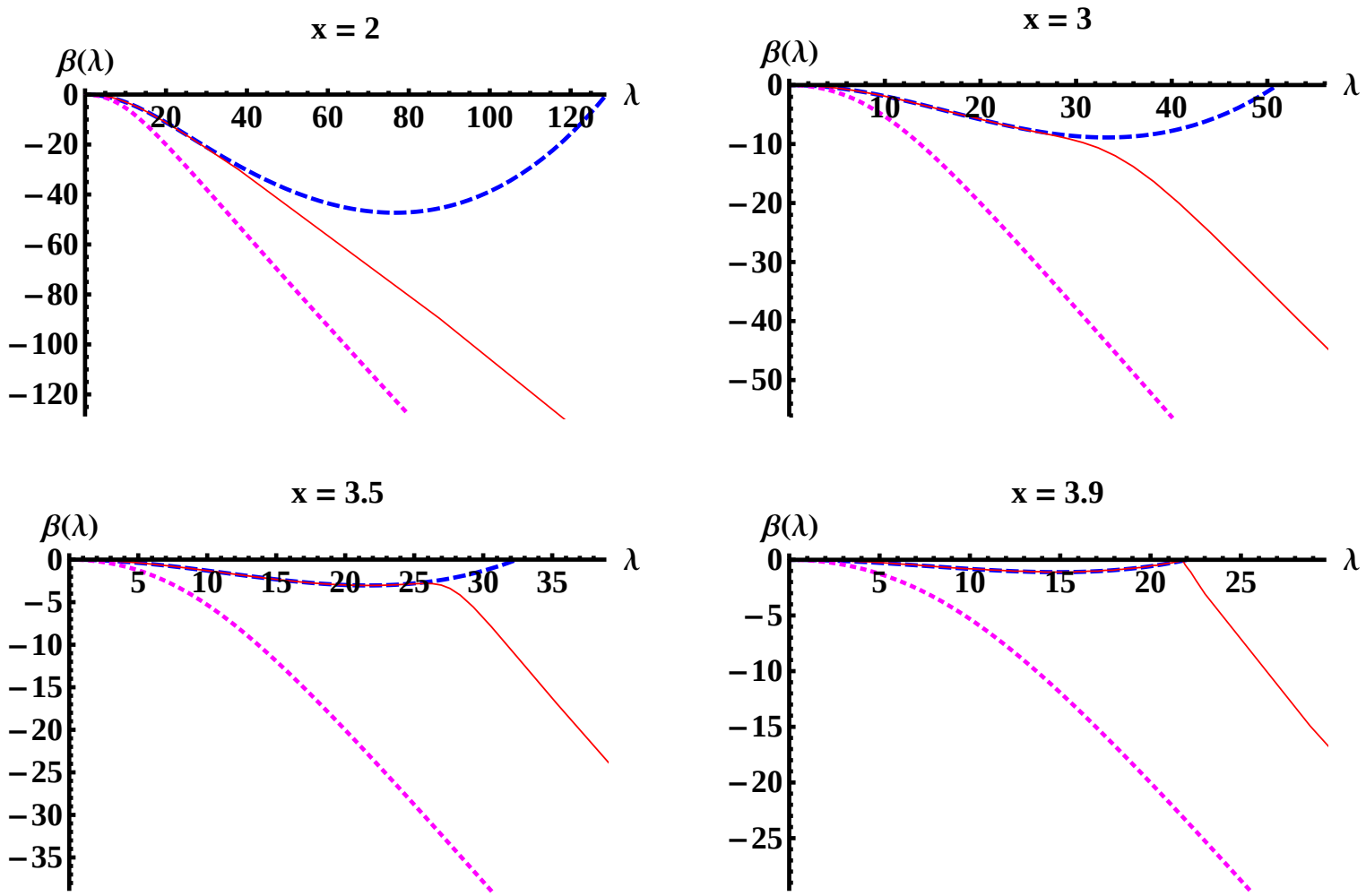

The β-functions for vanishing quark mass for various values of x. The red solid, blue dashed, and magenta dotted curves are the β-functions corresponding to the full numerical solution $(d\lambda/dA)$ along the RG flow, the potential $V_{\text{eff}} = V_g - xV_{f0}$, and the potential V_g, respectively.

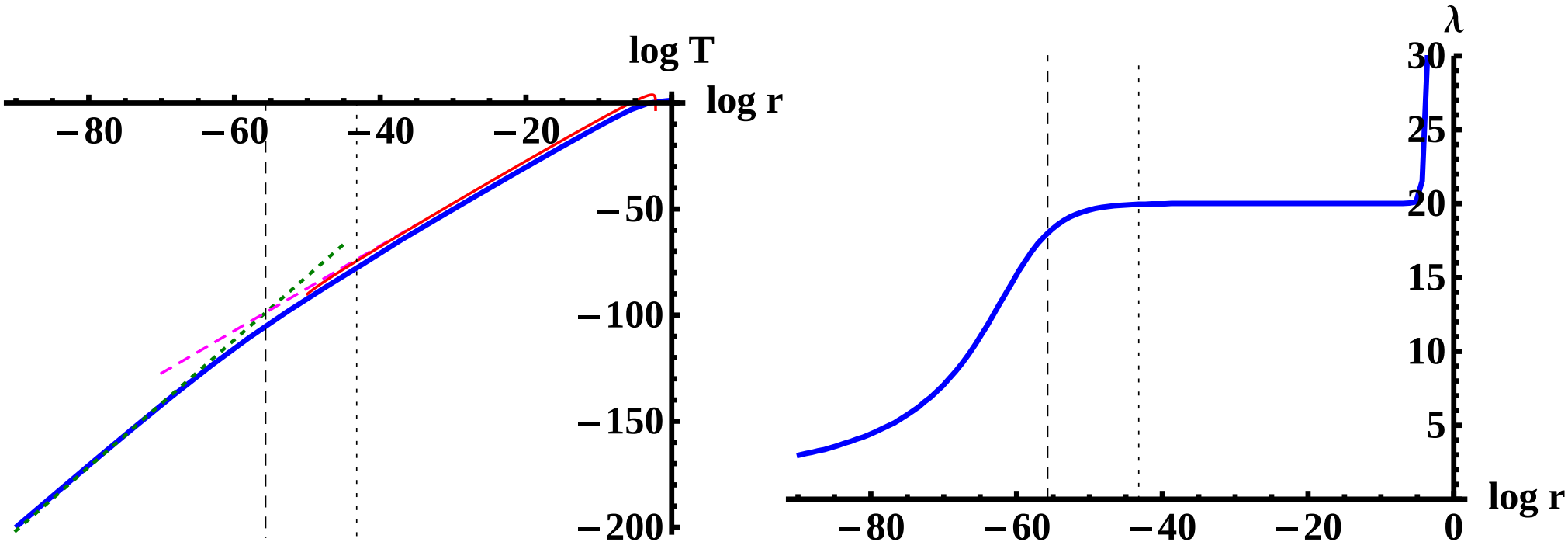

The tachyon $\log T$ (left) and the coupling λ (right) as functions of $\log r$ for an extreme walking background with $x = 3.992$. The thin lines on the left hand plot are the approximations used to derive the BKT scaling.

Holographic β-functions

The second order equations for the system of two scalars plus metric can be written as first order equations for the β-functions

Gursoy+Kiritsis+Nitti

$$\frac{d\lambda}{dA} = \beta(\lambda, T) \quad , \quad \frac{dT}{dA} = \gamma(\lambda, T)$$

The equations of motion boil down to two partial non-linear differential equations for β, γ.

Such equations have also branches as for DBI and non-linear scalar actions the relation of $e^{-A}A'$ with the potentials is a polynomial equation of degree higher than two.

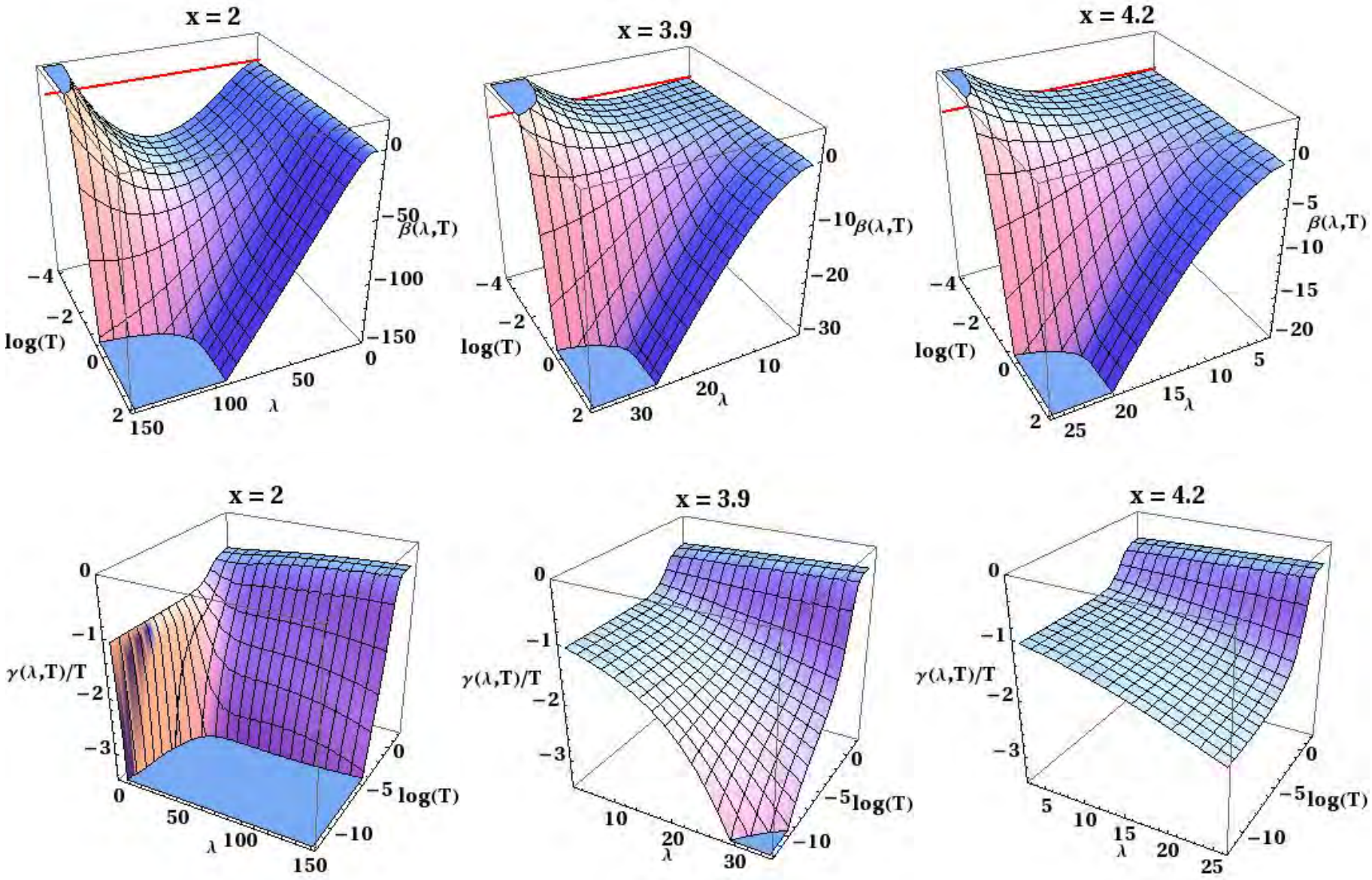

The red lines are added on the top row at $\beta = 0$ in order to show the location of the fixed point.

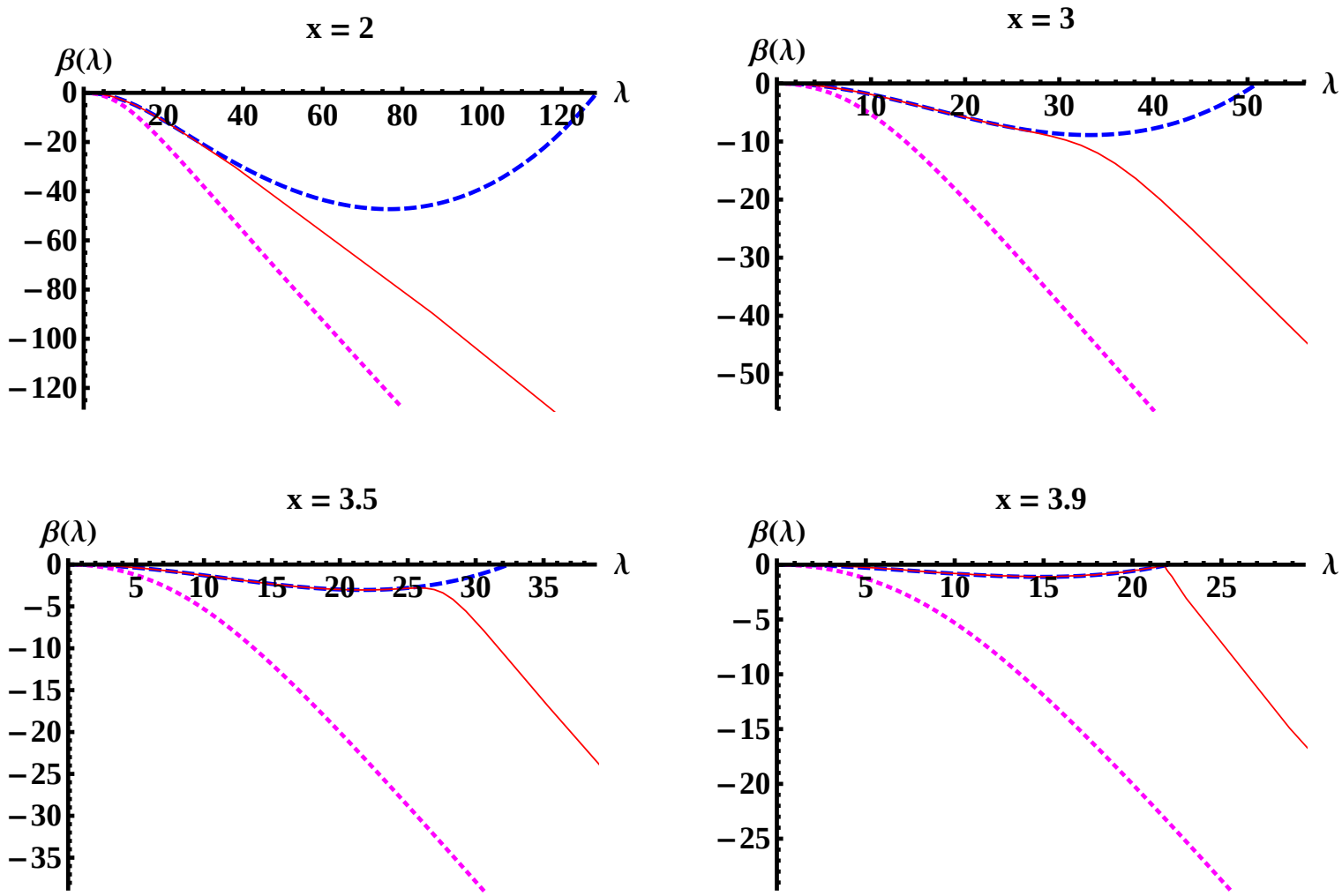

The β-functions for vanishing quark mass for various values of x. The red solid, blue dashed, and magenta dotted curves are the β-functions corresponding to the full numerical solution ($d\lambda/dA$) along the RG flow, the potential $V_{\text{eff}} = V_g - xV_{f0}$, and the potential V_g, respectively.

UV mass vs T_0 and r_1

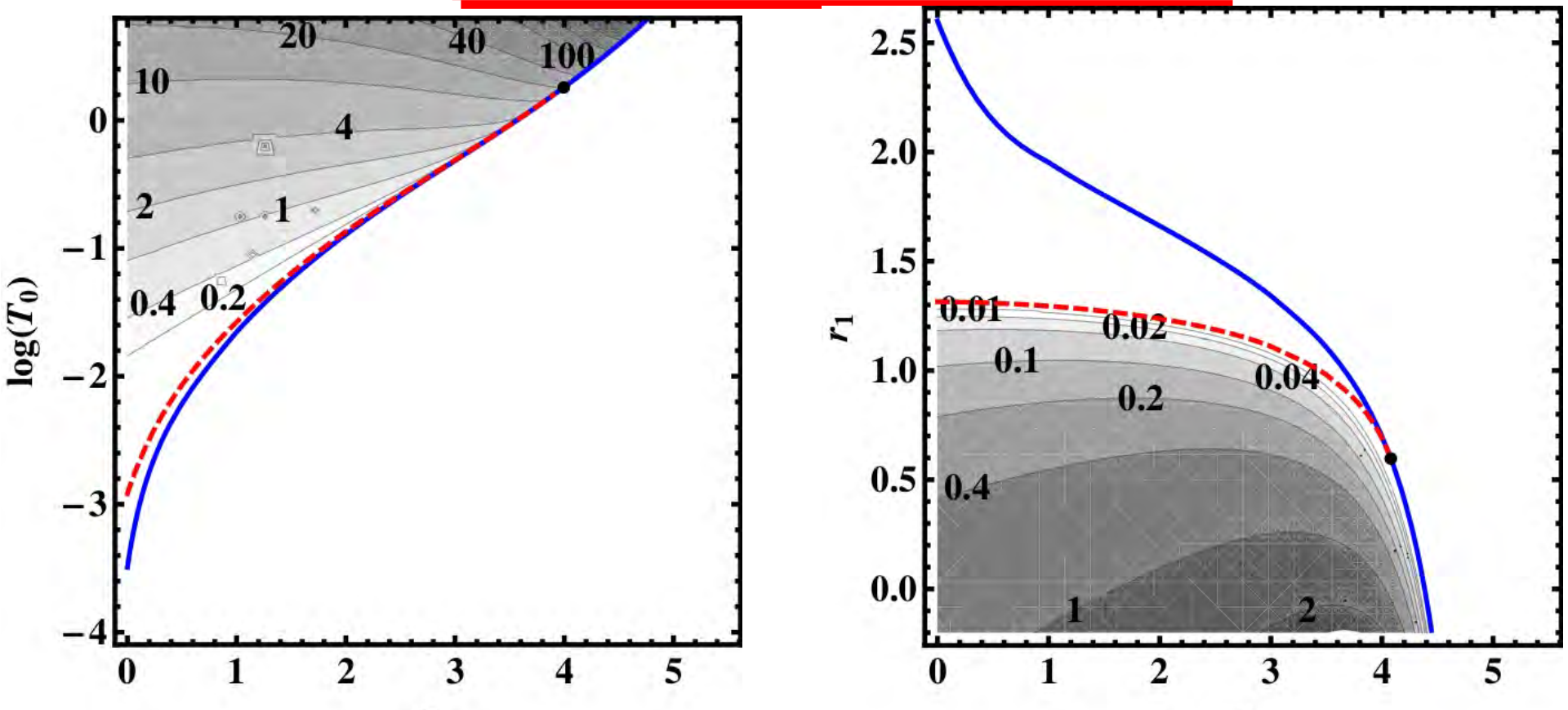

The UV behavior of the background solutions with good IR singularity for the scenario I (left) and parameter T_0 and scenario II (right) and parameter r_1.

The thick blue curve represents a change in the UV behavior, the red dashed curve has zero quark mass, and the contours give the quark mass. The black dot where the zero mass curve terminates lies at the critical value $x = x_c$. For scenario I (II) we have $x_c \simeq 3.9959$ ($x_c \simeq 4.0797$).

Numerical solutions: $T = 0$

$T \equiv 0$ backgrounds (color codes λ, A)

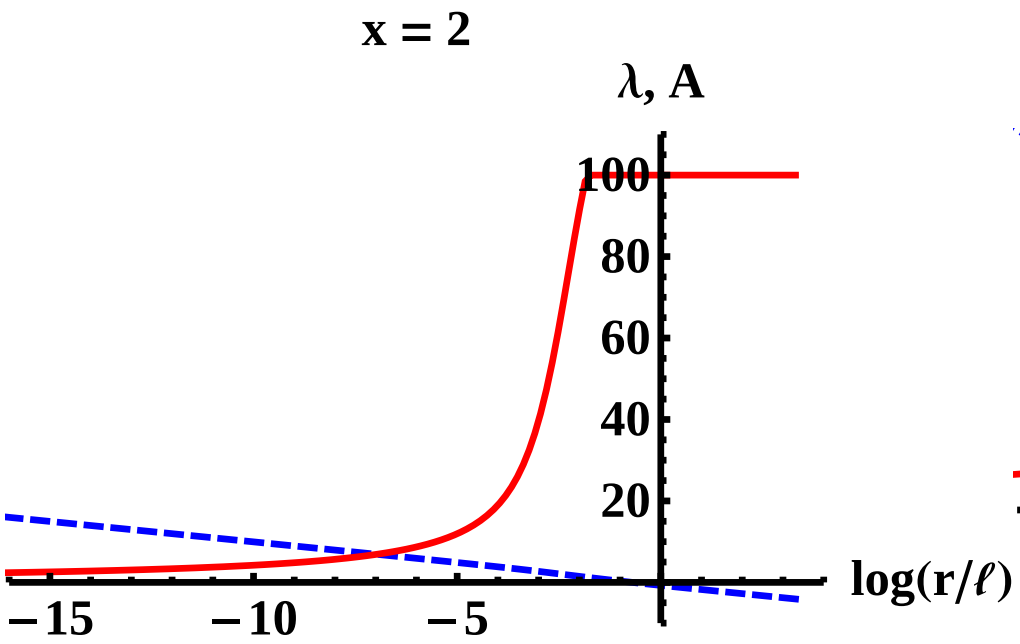

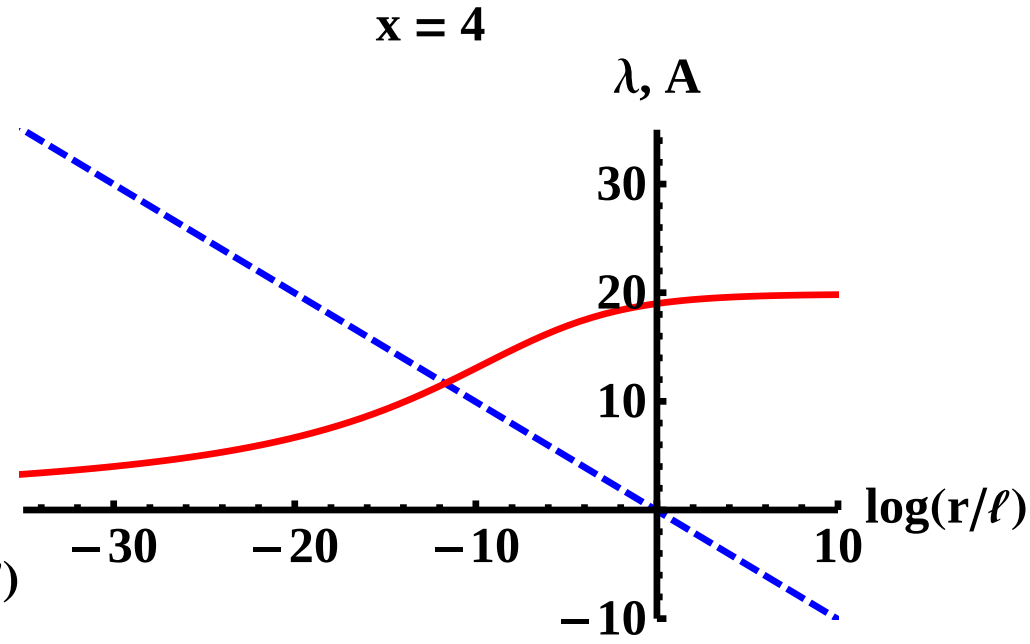

Numerical solutions: Massless with $x < x_c$

Massless backgrounds with $x < x_c \simeq 3.9959$ (λ, A, T)

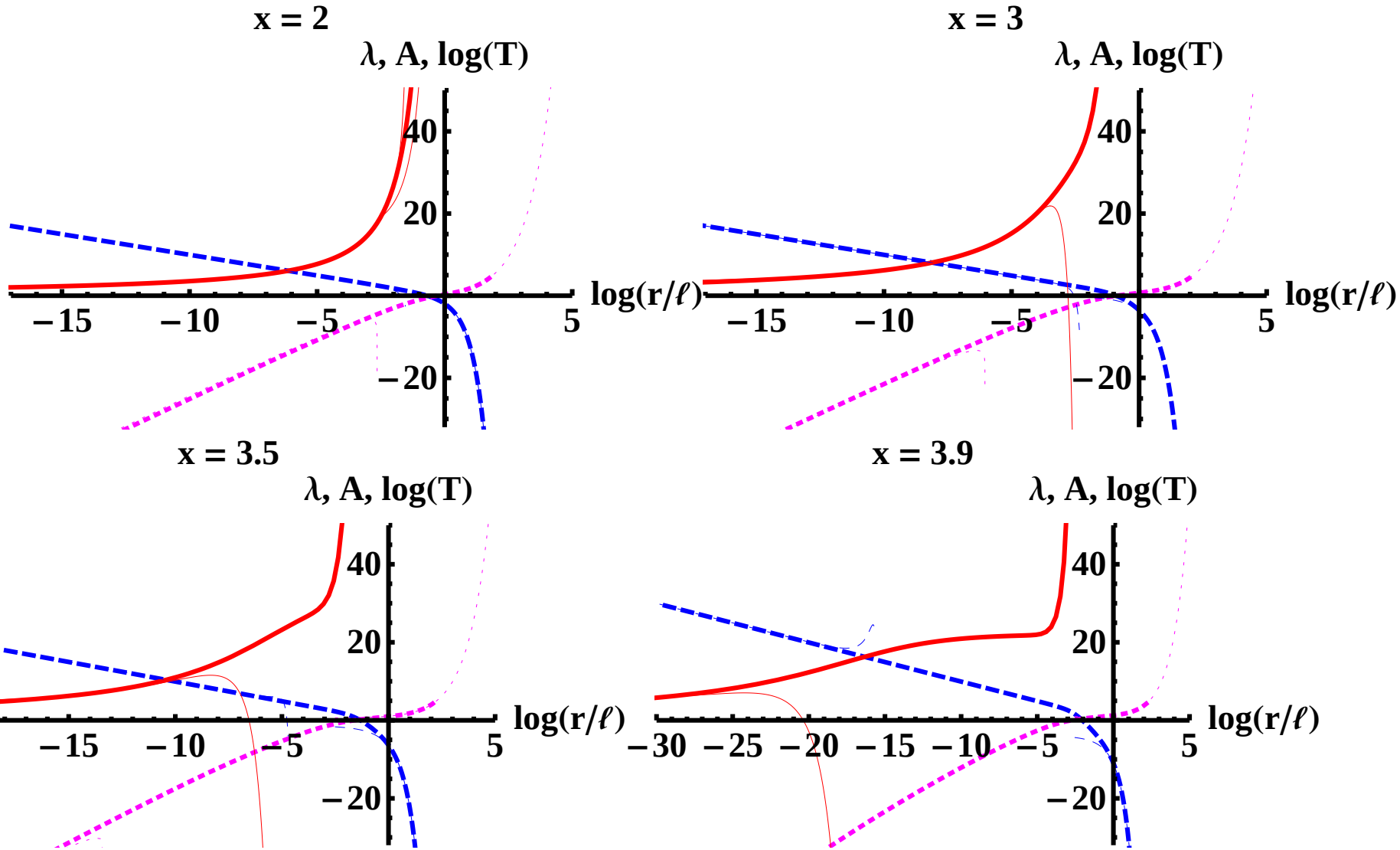

Massless backgrounds: beta functions $\beta = \frac{d\lambda}{dA}$, ($x_c \simeq 3.9959$)

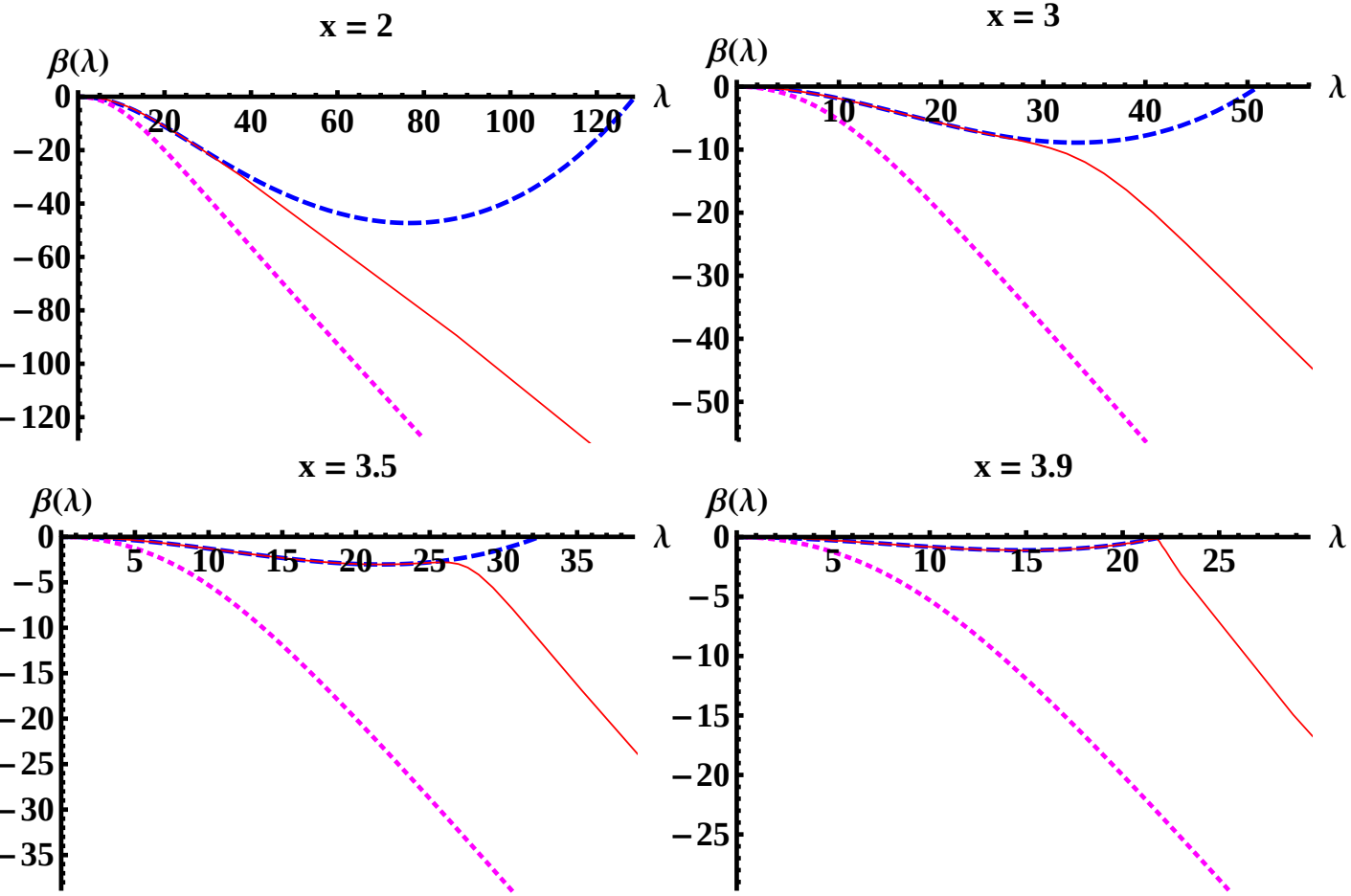

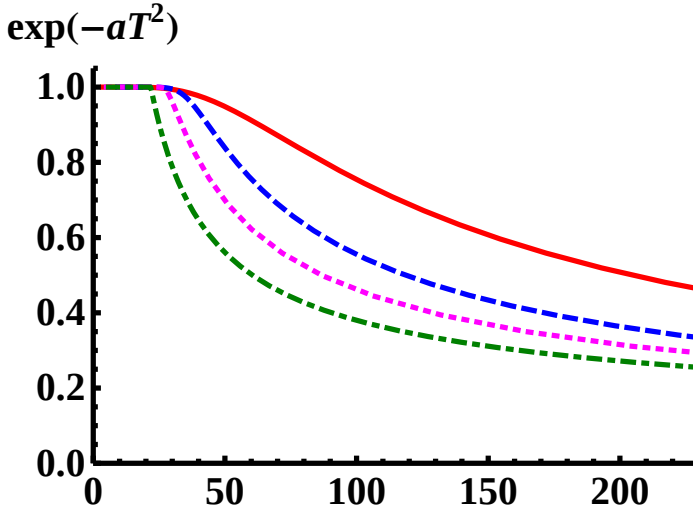

$x = 2, 3, 3.5, 3.9$

.

Massless backgrounds: gamma functions $\frac{\gamma}{T} = \frac{d \log T}{dA}$

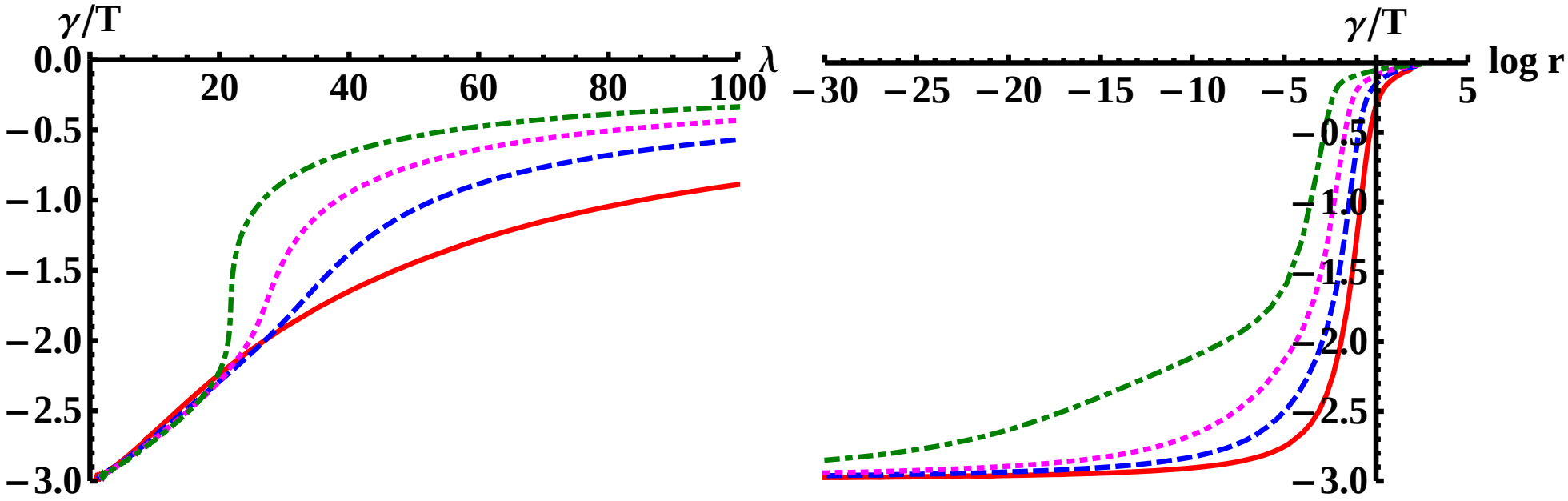

$x = 2, 3, 3.5, 3.9$

Matching to QCD: IR

• In the IR, the tachyon has to diverge $\Rightarrow$ the tachyon action $\propto e^{-T^2}$ becomes small

♠ $V_g(\lambda) \simeq \lambda^{\frac{4}{3}}\sqrt{\lambda}$ chosen as for Yang-Mills, so that a "good" IR singularity exists etc.

♠ $V_0(\lambda)$, $a(\lambda)$, and $h(\lambda)$ chosen to produce tachyon divergence: there are several possibilities.

♠ The phase structure is essentially independent of IR choices.

Choice I:

$$V_g(\lambda) = 12 + \frac{44}{9\pi^2}\lambda + \frac{4619}{3888\pi^4}\frac{\lambda^2}{(1+\lambda/(8\pi^2))^{2/3}}\sqrt{1+\log(1+\lambda/(8\pi^2))}$$

$$V_f(\lambda, T) = V_0(\lambda)e^{-a(\lambda)T^2}$$

$$V_0(\lambda) = \frac{12}{11} + \frac{4(33-2x)}{99\pi^2}\lambda + \frac{23473 - 2726x + 92x^2}{42768\pi^4}\lambda^2$$

$$a(\lambda) = \frac{3}{22}(11-x)$$

$$h(\lambda) = \frac{1}{\left(1+\frac{115-16x}{288\pi^2}\lambda\right)^{4/3}}$$

For which in the IR

$$T(r) \sim T_0 \exp\left[\frac{81\ 3^{5/6}(115-16x)^{4/3}(11-x)}{812944\ 2^{1/6}}\frac{r}{R}\right] \quad , \quad r \to \infty$$

R is the IR scale of the solution. T_0 is the control parameter of the UV mass.

Choice II:

$$a(\lambda) = \frac{3}{22}(11-x)\frac{1+\frac{115-16x}{216\pi^2}\lambda+\frac{\lambda^2}{\lambda_0^2}}{(1+\lambda/\lambda_0)^{4/3}}$$

$$h(\lambda) = \frac{1}{(1+\lambda/\lambda_0)^{4/3}}$$

for which in the IR

$$T(r) \sim \frac{27\ 2^{3/4}3^{1/4}}{\sqrt{4619}}\sqrt{\frac{r-r_1}{R}} \quad , \quad r \to \infty$$

R is the IR scale of the solution. r_1 is the control parameter of the UV mass.

Comparison to previous "guesses"

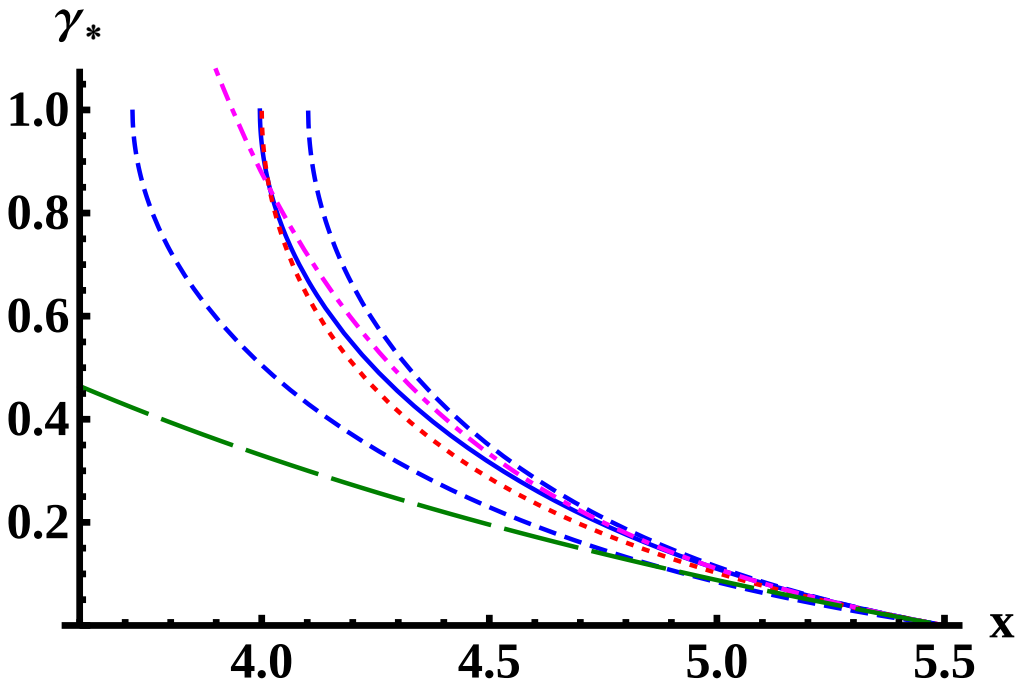

The anomalous dimension of the quark mass at the IR fixed point as a function of x within the conformal window in various approaches.

The solid blue curve is our result for the potential I.

The dashed blue lines show the maximal change as W_0 is varied from 0 (upper curve) to 24/11 (lower curve).

The dotted red curve is the result from a Dyson-Schwinger analysis, the dot-dashed magenta curve is the prediction of two-loop perturbative QCD, and the long-dashed green curve is based on an all-orders β-function.

Miransky scaling for the masses

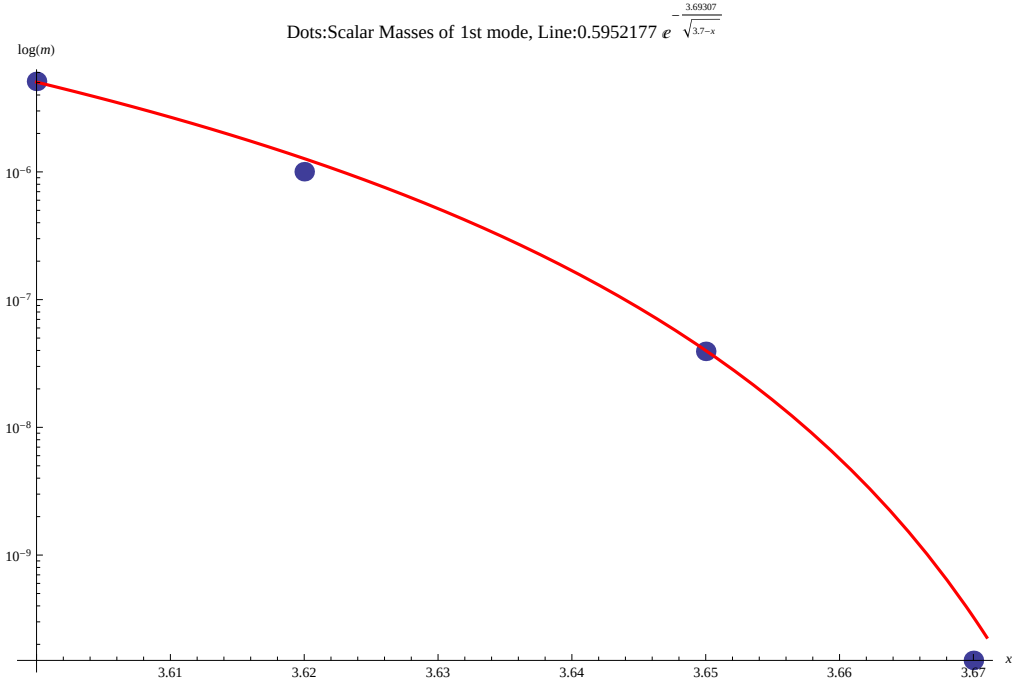

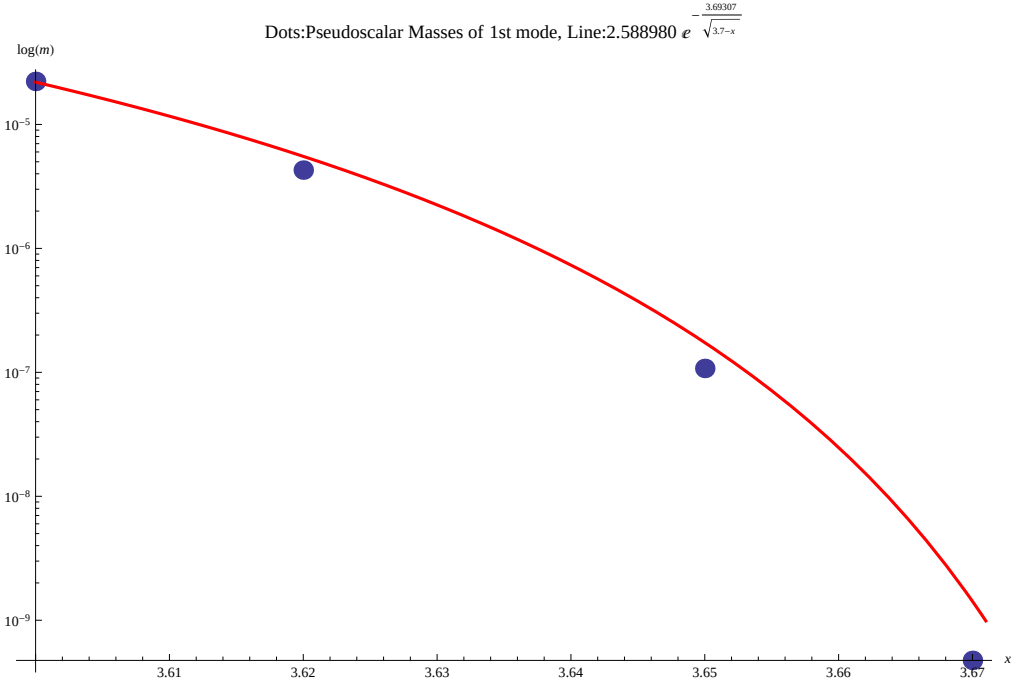

The plots depict the scalar and pseudoscalar masses of the first mode close to x_c fit to the Miransky exponential factor.

RETURN

Walking

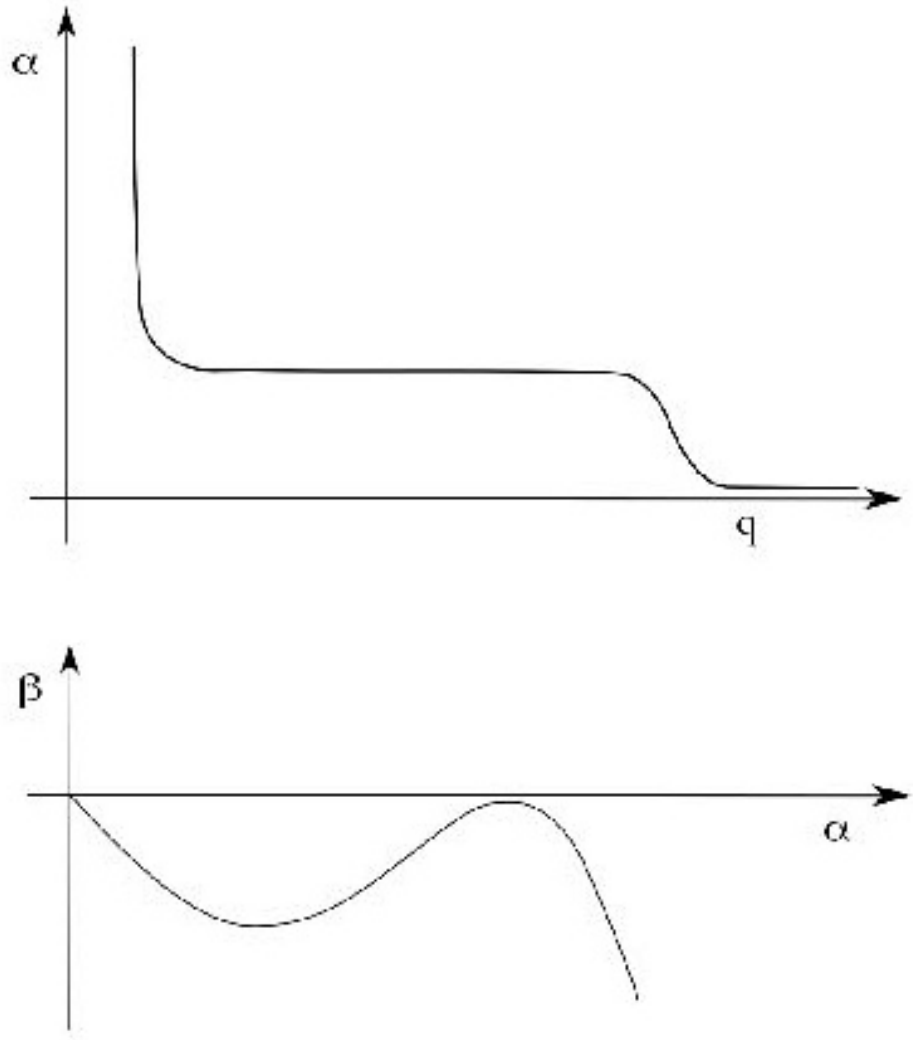

RETURN

The phase diagram

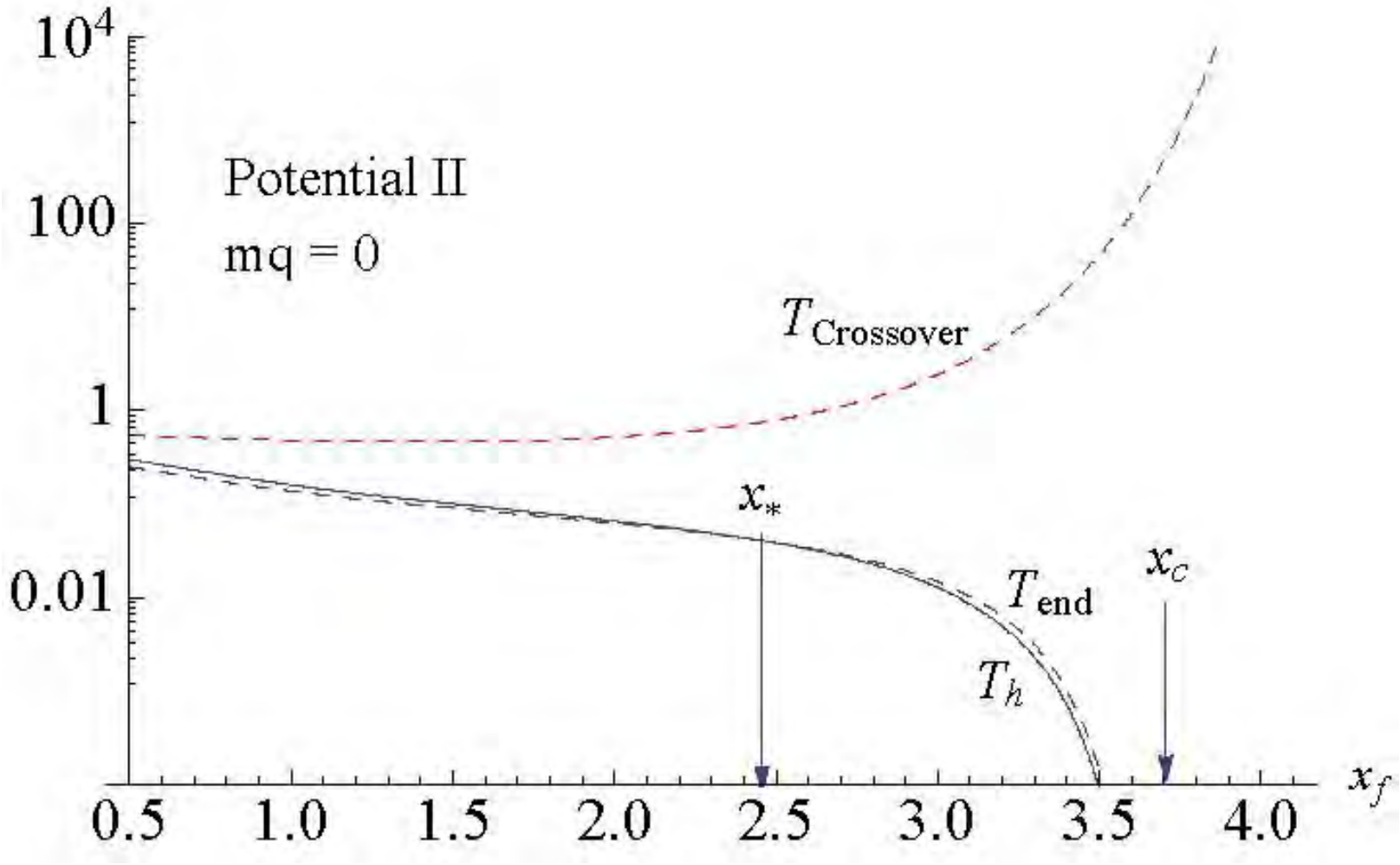

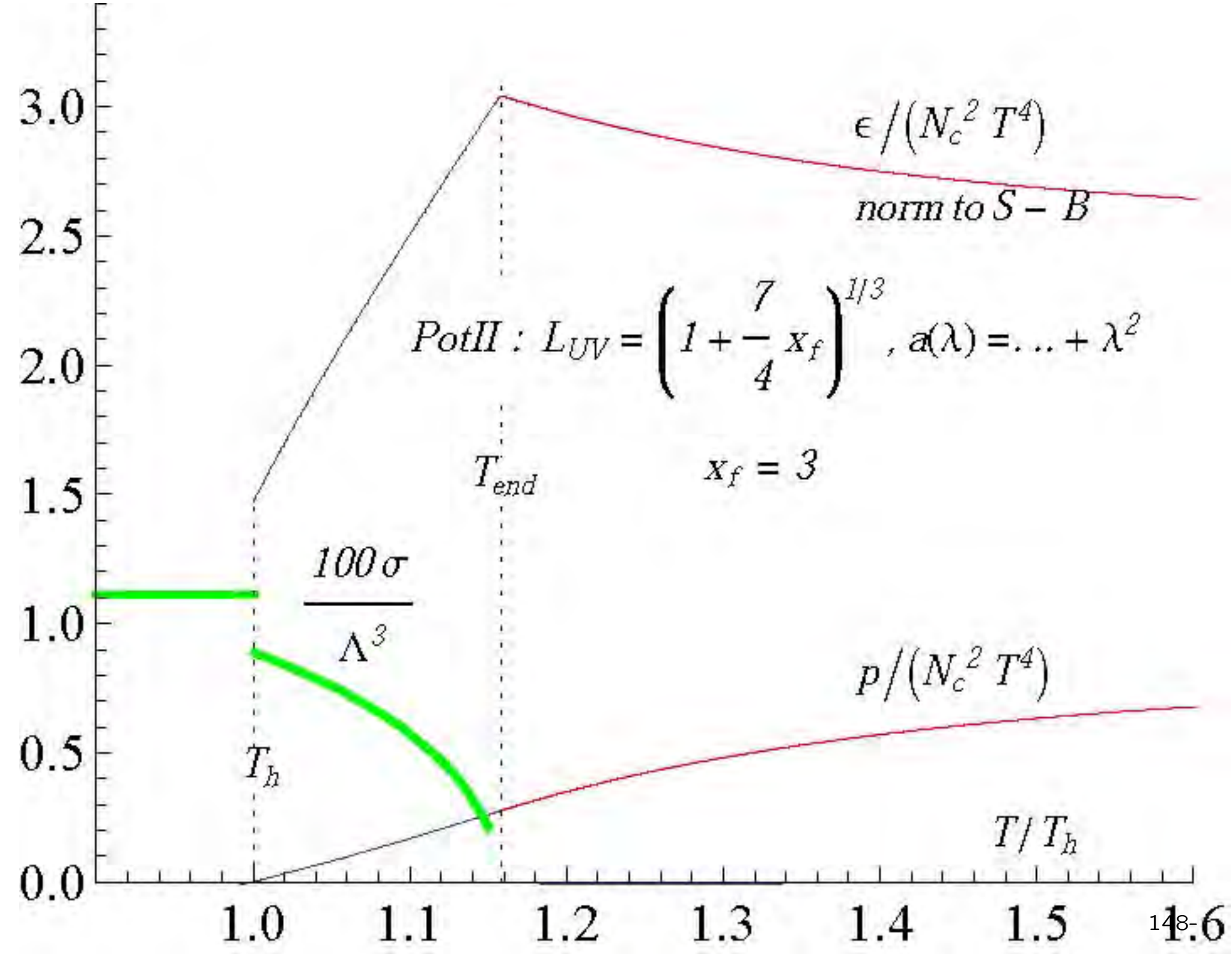
3.0
2.5
2.0
1.5
1.0
0.5
0.0
1.0
1.1
1.2
1.3
1.4
1.5
1.6
$\epsilon/(N_c^2 T^4)$
norm to $S-B$
$PotII: L_{UV} = \left(1 + \frac{7}{4} x_f\right)^{1/3}$, $a(\lambda) = \ldots + \lambda^2$
$x_f = 3$
T_{end}
$\frac{100\sigma}{\Lambda^3}$
T_h
$p/(N_c^2 T^4)$
T/T_h

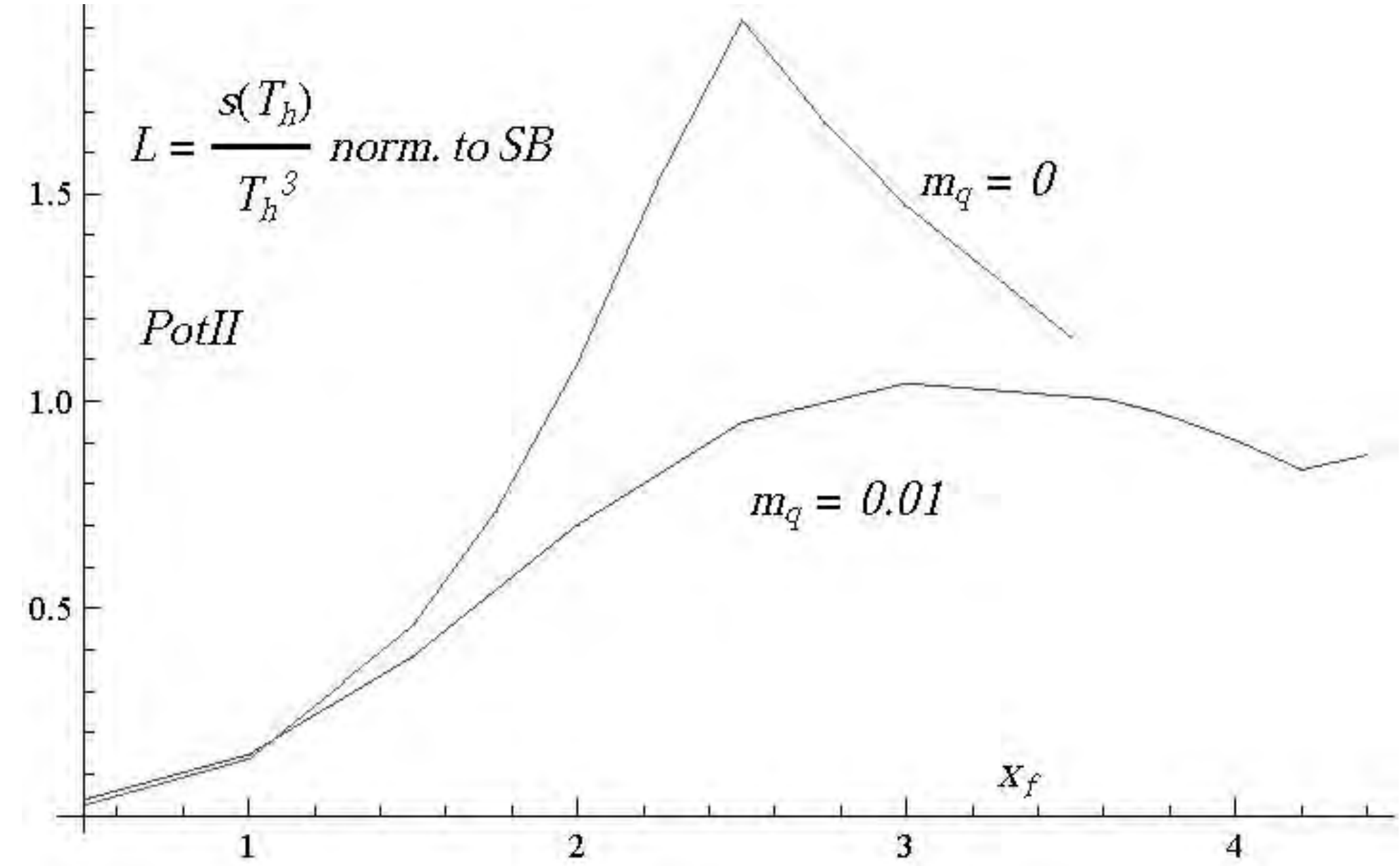
$L = \frac{s(T_h)}{T_h^3}$ norm. to SB
PotII
$m_q = 0$
$m_q = 0.01$
1.5
1.0
0.5
x_f
1
2
3
4

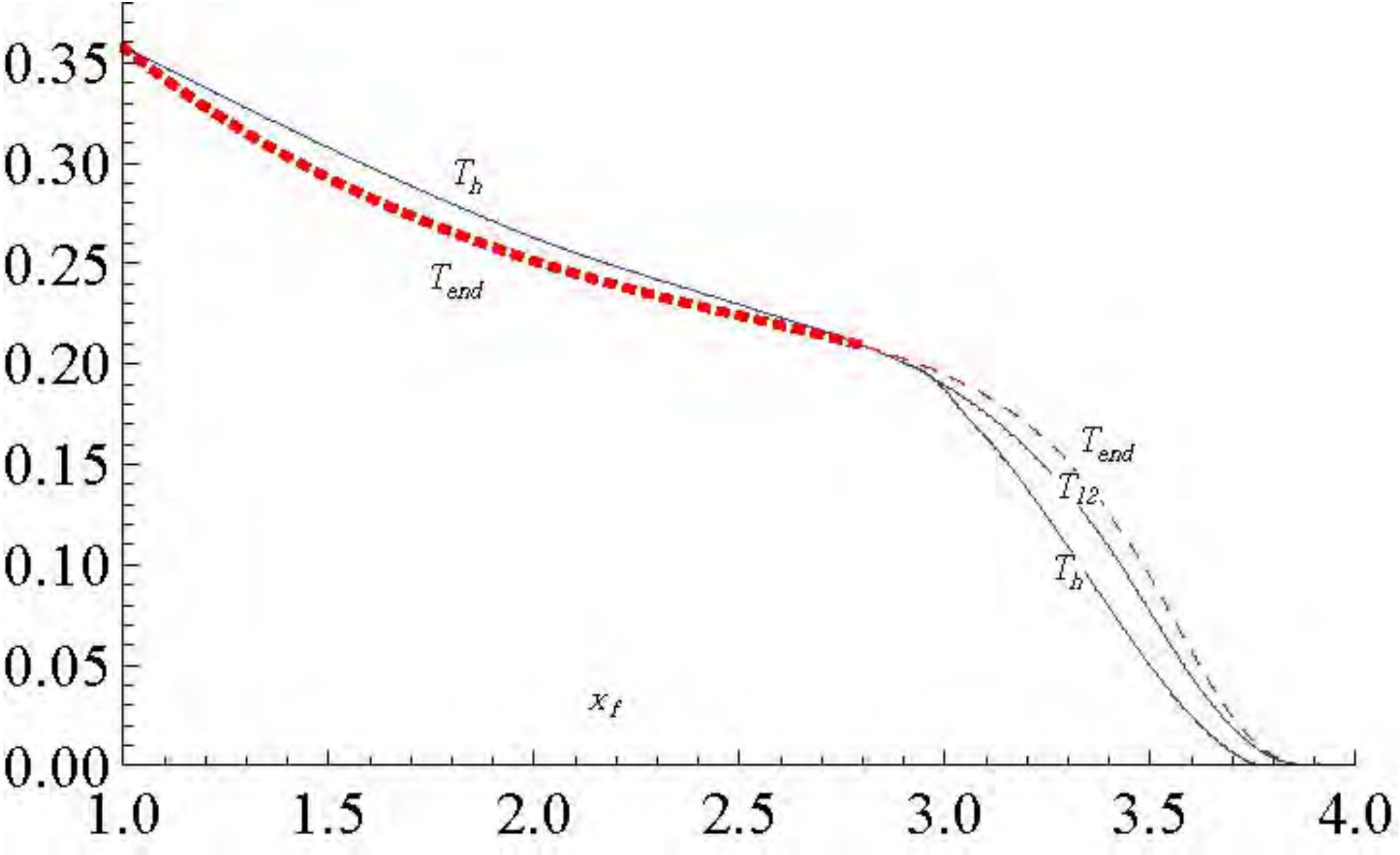
0.35
0.30
0.25
0.20
0.15
0.10
0.05
0.00
1.0
1.5
2.0
2.5
3.0
3.5
4.0
T_h
T_{end}
T_{end}
T_{12}
T_h
x_f

The speed of sound

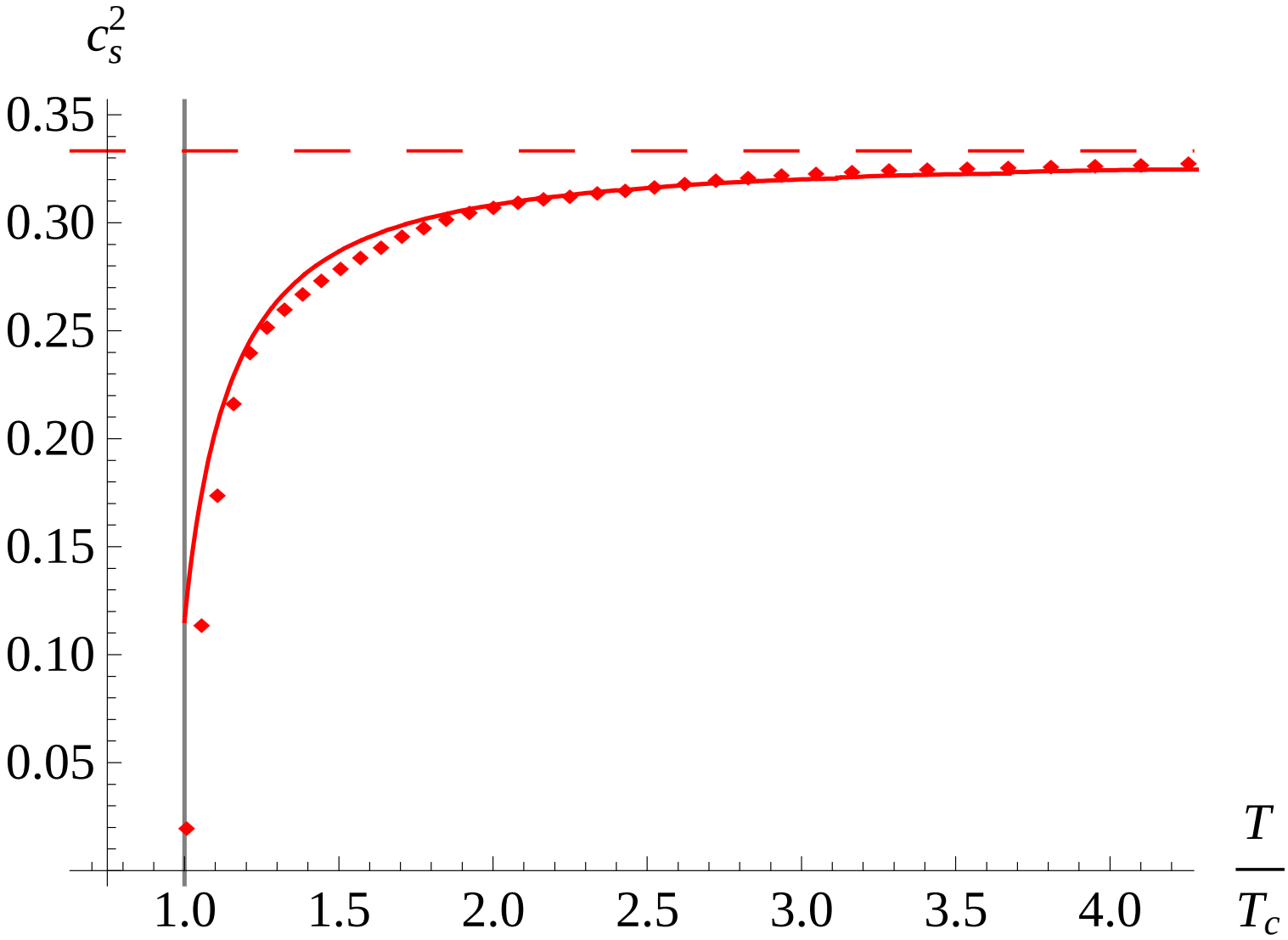

The improved Sen tachyon action

• The Sen action is conjectured for unstable branes and $D\bar{D}$ pairs in flat space. It passes several constraints on its dynamics.

• There are background independent arguments that $V_f \to 0$ when D-branes annihilate.

Sen

• The IhQCD background for glue, becomes flat in the string frame in the IR. The dilaton runs however (quadratically).

• The Sen action is expected to have open string corrections: these are not expected to change it basic asymptotics: $V_f \to 0$.

• The $\sqrt{|DT|^2}$ at large T is subleading and does not affect qualitatively the dynamics.

RETURN

Characterizing IR asymptotics

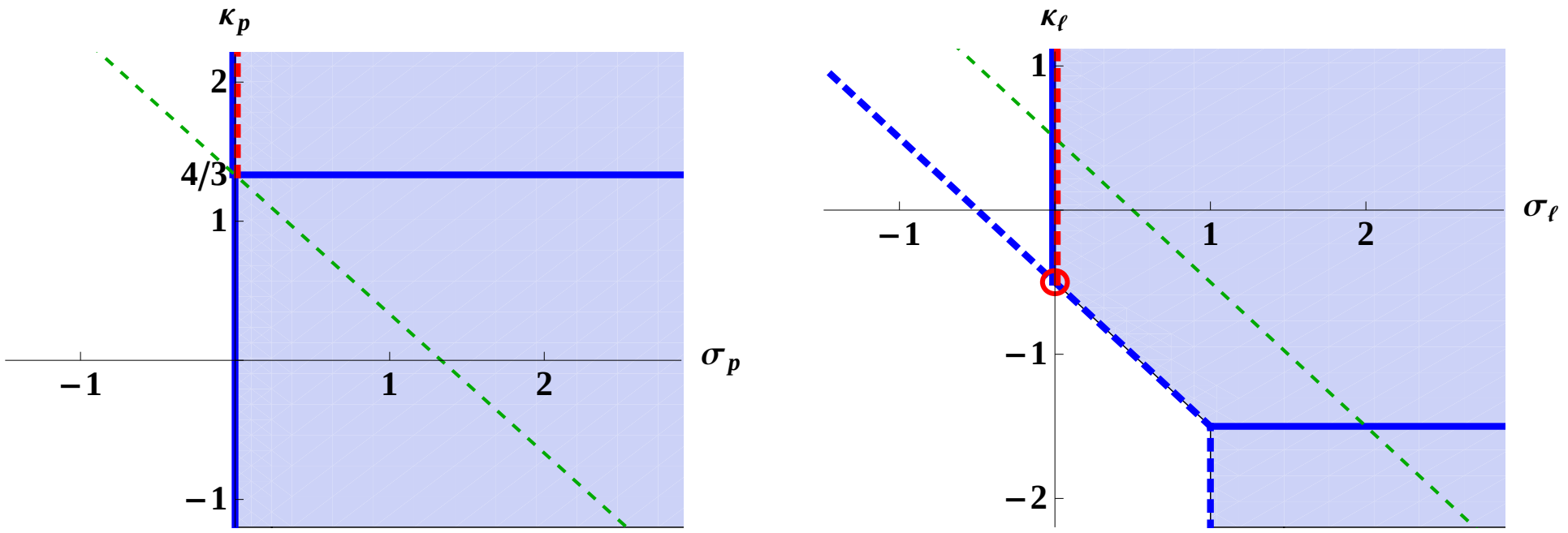

Map of the acceptable IR asymptotics of the functions $\kappa(\lambda) \sim \lambda^{-\kappa_p}(\log\lambda)^{-\kappa_\ell}$ and $a(\lambda) \sim \lambda^{\sigma_p}(\log\lambda)^{\sigma_\ell}$. Left: qualitatively different regions of tachyon asymptotics as a function of the parameters κ_p and a_p characterizing the power-law asymptotics of the functions. Right: regions of tachyon asymptotics at the critical point $\kappa_p = 4/3$, $a_p = 0$ as a function of the parameters κ_ℓ and a_ℓ characterizing the logarithmic corrections to the functions. In each plot, the shaded regions have acceptable IR behavior, and the thick blue lines denote changes in the qualitative IR behavior of the tachyon background. On the solid blue lines good asymptotics can be found, whereas on the dashed lines such asymptotics is absent. The thin dashed green line shows the critical behavior where the BF bound is saturated as $x \to 0$. Potentials above this line are guaranteed to have broken chiral symmetry at small x.

Finally, on the red dashed lines the asymptotic meson mass trajectories are linear with subleading logarithmic corrections. The red circle shows the single choice of parameters where the logarithmic corrections are absent.

Walking

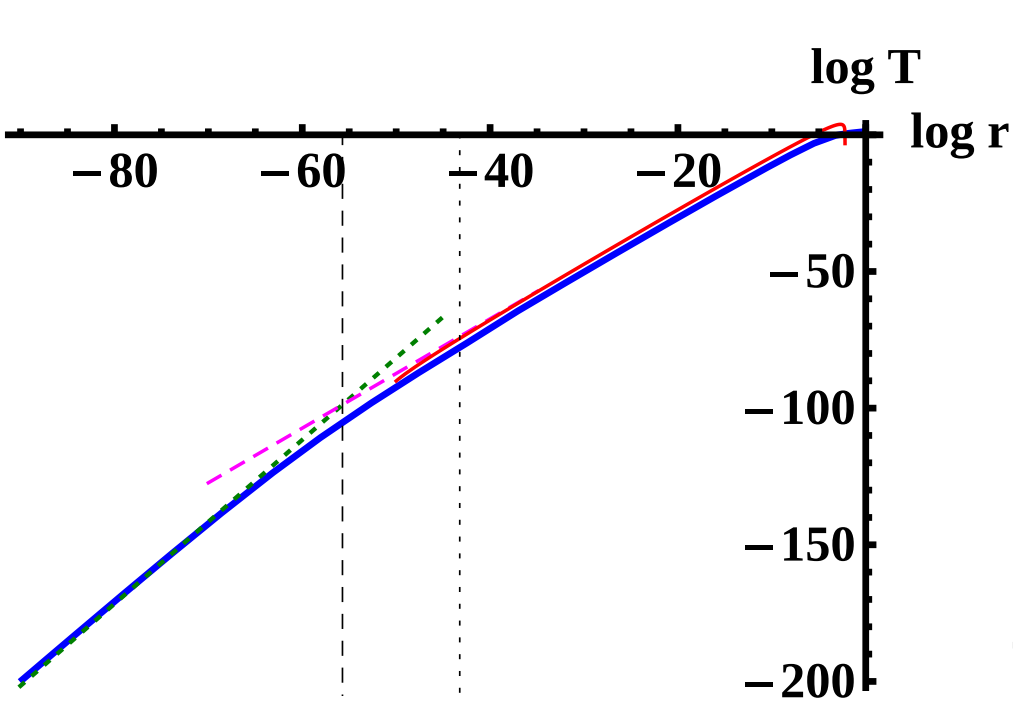

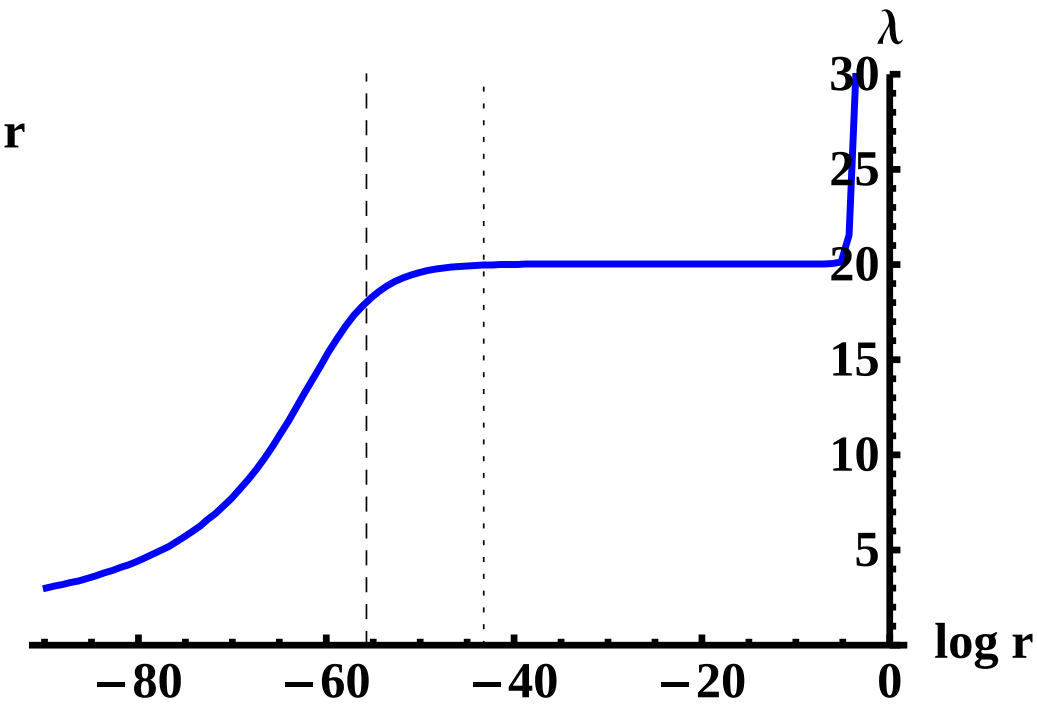

The tachyon $\log T$ (left) and the coupling λ (right) as functions of $\log r$ for an extreme walking background with $x = 3.992$. The thin lines on the left hand plot are the approximations used to derive the BKT scaling.

BKT/Miransky scaling

We obtain BKT-Miransky scaling:

$$\sigma \sim \Lambda_{\rm UV}^3 \ \exp\left(-\frac{2K}{\sqrt{\lambda_* - \lambda_c}}\right) \sim \Lambda_{\rm UV}^3 \ \exp\left(-\frac{2\hat{K}}{\sqrt{x_c - x}}\right) \ .$$

and the function that controls $K, \hat{K}$ is

$$\Delta_{\rm IR}(4-\Delta_{\rm IR}) = -m_{\rm IR}^2 \ell_{\rm IR}^2 = G(\lambda_*, x) \equiv \left.\frac{24a(\lambda)}{h(\lambda)(V_g(\lambda) - xV_{f0}(\lambda))}\right|_{\lambda=\lambda_*} ,$$

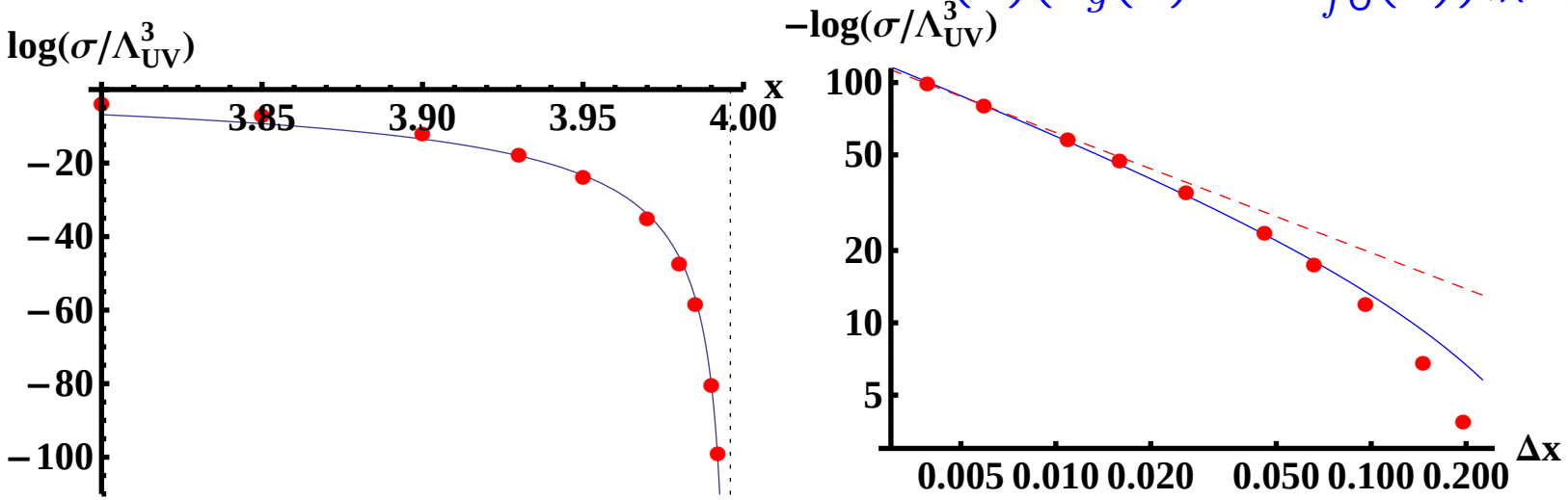

Left: $\log(\sigma/\Lambda^3)$ as a function of x (dots), compared to a BKT scaling fit (solid line). The vertical dotted line lies at $x = x_c$. Right: the same curve on log-log scale, using $\Delta x = x_c - x$.

Spectra

• The main difference from all previous calculations is that here flavor back reacts on color.

• In the singlet sector the glueballs and mesons mix to leading order and the spectral problem becomes complicated.

• The conclusions are:

♠ All masses follow Miransky scaling in the walking region.

♠ There is no dilaton. Instead all (bound-state) masses go to zero exponentially fast.

♠ There are several level crossings as x_f varies but they seem accidental

♠ There is a subtle (and unexpected) discontinuity associated with the S-parameter.

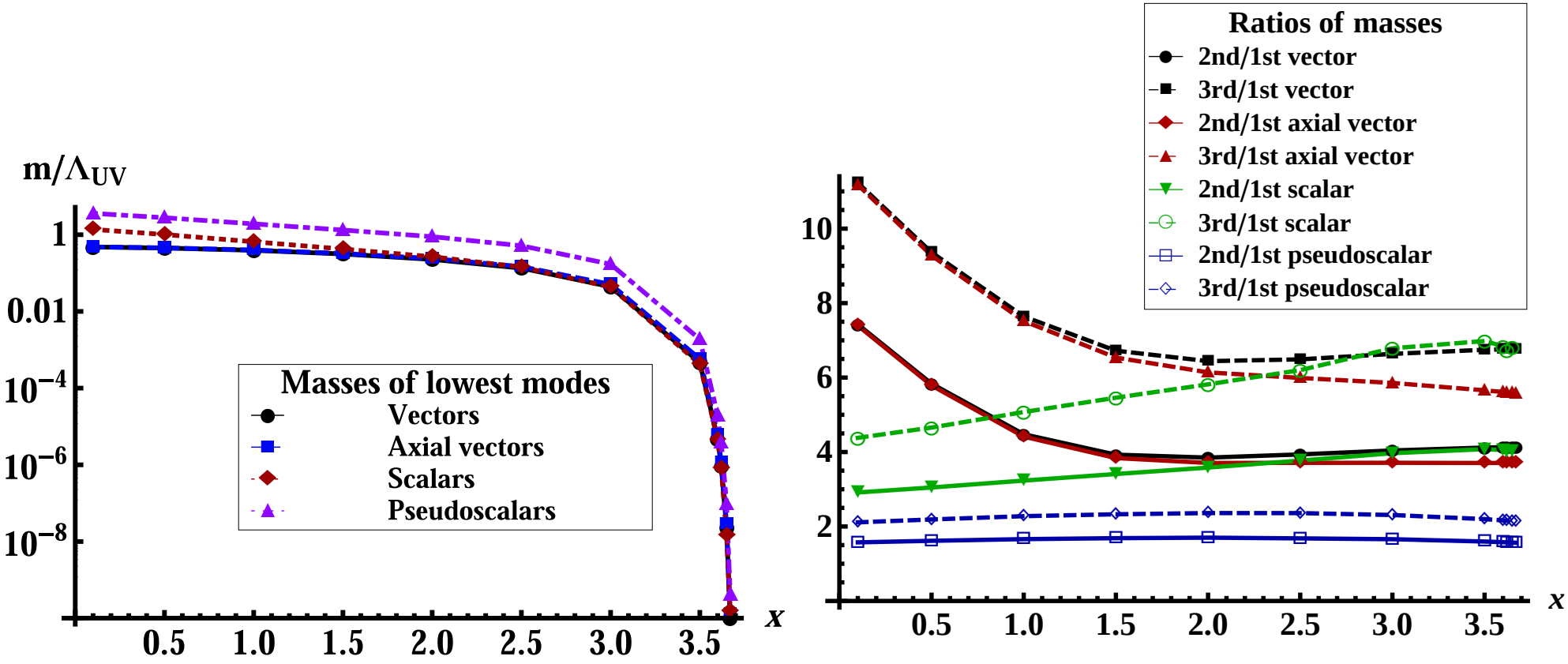

Non-singlet meson spectra in the potential II class with Stefan-Boltzmann (SB) normalization for W_0, with $x_c \simeq 3.7001$. Left: the lowest non-zero masses of all four towers of mesons, as a function of x, in units of Λ_{UV}, below the conformal window. Right, the ratios of masses of up to the fourth massive states in the same theory as a function of x.

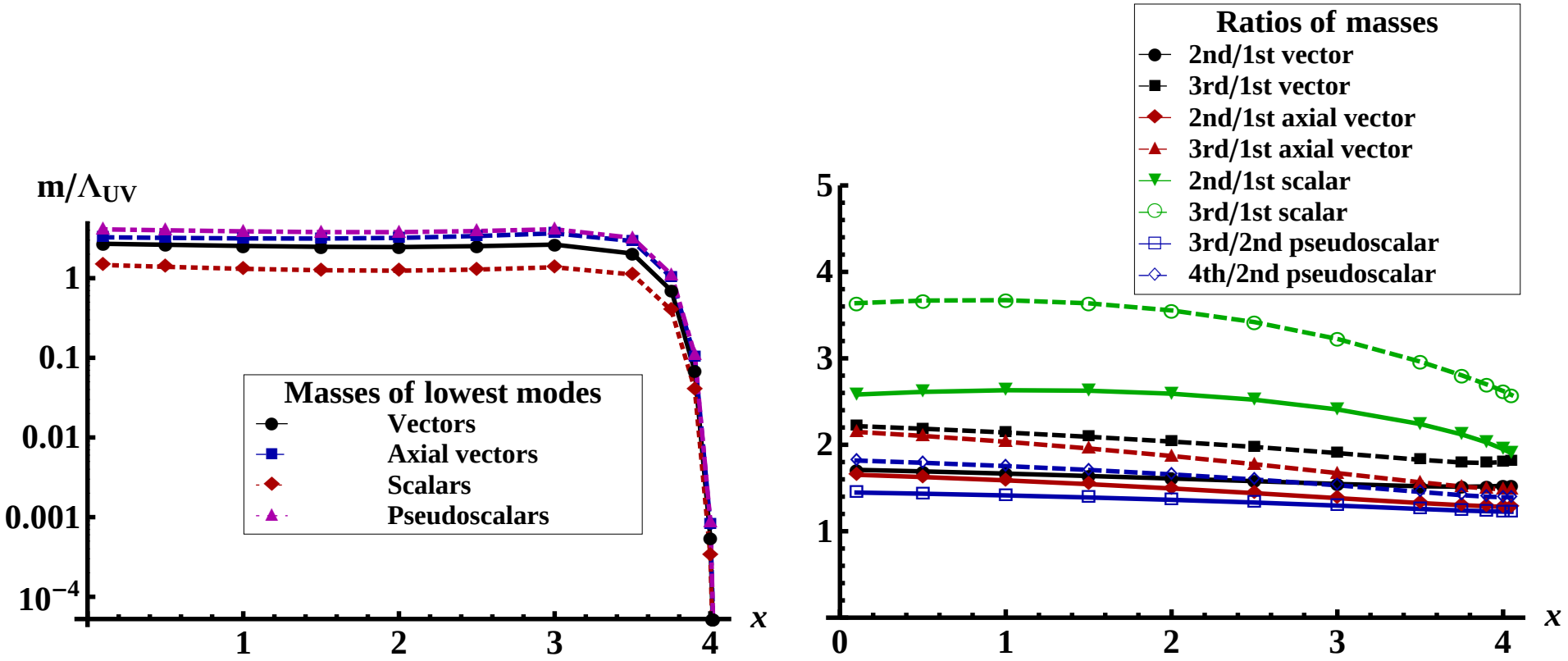

Non-singlet meson spectra in the potential I class ($W_0 = \frac{3}{11}$), with $x_c \simeq 4.0830$. Left: the lowest non-zero masses of all four towers of mesons, as a function of x, in units of $\Lambda_{\rm UV}$, below the conformal window. Right, the ratios of masses of up to the fourth massive states in the same theory as a function of x.

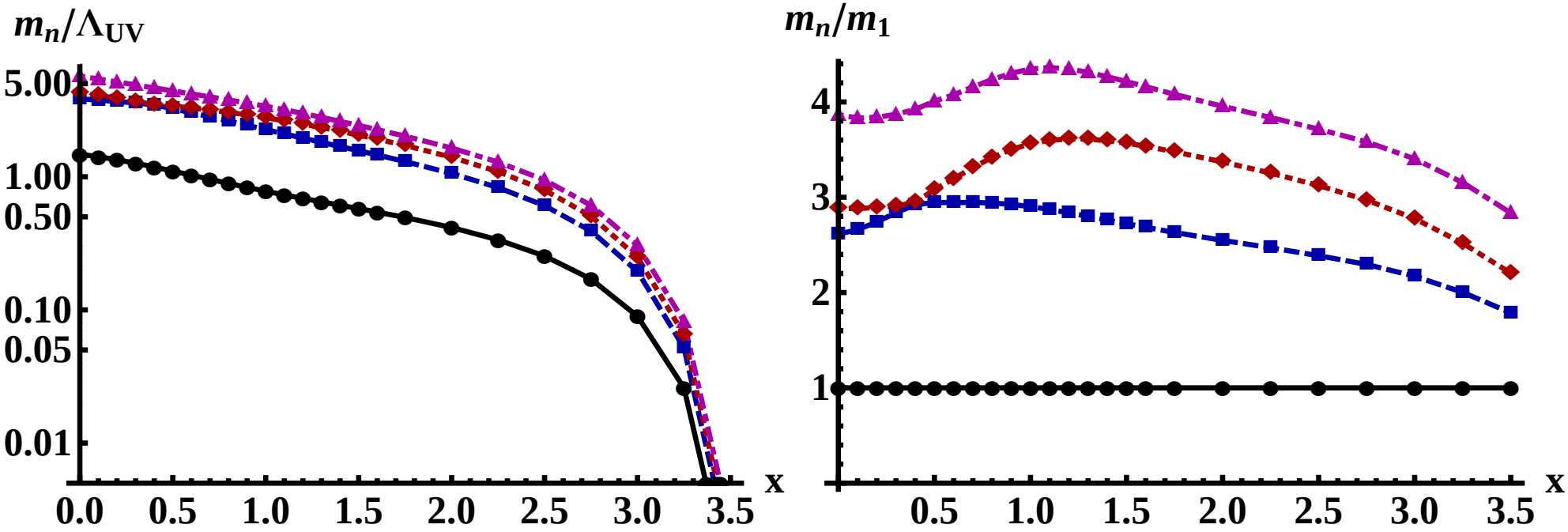

Singlet scalar meson spectra in the potential II class with SB normalization for W_0. They contain the 0^{++} glueballs and the singlet 0^{++} mesons that mix here at leading order. Left: the four lowest masses as a function of x in units of Λ_{UV}. Right: the ratios of masses of up to the fourth massive states as a function of x.

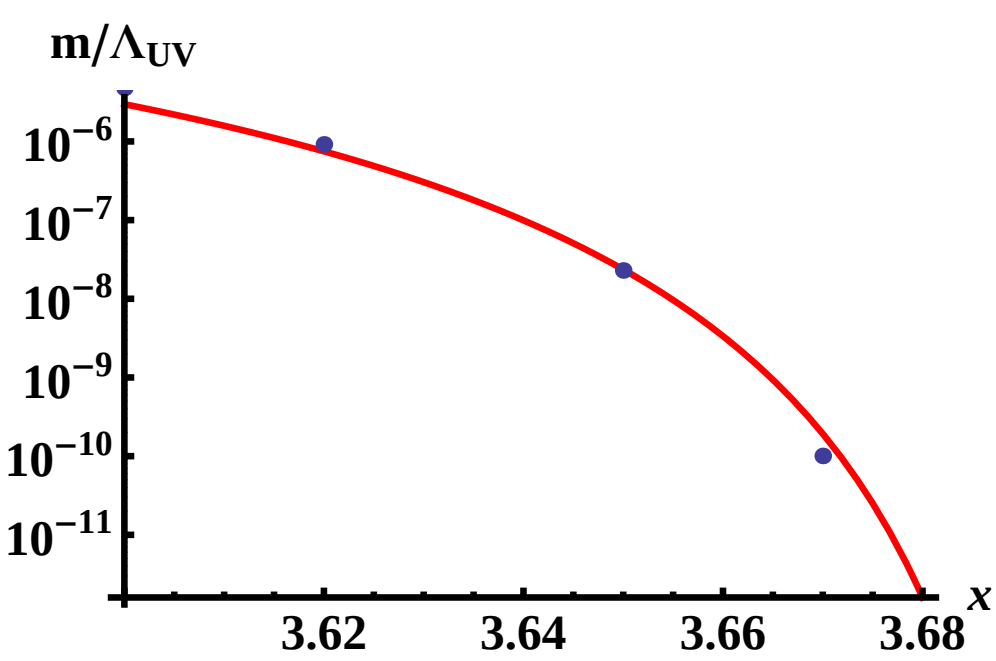

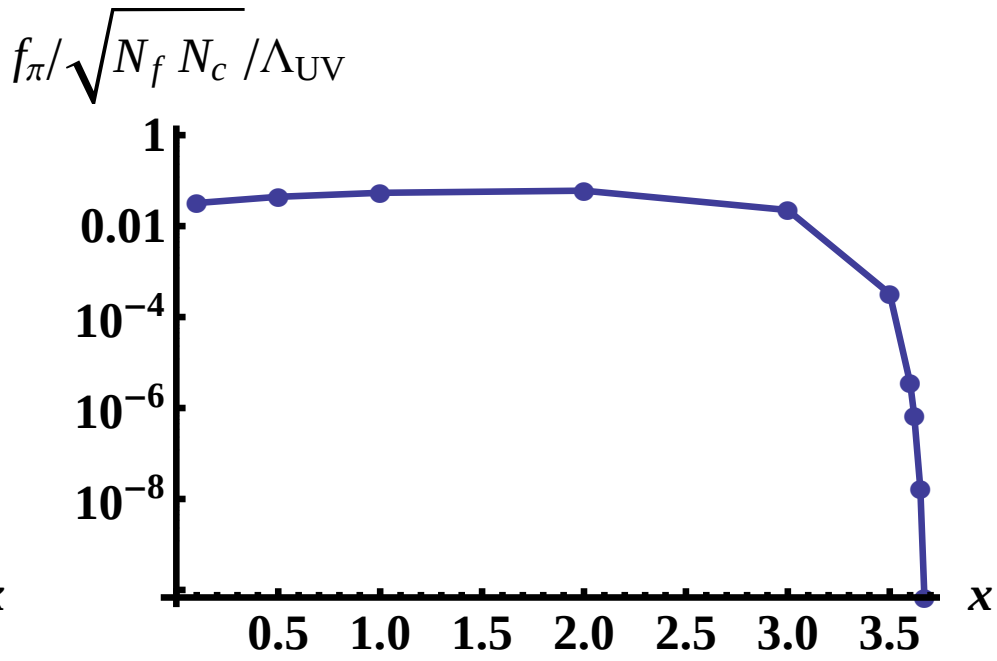

Potential II with SB normalization for W_0. Left: A fit of the ρ mass to the Miransky scaling factor, showing that it displays Miransky scaling in the walking region. Right, f_π as a function of x in units of Λ_{UV}. It vanishes near x_c following again Miransky scaling.

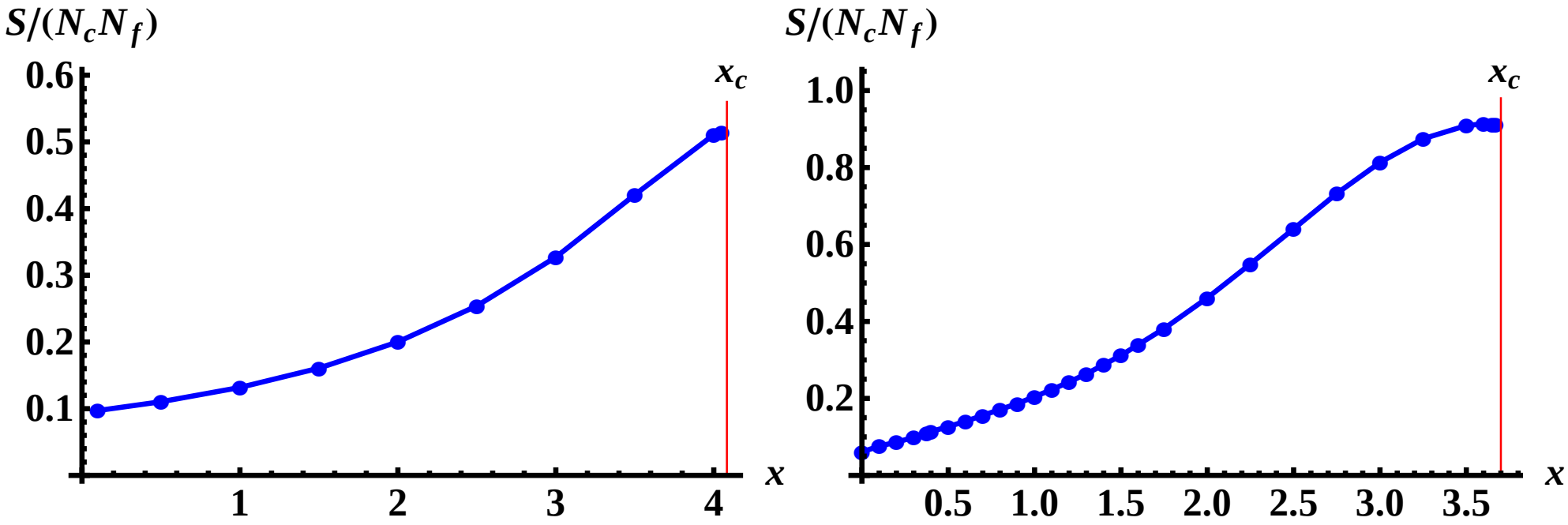

Left: The S-parameter as a function of x for potential class I with $W_0 = \frac{3}{11}$. Right: The S-parameter as a function of x for potential class II with SB normalization for W_0. In both cases S asymptotes to a finite value as $x \to x_c$.

Finite Temperature: the generic phase diagram

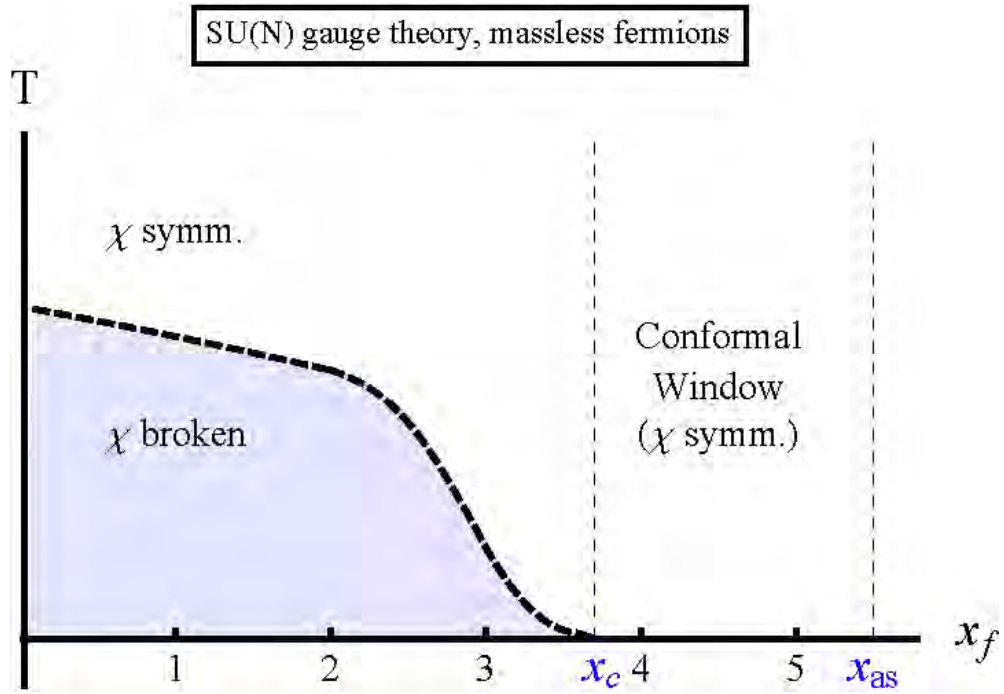

Qualitative behavior of the transition temperature between the low and high T phases of V-QCD matter.

- How does the deconfinement transition compete with the chiral transition?

- Are there further transitions (or crossovers) ?

The different types of blackholes

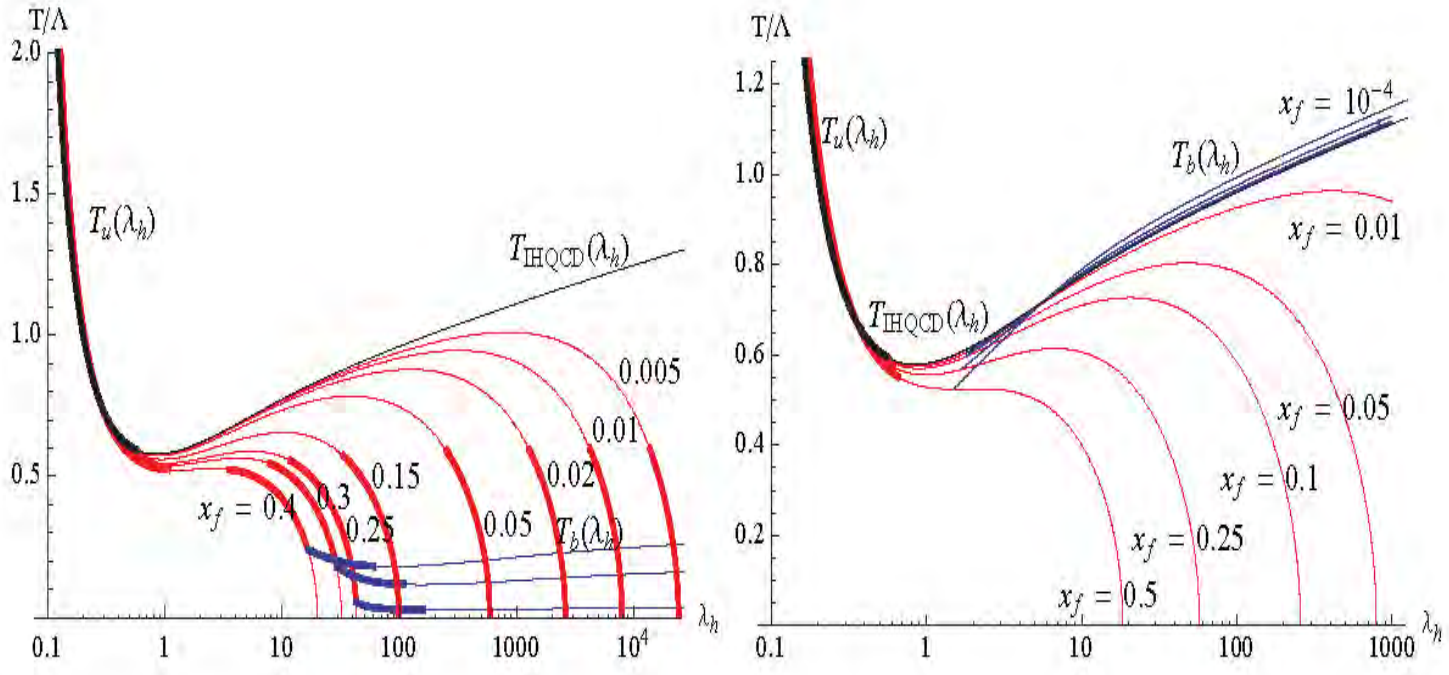

Figure 22: $T(\lambda_h)$ for various small values of x_f and for potential I, $W_0 = 24/11$ (*Left*) or for potential II, $W_0 = 12/11$ (*Right*). The black curve is the IHQCD limit. The chirally symmetric $T_u(\lambda_h) \equiv T(\lambda_h, \tau = 0)$ branch asymptotes to the IHQCD curve as $x_f \to 0$, for both potentials. The chirally broken $T_b(\lambda_h) \equiv T(\lambda_h, \tau_h(\lambda_h, m_q = 0))$ branches behave very differently for PotI and PotII. For PotI T_b is absent at such low x_f and all phases are chirally symmetric (see also Fig. 18). For PotII the curves T_b follow very closely T_s and, correspondingly, $T_h \approx T_s$ (see Fig. 15).

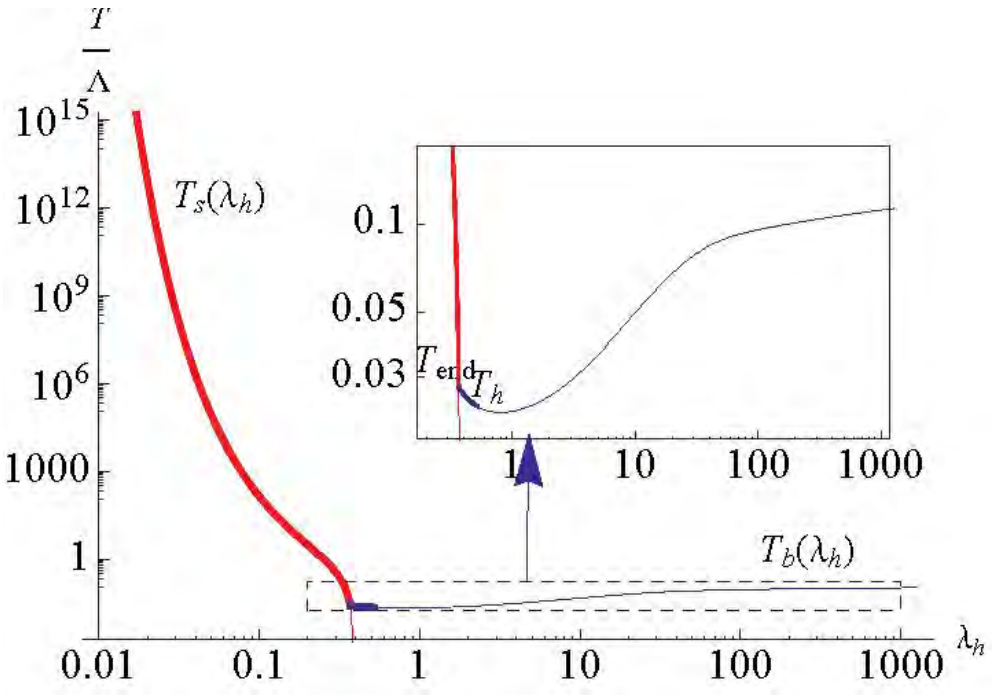

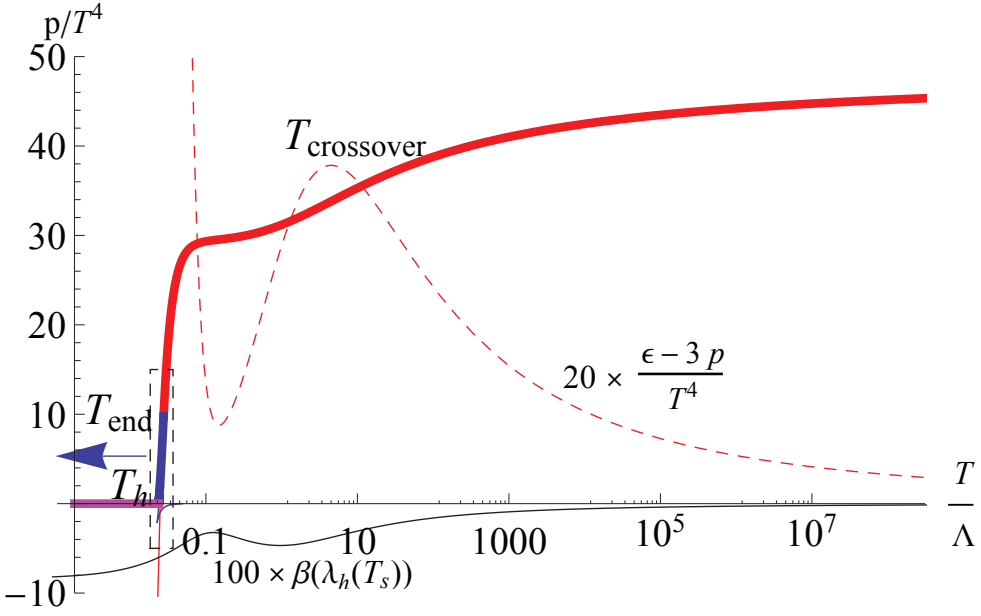

Examples of the T_{end}, T_h and $T_{\mathsf{crossover}}$ transitions in potential II with Stefan-Boltzmann -normalization of $\mathcal{L}_{\mathsf{UV}}$ and with $x_f = 3$ The curving of $T_s(\lambda_h)$ at $\lambda_h \sim 0.2$, $T \sim 2$ is related to the crossover transition. *Right*: an overview of the pressure in the same case, also showing the interaction measure, the peak of which determines the position of $T_{\mathsf{crossover}}$. The black curve shows the vacuum beta function, scaled to fit, as a function of temperature in the symmetric phase, so that $\beta(T) = \beta(\lambda_s(T))$, where $\lambda_s(T)$ is the inverse function of $T_s(\lambda_h)$. The walking maximum of the beta function clearly coincides with the plateau related to $T_{\mathsf{C}rossover}$, confirming that the $p/T^4 \sim$ constant phase below $T_{\mathsf{C}rossover}$ is indeed the quasi-conformal phase related to walking dynamics.

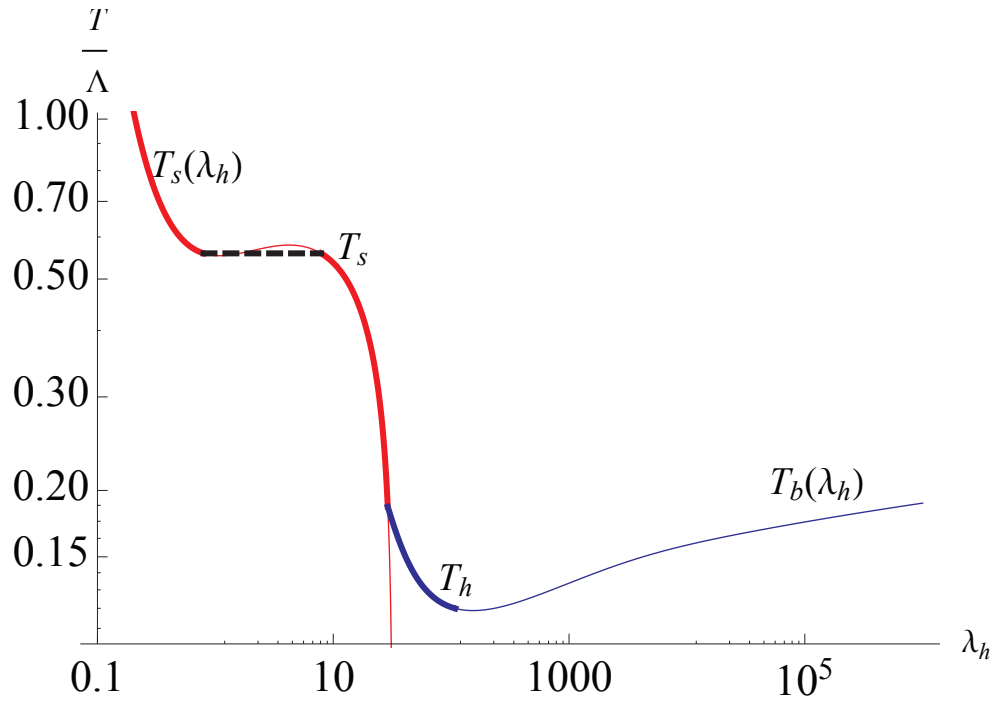

An example of the T_S transition in potential I with $W_0 = 24/11$ and with $x_f = 0.3$ The local maximum and minimum which generate the 1st order T_S -transition.

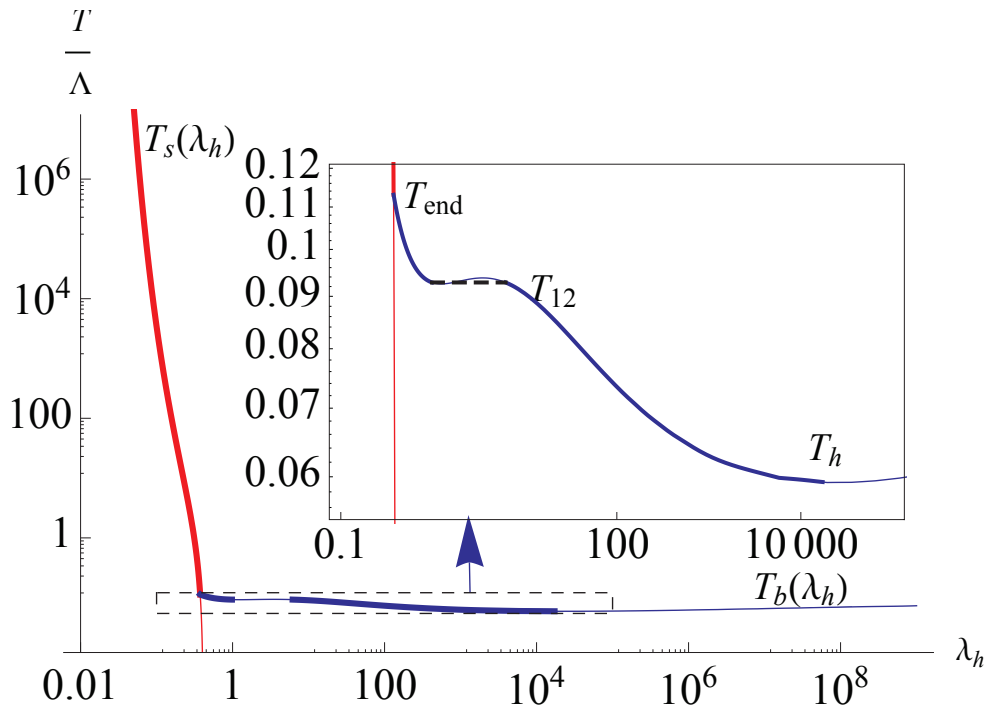

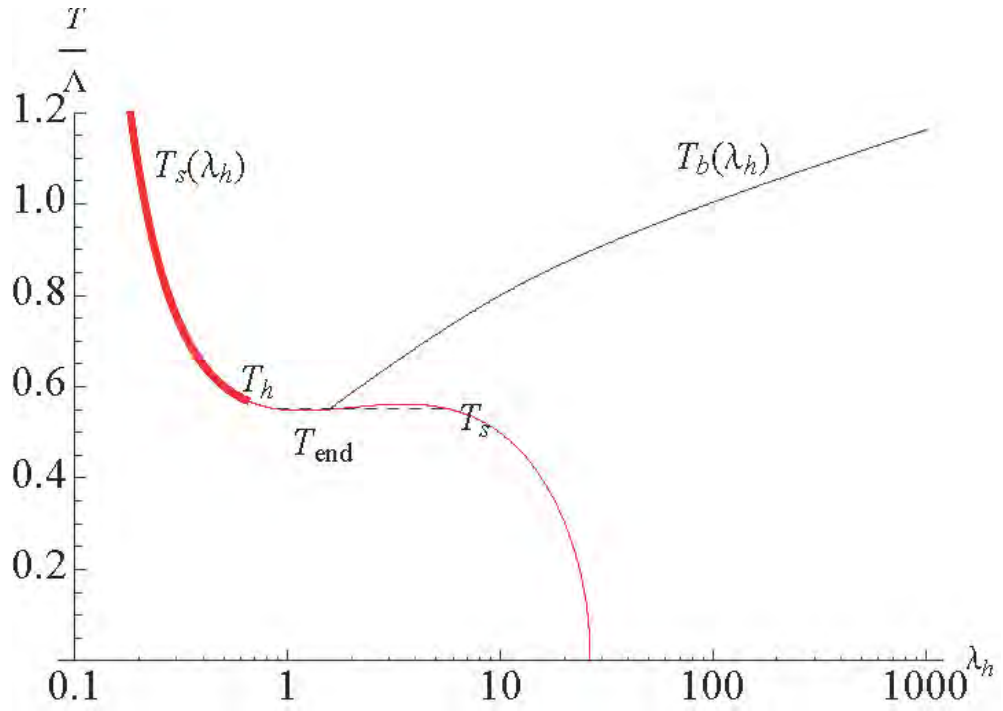

Left: An example of the T_{12} transition in potential I with $W_0 = 12/11$ and with $x_f = 3.5$. The overall structure of $T(\lambda_h)$, with an inset showing the maximum and minimum in more detail.

Right: An example of a configuration where all but the crossover and hadronisation transitions $T_{\rm crossover}$, T_h, are in the thermodynamically unstable region, in the initial stages of the approach to the IHQCD limit. The potential is II with $W_0 = 12/11$ and with $x_f = 0.4$ Note that everything to the right of the T_h transition is in the unstable phase.

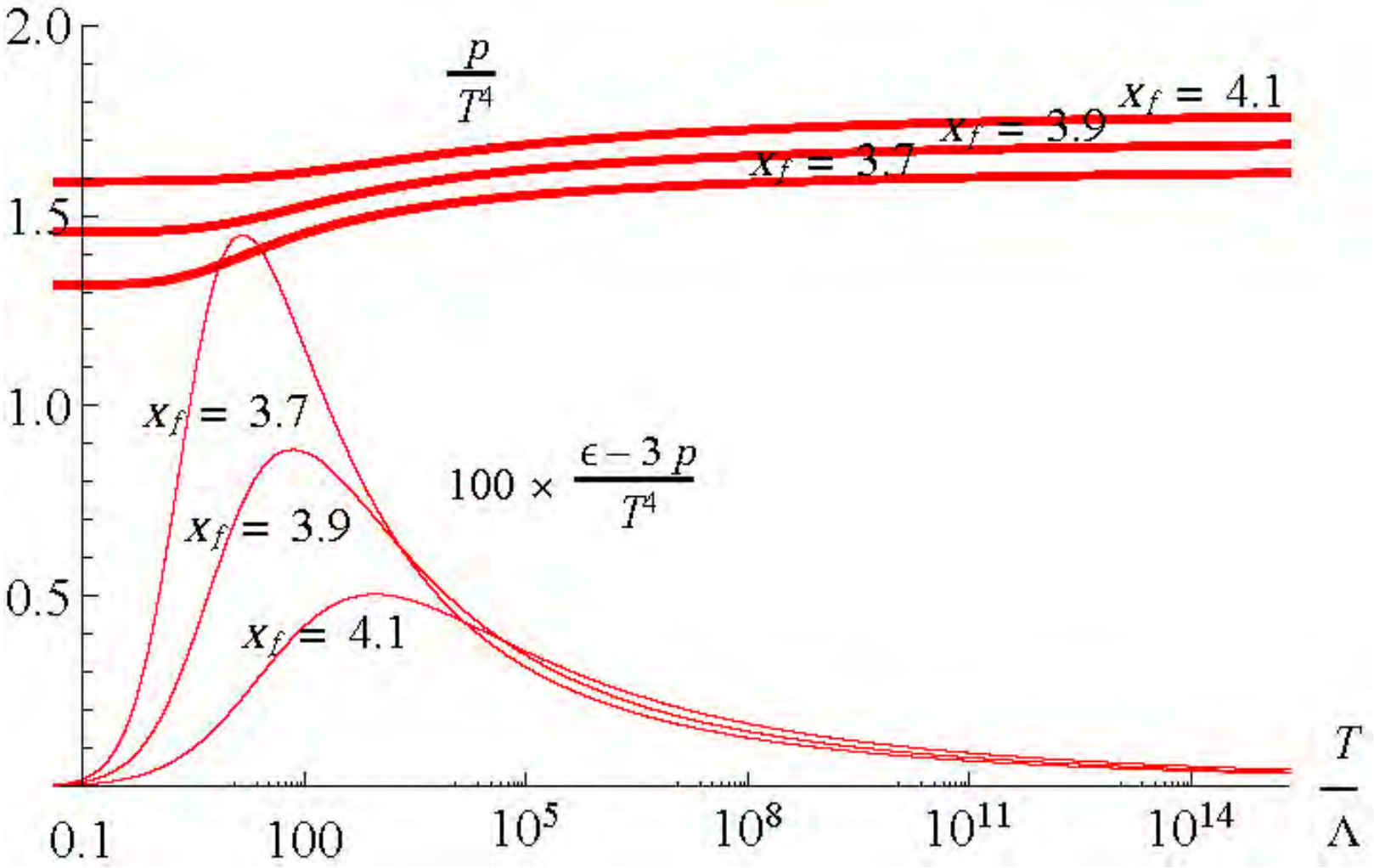

Thermodynamics for some values of x_f within the conformal window, computed for PotI. Note that in the conformal window always $\tau = 0$ and the functions $a(\lambda)$, $\Phi(\lambda)$ do not affect the result.

Finite small mass

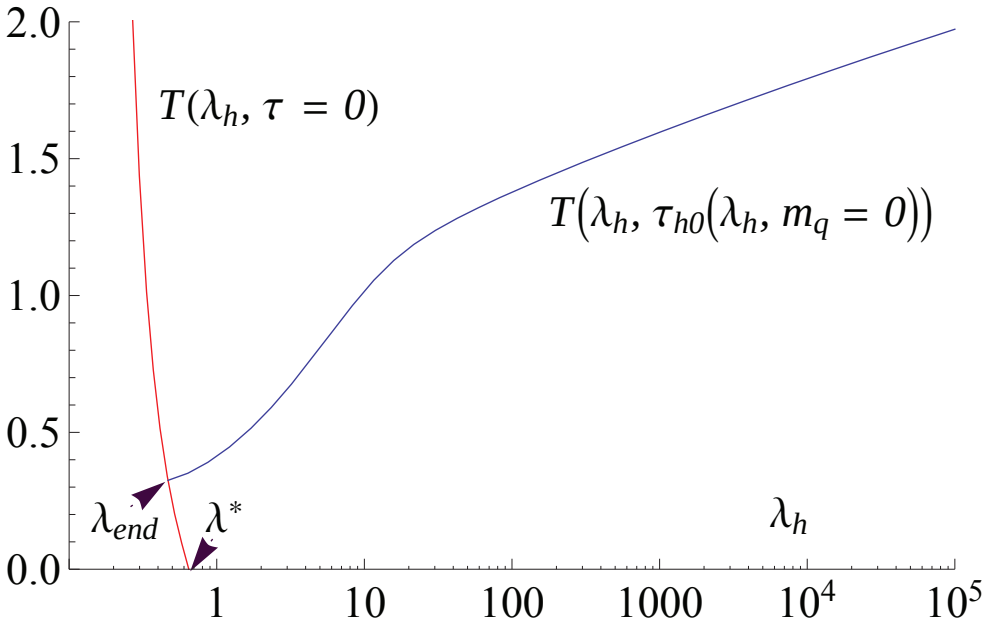

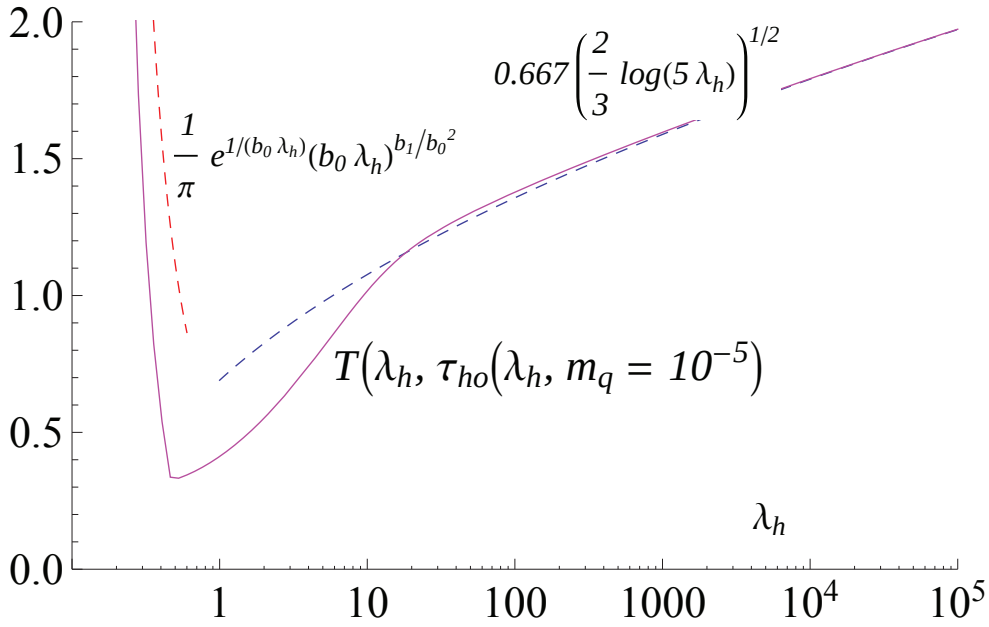

The phase diagrams

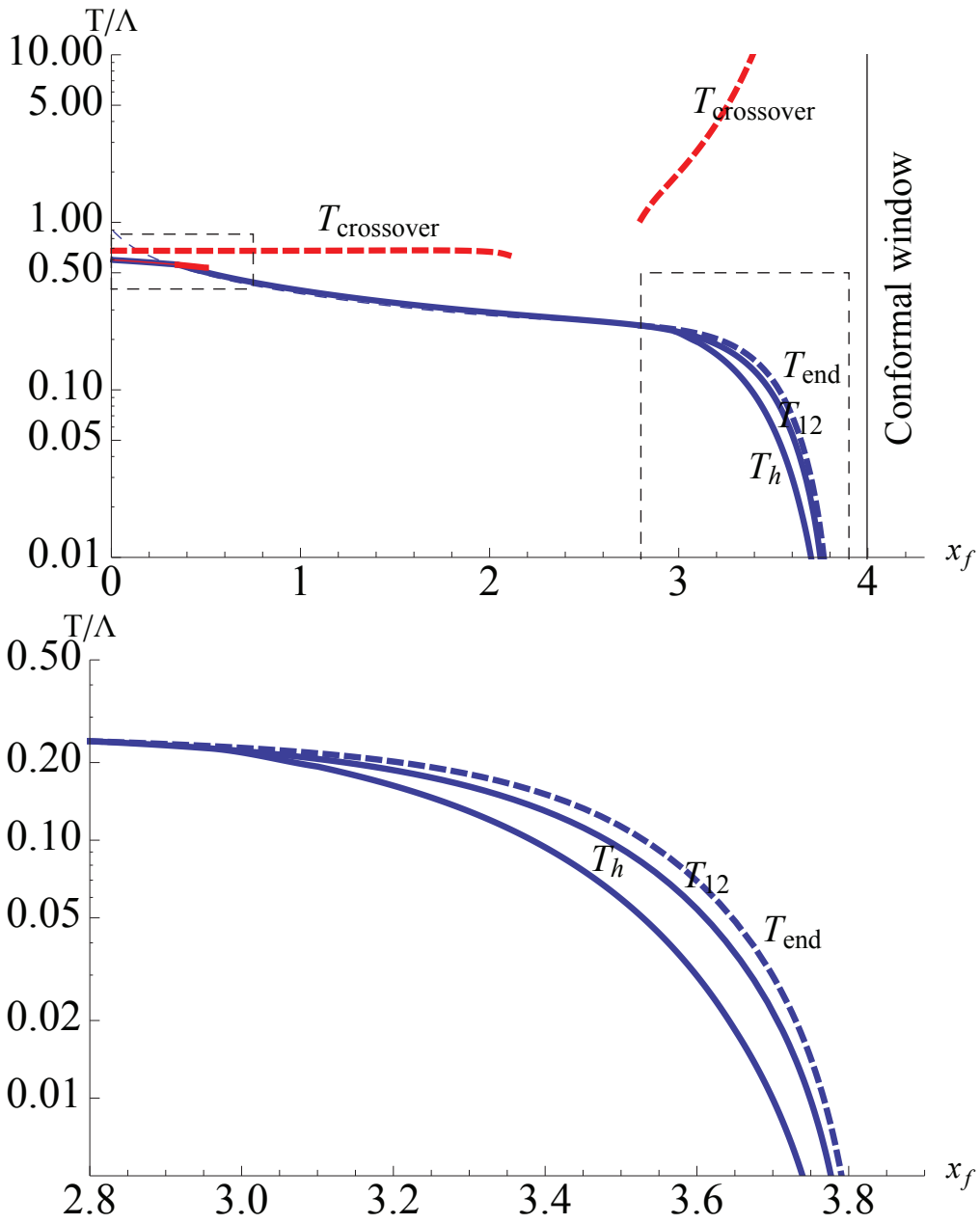

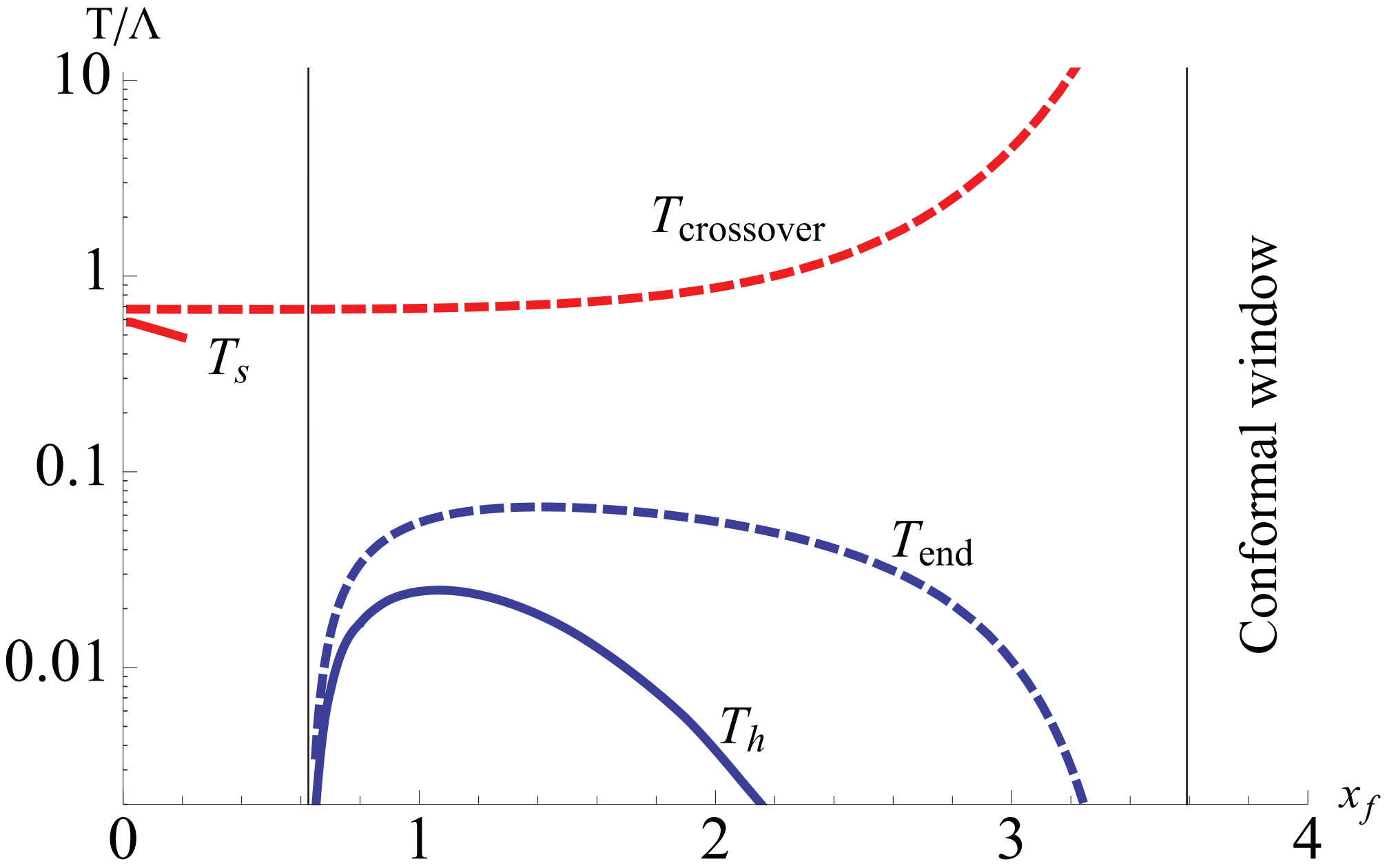
T/Λ
10
1
0.1
0.01
0
1
2
3
4
x_f
$T_{\text{crossover}}$
T_s
T_{end}
T_h
Conformal window

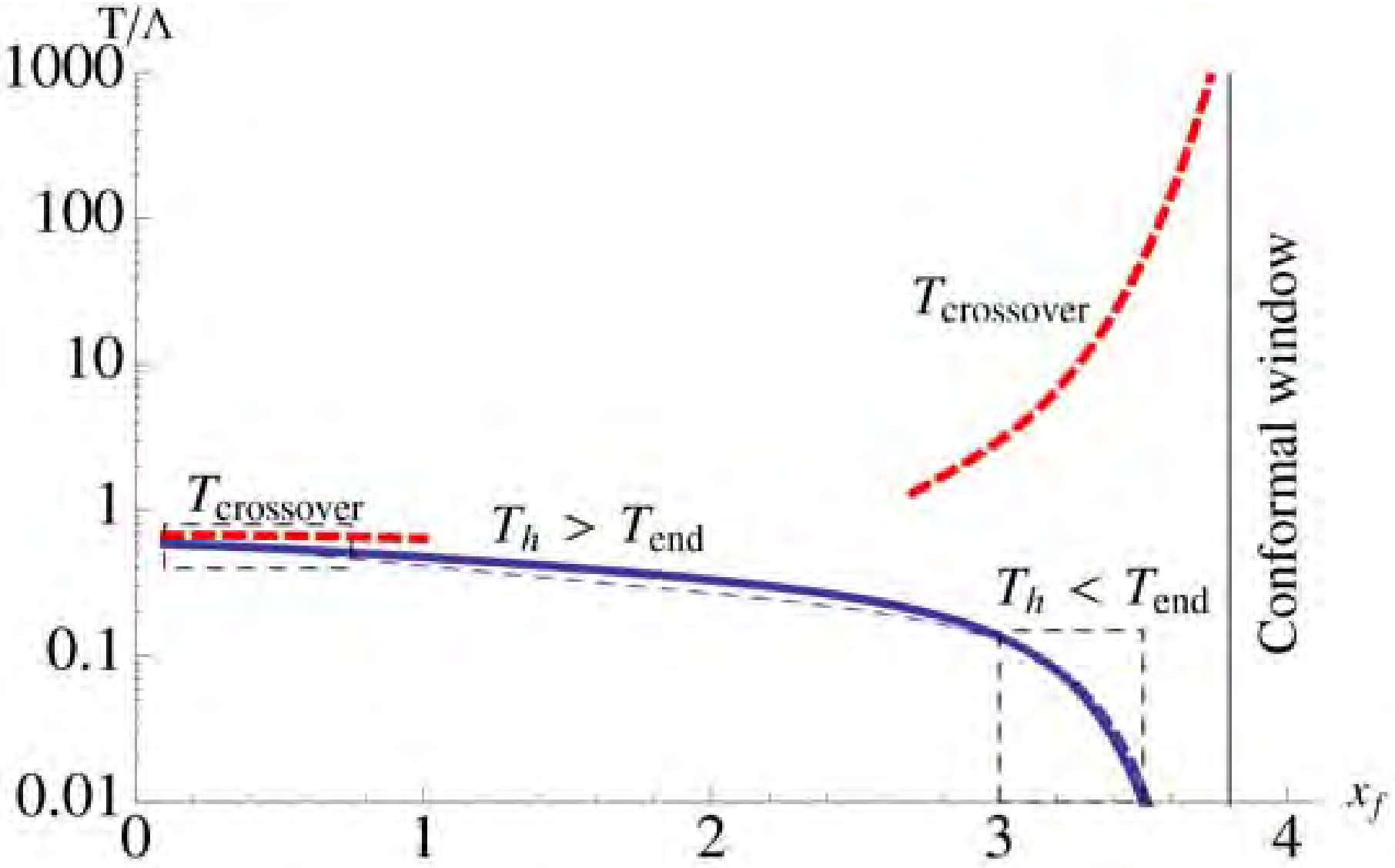

The phase diagram for potential II, $W_0 = 24/11$, $x_c = 3.80$.

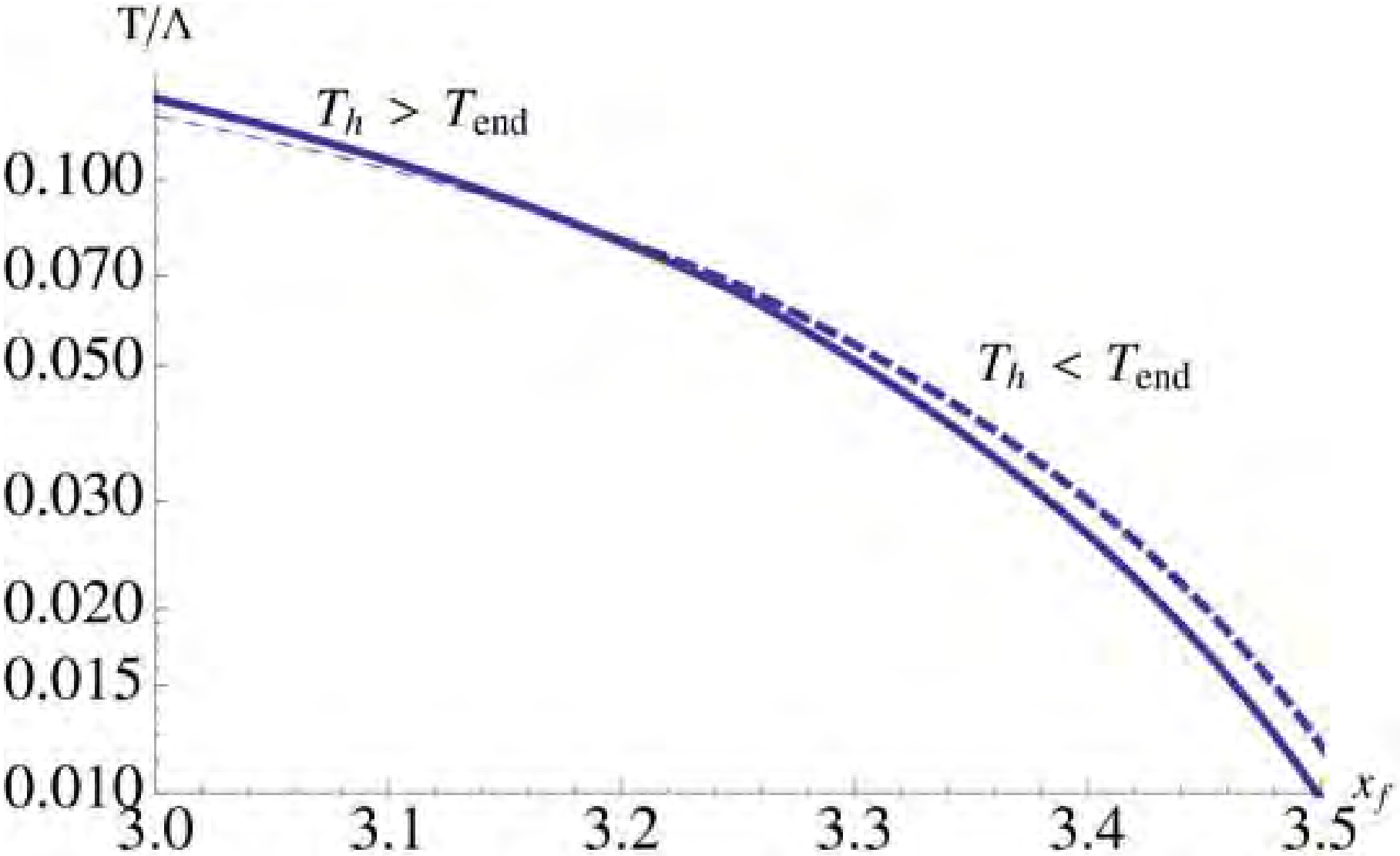
T/Λ
$T_h > T_{\rm end}$
$T_h < T_{\rm end}$
0.100
0.070
0.050
0.030
0.020
0.015
0.010
3.0
3.1
3.2
3.3
3.4
3.5
x_f

Detailed plan of the presentation

- Title page 1 minutes
- Introduction 2 minutes
- QCD 10 minutes
- Holography for YM theory 14 minutes
- Holographic Phenomenology 15 minutes
- A string theory for QCD:(Very) basic expectations 19 minutes
- Holographic YM: a model 21 minutes
- The holographic RG flow 24 minutes
- The UV regime 25 minutes
- The IR regime 27 minutes

Finite temperature considerations

- Finite temperature 30 minutes
- The pressure from the lattice at different N 32 minutes
- The entropy from the lattice at different N 33 minutes
- The trace from the lattice at different N 34 minutes

- The bulk viscosity in IhQCD 35 minutes

Adding Flavor

- Adding the quarks 36 minutes
- The Veneziano Limit 38 minutes
- The phase diagram 40 minutes
- Results 42 minutes
- The finite density diagram 44 minutes
- Outlook and Open problems 45 minutes
- Collaborators 45 minutes
- Bibliography 45 minutes

Support slides

General Comments

- Wilson loops and confinement 122 minutes
- Comments on confining backgrounds 125 minutes
- General criterion for confinement 128 minutes
- Classification of confining superpotentials 131 minutes
- Confining β-functions 134 minutes
- Selecting the IR asymptotics 137 minutes
- Particle Spectra: generalities 143 minutes
- Summary 145 minutes
- Linearity of the glueball spectrum 147 minutes
- Comparison with lattice data (Meyer) 149 minutes
- Shortcomings 151 minutes
- The lattice glueball data 152 minutes
- The glueball wavefunctions 153 minutes
- Comparison of scalar and tensor potential 154 minutes
- α-dependence of scalar spectrum 155 minutes
- The fit to glueball lattice data 157 minutes

Finite Temperature YM

- The gauge theory at finite temperature 159 minutes
- Temperature versus horizon position 162 minutes
- The free energy 165 minutes
- The free energy versus horizon position 166 minutes
- The transition in the free energy 167 minutes

- Thermodynamic variables 169 minutes
- Parameters 171 minutes
- Fit and comparison 175 minutes
- Equation of state 177 minutes
- The conformal anomaly in flat space 180 minutes
- The specific heat 181 minutes
- Parameters 185 minutes
- Speed of sound: comparing to Gubsers' formula 187 minutes

The axion

- The axion 188 minutes
- The axion background 196 minutes

Viscosity

- Shear viscosity and RHIC data 198 minutes
- Viscosity 203 minutes
- The bulk viscosity in lattice YM 205 minutes
- The Buchel bound 206 minutes
- The sum rule method 208 minutes
- Elliptic Flow vs bulk viscosity 210 minutes
- Spatial String Tension 213 minutes

Heavy quarks, Energy Loss and Langevin Diffusion

- Meson Spectra 306 minutes
- Mass dependence of f_π 307 minutes
- Linear Regge trajectories 308 minutes
- Spectra of "$s\bar{s}$ states 312 minutes

Veneziano Limit QCD

- The Veneziano limit: motivation 314 minutes
- N=1 sQCD 318 minutes
- Walking, Technicolor, S-parameter, Dilatons 323 minutes
- The Banks-Zaks region 325 minutes
- Strategy 326 minutes
- Fusion 329 minutes
- Parameters 330 minutes
- The effective potential 332 minutes
- Condensate dimension at the IR fixed point 334 minutes
- UV mass vs IR parameter 338 minutes
- Recap 339 minutes
- Below the BF bound 342 minutes

- Matching to QCD: UV 345 minutes
- Potential Choices 348 minutes
- Varying the model 350 minutes
- The IR fixed point 351 minutes
- Matching to QCD :IR 352 minutes
- The free energy 354 minutes
- Walking 359 minutes
- Holographic β-functions 362 minutes

- UV mass vs T_0 and r_1 368 minutes
- Numerical solutions :$T = 0$ 370 minutes
- Numerical solutions: Massless with $x < x_c$ 375 minutes
- Matching to QCD 376 minutes
- Comparison to previous guesses 377 minutes
- Miransky scaling for the masses 378 minutes
- Walking 379 minutes
- Phase diagram 380 minutes
- The tachyon action 381 minutes
- Characterizing IR asymptotics 382 minutes
- Walking 383 minutes
- BKT/Miransky scaling 385 minutes
- Spectra 392 minutes

Finite Temperature V-QCD

- Finite Temperature: The generic phase diagram 394 minutes
- The different black hole solutions 402 minutes
- Finite small mass 403 minutes
- The phase diagrams 405 minutes
- The speed of sound 406 minutes